A STUDY OF THE RELATIONSHIP BETWEEN VARIOUS SLURRY MATERIAL CHARACTERISTICS AND THE FLOW BEHAVIOUR OF CO-DISPOSED KIMBERLITE TAILINGS UPON DEPOSITION

Fredré Dunn

A dissertation submitted to the Faculty of Engineering and the Built Environment, University of Witwatersrand, Johannesburg, in fulfilment of the requirements for the degree of Master of Science in Engineering.

Johannesburg, 2004

DECLARATION

I declare that this dissertation is my own, unaided work. It is being submitted for the Degree of Master of Science in the University of the Witwatersrand, Johannesburg. It has not been submitted before for any degree or examination in any other university.

_____

(Signature of candidate)

_____ day of _____ (year) _____

ABSTRACT

The most significant benefit of co-disposal of tailings based on the "Paste and Thickened Tailings Disposal" concept is the improved ability to "design" the properties of the co-disposed tailings material to suit the surrounding environment. The overall aim of this study was to gain a better understanding of the relationship between the key slurry material characteristics and the flow behaviour of co-disposed tailings upon deposition, for the case of montmorillonite clay-based kimberlite tailings. A fundamental understanding of this relationship will enable the successful manipulation and exploitation of the co-disposed tailings rheology for optimal tailings disposal and the minimisation of associated financial, environmental and social risks.

The key material characteristics selected for investigation were the vehicle solids concentration, suspension pH and vehicle to load ratio. The yield stress was selected as the key rheological property representing both the vehicle component rheology and co-disposed tailings rheology. Two yield stress measurement techniques were used, namely (1) direct yield stress measurement with the vane method and (2) indirect yield stress measurement with the slump test method. The correlation between these two methods was investigated as a secondary objective of this study.

It was concluded that the suspension pH strongly influences the degree of microscopic particle interaction of the vehicle component and that manipulation of the suspension pH could move the material between interactive and non-interactive states.

It was further concluded that increasing load mass percentage leads to a significant increase in the co-disposed material yield stress. It is believed that the load component mainly affects the co-disposed material yield stress through its contribution to the total solids concentration, which in turn results in an exponential increase in the material yield stress.

The findings of this study showed remarkable flexibility in the manipulation of the various input parameters to produce the same yield stress value. It is therefore now possible to maintain a constant yield stress value as required by the environmental depositional requirements through various combinations of the input parameters and so keep the integrity of the deposition site intact.

The correlation obtained in this study between the vane and slump test yield stress measurement techniques was fairly poor. The slump test only provided an accurate prediction of the yield stress when the material was in a highly interactive state.

It is recommended that future research focuses on the thixotropic nature of the vehicle component as a function of suspension pH, the accuracy of the correlation between the vane and slump measured yield stress and the effect of the load on the bulk rheology of the co-disposed material.

ACKNOWLEDGEMENTS

I would like to thank each of the following people for the special contribution they made towards the successful completion of this research :

- Prof. Andy Fourie, for his guidance, insight and encouragement.
- Andrew Vietti, for his inspiration, interest and advice.
- De Beers Consolidated Mines, for financial support during the first year of my studies, supplying the raw materials and allowing me to use their laboratory facilities for the preparation of the test materials.
- My parents, Hannes and Yvonne Maasdorp, for their interest and encouragement.
- My husband, Arno Dunn, for his immense support, understanding and love.

CONTENTS

Page

DECLARATION 2
ABSTRACT 3
ACKNOWLEDGEMENTS 5
CONTENTS 6
LIST OF FIGURES 9
LIST OF TABLES 12
1. INTRODUCTION 14
1.1 Why Consider the Co-disposal of Tailings ? 14
1.1.1 Problems associated with conventional tailings disposal 14
1.1.2 Paste and Thickened Tailings Disposal – a solution ? 20
1.1.3 The added benefits of co-disposal of tailings 34
1.2 Identified Knowledge Gap 39
2. REVIEW OF PREVIOUS WORK 41
2.1 Different Methods of Co-disposal of Tailings 41
2.1.1 Fine tailings + coarse tailings 42
2.1.2 Fine tailings + coarse tailings + waste rock 50
2.1.3 Fine tailings + waste rock 51
2.2 General Introduction to Rheology 54
2.3 Manipulation of Thickened Tailings Rheology 60
2.3.1 The importance of rheology in P&TTD 60
2.3.2 General thickened tailings rheology 62
2.3.3 Kimberlite thickened tailings rheology 71
2.4 Manipulation of Co-disposed Tailings Rheology 93
2.4.1 Vehicle and load components 93
2.4.2 Co-disposed tailings rheology 94
2.5 Current Status of Identified Knowledge Gap 103
3. OBJECTIVES AND SCOPE OF STUDY 105
3.1 Objectives 105
3.2 Scope 106
3.2.1 Specific method of co-disposal of tailings 106

3.2.2 Type of tailings material 107
3.2.3 Research approach 108
3.2.4 Parameters under consideration 108
4. MATERIAL CHARACTERISTICS AND PREPARATION 111
4.1 Raw Material Characteristics 111
4.1.1 Vehicle 111
4.1.2 Load 113
4.2 Vehicle Preparation 115
4.2.1 Slurry preparation 115
4.2.2 Flocculation and settling 115
4.2.3 Sun drying 117
4.3 Load Preparation 117
4.4 Co-disposed Material Preparation 118
4.5 Manipulation of Variable Input Parameters 119
4.5.1 Vehicle solids concentration 119
4.5.2 Suspension pH 120
4.5.3 Vehicle to load ratio 122
5. MEASUREMENT TECHNIQUES AND EQUIPMENT 124
5.1 General Introduction 124
5.2 Overview of Yield Stress Measurement Techniques 126
5.2.1 Indirect measurement techniques 127
5.2.2 Direct measurement techniques 129
5.3 Description of Yield Stress Measurement Equipment 134
5.3.1 Vane test equipment 134
5.3.2 Slump test equipment 136
6. EXPERIMENTAL PROCEDURES 138
6.1 Preliminary Tests to Establish Experimental Procedures 138
6.1.1 Sensitivity of the vehicle rheology to shear history 138
6.1.2 Vane rheometer settings 143
6.2 Experimental Procedures 147
6.2.1 Direct yield stress measurement with the vane test 147
6.2.2 Indirect yield stress measurement with the slump test 148

7. RESULTS AND DISCUSSIONS 150
7.1 Vehicle Component 150
7.1.1 Manipulation of vehicle component yield stress 150
7.1.2 Correlation between yield stress measurement techniques 157
7.2 Co-disposed Tailings 168
7.2.1 Manipulation of co-disposed tailings yield stress 168
7.2.2 Correlation between yield stress measurement techniques 176
8. CONCLUSIONS AND RECOMMENDATIONS 179
8.1 Vehicle Component 179
8.2 Co-disposed Tailings 184
8.3 Recommendations for Future Work 189
REFERENCES 191
APPENDIX A : Material characteristics and preparation raw data 202
APPENDIX B : Preparation of co-disposed tailings 206
APPENDIX C : Calculation of vehicle solids concentration 208
APPENDIX D : Calculation of co-disposed tailings total solids concentration . 210
APPENDIX E : Preparation of acidic and alkaline solutions 213
APPENDIX F : US 200 Paar Physica software instructions 217
APPENDIX G : Preliminary test work - raw data summary 220
APPENDIX H : Vehicle yield stress - raw data summary 223
APPENDIX I : Vehicle yield stress - raw data sheets 230
APPENDIX J : Vehicle vane tests - torque-time curves 242
APPENDIX K : Co-disposed tailings yield stress – raw data summary 268
APPENDIX L : Co-disposed tailings yield stress – raw data sheets 278
APPENDIX M : Co-disposed tailings vane tests – torque-time curves 297

LIST OF FIGURES

Page

Figure 1.1 : The thickened tailings continuum 21
Figure 1.2 : Increased storage capacity of a P&TTD system 26
Figure 2.1 : Co-disposal of fines filter cake and coarse tailings 49
Figure 2.2 : Co-disposal of fine and coarse tailings and waste rock 50
Figure 2.3 : Two Plate Model for the definition of rheological terms 54
Figure 2.4 : Typical non-Newtonian flow behaviours 56
Figure 2.5 : Structural changes resulting in shear thinning behaviour 59
Figure 2.6 : Yield stress as a function of solids concentration in general 63
Figure 2.7 : Viscosity vs. shear rate for a range of red mud samples 64
Figure 2.8 : Variation of red mud flow properties as a function of shear history . 65
Figure 2.9 : Thixotropic behaviour of red mud thickened tailings 66
Figure 2.10 : Thixotropic strength gain after deposition 67
Figure 2.11 : Aggregation through poly-electrolyte coagulant addition 69
Figure 2.12 : Aggregation through flocculant addition 69
Figure 2.13 : Dispersion through steric repulsion 70
Figure 2.14 : Montmorillonite clay crystal structure 73
Figure 2.15 : pH dependency of clay platelet edge charges 74
Figure 2.16 : Electrical double layer model 76
Figure 2.17 : Aggregation through electrical double layer compression 80
Figure 2.18 : pH dependency of clay platelet electrical charges 81
Figure 2.19 : Particle interaction as a function of suspension pH 81
Figure 2.20 : Particle interaction as a function of suspension pH 83
Figure 2.21: Rheological effect of controlled and uncontrolled clay dispersion .. 88
Figure 2.22 : Advanced sedimentation behaviour of controlled clay dispersion .. 89
Figure 2.23 : Rheological behavioural model for kimberlite thickened tailings ... 90
Figure 2.24 : Rheologial behavioural model in terms of mud bed compaction 91
Figure 2.25 : Co-disposed tailings rheology 96
Figure 3.1 : Co-disposal of tailings based on the P&TTD concept 107
Figure 4.1 : Vehicle particle size distribution 112
Figure 4.2 : Vehicle clay fraction mineralogy 113

Figure 4.3 : Load particle size distribution 114
Figure 4.4 : Levels of suspension pH 121
Figure 5.1 : Slump test 128
Figure 5.2 : Vane test 131
Figure 5.3 : Typical torque-time curve 131
Figure 5.4 : Inclined plane test 133
Figure 5.5 : Vane rheometer 135
Figure 5.6 : Small slump test equipment 137
Figure 5.7 : Large slump test equipment 137
Figure 6.1 : Influence of time of shear on vehicle rheology 140
Figure 6.2 : Influence of time of recovery on vehicle rheology 141
Figure 6.3 : Typical torque-time curve at standard rheometer settings 144
Figure 6.4 : Typical torque-time curve at most suitable rheometer settings 146
Figure 7.1 : Vehicle component yield stress 150
Figure 7.2 : Proposed effect of particle interaction 152
Figure 7.3 : Shape of typical vehicle component torque-time curves 154
Figure 7.4 : Radius of slumped material radial flow distance 155
Figure 7.5 : Relationship between slump height and radial flow distance 155
Figure 7.6 : Correlation between direct and indirect vehicle yield stress 157
Figure 7.7 : Vehicle component yield stress 160
Figure 7.8 : Correlation between direct and indirect vehicle yield stress 161
Figure 7.9 : Vehicle component yield stress 162
Figure 7.10 : Vehicle component yield stress 163
Figure 7.11 : Vehicle component yield stress 164
Figure 7.12 : Shape of torque-time curves for a non-interactive vehicle 165
Figure 7.13 : Vehicle component yield stress 165
Figure 7.14 : Correlation between direct and indirect vehicle yield stress 166
Figure 7.15 : Co-disposed tailings yield stress 169
Figure 7.16 : Co-disposed tailings yield stress 171
Figure 7.17 : Shape of typical co-disposed material torque-time curves 173
Figure 7.18 : Radius of slumped material radial flow distance 174
Figure 7.19 : Correlation between direct and indirect co-disposed yield stress .. 176

Figure A 1 : Flocculated slurry settling curve 205

Figure G 1 : Influence of shear time on vehicle rheology – raw data curves 221
Figure G 2 : Influence of recovery time on vehicle rheology – raw data curves 222

Figure H 1 : Vehicle yield stress - pH 8.6 (non-interactive) 224
Figure H 2 : Vehicle yield stress - pH 6.2 (interactive) 225
Figure H 3 : Vehicle yield stress - pH 11.5 (interactive) 226
Figure H 4 : Vehicle yield stress – pH 8.5 (interactive) 228
Figure H 5 : Vehicle yield stress – pH 8.7 (non-interactive) 229

Figure K 1 : Co-disposed tailings yield stress (pH 8.6, v : l = 86:14 %) 269
Figure K 2 : Co-disposed tailings yield stress (pH 8.6, v : l = 60:40 %) 270
Figure K 3 : Co-disposed tailings yield stress (pH 8.6, v : l = 50:50 %) 271
Figure K 4 : Co-disposed tailings yield stress (pH 6.2, v : l = 86:14%) 272
Figure K 5 : Co-disposed tailings yield stress (pH 6.2, v : l = 60:40 %) 273
Figure K 6 : Co-disposed tailings yield stress (pH 6.2, v : l = 50:50 %) 274
Figure K 7 : Co-disposed tailings yield stress (pH 11.5, v : l = 86:14 %) 275
Figure K 8 : Co-disposed tailings yield stress (pH 11.5, v : l = 60:40 %) 276
Figure K 9 : Co-disposed tailings yield stress (pH 11.5, v : l = 50:50 %) 277

LIST OF TABLES

Page

Table 3.1 : Parameters under consideration in this study 110
Table 4.1 : Batch preparation for slurry flocculation and settling..... 116
Table 4.2 : Levels of vehicle to load ratio..... 122
Table 4.3 : Levels of vehicle to load ratio (dry solids basis) 123
Table 5.1 : Vane characteristics..... 135
Table 5.2 : Slump container characteristics 136
Table 6.1 : Preliminary settings of vane rheometer..... 139
Table 6.2 : Most suitable vane rheometer settings 146
Table 7.1 : Exponential trend line information 151
Table 7.2 : Vehicle yield stress as a function of pH 153
Table 7.3 : Example of input parameter combinations 156
Table 7.4 : Relative error between direct and indirect vehicle yield stress 158
Table 7.5 : Exponential trend line information 160
Table 7.6 : Relative error between direct and indirect vehicle yield stress 162
Table 7.7 : Exponential trend line information 166
Table 7.8 : Relative error between direct and indirect vehicle yield stress 167
Table 7.9 : Example of input parameter combinations 172
Table 7.10 : Comparison of co-disposed material slump heights 175
Table 7.11 : Relative error between direct and indirect co-disposed yield stress 177

Table A 1 : Vehicle particle size distribution..... 203
Table A 2 : Vehicle clay fraction mineralogy 204
Table A 3 : Load particle size distribution..... 204
Table A 4 : Load specific gravity 204
Table A 5 : Load void ratio 204
Table A 6 : Optimum flocculant selection 205
Table A 7 : Flocculated slurry settling data 205

Table E 1 : Preparation of 5M solution of 33% HCl 215
Table E 2 : Preparation of NaOH and $Ca(OH)_2$ solution..... 216

Table G 1 : Influence of shear time on vehicle rheology – raw data..... 221
Table G 2 : Influence of recovery time on vehicle rheology – raw data 222

Table H 1 : Vehicle yield stress - pH 8.6 (non-interactive) 224
Table H 2 : Vehicle yield stress - pH 6.2 (interactive) 225
Table H 3 : Vehicle yield stress - pH 11.5 (interactive) 226
Table H 4 : Average radius of slumped material radial flow distance 227
Table H 5 : Vehicle yield stress – pH 8.5 (interactive)..... 228
Table H 6 : Vehicle yield stress – pH 8.7 (non-interactive)..... 229

Table K 1 : Co-disposed tailings yield stress (pH 8.6, v : l = 86:14 %) 269
Table K 2 : Co-disposed tailings yield stress (pH 8.6, v : l = 60:40 %) 270
Table K 3 : Co-disposed tailings yield stress (pH 8.6, v : l = 50:50 %) 271
Table K 4 : Co-disposed tailings yield stress (pH 6.2, v : l = 86:14 %) 272
Table K 5 : Co-disposed tailings yield stress (pH 6.2, v : l = 60:40 %) 273
Table K 6 : Co-disposed tailings yield stress (pH 6.2, v : l = 50:50 %) 274
Table K 7 : Co-disposed tailings yield stress (pH 11.5, v : l = 86:14 %) 275
Table K 8 : Co-disposed tailings yield stress (pH 11.5, v : l = 60:40 %) 276
Table K 9 : Co-disposed tailings yield stress (pH 11.5, v : l = 50:50 %) 277

1. INTRODUCTION

The first chapter serves as a general introduction to this study. In addition to background information, it provides a high level description of the identified knowledge gap and ultimate aim of this study.

1.1 Why Consider the Co-disposal of Tailings ?

The generation of large quantities of unwanted material, generally referred to as "tailings", is an inevitable part of the processes employed in the mining and mineral processing industries to extract and recover a valuable product. The lack of value normally associated with tailings results in an inability to sell it, leaving long term containment and storage as the only other option. The sheer volume of tailings that has to be dealt with on an annual basis necessitates operators to make use of tailings management practices that are economically viable. However, operators are also under increasing pressure from government regulatory bodies, local communities and environmental watchdog groups to manage their tailings in an environmentally responsible manner.

The following sections deal with the progression of tailings management and disposal practices in order to reduce financial, environmental and social risks.

1.1.1 Problems associated with conventional tailings disposal

Types of tailings

Mining and mineral processing operations produce a wide variety of tailings materials, which could roughly be classified into (1) waste rock, (2) coarse tailings and (3) fine tailings.

Waste rock is defined as barren rock, which naturally occurs within the same vicinity as the ore containing the valuable product. The waste rock is generally not

of value and therefore does not warrant treatment. It is normally removed before treatment where possible.

Coarse tailings generally refer to the crushed barren ore from which the valuable product was removed during treatment in a mineral processing plant. It typically comprises of the ore particles above the bottom cut-off size on the screen panels and below the crusher gap size. In some mineral processing operations, a coarse tailings fraction may be absent and only a fine tailings fraction is generated, depending on the nature of the valuable product extraction and recovery processes.

Fine tailings, a direct result of the wet mineral processing stage, can be described as a dilute slurry consisting of water (and process chemicals in some cases) and the very fine ore particles below the bottom cut-off size on the screen panels, e.g. 1 mm. Fine tailings are often also referred to as “slimes”.

Conventional tailings storage facilities

Waste rock and coarse tailings are conventionally stored in separate tailings dumps. The material is either trucked or conveyed to the respective tailings dump where it is dumped and allowed to come at rest at its natural angle of repose. Waste rock and coarse tailings dumps normally have steep side slopes and may be built up to substantial heights.

The conventional method of disposal related to the dilute fine tailings slurry involves limited thickening in large diameter conventional thickeners followed by centrifugal pumping of the low density thickener underflow product to a conventional tailings storage facility or “slimes dam”. Typically, segregation and subsequent hydraulic sorting of the high volume, low solids content fine tailings slurry take place upon deposition. As a result, the coarser (sand) fraction is deposited first close to the discharge point, while the finer (slimes) fraction is carried further along the beach and deposited progressively towards the centre pool. The hydraulic sorting effect generates a concave beach profile with the

highest point around the perimeter from where the fine tailing slurry is normally discharged and the lowest point at the centre pool where the excess water accumulates for recycle back to the mineral processing plant through a decantation system. In most cases, the coarser fraction of the fine tailings slurry itself is used in the perimeter wall construction.

Problems

The problems associated with waste rock and coarse tailings dumps are mainly slope failures of high storage facilities in steep terrain, surface water management to limit erosion and run-off, dust generation and acid generation (MMSD, 2002). Additional problems include land sterilisation and aesthetic unacceptability.

However, the problems associated with the conventional tailings storage facilities of the fine tailings slurry are of more interest and relevance to this study and will form the focus of this section.

High failure risk - The failure of conventional tailings storage facilities has severe consequences and is probably the most serious problem faced by all parties involved. A failure can generally be described as a breach in the perimeter wall with the subsequent release of tailings to the surrounding environment.

The International Commission on Large Dams (ICOLD) collected a total of 221 case records on failures of conventional tailings storage facilities over the period 1917 to 2000. The occurrence of major incidents was reported at an average of more than one per year. ICOLD concluded that the main causes for these failures were lack of control of the water balance and lack of control of construction. Of the cases reported, the majority of failures were due to overtopping, slope instability, seepage and erosion, which are all the result of a lack of control of the water balance within the facility (ICOLD, 2001).

According to ICOLD (2001) the failure of a conventional tailings storage facility has serious consequences for public safety, the environment and the owner or

operator of the facility. The following paragraphs discuss these consequences in more detail:

- Public safety – In the past, a number of failures resulted in the loss of human life. Fourie (2002a) lists some of the more disastrous failures over the period 1928 to 2001, which together have resulted in more than 1 100 fatalities. The safety of operating personnel and surrounding communities are at stake when large volumes of tailings flow uncontrolled from a breached facility, destroying everything in its path.

- Environment – The numerous environmental impacts of a failure include (1) pollution of surface water supplies when tailings (often containing contaminants) flow into nearby streams and rivers, (2) termination of natural fauna and flora, either by flooding with tailings or pollution of habitat and (3) destruction of buildings and or property (ICOLD, 2001; DNRE, 2002).

- Owner or operator – The impacts on the owner or operator can best be related to in economic terms and include (1) extended production interruption leading to loss in cash flow, (2) tailings storage facility reparation or replacement costs, (3) environmental clean-up costs and (4) compensation costs to affected parties. Legal responsibility and damage to the public image of the company might further affect the financial status of a company and in some cases even lead to bankruptcy (ICOLD, 2001; Russell, 2001; Rice and Davies, 2002).

Poor water recovery – In conventional tailings disposal, water is recovered from the fine tailings stream for re-use in the mineral processing plant in two places, i.e. the thickeners and the pool at the tailings storage facility. The large diameter conventional thickeners are not very efficient in terms of water recovery and are further limited by the centrifugal pumping system to produce only low density underflows. Water available for recovery from the tailings storage facility pool is again subjected to evaporation and seepage losses, especially in dry climates where low rainfall and high evaporation rates are common (Brzezinski, 2001).

High seepage gradients – Groundwater contamination through seepage is a direct result of the presence of the pool on a conventional tailings storage facility. The pool provides the hydrostatic head that drives the seepage of process and rainwater through the perimeter wall and base of the tailings storage facility. The problems associated with groundwater contamination are obviously increased if the tailings contain any toxins or have the potential to generate acid mine drainage (Robinsky, 1999; Brzezinski, 2001).

Erosion and dust – The outer surfaces of the steep perimeter walls of conventional tailings storage facilities tend to rill quite dramatically as a result of wind erosion in dry climates (or water erosion in wet climates). In areas with high erosion rates, large quantities of material can be removed from the perimeter wall slopes in a short period of time and lead to a "halo" of constantly moving unconsolidated tailings around the tailings storage facility (Jones, 2002).

The beaches of conventional tailings storage facilities consist of fine particles, which can be easily picked up by the wind, resulting in major dust problems. Depending on the prevailing wind direction and intensity, tailings material can be transported over several kilometres. Dust is a serious problem for nearby residents in terms of health issues and the impact on agricultural activities (Brzezinski, 2001; MMSD, 2002).

Poor rehabilitation potential – Rehabilitation of a conventional tailings storage facility can only start at the end of its operational life and then it could still be delayed for many years until consolidation of the tailings progressed to a point where traffic could be supported on the surface of the facility. Ruse (2003) noted that the delay in rehabilitation could create a long-term financial liability due to the fact that closure certification cannot be obtained, while on-going monitoring and maintenance of the facility have to take place.

Rehabilitation of a conventional tailings storage facility involves significant earthworks to create a long-term stable landform. In particular, the flat surfaces

and straight lines of the perimeter walls and surface of the facility need to be re-worked into a curved landform, which is aesthetically pleasing and fits in with the surrounding environment. The resultant slopes should be gentle enough to resist erosion and to sustain vegetation (Jones, 2002).

In many cases, the tailings storage facility is rehabilitated through the re-establishment of natural vegetation. However, due to the poor physical composition of the fine tailing slurry, vegetation establishment is hampered by the poor water storage capacity of the tailings due to low permeability and the mobilisation of fine particles by wind, causing sandblasting and burying of plants. In addition, the fine tailings are often devoid of plant nutrients and could contain contaminants, which are toxic to certain plants (Jones, 2002).

Public perceptions driving change

In today's world people are more aware of what is going on around them and how that could affect the quality of their lives. The preservation of a high quality life is a main priority for many people and as a result, people are more determined to eliminate threats to their health and surrounding environment. This attitude is fuelled by the perceptions that are created from what people see and hear in relation to potentially harmful activities. All of the problems discussed above contribute to an increasingly negative public perception of tailings disposal and the mining and mineral processing industries in general.

Fourie (2002b) pointed out how easily public perceptions are moulded in today's era of instant global communication. Information on environmental disasters related to tailings disposal is easily accessed by otherwise unaffected people. Fourie (2002b) further noted that the concerns (real or imagined) of the public could force governments to impose ever-stricter legislation and ultimately make mining unviable in some areas.

According to Regensburg and Tacey (2002), the stricter legislation results in permitting complexities and delays for new mining ventures as most regulatory

assessments include public consultation steps. The ability to obtain regulatory approval can be strongly influenced by public perceptions. This problem is often referred to as the "public licence to operate". It is therefore clear that operators have to win the acceptance of both the government and the community in regard to the manner in which they operate and dispose of their tailings. Regensburg and Tacey (2002) suggest that having an operation that poses no threat to public safety and the environment is a powerful tool in obtaining this acceptance. A further persuasive bonus would be to create a post-closure landscape that is safe and valuable for re-use.

It is evident that due to the enormous problems associated with it, conventional tailings management and disposal methods are no longer a viable option – not for governments, the public, the environment or the operator. As a result, the mining and mineral processing industries started to investigate alternative tailings disposal methods. The emerging technology of "Paste and Thickened Tailings Disposal" appears to be a potential solution.

1.1.2 Paste and Thickened Tailings Disposal – a solution ?

This section starts off with a high level description of the concept of Paste and Thickened Tailings Disposal (P&TTD), followed by a discussion of the benefits and challenges associated with this technology in an attempt to answer the question if P&TTD is the solution to conventional tailings disposal problems.

The concept of Paste and Thickened Tailings Disposal (P&TTD)

The concept of P&TTD was developed by Eli Robinsky in the 1970's (Robinsky, 1975). The first attempt to implement the method was made in 1973 at the Kidd Creek copper/zinc mine in Ontario, Canada. However, successful implementation was only achieved in 1995 after developments in thickening technology resulted in the availability of thickeners capable of producing high density underflows of paste-like consistency (Robinsky, 2002).

Robinsky (1999), sometimes called “the father of paste”, stated that the aim of a P&TTD system is to create a self-supporting ridge or hill of tailings to minimise the requirements of perimeter walls and at the same time to eliminate the need for a centre pool. To achieve this, the tailings consistency must be increased through dewatering.

The concept of P&TTD is best understood when viewed as a continuum. Figure 1.1 describes the thickened tailings continuum as presented by Jewell (2002). The curve represents a plot of a measure of strength (i.e. yield stress or shear stress) against a measure of concentration (i.e. solids concentration or density) for a tailings sample.

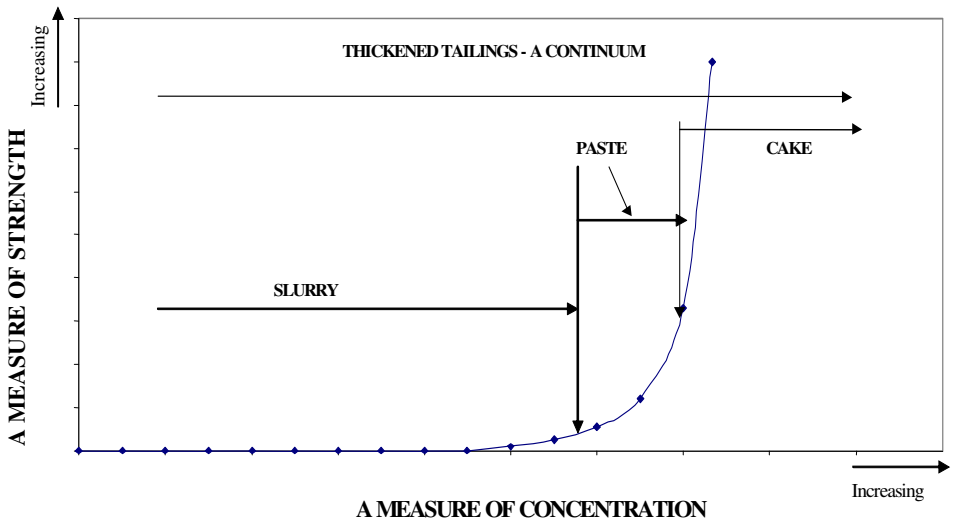

Figure 1.1 : The thickened tailings continuum
(Jewell, 2002)

The removal of water from the fine tailings slurry, in other words increasing the solids concentration, results in an exponential increase in the strength of the material. Within the thickened tailings continuum, terms such as “slurry”, “paste” and “cake” are frequently used to describe the consistency of a thickened tailings material. These terms provide an indication of the types of equipment required to produce and transport a specific material, as well as its behaviour upon deposition.

The respective boundaries between slurry, paste and cake are still somewhat subjective at this stage (Jewell, 2002).

The tailings consistency produced is directly related to the degree of dewatering and therefore also the type of dewatering equipment that was used. In an over simplification of this aspect, it could be said that a high density slurry is normally produced from high rate thickeners, a paste from deep cone thickeners and a cake from filter presses. Similarly, a slurry is normally transported by centrifugal pumps, a paste by centrifugal or positive displacement pumps (depending on the pumping distance) and a cake by conveyor (if it is not re-slurried to paste again).

Although various types of equipment are used to produce and transport material within the thickened tailings continuum, there is a common goal when it comes to deposition and that is to dispose of a material that is non-segregating, releases the minimum amount of bleed water upon deposition and has the ability to stack at a gentle slope. As a result of the thickened tailings consistency, no hydraulic sorting takes place upon deposition, which creates a planar beach profile. The necessity for perimeter walls is reduced or even eliminated, due to the fact that thickened tailings material is self-supporting and no containment as such is required. The high solids concentration of thickened tailings material results in minimum or no free water on the deposition site. In dry climates the material dries out quickly with extensive cracking visible within days. A centre pool where free water accumulates for recycle is therefore completely eliminated. Apart from rainfall run-off, no water is recovered from a thickened tailings disposal site (Robinsky, 1999; Bentel, 2002).

There are various deposition methods available for P&TTD, which include single or multiple point discharge onto a flat area to develop low conical hills around central riser pipes (often called central thickened discharge or CTD), in-pit disposal where old mined out pits are used as tailings storage areas, down-valley discharge where a valley is filled with thickened tailings, discharge from an existing embankment or side of a hill where the thickened tailings are allowed to

fan out over flatter ground and discharge into paddocks (Bentel, 2002). The choice of deposition method is however dependent on site specific and material specific factors.

Benefits

The potential of the P&TTD technology to address the problems that the mining and mineral processing industries are facing in relation to tailings disposal will become clear during the following discussion on the benefits of P&TTD.

Reduced failure risk – The failure risk of a P&TTD deposit is significantly reduced as a result of (1) the absence of a centre pool and (2) the increased strength of the material.

As discussed earlier, the most common causes of conventional tailings storage facility failures were all related to the storage of large quantities of water on top of unconsolidated tailings. Brzezinski (2001) noted that very few failure incidents were reported of inactive tailings storage facilities where ponded surface water was permanently removed. By definition, thickened tailings contain the minimum amount of water, which means that no water storage takes place on a properly operated P&TTD deposit. The most common failure modes are therefore greatly reduced or even eliminated (Regensburg and Tacey, 2002).

Robinsky (1999) pointed out that the unique features of the P&TTD system allow for very effective strengthening of the tailings material through dessication. It is desirable to deposit the thickened tailings in layers that would be allowed to reach the shrinkage limit upon consolidation and drying. This is made possible through the design of the position of the tailings discharge points and the manipulation of the discharge schedule. The result is a dense, self-supporting deposit at a gentle slope.

It is evident that due to the absence of stored water and increased strength of the material, P&TTD deposits are less mobile. Therefore, the likelihood of a failure is

reduced and even more important, the consequences associated with a failure is much less severe (Regensburg and Tacey, 2002). As a result, public safety is enhanced, environmental pollution is reduced or prevented and the operator is saved from much of the costs incurred around a failure.

Improved water conservation - The potential for significant water savings is one of the main advantages of the P&TTD technology, especially for operations situated in dry climatic areas such as Central and Western Australia, Southern Africa and Northern Chile, to name a few (Brzezinski, 2001).

The specific case of Southern Africa, as discussed by Dunn and Vietti (2003), is compounded with a foreseeable water scarcity crisis in certain parts of the area by as early as 2025, due to expected increases in population and climatic change based on studies carried out by the United Nations. The efficient recovery and re-use of water are therefore vital to reduce the fresh water intake from the environment. A water scarcity problem could have a severe impact on the development of new mining ventures, as well as the life of existing mines, to the extent that certain mining deposits could be regarded as too costly to develop further.

Dunn and Vietti (2003) also discussed the consequences of the implementation of the new National Water Act (No.36 of 1998) in South Africa. This Act recognises that water is a scarce and unevenly distributed natural resource, which belongs to all people and that the discriminatory practices and laws of the past prevented equal access to the use of water resources. Therefore, the Act provides for the regulation of water use through a system of water allocation to users, water licensing and water charges, which mean that it will not be a free or cheap resource any longer. Situations could arise in future where the probability of obtaining a mining license is reduced in areas where strict environmental legislation protects a stressed environment or where water resources have to be shared by numerous other non-mining functions.

It is evident that the conservation of water is a high priority and in some cases of strategic nature for many operations. Fourie (2002b) stated that the potential for recovering large volumes of water at the mineral processing plant instead of trying to collect and return water for re-use from a conventional tailings storage facility where evaporation and seepage losses are impossible to prevent, is seen as an extremely attractive feature of the P&TTD technology. The greater process water recycle rate reduces the supplement volume of fresh water required from the environment.

Regensburg and Tacey (2002) claim that the reduction in capital and operating costs associated with water savings could easily justify a P&TTD system in areas where water is particularly scarce or expensive. This is relevant at operations where production is frequently disrupted by water shortages or where operators have to purchase water or pump it from water resources at extreme distances from the operation.

Improved energy conservation – The conservation of energy through the adoption of P&TTD is possible at operations situated in cold climates or where mineral processing requires process water above the ambient temperature. Energy savings are realised when the process water is recovered directly at the mineral processing plant close to operating temperature, instead of being discharged to a conventional tailings storage facility where it will cool off in the centre pool before returning to the mineral processing plant (Robinsky, 1999; Regensburg and Tacey, 2002).

Improved reagent conservation – Some mineral processing operations need to recover process chemicals from tailings for economic and/or environmental reasons. Examples of these are cyanide in the gold industry and caustic soda in the alumina industry. Substantial savings in reagent costs and pollution of the environment can be prevented by recovery of process chemicals directly at the mineral processing plant through P&TTD, avoiding partial or complete loss of the reagents to the environment through conventional tailings disposal (Brzezinski, 2001; Regensburg and Tacey, 2002).

Reduced risk to groundwater contamination – Seepage losses and therefore the risk for groundwater contamination is significantly reduced by the elimination of the centre pool, which normally provides the hydrostatic head for seepage to occur. Seepage losses are further reduced by the fact that the initial amount of water within the thickened tailings is at a minimum (Fourie 2002b; Robinsky, 1999).

Increased storage capacity – As discussed earlier, in most cases conventional tailings disposal involves the discharge of tailings from the perimeter, resulting in a concave beach profile with a centre pool. This has to the effect that a large volume within the disposal area remains unoccupied by tailings. Robinsky (1999) pointed out that thickened tailings have sufficient strength to enable stacking of the material at a gentle slope. The fact that the material is self-supporting opens up opportunities to discharge the thickened tailings from the centre or from a natural elevated point in the area. P&TTD leads to the development of a planar or convex beach profile with the highest point at the discharge end and the lowest point at the perimeter. It is therefore obvious that regardless of the topography of the disposal site, it would be possible to store more tailings within a given area with the P&TTD system than with conventional tailings disposal. This feature, as illustrated by Robinsky (1999), is presented in Figure 1.2.

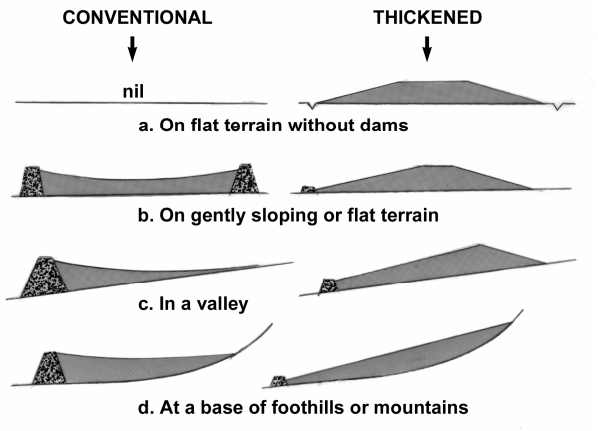

Figure 1.2 : Increased storage capacity of a P&TTD system (Robinsky, 1999)

Insignificant perimeter walls – A further benefit from the ability of thickened tailings to form a self-supporting stack is that the necessity for high perimeter walls is eliminated or reduced. A P&TTD deposit has its lowest point at the perimeter of the structure and therefore only requires a low perimeter wall (if any) at the toe of the deposit for the containment of precipitate run-off or to contain the extent of the deposit in steep topographical areas. Substantial cost savings could be realised through the reduced need for high specification engineered perimeter walls (Robinsky, 1999; Regensburg and Tacey, 2002).

Both Williams and Seddon (1999) and Brzezinski (2001) refer to the usefulness of "leaking" perimeter walls, which essentially refers to the construction of the perimeter walls out of pervious material. Precipitate run-off is allowed to leak through the perimeter wall and accumulate in a run-off pond outside the P&TTD deposit from where it could be returned to the mineral processing plant for re-use. It is therefore clear that the perimeter walls need not to be designed as watertight structures as required by conventional tailings disposal.

Flexibility in terms of site selection – The P&TTD system could be accommodated at almost any topography (i.e. flat terrain, valleys, hills, etc.) due to its inherent ability to form self-supporting landforms.

The P&TTD system also results in a reduction of tailings volumes to be pumped to the deposition site due to the extensive dewatering of the fine tailings slurry at the mineral processing plant. The reduced pumping volumes lead to smaller discharge pipelines and potential savings on pipeline and installation costs.

The fact that the discharged thickened tailings contain the minimum amount of water has the effect, particularly in dry climates, that no water is returned from the P&TTD deposit. In wet climates only precipitate run-off is returned for re-use at the mineral processing plant. The need for return water facilities is therefore reduced or even eliminated, which further results in cost savings.

It is evident that there is considerable flexibility in choosing a deposition site when it comes to P&TTD. The benefits are not only seen in the variety of adequate topographies, but also in the possibility of considering sites that are further away from the mineral processing plant, made possible through a reduction in pumping volumes and the elimination of return water facilities (Robinsky, 1999).

Rapid drainage – Rapid drainage is one of the advantages of the sloped surface of a P&TTD deposit, during both active disposal and post-closure. Free water on a P&TTD site is minimal – if any bleed water is released it evaporates quickly leaving the deposit dry and close to its shrinkage limit. In the event of precipitation, the sloping deposit provides rapid run-off, which prevents infiltration. This latter aspect is often referred to as the deposit having a "self shedding" nature (Robinsky, 1999; Brzezinski, 2001; Bentel, 2002).

Reduced erosion – The rate of erosion of a slope is dependent on the slope angle, the slope length and the shear strength of the surface material. P&TTD deposits are normally designed to have gentle, flat slopes in order to minimise erosion. However, in some cases the flatter slopes could be very long, resulting in little overall benefit in terms of erosion resistance. The increased shear strength of thickened tailings material adds to the erosion resistance of a P&TTD deposit in the sense that higher erosion forces are required to remove surface particles from the stable deposit (Jones, 2002; Fourie, 2002c).

Improved rehabilitation potential – Improved rehabilitation potential of a P&TTD site includes aspects such as progressive rehabilitation, accelerated rehabilitation, reduced rehabilitation and closure costs and reduced post-closure liability.

In the first place, the rehabilitation potential of a P&TTD site is improved through the formation of gentle slopes, which sufficiently reduce erosion and provide good drainage to sustain vegetation (Robinsky, 1999).

Robinsky (1999) suggested the use of progressive rehabilitation in conjunction with P&TTD. Progressive rehabilitation involves the closure and rehabilitation of one end of the P&TTD deposit as the discharge end is progressively moved in the opposite direction. The result is a smaller active disposal area, which is an attractive feature when it comes to regulatory approval of operational methods. Progressive rehabilitation is largely dependent on the type of deposition method employed and the topography of the deposition site and is not always possible in all implementations of P&TTD.

The rapid consolidation and drying of thickened tailings material allow for accelerated rehabilitation, which essentially refers to the early accessibility of traffic on the P&TTD surface shortly after deposition ended (Bentel, 2002; Jones, 2002). Brzezinski (2001) also recommended the inclusion of soil treatments, fertiliser and plant seeds with the last layer of thickened tailings in order to accelerate vegetation establishment.

P&TTD has the potential to reduce the costs associated with rehabilitation and closure. In the first place, minimal (if any) earthworks are required to change the P&TTD deposit into a long-term stable landform (Jones, 2002). Where the site topography and deposition method permit, P&TTD could result in a smaller footprint area, which means that the subsequent rehabilitation costs could be less.

Regensburg and Tacey (2002) stated that the P&TTD technology has the potential for improved long-term predictability of the deposit performance. This enables the early development of rehabilitation and closure plans with an increased level of confidence, facilitating accurate financial provision for closure.

The benefits associated with the rehabilitation of a P&TTD site culminates in the significant reduction of post-closure liability for the operator and the realisation of savings in terms of insurance costs (Regensburg and Tacey, 2002).

Aesthetically acceptable – Thickened tailings offer significant landscaping opportunities. It is possible with a P&TTD system to build a specific landform through the proper design of the initial deposition system. As a result, P&TTD deposits are designed to fit in with the natural surrounding topography and are therefore much more aesthetically acceptable than conventional tailings storage facilities (Jones, 2002).

Reduced regulatory risk – Regulatory risk is defined by Regensburg and Tacey (2002) as the risk associated with the duration and uncertainty of obtaining permits or other regulatory approval for new mining operations. The potential environmental impacts of a mining operation and therefore also its tailings management and disposal strategies, are under intense scrutiny during the permitting phase. Hayley (2000) suggested that the use of inherently risky tailings disposal methods in today's world would lead to considerable permitting and project start-up delays. The cost of a delay in project start-up and therefore production as a result of regulatory approval problems could have a significant financial impact on the operator.

The P&TTD technology offers several benefits related to the reduction of risk, both during active operation and post-closure (as discussed in the preceding paragraphs), which could lead to shorter timelines and increased certainty in the achievement of regulatory approval.

As mentioned before, most regulatory approval processes include a public consultation stage. As a result, the ability to obtain regulatory approval can be strongly influenced by public perception. It would be fair to expect that in future, approval for new mining ventures would not be provided by governments or regulatory bodies, but by the affected local people. Regensburg and Tacey (2002) suggested that the general public would perceive P&TTD deposits as "safe" and "not environmentally risky" in comparison with conventional tailings storage facilities. Positive public perceptions reduce the likelihood of the public submitting numerous and complex complaints to the regulatory body, of which

the investigation and assessment slow down the regulatory approval process (Hayley, 2000; Regensburg and Tacey, 2002).

Challenges

Apart from the numerous benefits that could be realised from the implementation of the P&TTD technology, it is important to be aware also of the challenges and problems related to it. The following section highlights some of the main challenges associated with P&TTD.

Costs – There is a perception that implementation of the P&TTD technology is associated with high cost. This perception is mainly due to the fact that operators are blinded by the high capital costs associated with certain process equipment such as high rate and deep cone thickeners, filters, positive displacement pumps, high pressure pipelines and fittings, etc. The cost of these pieces of equipment could amount to millions of rands, however the various cost savings related to the benefits of the P&TTD system as discussed in the previous section, could offer a partial off-set (Regensburg and Tacey, 2002).

Even more important is the economic evaluation of a P&TTD system based on "full life-cycle costs", as described by Regensburg and Tacey (2002). Capital costs, operating costs, timing and the time value of money need to be assessed across the entire life of the mine from inception to closure. It is often necessary to run the mine and tailings disposal plans to the point of final closure to fully understand the benefits of the P&TTD technology. Social and environmental benefits might be difficult to quantify, but could hold significant value and should therefore not be excluded from evaluations. Regensburg and Tacey (2002) stated that a definite *reduction* in costs and financial risk could be realised from P&TTD if it is based on full life-cycle costs.

It is however, a challenge to change the perceptions of many operators in this regard.

Process control – Conventional tailings storage facilities have the ability to tolerate and accommodate significant variations in the fine tailings slurry properties. Therefore not much effort is made to exercise control over key slurry properties. This is however, not the case with the P&TTD technology where fluctuations in the thickened tailings consistency could seriously compromise the integrity of the P&TTD deposit. According to Fourie (2002b) the success or failure of a P&TTD system rest on the initial preparation and transport of the thickened tailings material to the deposition site.

Regensburg and Tacey (2002) stated that a high level of process control is required to manage the properties of the thickened tailings material within the desired limits, between the source of the tailings stream and the deposition site.

Fourie (2002b) referred to an important shift that is taking place in the P&TTD field and that is not the question if thickened tailings can be produced, but if it can be produced consistently. The latter remains a significant challenge for the industry.

Footprint – Although a P&TTD deposit offers increased storage capacity as discussed in the previous section, the large footprint associated with some of the deposition methods is a challenge to many operators.

Williams and Seddon (1999) stated that the central thickened discharge (CTD) method, which typically forms a low conical hill with flat slopes, requires a large area, often two to three times the area required for conventional impounded tailings disposal of equivalent tonnage. This is of course dependent on the natural beach slope of the thickened tailings material and the degree of perimeter bunding that is employed (Bentel, 2002). Examples of large footprint CTD systems include the Mt Keith nickel mine in Western Australia with a diameter of 5 km and a perimeter of 17 km (Jewell, 2000) and the Peak gold mine in New South Wales, Australia with a footprint area of around 100 ha in December 2000 (Williams, 2002).

In some cases, as the two just mentioned, the large footprint area seems not to be of great concern, but as mentioned by Fourie (2002b), most operators do not have large areas of land available and are under increasing pressure from regulatory bodies to reduce the footprint of their tailings storage facilities.

The larger footprint area further has negative impacts on land sterilisation and therefore the rehabilitation costs of such a facility (Bentel, 2002; Jones, 2002). In addition to that, the large footprint area of a CTD system acts as a large surface catchment area, which means that the management of precipitation run-off and erosion could be more complex and even problematic (Jones, 2002).

Brzezinski (2001) attempted to address the footprint challenge at Auginish Alumina in Ireland through the staged construction of bunds on top of the P&TTD deposit in order to increase the beach slope above the natural angle of repose of the thickened tailings material and so occupy a smaller land area.

Dust – Dust generation could occur sooner after deposition in the case of P&TTD due to the fact that drying of the thickened tailings material is accelerated by the relative lack of water in the tailings. The thickened tailings material reaches its shrinkage limit in a relatively short time, which means that in many cases, despite the increased shear strength of the material and supposedly higher resistance to erosion, dust generation could occur sooner and more extensively than would be expected (Regensburg and Tacey, 2002).

Conclusion

At the start of Section 1.1.2, the question was raised if P&TTD could be the solution to conventional tailings disposal problems. From the above discussions, it is concluded that the P&TTD technology certainly presents an exceptional ability to address the common problems associated with conventional tailings disposal. The benefits far outweigh the limitations and it is believed that the few existing challenges will be put to rest as the technology is more widely implemented.

However, several workers in this field (Fourie, 2002b; Jewell, 2003) pointed out that P&TTD is not a universal solution to all the problems that will ever be encountered in tailings disposal and should not be viewed as such. The implementation of P&TTD still brings about costs and difficulties, mainly due to a lack of understanding of the entire system and site or material specific problems. These problems could be enough justification in some cases, to reject the technology. It is therefore of the utmost importance to evaluate each project based on its own requirements and then only to make a decision if P&TTD is the most appropriate option.

1.1.3 The added benefits of co-disposal of tailings

Taking the P&TTD concept one step further to incorporate one or more other tailings streams could present several added benefits towards minimising the environmental and social impact of tailings management and disposal practices. This section provides a high level description of the concept of co-disposal of tailings, followed by a discussion of the added benefits.

The concept of co-disposal of tailings

The co-disposal of tailings, in the most general sense, can be described as the combined disposal of two or more of the tailings streams discussed in Section 1.1.1 (i.e. fine tailings, coarse tailings and waste rock). However, the concept is interpreted in many different ways throughout the mining and mineral processing industries, resulting in a wide variety of co-disposal methods. These will be discussed in more detail in Section 2.1 as part of the review of previous work.

The co-disposal of tailings based on the P&TTD concept is the main focus of this study. By implication all the P&TTD principles apply, which means that this type of co-disposal essentially refers to the pre-existence of a thickened tailings material, which is combined with coarse tailings or waste rock material for disposal. Co-disposal is achieved through either combined or separate transport of the various tailings types to the deposition site. In other words, the various tailings

materials are blended before deposition and transported as a combined product to the deposition site or it is transported separately and only blended upon deposition. In any event, the final co-disposed tailings material typically consists of coarse particles in loose contact, with the voids between them filled with thickened tailings material (MMSD, 2002).

Added benefits

Why consider the co-disposal of tailings? Close to all of the problems related to conventional tailings disposal are already addressed through the P&TTD technology. What further benefits could be realised through the incorporation of one or more tailings streams? Certainly not further water savings. The latter is only recognised in the enhanced dewatering associated with the production of thickened tailings.

This section discusses the added benefits of co-disposal of tailings based on the P&TTD concept and attempts to answer the question why this option should even be considered by operators.

One tailings disposal site – The co-disposal of tailings implies that various tailings streams are stored together in the same area. This leads to a reduction in the number of tailings storage facilities requiring monitoring, rehabilitation and closure.

Implementation of the co-disposal of tailings based on the P&TTD concept eliminates both the problematic conventional tailings storage facility and the unsightly coarse tailings (or waste rock) dump. They are replaced by one tailings storage facility called the "co-disposed tailings dump", which is more aesthetically pleasing and easier to rehabilitate than each of the separately disposed tailings storage facilities.

The fact that the operator is concerned with only one tailings storage facility simplifies rehabilitation and closure planning and opens up possibilities for cost savings and accelerated regulatory approval.

Improved drainage and strength gain – Co-disposed tailings are normally better graded than the separately disposed tailings streams, resulting in several benefits. The wider particle size distribution leads to a reasonably high permeability that permits rapid drainage and therefore increases the rate of consolidation and strength gain of the material (MMSD, 2002; DNRE, 2002).

Improved rehabilitation potential – According to Van Rensburg and Maboeta (2003) coarse tailings (or waste rock) dumps are generally devoid of organic matter, deficient in nutrients, without structure and have low water-holding capacity. These problems limit the rehabilitation of coarse tailings dumps through re-vegetation, especially in dry climates.

Fine tailings have similar problems in terms of organic matter and nutrient deficiencies, but could present better water-holding capacity due to the presence of clay materials. However, water infiltration is often limited due to poor structural characteristics. Narrow graded fine tailings at high bulk densities present a deep and highly compacted profile resistant to plant root penetration and development (Van Rensburg and Maboeta, 2003; Jones, 2002).

The particle size distribution of co-disposed tailings closely represents normal soil conditions, which means that it would be more amenable to rehabilitation through vegetation than the separately disposed tailings. As mentioned before, the wider particle size distribution leads to a reasonable permeability (less than coarse tailings or waste rock, but greater than fine tailings), which means that a middle ground could possibly be obtained in terms of water-holding capacity, aeration, nutrient distribution and resistance to plant root penetration, thereby accelerating rehabilitation (MMSD, 2002; Jones, 2002, Van Rensburg and Maboeta, 2003).

Acid mine drainage (AMD) control – Acid mine drainage (AMD), sometimes also referred to as acid rock drainage (ARD), refers to the breakdown of sulphide minerals in the presence of atmospheric oxygen and water to produce sulphuric acid. The sulphuric acid has the ability to leach out various heavy metal components from the tailings material. Drainage water or seepage containing sulphuric acid and heavy metals could be extremely harmful to the environment (MMSD, 2002).

Waste rock dumps in particular (and also some coarse tailings types) are prone to AMD generation, because the high void ratio of the material allows for air and water to enter the coarse particle network. Co-disposal of waste rock with thickened tailings could contribute significantly to prevent and control AMD. The thickened tailings material would (1) coat the coarse particles, thereby limiting the exposed surfaces for oxidation and (2) fill the voids between coarse particles, thereby limiting the infiltration of air and water. As a result, the rate of sulphide oxidation would be reduced and AMD generation controlled (MMSD, 2002).

Tailings "design" opportunities – When the various types of tailings are separately disposed, the resultant tailings storage facilities exhibit the inherent characteristics of each tailings type. However, with the co-disposal of two or more tailings streams the opportunity arises to "design" a combined tailings product with modified and more desirable characteristics than those of each of the separate tailings materials (MMSD, 2002). This is a very powerful ability and probably the most significant benefit of co-disposal.

The concept of manipulating tailings properties to suit the environment, rather than trying to manipulate the environment to accommodate the tailings, was first brought up by Boger (2002) in association with the P&TTD technology. This concept further progressed into the development of a reversed design approach for P&TTD systems where the design sequence starts at the deposition site and works upstream to the thickening stage. This design approach includes the consideration of the rheological properties of the thickened tailings material at each design step

and the development of methods to manipulate the rheology of the thickened tailings in order to produce the desired deposition characteristics (Boger, 2002).

Although the concept of designing tailings properties is not new, the co-disposal of tailings just offers so much more in this regard than general P&TTD. Not only is it possible to manipulate the rheological properties of the thickened tailings (one of the constituents of the co-disposed material) as suggested by Boger (2002), but the manipulation of the mixing ratio of thickened tailings to coarse tailings (or waste rock) could produce a wide range of different tailings flow properties. The improved ability to design the properties of co-disposed tailings opens up more opportunities for the application of co-disposal as it could be the answer to tailings disposal problems where other methods failed to present a workable solution.

Conclusion

The above discussion made it clear that there are definite advantages in taking the P&TTD system one step further to include one or more other tailings streams for disposal. Most of the benefits of general P&TTD, as discussed in Section 1.1.2, still apply, but there is a significant enhancement of these benefits through co-disposal.

Most of the added benefits of co-disposal are having an impact on long-term issues such as rehabilitation and closure. These benefits are difficult to quantify, but that should not be an excuse for exclusion. It is often these long-term issues that offer the most scope for cost savings.

The single most important benefit of the co-disposal of tailings based on the P&TTD concept is the ability to "design" the co-disposed tailings properties. The flexibility provided to operators in terms of what they need to produce and how they need to store it without affecting the natural environment is obvious and should be a serious consideration for adopting the technology.

1.2 Identified Knowledge Gap

The previous section dealt with the question of why the co-disposal of tailings should be considered by the mining and mineral processing industries. In an attempt to answer this question, quite a number of benefits were pointed out that could be realised through the adoption of the co-disposal technique. However, in spite of the obvious benefits related to the co-disposal of tailings, there are very few operations who have actually implemented the technology. The main reasons are related to (1) operators wanting to re-treat one of the tailings streams in the future and (2) lack of knowledge in terms of the behaviour of co-disposed tailings material.

Operators are often resistant to the co-disposal of tailings due to the fact that developments in mineral processing technologies could facilitate the re-treatment of coarse tailings in the future. It is therefore more acceptable to operators to store tailings separately for easier re-treatment. The economic viability of such a decision requires careful consideration as cost savings related to rehabilitation, closure and regulatory approval of a co-disposed tailings facility could be far more than the financial benefits related to the recovery of a small amount of valuable product from low grade tailings.

The lack of knowledge in terms of the transport and deposition behaviour of co-disposed tailings is a more complex problem. Very few operators have a full understanding of their tailings properties and how it could be manipulated to produce specific behaviour. Without a fundamental understanding of the parameters and the extent of their influence, that affect the rheology of a co-disposed tailings material it would be impossible to carry out the successful design, construction and operation of such a facility.

It is this knowledge gap that is addressed through this study for the specific case of co-disposed kimberlite tailings. The overall aim of this study is to gain a better understanding of the relationship between the key tailings material characteristics

and the flow behaviour of co-disposed kimberlite tailings upon deposition. It is believed that improved insight of this relationship will enable the design of a co-disposed tailings material with the desired characteristics to successfully minimise financial, environmental and social risks.

2. REVIEW OF PREVIOUS WORK

A review of previous work is presented in this chapter in order to provide detailed background to the problem addressed in this study and to establish the current status of the identified knowledge gap.

Previous work was reviewed through a literature survey. The main focus of the literature survey was to find information related to the manipulation of co-disposed tailings rheology. This focus was extended to include the manipulation of thickened tailings rheology for the reason that thickened tailings form a major part of the specific type of co-disposed tailings considered in this study. The section on thickened tailings rheology is also further divided into general thickened tailings and kimberlite thickened tailings. These sections are preceded by a general introduction to rheology in order to explain various concepts and terms that would be used later on.

However, since the co-disposal of tailings is not yet widely implemented, it was thought necessary to also present the different methods of co-disposal of tailings that were encountered during the literature survey, for interest sake.

2.1 Different Methods of Co-disposal of Tailings

The review of previous investigations and implementations of the co-disposal of tailings showed that most co-disposal methods fitted one of the following general descriptions:

- Fine tailings blended with coarse tailings or waste rock prior to deposition, which implies the transport of a combined tailings product to the deposition area.

- Fine tailings blended with coarse tailings or waste rock upon deposition, which implies the separate transport of various tailings materials to the deposition area. This is also referred to as simultaneous deposition.

- Fine tailings placed as discreet deposits within already placed coarse tailings or waste rock.

- Fine tailings and coarse tailings and/or waste rock placed in a paddock type arrangement.

However, in order to provide a better understanding of the differences between the various co-disposal methods, it was found easier to classify the various co-disposal methods according to the combination of tailings involved, i.e. fine tailings, coarse tailings or waste rock.

It was found that the state of the fine tailings had a significant impact on the characteristics of the co-disposed material and final co-disposed dump. Therefore, in some cases it was deemed necessary to further subdivide the various co-disposal methods based on the state of the fine tailings, i.e. conventional slurry, thickened tailings or filter cake.

2.1.1 Fine tailings + coarse tailings

Conventional fine tailings slurry + coarse tailings

Applications of this type of co-disposal of tailings were found at coal, mineral sands and oil sands operations. The implication here is that the fine tailings slurry underwent limited or no thickening before co-disposal with the coarse tailings. The resultant co-disposed tailings material was often prone to segregation and the release of large amounts of free water upon deposition.

Coal - Williams and Kuganathan (1992) first discussed the co-disposal of conventional fine coal tailings with coarse coal tailings (reject) at the Jeebropilly

Mine in Queensland, Australia. The fine tailings slurry, of which the solids consisted of 70% silt and clay sized particles, was subjected to conventional thickening before it was combined with the coarse tailings, ranging in particle size between 1 mm and 100 mm, in a mixing hopper. The combined tailings was pumped at a total solids concentration of about 30% by mass over a distance of close to 1 km using a centrifugal pump to old open cuts for disposal. The ratio of coarse tailings to fine tailings was in the order of 86:14. Upon deposition the co-disposed tailings material underwent hydraulic sorting according to particle size and specific gravity. Segregation of the co-disposed tailings upon deposition was seen as a limiting factor in the realisation of the full benefits of the co-disposal concept, however increasing the solids concentration in order to counteract segregation was not seen as a solution at the time due to a fear of pipeline blockages (Williams and Kuganathan, 1992; Morris and Williams, 1997; Morris and Williams, 1999).

Mineral sands - Jewell (2000) described field trials undertaken at the Iluka Yoganup North mineral sands operation in Western Australia to investigate two different methods of co-disposal of "slimes" and "sand" fractions – (1) blending of the un-thickened slimes and sand fractions upon deposition (simultaneous deposition) and (2) mixing of the un-thickened slimes and sand fractions in a trommel screen before deposition of the combined product. Several problems were encountered in terms of finding the right mixing ratio between the slimes and sand fractions in order to dispose of a significant amount of slimes and still produce a stable end product. After considerable geotechnical test work this ratio was found to be in the order of 3:1 sand to slimes by mass. A major challenge was to retain a certain amount of flexibility to handle the variations in the proportions of sand to slimes, which occurred naturally within the ore body, through co-disposal (Jewell, 2000).

Oil sands - Lord (2002) discussed the development and implementation of "Composite Tailings" disposal at the Syncrude oil sands operations in Alberta, Canada. Oil sands are composed of bitumen, sand, silt, clay and water. The

bitumen extraction processes at Syncrude produced two tailings products – a coarse tailings (sand), which consisted of 95% quartz at a d_{50} of 150 μm and a fine tailings (silt and clay), which consisted of 39% kaolin, 12% illite and 45% quartz with a d_{50} of 2 μm. Co-disposal of the coarse and fine tailings involved the production of a combined product called "Composite Tailings" prior to deposition. Coarse tailings from the bitumen extraction plant was dewatered and densified by hydrocyclones before it was added to the fine tailings (also known as Mature Fine Tailings) from the settling ponds of conventional tailings storage facilities. Gypsum was added to coagulate the fine tailings and change the slurry viscosity in order to produce a non-segregating final product. The homogeneous Composite Tailings material was deposited in mined out pit areas where rapid drainage occurred to create a deposit with the geotechnical character of loose sand (Lord, 2002).

Fine thickened tailings + coarse tailings

Applications of the co-disposal of fine and coarse tailings based on the P&TTD concept were found at mineral sands, oil sands and diamond-bearing kimberlite operations. In this case the fine tailings slurry was thickened to a paste consistency before it was co-disposed with the coarse tailings. In most cases, the resultant co-disposed material had similar characteristics to thickened tailings.

Mineral sands - Hutcheson (2001) described field trials involving the co-disposal of fine and coarse tailings in the form of thickened tailings and sand, at the Jangardup Mine of the Cable Sands mineral sands operation in Western Australia. Two different methods were investigated for the sub-aqueous co-disposal of fine thickened tailings and sand on a field trial basis. The first set of tests involved the evaluation of the two co-disposal methods in an 8 m long by 1 m square viewing tank filled with water. The fine tailings slurry (d_{50} of 3.6 μm) was withdrawn from the dredging pond at 5% solids and then thickened to 25-30% solids by mass. The coarse tailings sand from the dredging operation was dewatered by a cyclone and a screen to 85% solids by mass. The first method of co-disposal involved the mixing of the thickener underflow and dewatered sand in a mixing hopper from

where the combined product was pumped and discharged underwater in the viewing tank. The second method can be described as simultaneous deposition of the two tailings products. The thickened underflow was separately fed towards the base of the viewing tank through a pipe ending in a T-piece, while at the same time the sand was deposited from a sand distribution system at the top of the viewing tank. In both cases, the total solids concentration targeted for discharge into the viewing tank was in the region of 65-73% solids by mass and the sand to fines ratio which resulted in non-segregating behaviour was in the range of 10:1 down to 5:1 (Hutcheson, 2001).

The second method, described as simultaneous discharge, proved to be the preferred method as it resulted in a robust matrix of "blobs" of thickened fines surrounded by sand. Further test work confirmed the success of the method and led to the implementation of the simultaneous discharge of fine thickened tailings and sand into the mined out area behind the dredge in the operational dredge pond at Jangardup Mine (Hutcheson, 2001).

Oil sands - As a result of the increasing interest in P&TTD, the oil sands industry also started to investigate the use of thickened tailings in their Composite Tailings concept. Lord (2001) discussed research conducted on the co-disposal of fine thickened tailings and coarse tailings as Composite Tailings at Syncrude in Alberta, Canada.

The envisaged co-disposal strategy involved the production of thickened tailings from two potential fine tailings streams, i.e. the fine tailings slurry from the bitumen extraction plant with a fines content (the minus 22 μm fraction) of 50% and the run-off from the hydraulically placed coarse tailings with a fines content of 90%. The fine thickened tailings would then be disposed of as discrete deposits within the previously placed coarse tailings (sand) deposits. The original Composite Tailings disposal method involved the mixing of the two tailings streams before deposition, while this new adaptation of the method to include

thickened tailings is best described as the placement of fine tailings into previously placed coarse tailings (Lord, 2001).

Kimberlite - The specific process of the co-disposal of kimberlite tailings streams based on the principles of P&TTD, as developed by De Beers Consolidated Mines was described by Vietti (2003a). A typical diamond mine mineral processing plant produces the following three processed kimberlite products (tailings streams) characterised by their particle size ranges (Vietti, 2003a):

- Slimes slurry (-0.3 mm)
- Grits (-1.5+0.3 mm)
- Coarse tailings (-8+1.5 mm)

The De Beers vision for the co-disposal of tailings involves the combined disposal of all three of the above tailings streams through the co-thickening of the slimes and grits streams to a high density thickened tailings material of paste consistency, before it is combined with the barren coarse tailings prior to or at deposition in order to generate a single tailings storage facility (Vietti, 2003a; Dunn and Vietti, 2003).

Helfer (2001a, 2001b) and Dunn et al (2001) discussed the successful pilot scale implementation of the co-disposal of kimberlite tailings streams based on the combination of the tailings before deposition at De Beers' Finsch Mine in South Africa during 2001. The fine tailings slurry consisting of both slimes and grits fractions (all the minus 1.5 mm material), was thickened to about 60% solids by mass. The co-thickened tailings was pumped with a positive displacement pump to a mixing hopper where it was introduced to dry coarse tailings (-6+1.5 mm). The mixing ratio of co-thickened tailings to coarse tailings, based on mass percentage, was 60:40. The combined tailings product was pumped with a concrete pump to large scale trenches (flumes) for further geotechnical and rehabilitation test work.

Although the combination of the tailings products before deposition was successful on a pilot scale, the large scale implementation of this co-disposal method was seen as having significant technical risk at the time due to a lack of confidence in mixing and transportation equipment and a lack of understanding in terms of co-disposed tailings material rheology. De Beers therefore opted to start with the implementation of large scale co-disposal on the basis of simultaneous deposition, while the risks associated with the previous method are addressed.

Vietti (2002) discussed the implementation of co-disposal of kimberlite tailings through simultaneous deposition at two De Beers operations, namely the Daberas mobile plant on the banks of the Orange River in South Africa and the Williamsons Mine in Tanzania. At the Daberas mobile plant the slimes and grits fractions are co-thickened to a thickened tailings product, which is then centrifugally pumped to the deposition area. The underflow pipeline follows the coarse tailings conveyer to the deposition area where the two tailings streams are blended by simultaneous deposition.

At Williamsons Mine in Tanzania, the coarse tailings dumps are re-treated by contractors making use of old pan technology. The coarse tailings from the re-treatment operations are conveyed to a coarse tailings dump. The tailings stream from the pans, also known as “puddle”, closely resembles thickened tailings material and is pumped to the base of the coarse tailings dump. As a result, a layering effect of thickened tailings and coarse tailings is created, which causes the dump to slump from time to time, allowing the two tailings streams to blend even more and flow under gravity over a wider area (Vietti, 2002).

The Combined Treatment Plant in Kimberley, South Africa can be described as De Beers’ flagship operation in terms of the implementation of P&TTD technology. Currently the slimes and grits fractions are co-thickened to a paste consistency, after which the underflow is pumped via positive displacement pumps over a distance of about 5.5 km to a central thickened discharge deposition area. The coarse tailings are currently conveyed to a coarse tailings dump. The

separate disposal of the two tailings streams will continue to carry on in this manner for close to another 10 years. However, after this initial period of 10 years, which is required to complete mining activities in a nearby pit, the two tailings streams will be co-disposed in the mined out pit. It is planned to pump the co-thickened tailings and convey the coarse tailings both to the edge of the mined out pit where blending will take place upon simultaneous deposition (Dunn and Vietti, 2003; Johnson and Vietti, 2003).

Fines filter cake + coarse tailings

Applications of the co-disposal of the fine tailings as a filter cake with the coarse tailings were found in coal and copper operations. In this case, the fine tailings slurry is dewatered by a filter or thickener/filter combination to produce a cake prior to co-disposal with the coarse tailings. In most cases, the resultant co-disposed tailings deposit takes the form of a stable dump, similar to a coarse tailings dump.

<u>*Coal*</u> - Lord (2003) described the co-disposal operation of fines filter cake and coarse tailings, at the Luscar Line Creek coal mine in British Columbia, Canada. The fine tailings slurry, consisting of fine coal and clay, all minus 150 μm in particle size, is thickened to a density of about 30-36% solids by mass. The thickener underflow is then dewatered further into a cake by continuous belt filters. The fines filter cake is conveyed to a mixing hopper where it is introduced to the coarse coal tailings (reject) from the thermal and metallurgical plants. The coarse tailings, consisting of 50-64 mm lumps, are also dewatered by centrifuge to about 8% moisture content before arriving at the mixing hopper. The combined material is trucked from the mixing hopper to the disposal area where it is off-loaded and pushed over the crest of the dump. The co-disposed tailings dump is currently up to 40 m high with a slope angle of about 45 degrees, similar to a typical coarse tailings dump (Lord, 2003).

<u>*Copper*</u> - The co-disposal of fines filter cake and coarse tailings was also observed by the author during a technical visit in 2003 to the Anglo American Mantos

Blancos copper mine north of Antofagasta in Chile. The coarse tailings of the oxide plant are used to build the walls of a paddock type containment into which the fine tailings of the sulphide plant are deposited as a filter cake. The two tailings streams are not mixed prior to or at deposition, but could still be regarded as co-disposal due to the fact that only one site is occupied. The fine tailings slurry is conventionally thickened to about 60% solids by mass, after which the underflow is further dewatered by continuous band filters to about 80% solids by mass. The fines filter cake is then conveyed to the combined deposition area, as shown in Figure 2.1.

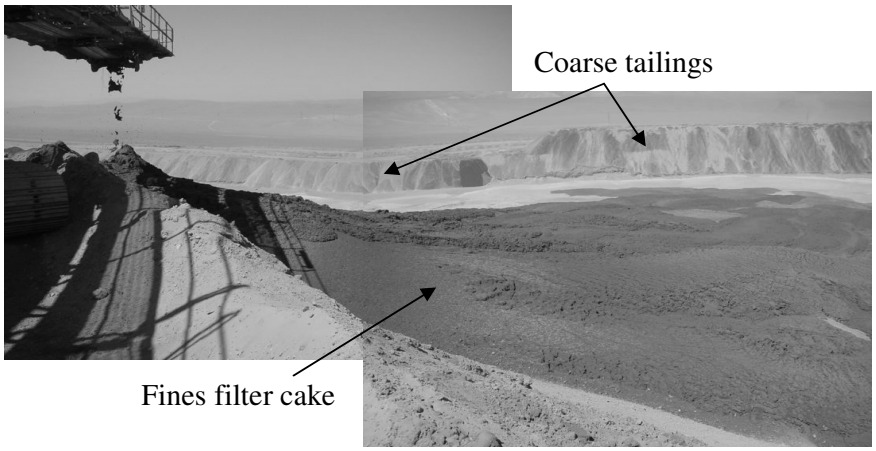

Figure 2.1 : Co-disposal of fines filter cake and coarse tailings
Mantos Blancos copper operation in Chile

Further planned expansion of the mine and the subsequent production increase also prompted the investigation of P&TTD. The co-disposal strategy would then be adapted to deposit the fines as both thickened tailings and filter cake in the paddock type containment area.

2.1.2 Fine tailings + coarse tailings + waste rock

Application of the co-disposal of fine tailings, coarse tailings and waste rock streams was found in a paddock type arrangement at a diamond-bearing kimberlite operation.

Vietti (2002) discussed the co-disposal of all waste streams (fine tailings, coarse tailings and waste rock) at De Beers' Oaks Mine in South Africa. The waste rock is used to build paddock type cells into which fine tailings (as thickened tailings) and coarse tailings are disposed of separately, as shown in Figure 2.2.

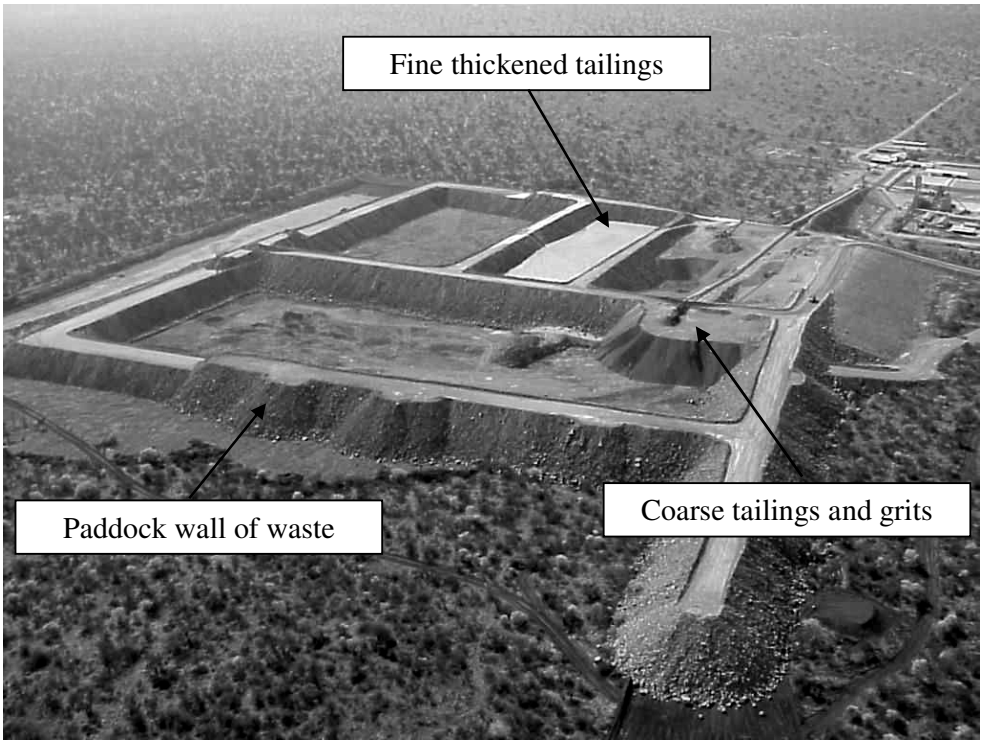

Figure 2.2 : Co-disposal of fine and coarse tailings and waste rock
De Beers' Oaks Mine in South Africa (Vietti, 2002)

The fine tailings slurry from the mineral processing plant is split up in the separate slimes and grits fractions by means of a de-grit cyclone, ahead of the thickening stage. The grits fraction (de-grit cyclone underflow) joins the coarse tailings on the main tailings conveyor and is transported to the specific paddock cell allocated

for grits and coarse tailings storage. The slimes fraction (de-grit cyclone overflow) is thickened to a density of about 1.5 t/m^3. The fine thickened tailings are centrifugally pumped to the specific paddock cell allocated for fine tailings storage. When the fine tailings paddock cell is completely filled, it is covered with a layer of grits and coarse tailings. Closed paddock cells are progressively covered with top soil to allow for the natural establishment of vegetation (Vietti, 2002, 2003a).

2.1.3 Fine tailings + waste rock

Applications of the co-disposal of fine tailings and waste rock were found to fit one of the following general descriptions, regardless of the state of the fine tailings stream, although in most cases the fine tailings were prepared as a thickened tailings material before co-disposal:

- Blending of the fine tailings and waste rock before deposition
- Blending of the fine tailings and waste rock through simultaneous deposition
- Placement of the fine tailings in discreet cells or layers within the waste rock
- Placement of a thin veneer of fine tailings on top of the waste rock, allowing infiltration
- Injection of fine tailings into the waste rock, allowing infiltration

Chambers and Plewes (2002) described the co-disposal of fine tailings and waste rock at the Placer Dome Porgera Mine in Papua New Guinea. Field trials were conducted at the Kogai waste rock dump site of Porgera Mine. The first co-disposal method tested was the placement of fine tailings in discreet cells within the waste rock dump. Different cell geometries were tested, including a v-notch cell. It was concluded that the co-disposal of cells of fine tailings within coarse waste rock appeared to be a promising co-disposal method. It was proposed that large scale implementation should include the filling of 1.5-2 m deep cells with fine tailings and the covering of the cells with 10 m thick layers of waste rock. An adaptation of this method was also proposed where the fine tailings and waste

rock are blended before the combined product is deposited into discreet cells, but the focus here was the development of saturated mixtures to reduce the potential for acid generation (Chambers and Plewes, 2002).

The second co-disposal method investigated involved the deposition of a thin veneer of fine tailings onto the face of the waste rock dump. The fine tailings were allowed to flow under gravity from a tanker truck stationed at the tip head of the waste rock dump. A significant amount of the fine tailings infiltrated the waste rock face, but in some cases the fine tailings caused a limited amount of debris flow at the toe of the dump. This co-disposal method was also recognised as promising and it was proposed for large scale implementation that the fine tailings are transported by tanker truck or pipeline to the waste rock tip head where intermittent fine tailings and waste rock deposition will take place in order to generate an inclined layered effect (Chambers and Plewes, 2002).

Leduc et al (2004) described the evaluation of similar methods of co-disposal of fine tailings and waste rock at the Esquel gold mine owned by Meridian Gold Inc. in Argentina. The first co-disposal method considered was the placement of fine tailings in discreet cells or layers within the waste rock dump. Implementation of this method involved the building of berms that would form cells for holding fine tailings. After a certain period of time the cells were covered with the next layer of waste rock and the cycle repeated. The main concern around this method was that if the next waste rock layer is placed too soon, pore water pressures will build up in the tailings and the new waste rock layer could be subjected to a sudden failure. In order to overcome this problem, it was suggested that binder material such as cement could be used in conjunction with the fine tailings to increase its strength (Leduc et al, 2004).

The second method of co-disposal considered was the blending of fine tailings and waste rock at the face of the waste rock dump. Three different blending configurations were investigated for the Esquel project, namely (1) placing of both the fine tailings and waste rock close to the crest of the waste rock dump and

pushing it over the edge of the face, (2) placing the fine tailings in a haul truck already containing waste rock and dumping the relatively un-mixed material out on the waste rock dump face and (3) mixing of the fine tailings and waste rock by simultaneous deposition on a conveyor belt before the relatively well mixed material is dumped on the waste rock face. The main advantage of these methods were seen as the generation of a homogenous mixture, which would provide more uniform characteristics throughout the co-disposed dump (Leduc et al, 2004).

The third co-disposal method considered involved the injection of fine tailings as a thickened tailings material, into the body of the waste rock dump. Implementation of this method involved the placement of perforated pipes on the inclined waste rock face and then covering the pipes with waste rock material. Once the waste rock dump advanced significantly, the pipes were connected to the fine tailings distribution system and the fine tailings injected into the body of the waste rock dump. Alternatively, pipes could be put into place by drilling vertical holes and fitting slotted pipes in the holes. The main advantage of the latter arrangement is that old inactive waste rock dumps could also be utilised for co-disposal in this manner (Leduc et al, 2004).

The fourth co-disposal method investigated involved the placing of a thin veneer of fine thickened tailings on the waste rock face and then allowing the tailings to infiltrate the waste rock and dry. After a certain time period, the veneer was covered by the next waste rock layer. The fine thickened tailings layer was 20-40 cm thick, while the waste rock layer was 1.5-3 m thick. The thin veneer of fine tailings was allowed to flow onto the waste rock from a perforated pipe on top of the waste rock face. The main advantage of this method was the fact that the pore water pressure build up concerns of the cell method are eliminated due to the thin nature of the veneer and expected high infiltration. The method requires significant monitoring to avoid erosion in the wet season (Leduc et al, 2004).

2.2 General Introduction to Rheology

Rheology is the science of deformation and flow of matter (Boger, 2002). The main rheological parameters are best described according to the Two Plate Model in Figure 2.3 (Coghill, 2003; Vietti and Dunn, 2003a).

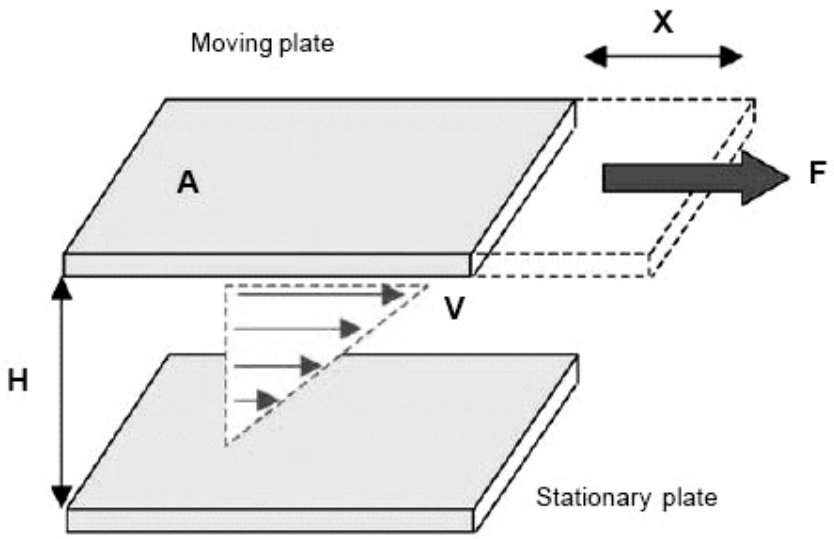

Figure 2.3 : Two Plate Model for the definition of rheological terms (Coghill, 2003; Vietti and Dunn, 2003a)

Figure 2.3 describes the shearing of a fluid between two parallel plates. The space between the two parallel plates, a distance *H* apart, is filled with a fluid. The upper plate, with surface area *A*, is moved with a velocity *V* under the force *F*, while the lower plate remains stationary. The top layer of the fluid adjacent to the upper plate moves with the plate at a velocity *V*, while the bottom layer of the fluid adjacent to the lower plate remains stationary at zero velocity. As a result, a velocity gradient (*dV/dH*) develops across the space between the two plates where *dV* refers to the velocity differential between adjacent layers of fluid and *dH* refers to the differential thickness of a layer of fluid (Vietti and Dunn, 2003a).

The term *shear stress* is defined as the shearing force per surface area and is described in terms of the Two Plate Model in Equation 2.1 (Coghill, 2003; Vietti and Dunn, 2003a).

Equation 2.1 :

$$\tau = F / A$$

where τ = shear stress [N/m^2 = Pa]

F = shearing force [N]

A = surface area [m^2]

The term *shear rate* is defined as the change of deformation per unit time and is described in terms of the Two Plate Model in Equation 2.2 and Equation 2.3. The shear rate equals the velocity gradient (Coghill, 2003; Vietti and Dunn, 2003a).

Equation 2.2 :

$$\dot{\gamma} = dV / dH = dX / dt \times 1 / dH = d\gamma / dt$$

Equation 2.3 :

$$\gamma = X / H$$

where $\dot{\gamma}$ = shear rate [1/s]

dV/dH = velocity gradient [1/s]

γ = shear or deformation

X = distance of deformation [m]

H = distance between parallel plates [m]

t = time of deformation [s]

The term *viscosity* is defined as the ratio of shear stress to shear rate and is described according to the Two Plate Model in Equation 2.4. In general terms viscosity is described as a material's resistance to flow (Coghill, 2003; Vietti and Dunn, 2003a).

Equation 2.4 :

$$\eta = \tau / \dot{\gamma}$$

where η = dynamic viscosity [Pa.s]

τ = shear stress [Pa]

$\dot{\gamma}$ = shear rate [1/s]

In terms of fluid behaviour, materials can be classified as Newtonian or non-Newtonian fluids. Newtonian fluids exhibit a linear relationship between shear stress and shear rate and therefore a constant viscosity over a wide range of shear rates, as illustrated in curve **A** in Figure 2.4. Fluids that do not exhibit a linear relationship between shear stress and shear rate are referred to as non-Newtonian fluids. In the case of non-Newtonian fluids the viscosity is not constant, but varies with shear rate and is referred to as the apparent viscosity. Figure 2.4 provides a summary of the most common rheological behaviours encountered in non-Newtonian fluids (Boger, 2002; Vietti and Dunn, 2003a).

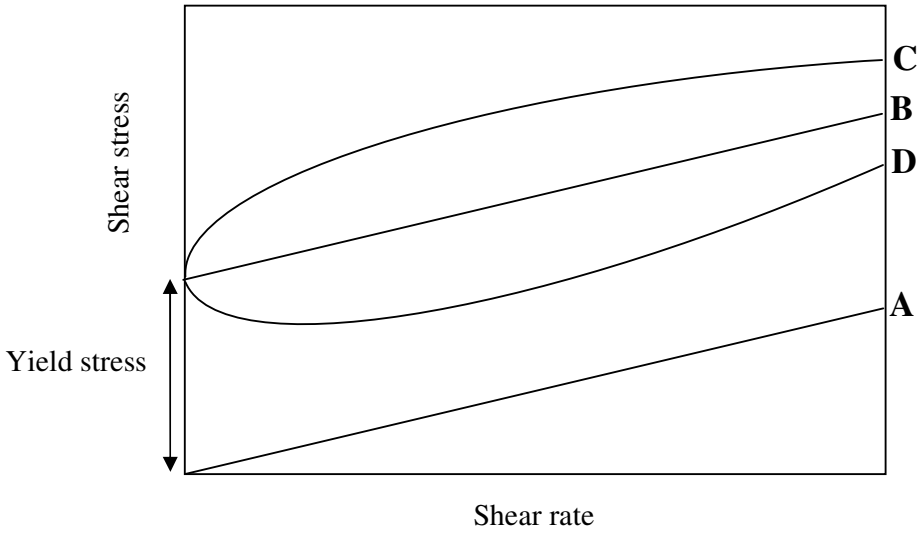

Figure 2.4 : Typical non-Newtonian flow behaviours
(Boger, 2002; Vietti and Dunn, 2003a)

Most non-Newtonian fluids possess a *yield stress*, which is defined as the minimum shear stress that must be exceeded for material deformation and flow to occur (Boger, 2002). A more comprehensive description of the yield stress is provided by Nguyen and Boger (1983). They stated that the yield stress is usually exhibited in suspensions where inter-particle interactions result in a continuous three-dimensional network structure extending throughout the entire volume of the material. The yield stress has been related to the strength of this network structure as the force per unit area required to breakdown the structure, followed by a rupture of network bonds and links between flow units. Therefore, fluids with a yield stress will only begin to flow once the applied external shearing forces exceed the internal structural forces of the material. When the applied shearing forces remain below the yield stress, the network structure will deform elastically, with complete recovery upon removal of the stress. However, once the applied shearing forces exceed the yield stress, the material exhibits viscous liquid flow behaviour with the viscosity a function of shear rate (Boger, 2002; Vietti and Dunn, 2003a).

The non-Newtonian rheological behaviour described by curve **B** in Figure 2.4 exhibits a yield stress followed by a linear relationship between shear stress and shear rate. This is commonly referred to as Bingham plastic behaviour and is described by Bingham plastic model presented in Equation 2.5 (Boger, 2002; Vietti and Dunn, 2003a).

Equation 2.5 : Bingham plastic model

$$\tau = \tau_y + K\dot{\gamma}$$

where τ = shear stress [Pa]

τ_y = Bingham yield stress [Pa]

K = fluid consistency index or Bingham viscosity [Pa.s]

$\dot{\gamma}$ = shear rate [1/s]

The non-Newtonian rheological behaviours described respectively by curves **C** and **D** in Figure 2.4 are referred to in general as shear thinning and shear thickening behaviour. As the shear rate is increased, shear thinning (pseudoplastic) materials exhibit a decrease in viscosity, while shear thickening (dilatant) materials exhibit an increase in viscosity. Shear thinning and shear thickening behaviour without the presence of a yield stress are described by the Ostwald-De Waele rheological model (also known as the Power Law model) presented in Equation 2.6. Shear thinning and shear thickening behaviour of materials possessing a yield stress (curves **C** and **D**) are described by the Herschel Bulkley model presented in Equation 2.7 (Boger, 2002; Vietti and Dunn, 2003a).

Equation 2.6 : Ostwald-De Waele model

$$\tau = K\dot{\gamma}^n$$

Equation 2.7 : Herschel Bulkley model

$$\tau = \tau_y + K\dot{\gamma}^n$$

where τ = shear stress [Pa]

τ_y = yield stress [Pa]

K = fluid consistency index [Pa.s^n]

$\dot{\gamma}$ = shear rate [1/s]

n = flow behaviour index

Shear thinning behaviour is quite common, while true shear thickening behaviour is relatively rare. The decrease in viscosity with increasing shear rate that typifies shear thinning behaviour is a result of inter-particle network structural changes, as illustrated in Figure 2.5. The interactive forces between particles are reduced due to the breakdown, deformation and/or re-orientation of the inter-particle network structure and therefore the resistance to flow decreases (Coghill, 2003; Vietti and Dunn, 2003a).

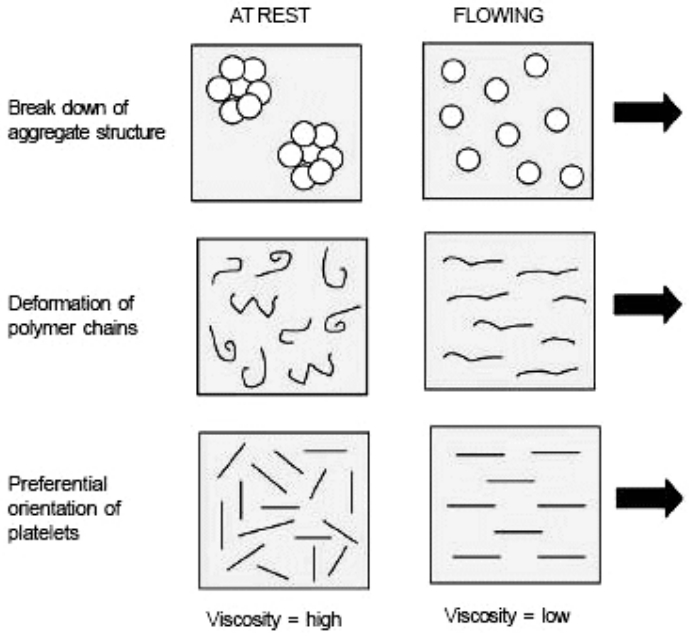

Figure 2.5 : Structural changes resulting in shear thinning behaviour (Coghill, 2003; Vietti and Dunn, 2003a)

The time dependency of non-Newtonian fluids results in complex rheological behaviour. Time independent behaviour results in the immediate reversible return of the material to its original state before shear, when the applied shearing forces are removed. Time dependent behaviour is different in the sense that the reversible return of the material to its original state before shear is not immediate, but takes place over a period of time from the point when the applied shearing forces are removed. Time dependent shear thinning is referred to as *thixotropic behaviour* and time dependent shear thickening is referred to as *rheopectic behaviour*. Thixotropic behaviour is again much more common and could be described as the structural breakdown of the material over time under constant shear and is manifested as a decrease in the viscosity and yield stress of the material over time. As the time of shear increases, the rate of structural breakdown will decrease as fewer structural bonds are available for breakdown. At the same time, structural recovery or reformation could be taking place and the rate of this will increase with time of shear due to the increasing number of broken bonds available. An equilibrium state is often reached where the rate of structural

breakdown equals the rate of structural recovery. However, when the applied shearing forces are removed, the material remains at rest and the rate of structural recovery increases so that the material is brought back to its original state before shear over a certain time period. The specific time period in question is strongly related to the material characteristics (Coghill, 2003; Boger, 2002; Paar Physica, 2002; Vietti and Dunn, 2003a).

In some cases the recovery of the inter-particle network structure is not reversible. The permanent breakdown of the network structure with no recovery upon rest is referred to as *rheomalaxis* (Paterson and Cooke, 2000; Vietti and Dunn, 2003a).

2.3 Manipulation of Thickened Tailings Rheology

Before the manipulation of thickened tailings rheology is addressed, it is necessary to first deal with the issue of why rheology is important in tailings disposal.

2.3.1 The importance of rheology in P&TTD

The rheology of tailings was largely ignored in conventional tailings disposal practices where high volume, low solids concentration tailings slurries were generated and stored in conventional tailings storage facilities or slimes dams. However, since the advent of P&TTD, the volume of tailings slurries is potentially significantly reduced by dewatering to produce low volume, high solids concentration thickened tailings. As the solids concentration of the tailings slurry increases, the material proceeds from simple Newtonian to much more complex non-Newtonian flow behaviour. The successful design and implementation of any P&TTD system requires a thorough understanding of the rheology of non-Newtonian thickened tailings in terms of dewatering, pumping and deposition (Boger, 2003).

Boger (2002) discussed the rheological requirements of each step in the P&TTD system according to the reversed design sequence. It was thought necessary to highlight some of these aspects in order to emphasise the importance of rheology in thickened tailings disposal.

The choice of the deposition site and method defines the desired footprint and shape of the deposit. The main depositional requirement is therefore the delivery of thickened tailings to the deposition site with specific rheological characteristics to ensure that the desired angle of repose for maximum storage capacity is achieved. In addition to the angle of repose, the non-segregating behaviour and spreading characteristics of the thickened tailings are also controlled by the rheology (Boger, 2002).

The pumping and pipeline transport requirements are related to the optimum transport of thickened tailings whilst ensuring the material reaches the deposition site with the desired rheological properties. The thickened tailings rheology defines the minimum pressure differential required for flow to occur (pumping energy), frictional pressure losses in the pipeline and the pressure gradient for various combinations of pipe diameter, flow rate and throughput. Pumping and pipeline transport might alter the rheology of the thickened tailings between the thickening and deposition stages. An understanding of the shear history dependence of the thickened tailings rheology is therefore vital to ensure that the material reaches the deposition site in the desired state (Boger, 2002).

The latter also defines the rheological characteristics of the thickener underflow and therefore dictates thickener operation. The requirements of the thickening stage are related to efficient water recovery and production of a thickened underflow with the desired characteristics as dictated by the transport and deposition stages. The flocculation and operating conditions within the thickener are defined by both the shear and compression rheology of the thickened tailings. The compression rheology provides an indication of the dewatering feasibility of the material to the desired solids concentration. An understanding of the

compression rheology of the material and its relationship with factors such as flocculant dosage and shear history will facilitate optimum thickener performance (Boger, 2002).

Boger (2000) made the following statement: "Environmental considerations dictate that we must manipulate tailings to fit a particular environment rather than manipulating the environment to contain the tailings. Understanding and exploiting the rheology of tailings help us do this". This statement confirms the changing attitude towards tailings disposal, but more importantly brings across the remarkable flexibility of P&TTD when the thickened tailings rheology is fully understood and exploited through manipulation to optimise the system.

Fortunately, the P&TTD technology has advanced to a point where most operators considering the implementation of a P&TTD system seek to understand the rheology of their own material. A considerable amount of work has therefore been done in this area. It is not attempted here to present everything that has been done by everybody, but rather to provide examples of the main factors that can be manipulated in order to exploit the thickened tailings rheology for optimum results.

2.3.2 General thickened tailings rheology

First, the manipulation of thickened tailings rheology is addressed in general, before attention is focused on kimberlite thickened tailings, the specific material used in this study. The main factors discussed in this section apply to the rheological manipulation of most thickened tailings materials and are as follows:

- solids concentration
- shear rate
- shear history
- degree of particle interaction
- particle physical characteristics

The effect of these main factors on the thickened tailings rheology is normally expressed in terms of the yield stress and viscosity.

Solids concentration

Changing the solids concentration of the thickened tailings material is the simplest rheology manipulation technique. As the solids content increases, the particles are brought closer to each other, which restricts their movement. As a result, the yield stress of the material increases due to the increased particle interaction and network structure strength. Shear thinning and thixotropic behaviours are also more pronounced at higher solids concentrations (Coghill, 2003).

The strong dependence of thickened tailings rheology on solids concentration is shown in Figure 2.6. The yield stress as a function of solids concentration is presented for a number of mineral slurries. Although the curves are spread out along the x-axis, all exhibit an exponential increase in yield stress with solids concentration (Sofra and Boger, 2000).

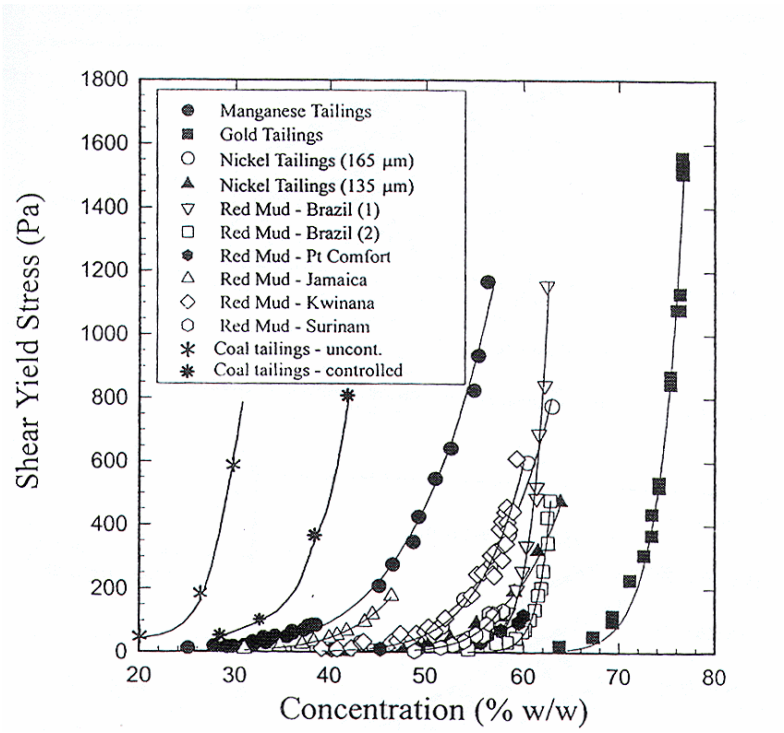

Figure 2.6 : Yield stress as a function of solids concentration in general (Sofra and Boger, 2000)

In practice, the solids concentration of thickened tailings material is manipulated through the degree of dewatering or thickening. It is normally desirable in P&TTD to recover as much of the process water as possible at the thickeners, thereby concentrating the solids content of the underflow to as high as possible.

Shear rate

The non-Newtonian nature of thickened tailings materials results in the ability to express the material viscosity as a function of shear rate. It is therefore possible to manipulate the viscosity of a material through changes in the shear rate.

Most thickened tailings materials exhibit shear thinning behaviour, which means that the viscosity decreases with increasing shear rate. In most cases, the increase in shear rate results in the alignment of particles in the direction of shear, which lowers the resistance to flow. Figure 2.7 shows the relationship between viscosity and shear rate for a number of shear thinning red mud samples at a range of solids concentrations (Sofra and Boger, 2000).

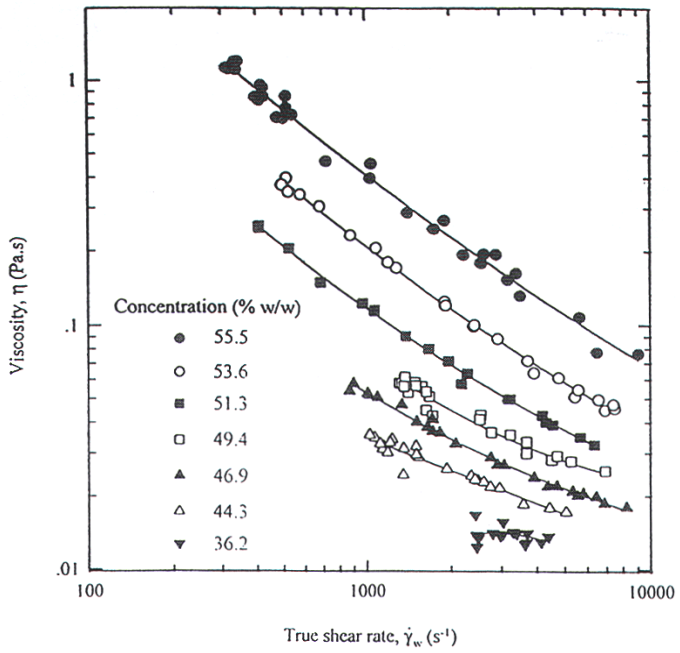

Figure 2.7 : Viscosity vs. shear rate for a range of red mud samples (Sofra and Boger, 2000)

In practice, the amount of shear to which a thickened tailings material is normally subjected to during pumping, results in the reduction of the viscosity, which is in turn beneficial for pipeline transport. Additional shear could be introduced to the material by adding a mechanical mixing stage.

Shear history

Shear history is concerned with both the rate of shear and the time of shear and it is therefore an effective rheology manipulation technique for thixotropic thickened tailings materials. Both the viscosity and the yield stress of the material can be drastically reduced through the introduction of prolonged shear, as illustrated for red mud thickened tailings in Figure 2.8. The data in Figure 2.8 was obtained by shearing (agitating) the material for increasing time periods in between measurement of the flow properties (Nguyen and Boger, 1998).

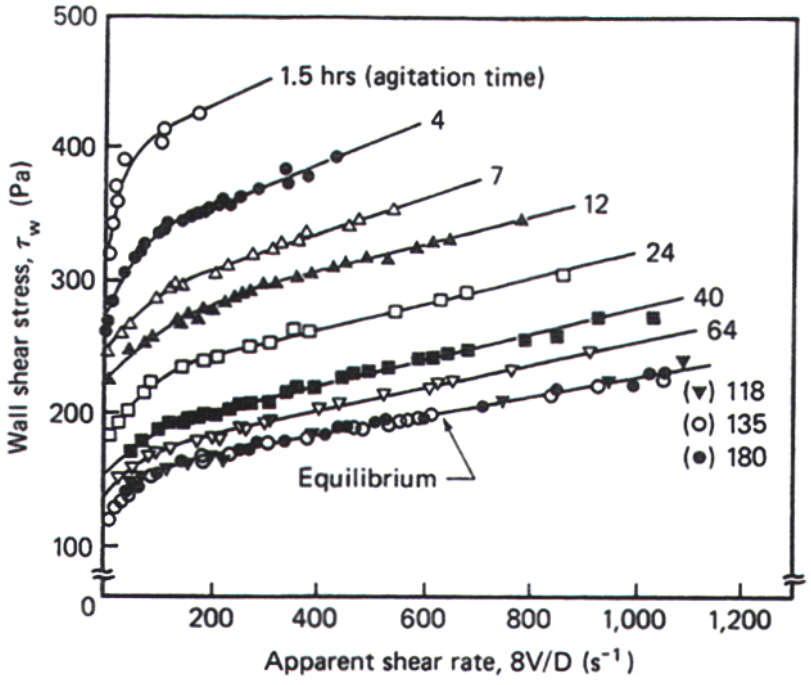

Figure 2.8 : Variation of red mud flow properties as a function of shear history (Nguyen and Boger, 1998)

The effect of shear history on thixotropic thickened tailings materials is not only manifested in the breakdown of the inter-particle network structure under prolonged shear, but also the recovery of the structure at rest, as described in Figure 2.9. The time of rest is just as important as the time of shear (Nguyen and Boger, 1998).

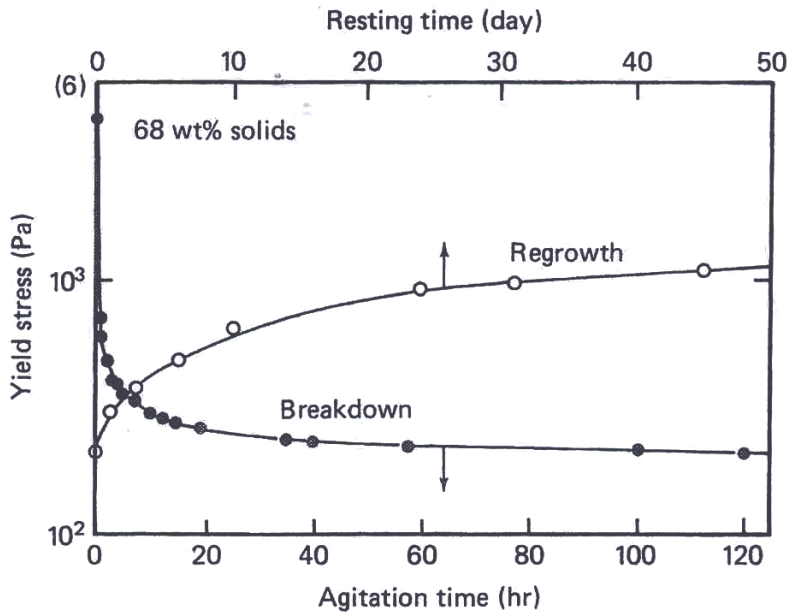

Figure 2.9 : Thixotropic behaviour of red mud thickened tailings (Nguyen and Boger, 1998)

There is normally quite a difference between the rate of structural breakdown and the rate of structural recovery, as illustrated in Figure 2.9. This aspect can be exploited to the advantage of thickened tailings pipeline transport and deposition (Nguyen and Boger, 1998). The optimum arrangement in practice would be for the material to be transported close to the equilibrium state, after which thixotropic strength gain would take place at rest after deposition as shown by Robinsky (1999) in Figure 2.10.

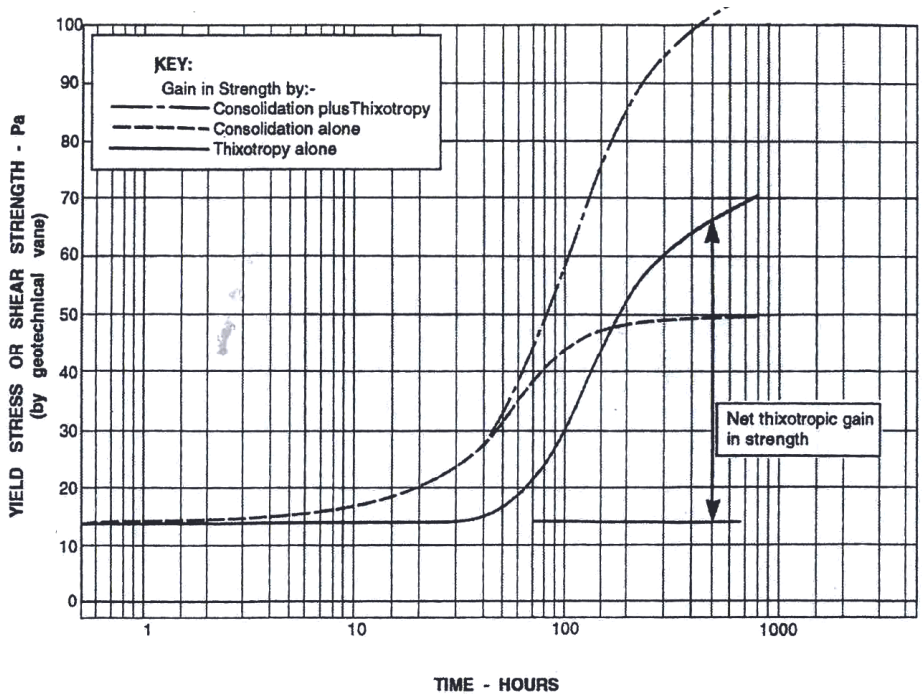

Figure 2.10 : Thixotropic strength gain after deposition (Robinsky, 1999)

Degree of particle interaction

The rheological behaviour of thickened tailings materials can be controlled by understanding and manipulating the strength of the inter-particle network structure and therefore the degree of particle interaction. A material can be *dispersed* by promoting a net repulsive force between particles. Under such circumstances, the particles repel each other and form a suspension with a high resistance to sedimentation, but with a low resistance to compression and flow. On the other hand, a material can be *aggregated* by promoting a net attractive force between particles. Under such circumstances, large inter-particle aggregates are formed in dilute suspensions, which is conducive to rapid sedimentation. In concentrated suspensions a continuous three-dimensional inter-particle network structure is formed with considerable mechanical strength and resistance to compression and flow. In recent years, the yield stress has been used as a measure of the strength of the inter-particle network structure. In simple terms it is therefore concluded that the yield stress can be increased through aggregation and

reduced through dispersion (Johnson et al, 2000; Coghill, 2003; Nguyen and Boger, 1983).

Aggregation and dispersion could be brought about in a mineral suspension on a macroscopic scale through the addition of reagents such as coagulants, flocculants and dispersants. For successful particle aggregation or dispersion in this manner, the particles have to be in the correct receptive state (microscopically aggregated), which is in turn determined by the microscopic scale manipulation of the surface chemistry characteristics of the colloidal particles. A brief description of the mechanisms of coagulation, flocculation and dispersion through reagent addition is provided in the following paragraphs. The surface chemistry manipulation of colloidal particles and the subsequent effects on the material rheology is discussed in Section 2.3.3 where the specific focus is on the rheological behaviour of the montmorillonite clays that are abundant in kimberlite thickened tailings material.

Coagulants are available in two forms, namely electrolytes and poly-electrolytes. The electrolytes are essentially inorganic salts such as lime, gypsum, etc., while the poly-electrolytes are positively charged low molecular weight polymers. The two forms of coagulants make use of different mechanisms of aggregation. The electrolyte mechanism of aggregation could be described as “electrical double layer compression”, which takes place on a microscopic scale and will be discussed later on when the manipulation of surface chemistry characteristics is covered in Section 2.3.3. The poly-electrolyte mechanism of aggregation could be described as “charge patch attraction” as illustrated in Figure 2.11. The positively charged short polymer chains attach as patches on the negatively charged surfaces of colloidal particles in suspension (Dunn, 2003a).

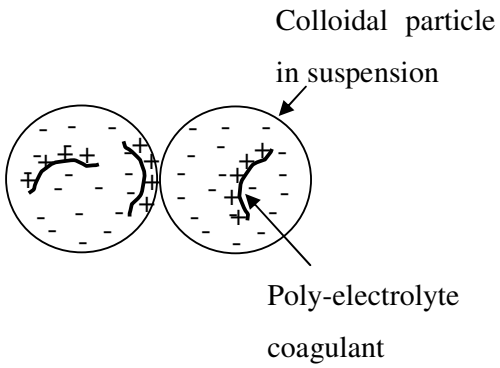

Figure 2.11 : Aggregation through poly-electrolyte coagulant addition (Dunn, 2003a)

Flocculants are high molecular weight polymers available in neutral, positively charged or negatively charged forms. Most commercial flocculants available are based on the poly-acrylamide monomer. The mechanism of aggregation utilised by flocculants can be described as "bridging attraction" and is illustrated in Figure 2.12. High molecular weight flocculants are associated with significant polymer chain length so that upon attachment to the surfaces of colloidal particles in suspension, "loops" and "tails" of polymer are formed, which extend into the bulk suspension. The loops and tails act as bridges and attach to the surfaces of nearby colloidal particles. The result is the aggregation of colloidal particles into multi-particle aggregates, sometime called flocs (Johnson et al, 2000; Dunn, 2003a).

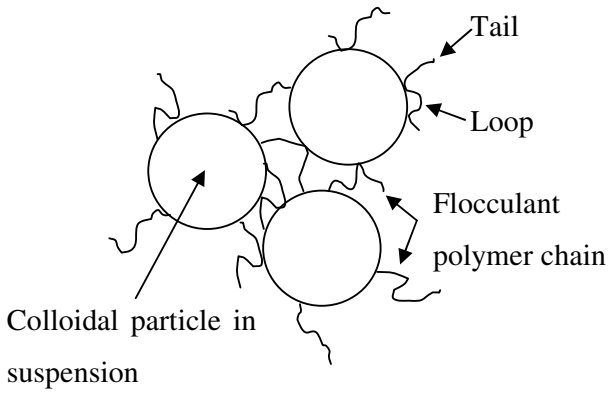

Figure 2.12 : Aggregation through flocculant addition (Dunn, 2003a)

Dispersants, also known as viscosity modifiers, are generally available as polymers and poly-electrolytes. The mechanisms of dispersion can be described as "steric or electrosteric repulsion". Steric repulsion normally takes place when the particle surfaces are completely coated with polymer as described in Figure 2.13. Similar repulsion forces are also observed for poly-electrolyte coated particle surfaces, however due to the excess charge carried by the poly-electrolyte, additional repulsive electrical double layer forces also occur (Johnson et al, 2000; Dunn, 2003a).

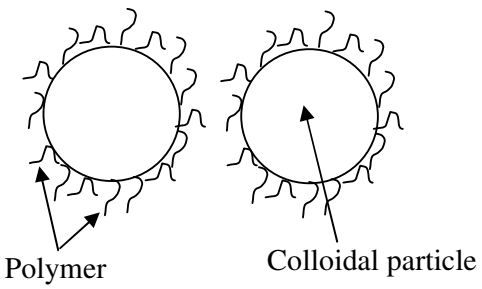

Figure 2.13 : Dispersion through steric repulsion
(Dunn, 2003a)

In practice, coagulation and/or flocculation are used to aid sedimentation and clarification during the thickening stage, while dispersion often precedes pumping and pipeline transport.

Particle physical characteristics

The physical characteristics of the mineral particles such as particle size distribution, particle shape and mineralogy, might not necessarily be easily manipulated, but nevertheless have an impact on the rheological behaviour of thickened tailings materials and are worth mentioning.

Thickened tailings materials with finer particle size distributions generally exhibit higher yield stress and viscosity values for the same solids concentration. In addition to the particle size distribution of a material, progressively changing the particle shape from spheres to rods to plates will also cause an increase in material

viscosity. This is mainly related to the ease with which particles can move with respect to each other when they are brought in closer proximity of each other as a result of increasing solids concentration through dewatering (Coghill, 2003).

The mineralogy of the solid particles is of interest in terms of the presence of clay minerals. Certain types of clay minerals exhibit complex surface chemistry characteristics, which could have a significant impact on the degree of colloidal particle interaction and subsequent strength of the inter-particle network structure. A particularly problematic group of clay minerals is the montmorillonite clays of the smectite group (Coghill, 2003).

2.3.3 Kimberlite thickened tailings rheology

Kimberlite ore is an ultrabasic igneous rock consisting of a cementing matrix material in which mineral inclusions of various crystal elements such as diamond are found. In most cases, the cementing matrix is composed of a range of clay minerals, of which the smectite group of clays are the most dominant, comprising anywhere from 50-90% of the clay mineral fraction (minus 2 μm). Within the smectite group of clays the montmorillonite clays are the major clay species found in kimberlite ores (Vietti, 2003b).

Since the characteristics of kimberlite thickened tailings are dominated by the characteristics of montmorillonite clays, a good understanding of how the clay surface chemistry influences particle interaction and ultimately the rheological behaviour of the material is essential for optimum thickened tailings disposal. Knowledge of the nature and properties of the clay is critical in this regard.

Clay characteristics

Structure - Clays belong to a mineral group called phyllosilicates, which are essentially alumino-silicates, i.e. oxides of aluminium and silicon with smaller amounts of metal ions substituted within the crystal. The basic building blocks of clay minerals are silicon-oxygen tetrahedral and aluminium-oxygen octahedral

units. These units are bonded together to form sheets. The combination of one octahedral sheet with one or two tetrahedral sheets is called a layer. The layers are stacked together in parallel. Clay minerals are classified based on the specific composition of the layers and the isomorphous substitution of other ions for aluminium and silicon within the crystal structure (Yong and Warkentin, 1966; Van Olphen, 1977).

The main clay mineral groups are kaolinites, chlorites, micas, montmorillonites and vermiculites. The kaolinite crystal is made of repeating layers consisting of one silica tetrahedral sheet and one alumina octahedral sheet, sharing a layer of oxygen atoms between them. Kaolinites are referred to as 1:1 layer clays. The repeating layers of the chlorite crystal consist of a silica tetrahedral sheet and an aluminium octahedral sheet followed by a second tetrahedral sheet and a second octahedral sheet and is therefore referred to as 2:2 layer clays. Micas, montmorillonites and vermiculites are all 2:1 layer clays, where the aluminium octahedral sheet is sandwiched between two silica tetrahedral layers. In the case of micas, the layers are bound together by potassium ions and in the case of vermiculites, the layers are separated by only two layers of water molecules. The repeating layers of the montmorillonite crystal are not bound together by a specific ion, but are kept together by attractive Van der Waals forces, as shown in Figure 2.14. Montmorillonite clays have the ability to adsorb several layers of water molecules between the clay platelet layers under certain circumstances. The "swelling" characteristics of montmorillonite clays are discussed in more detail in later sections (Yong and Warkentin, 1966; Van Olphen, 1977; Vietti, 2003b).

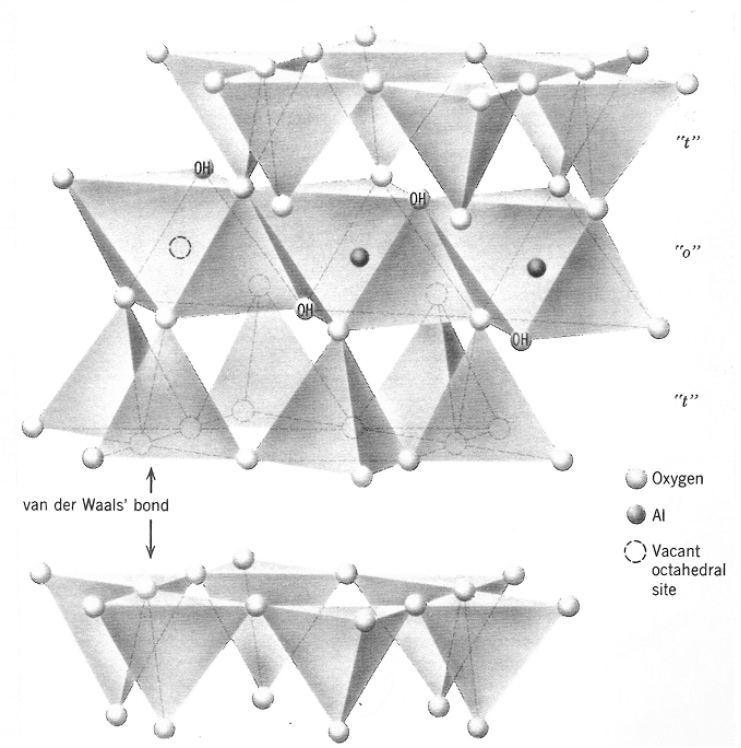

Figure 2.14 : Montmorillonite clay crystal structure
(Vietti, 2003b)

Electrical charge – Clay particles normally carry an excess negative charge as a result of isomorphous substitution and crystal lattice imperfections. Isomorphous substitution is the replacement of one ion with another of nearly equal size but lower valence, within the crystal structure. The main substitutions found are Al^{3+} for Si^{4+} in the tetrahedral sheet and Mg^{2+} or Fe^{2+} for Al^{3+} in the octahedral sheet. The resultant excess negative charge is distributed at the flat layer surfaces of the clay platelet. Cations from the pore water are attracted to the negative clay surfaces in order to maintain electrical neutrality. The excess negative charge is therefore compensated for by the adsorption of cations on the outer layer surfaces of the clay platelet. In the presence of water, these compensating cations are readily exchanged by other cations in solution and are therefore called "exchangeable cations". The amount of exchangeable cations adsorbed onto the clay surface is known as the "cation exchange capacity" (CEC) of the clay. Since the exchangeable cations compensate the unbalanced charge in the interior of the

layers resulting from isomorphous substitution, the CEC is an indication of the degree of substitution or in other words, the amount of negative charge per unit surface area of the clay (Yong and Warkentin, 1966; Van Olphen, 1977).

The second source of clay particle electrical charge is the occurrence of crystal lattice imperfections, especially at the edges of the clay platelet. The clay crystal lattice extends in two directions, but at the edges broken bonds occur between oxygen and silicon in the tetrahedral sheet and oxygen and aluminium in the octahedral sheet, resulting in unsatisfied valence charges at the layer edges. The exposed tetrahedral silicon and octahedral aluminium or other metal ions at these broken bonds attract hydroxyl groups (OH^-) from the pore water to fulfil the unsatisfied valences. In the presence of water, the hydroxyl bearing groups are protonated or deprotonated depending on the pH of the water, as described in Figure 2.15. In acidic conditions the hydroxyl groups become protonated so that the clay platelet edges carry an overall positive charge. As the pH is increased, the hydroxyl groups become deprotonated until a point of overall edge neutrality is reached. This pH value is referred to as the point of zero charge (PZC). Further increase of the pH will result in total deprotonation of the hydroxyl groups until the clay platelet edges carry an overall negative charge. While the clay platelet surfaces carry a permanent negative charge, the charge of the clay platelet edges is pH dependent (Yong and Warkentin, 1966; Van Olphen, 1977; Vietti, 1994; Vietti, 2003b).

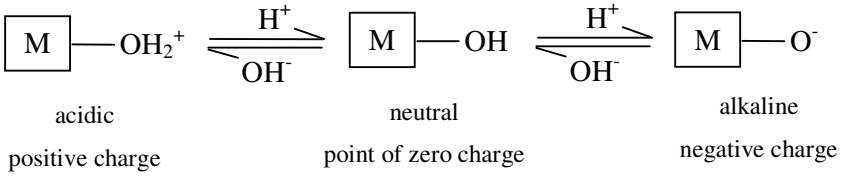

Figure 2.15 : pH dependency of clay platelet edge charges
(Vietti, 1994)

Clay – water interactions

In order to understand the interactions between clay particles in an aqueous environment it is necessary to first develop an understanding of colloidal particle theory and in particular the characteristics of the electrical double layer.

Electrical double layer formation – Colloidal particles normally carry a net surface charge, resulting from effects such as isomorphous substitution or crystal lattice imperfections as discussed in previous paragraphs. When the colloidal particle finds itself in an aqueous environment an electrical double layer is formed around the particle through the migration of charged ionic species in solution to the particle surface to balance the particle surface charge. The electrical double layer consists of (1) the layer of particle surface charge and (2) the layer of diffuse counter-ions balancing the particle surface charge. The latter consists of a layer of bound counter-ions adjacent to the particle surface, known as the Stern layer, which is surrounded by a more diffuse ionic "cloud" that extends into the bulk solution, as described in Figure 2.16. When two similarly charged colloidal particles approach each other due to their Brownian motion, their electrical double layers will overlap and start to interfere. This will give rise to a repulsive inter-particle force as a result of the higher concentration of ions between the particles than in the bulk solution (Van Olphen, 1977; Dunn, 2003a).

The electrical double layer force between homogenously charged colloidal particles is inherently repulsive. However, the electrical double layer force may be either attractive or repulsive for heterogeneously charged colloidal particles, such as montmorillonite clay platelets (Johnson et al, 2000).

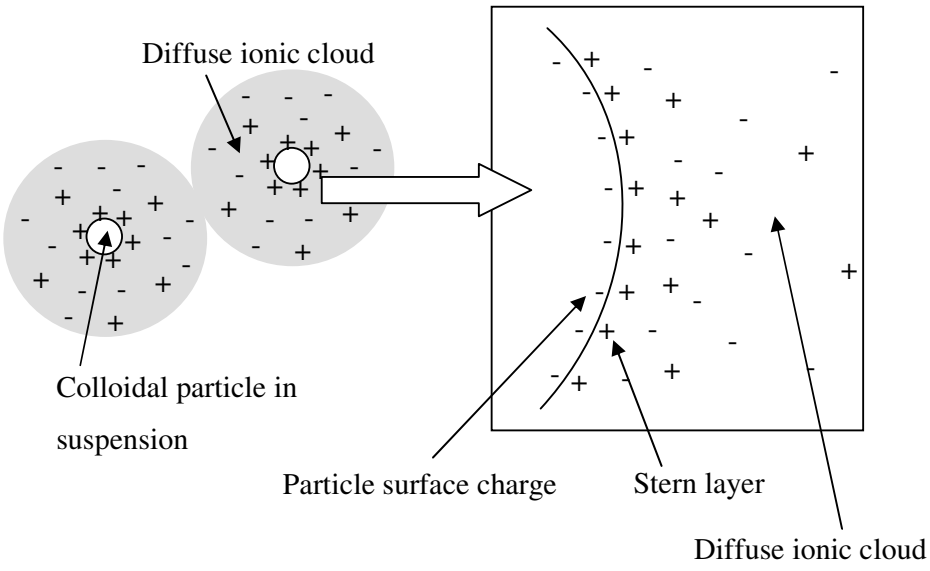

Figure 2.16 : Schematic representation of electrical double layer model (Dunn, 2003a)

In the case of montmorillonite clays, the exchangeable cations normally act as the counter-ions in the Stern layer and are, like any other counter-ions, exchangeable for other cations in the diffuse layer or bulk solution (Van Olphen, 1977).

Swelling characteristics – Montmorillonite clays are widely known for their enhanced swelling behaviour upon interaction with water. The swelling is due to the adsorption of water molecules between the clay platelet layers, thereby pushing them further apart. The swelling is based on to two mechanisms, namely interlayer swelling and osmotic swelling (Van Olphen, 1977).

Interlayer swelling can be described as the step-wise expansion of clay platelet layers as water molecules are adsorbed in successive monolayers. Hydrogen bonding between the surface oxygen groups of the tetrahedral sheet and the water molecules takes place. The surface hydration energy overcomes the attractive Van der Waals forces between the clay platelet layers, which causes more water molecules to enter between the layers. The hydrated clay forms a stable configuration, limited to one to four monolayers of water molecules between the

layers. The mode of swelling leads to, at most, the doubling of the volume of the dry clay (Van Olphen, 1977, Vietti, 1994).

Osmotic swelling is responsible for a much larger degree of swelling and has the potential to completely separate individual clay platelets. The exchangeable cations are not only adsorbed to the outer surfaces of the clay platelet layers, but also in between layers. In an aqueous environment the exchangeable cations hydrate and can be regarded as in solution. The concentration of ions is therefore higher between the clay platelet layers than in the bulk solution. Water molecules are drawn in between the layers under osmotic pressure in response to this ionic concentration gradient. The osmotic swelling continues until electrical double layers are formed around the negatively charged layer surfaces, resulting in electrical double layer repulsion between layers. The repulsive electrical double layer forces overcome the attractive Van der Waals forces and push the layers further apart. Osmotic swelling may continue indefinitely depending on the nature of the exchangeable cations and the nature and concentration of ions in the water (Van Olphen, 1977; Yong and Warkentin, 1966; Vietti, 1994).

Osmotic swelling leads to the formation of a voluminous clay platelet network, which contains large amounts of entrapped water. The swelled clay is highly resistant to dewatering and compression, resulting in unfavourable rheological properties for pipeline transportation at the high solids concentrations required for P&TTD systems. When the swelling is restricted through surface chemistry effects, the clay exhibit improved rheological properties at high solids concentration and consequently dewatering and pipeline transport is simplified (De Kretser et al, 1997; Sofra and Boger, 2000).

Manipulation of rheology through clay surface chemistry effects

The degree of particle interaction is one of the main factors through which thickened tailings rheology can be manipulated. In Section 2.3.2, the degree of particle interaction (i.e. aggregation or dispersion) and its effect on thickened tailings rheology were discussed on a macroscopic scale. However, it is also

possible in clay-based thickened tailings, such as kimberlite thickened tailings, to manipulate the degree of particle interaction and hence the rheology through clay surface chemistry effects on a microscopic scale.

The primary effects of particle interaction on thickened tailings rheology remain the same, regardless of the source of the interaction (macroscopic or microscopic). In other words, particle aggregation leads to an increase in strength, while particle dispersion leads to a decrease in strength of the inter-particle network structure, which is commonly expressed as the material yield stress. It is therefore concluded that dispersed materials are beneficial for compression, pumping and pipeline transport, while aggregated materials are beneficial for sedimentation, clarification and slope stability (Johnson et al, 2000). As discussed before, particle aggregation is the result of a net attractive force between particles, while particle dispersion is the result of a net repulsive force. The degree of particle interaction is therefore controlled by the net inter-particle force between colloidal particles, which in turn is controlled through clay surface chemistry effects.

In the simplest of cases, the net inter-particle force between colloidal particles is governed by a sum of the attractive Van der Waals forces and the repulsive electrical double layer forces. The attractive Van der Waals forces, which can be described as the attraction forces between the atoms of individual particles, are always present, but decrease rapidly with increasing distance between particles. Therefore the net inter-particle force is determined by the degree by which the attractive Van der Waals forces are counter-acted by the repulsive electrical double layer forces. The point at which the repulsive electrical double layer forces overcome the attractive Van der Waals forces is controlled by the type and concentration of ions in suspension (Johnson et al, 2000; Van Olphen, 1977).

The main factors discussed in this section that apply to the rheological manipulation of kimberlite thickened tailings through the surface chemistry manipulation of montmorillonite clays are as follows:

- suspension ionic concentration
- suspension pH
- ion exchanged nature of the clay

Each of these main factors is discussed separately in the following paragraphs, after which the concepts of "controlled and uncontrolled dispersion" are briefly touched upon as an integrated clay surface chemistry manipulation technique as described by De Kretser et al (1997). Finally, this section presents the kimberlite thickened tailings behavioural model recently postulated by Vietti (2003b, 2004).

Suspension ionic concentration - The characteristics of the electrical double layer around a colloidal particle in solution are strongly dependent on the ionic concentration of the suspension. At low ionic concentrations, the electrical double layer is wide and diffuse and therefore the particles remain at some distance from one another in a dispersed state. In this state, the short range Van der Waals attractive forces are exceeded by the electrical double layer repulsive forces. The extent of the electrical double layer decreases with increasing ionic concentration of the suspension. At high ionic concentrations the electrical double layer is compressed, allowing the particles to move close enough to each other for the attractive Van der Waals forces to dominate, causing particle interaction and aggregation, as illustrated in Figure 2.17. It is therefore possible to effect particle aggregation or dispersion through the manipulation of the electrical double layer force by changing the ionic concentration of the suspension (Van Olphen, 1977; Vietti, 1994; Dunn, 2003a).

The degree of electrical double layer compression is primarily determined by the concentration and valence of the ions in solution of opposite sign to the particle charge. The most common practical method in this regard is the addition of salts (electrolytes) at the Critical Coagulation Concentration (CCC), which is the concentration of the specific salt at which aggregation through electrical double layer compression is induced (Van Olphen, 1977; Vietti, 1994).

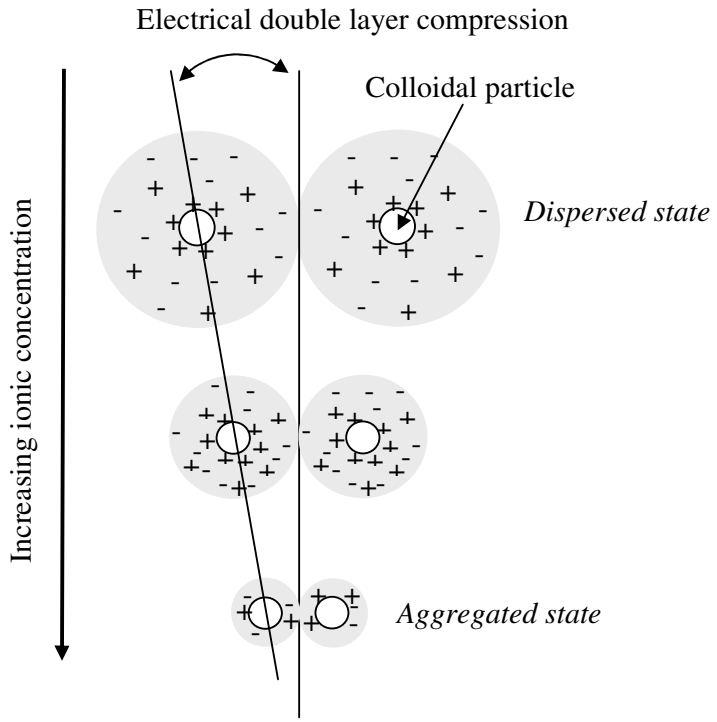

Figure 2.17 : Aggregation through electrical double layer compression (Dunn, 2003a)

Suspension pH – Montmorillonite clay platelets carry pH independent surface or face charges and pH dependent edge charges. In addition to Figure 2.15, the pH dependency of the clay platelet edge charges can also be expressed in terms of the clay platelet zeta potential, as illustrated for the case of montmorillonite clays in Figure 2.18 where the point of zero charge (PZC) on the clay platelet edges is around pH 8 (Vietti, 2003b). The clay platelet zeta potential is defined as the electrical potential in the double layer at the plane of shear between the fixed Stern layer and the mobile diffuse ionic cloud. The zeta potential provides an indication of the overall electrical charge of a colloidal particle (Vietti, 1994).

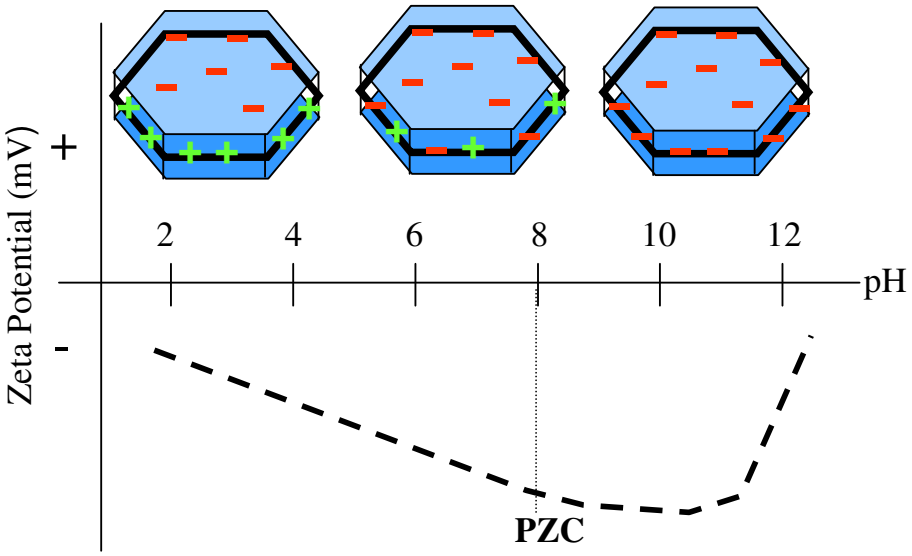

Figure 2.18 : pH dependency of clay platelet electrical charges (Vietti, 2003b)

Figure 2.18 implies that under certain pH conditions clay platelet face to edge attraction will occur, while under other pH conditions clay platelet face to edge repulsion will occur, as illustrated in Figure 2.19 (Vietti, 2003b).

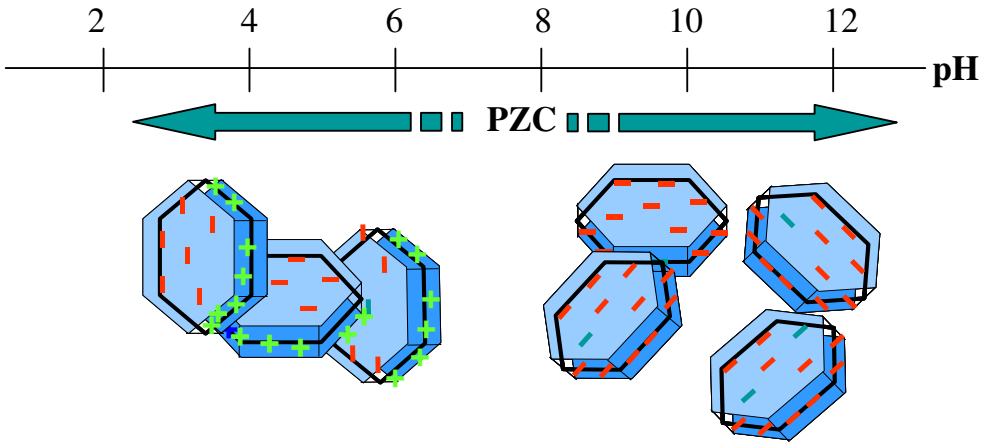

Figure 2.19 : Particle interaction as a function of suspension pH (Vietti, 2003b)

The effect of suspension pH on particle interaction is best observed at low ionic concentrations of the suspension. The electrical double layer compression effect overrides the pH effect at high ionic concentrations (Vietti, 2003b).

In suspension, the montmorillonite clay platelet develops electrical double layers around both the faces and edges of the clay platelet. At low ionic concentrations, both the face and edge double layers of the clay platelet are well enough developed to prevent particle attraction under short range Van der Waals attraction forces. At pH values above 8, both the faces and edges of the clay platelet are negatively charged, resulting in repulsive electrical double layer forces. At pH values below 8, the edges of the clay platelet are positively charged, resulting in electrostatic attraction between the oppositely charged face and edge double layers, leading to particle interaction in spite of the low ionic concentration of the suspension. Particle interaction is dominated by the pH effect at low ionic concentrations (Van Olphen, 1977).

The physical results of the different forms of particle interaction as a function of pH are described in Figure 2.20. Above pH 8, the clay platelets are in a dispersed state and generally pack in a parallel face to face (FF) fashion upon compaction, exhibiting a relatively low yield stress. Below pH 8, the clay platelets are in an edge to face (EF) aggregated state, which can be described as a voluminous "house of cards" structure due to the specific orientation of clay platelet faces and edges. The house of cards structure generally has high mechanical strength and therefore a high yield stress, but also contains large amounts of trapped water in the open spaces between the clay platelets. It is therefore evident that the FF type particle interaction generates higher solids concentrations than the EF type particle interaction under similar compaction forces (Van Olphen, 1977).

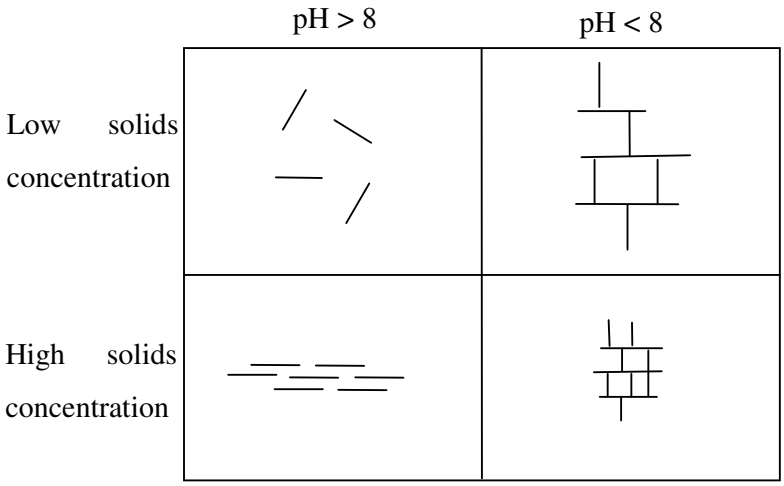

Figure 2.20 : Particle interaction as a function of suspension pH (Van Olphen, 1977)

Ion exchanged nature of the clay – In the case of montmorillonite clays, the main impact on the net inter-particle force is the degree to which the swelling behaviour of the clay is counter-acted through surface chemistry effects. The degree of osmotic swelling observed in montmorillonite clays is strongly dependent on the degree of octahedral substitution in the crystal lattice structure, the nature of the exchangeable cations and the nature and concentration of cations in the contacting water (Vietti, 2003b).

As discussed in previous paragraphs, the degree of isomorphous substitution is reflected in the cation exchange capacity (CEC) of a clay material (Van Olphen, 1977). Therefore, the higher the isomorphous substitution, the higher the CEC of the clay and this result in an increased ability of the clay to change its ion exchanged nature upon contact with the water.

The ion exchanged nature of a clay material typically refers to the dominant exchangeable cation bound to the outer surfaces of the clay platelet layers. The nature of the exchangeable cations has a significant impact on the swelling characteristics of montmorillonite clays. Monovalent exchangeable cations, such as sodium, tend to cause unlimited swelling, while divalent exchangeable cations,

such as calcium, generally restrict the swelling. This is mainly due to the fact that divalent cations have the ability to link adjacent clay platelet layers, thereby preventing water molecules from penetrating the layers and pushing them apart (Vietti, 1994).

It is possible to change the ion exchanged nature of a clay material to enhance or restrict swelling through the manipulation of the nature and concentration of cations in the contacting water. When clay colloidal particles come into contact with water, ion exchange reactions take place between the exchangeable cations on the clay platelet surfaces and the free cations in solution. The specific nature of the ion exchange reactions depends on the valence and concentration of the free cations in solution. The higher the valence of a cation, the stronger it is held at the clay platelet surface or on the other hand the greater its ability to replace cations held at the clay platelet surface when it appears in solution. The general order of preference for cations to adsorption to the clay platelet surfaces as exchangeable cations is shown in Equation 2.8. This is also the order of decreasing replacement power (Yong and Warkentin, 1966).

Equation 2.8 :

$$Al^{3+} \rangle Ca^{2+} \rangle Mg^{2+} \rangle NH_4^+ \rangle K^+ \rangle H^+ \rangle Na^+ \rangle Li^+$$

However, when a specific cation is present in solution at a much higher concentration than the rest, it will be favoured in the ion exchange reactions, regardless of its valence (Yong and Warkentin, 1966).

In the case of montmorillonite clays, the predominant exchangeable cations of interest are sodium and calcium, since they have profound effects on the swelling behaviour of the clay as discussed earlier. Equation 2.9 presents the specific ion exchange reaction where *X* refers to the clay exchange complex (Yong and Warkentin, 1966).

Equation 2.9 :

$$Na_2X + CaCl_2 \Leftrightarrow CaX + 2NaCl$$

In terms of mineral processing, the quality of the process water is therefore critical in determining the ion exchanged nature of the clay at an early stage when the clay comes into contact with the water for the first time. The Sodium Adsorption Ratio (SAR) of a water is used as an indicator of the likelihood of the generation of sodium exchanged clays when the clay and water come into contact with each other. The SAR is defined as the ratio of the monovalent to divalent cations present in the process water, as described by Equation 2.10 where the concentrations of sodium, calcium and magnesium ions in the process water are expressed in milli-equivalents per litre. Process waters with SAR values in excess of 15, are expected to generate sodium exchanged clays, while waters with lower SAR values are expected to generate calcium exchanged clays (Vietti, 1994; Richards, 1954; Van de Graaff and Paterson, 2001).

Equation 2.10 :

$$SAR = \left[Na^+\right] / \sqrt{\left(\left[Ca^{2+}\right] + \left[Mg^{2+}\right]\right) / 2}$$

The ion exchanged nature of montmorillonite clays are often expressed in terms of the Exchangeable Sodium Percentage (ESP), which is defined as the amount of exchangeable sodium held on the clay platelet surfaces expressed as a percentage of total cation exchange capacity (CEC), as described by Equation 2.11 where the concentrations of the exchangeable cations are expressed in milli-equivalents per litre. The ESP is typically used to classify problematic agricultural soils into the classes of saline, saline-alkali and non-saline-alkali soils. The characteristics of kimberlite clays are very similar to the non-saline-alkali soils, which are typified by an ESP of greater than 15%. An ESP value of 100% refers to a completely sodium exchanged clay, while an ESP value of 0% refers to a completely calcium exchanged clay, although these extremes are rare in practice (Richards, 1954; Van de Graaff and Paterson, 2001; Vietti, 2003b).

Equation 2.11 :

$$ESP\ (\%) = (\left[Na^{+}\right] / CEC) \times 100$$

It is therefore possible to alter the ion exchanged nature of the clay through the selection of a specific water source. The ESP value which the clay will reach when it is in equilibrium with the process water can be approximately predicted from the SAR value of the water (Richards, 1954).

If the desired ion exchanged nature of the clay cannot be achieved through the selection of an appropriate water source, the addition of sodium or calcium salts below the Critical Coagulation Concentration (CCC) could be used to alter the ion exchange nature of the clay (Vietti, 1994).

Controlled and uncontrolled dispersion – The concepts of controlled and uncontrolled dispersion are used as effective means of manipulating the degree of particle interaction in montmorillonite clays through the combined effects of the suspension ionic concentration and the ion exchanged nature of the clay. Sodium exchanged montmorillonite clays present several rheological problems due to its enhanced swelling behaviour, as discussed earlier. The degree of swelling of the clay can be restricted through two mechanisms – (1) altering the ion exchanged nature of the clay to calcium exchanged and (2) increasing the suspension ionic concentration to effect electrical double layer compression. Both of the above can be conducted through the addition of calcium salts to the process water. However, the order in which the calcium ions and clay particles are introduced to the process water has a profound effect on the resultant particle interaction and is the essence of the controlled and uncontrolled dispersion concepts (De Kretser et al, 1997; Nguyen and Boger, 1998; Sofra and Boger, 2000).

Controlled dispersion involves the pre-conditioning of the process water with calcium salts to ensure both the presence of calcium ions and high ionic strength. When the sodium exchanged clay is then brought into contact with the pre-conditioned process water, controlled dispersion of the clay platelets takes place.

Initial swelling of the clay upon wetting is restricted due to electrical double layer compression as a result of the high ionic concentration of the process water. In addition, the exchangeable sodium ions on the clay platelet surfaces are simultaneously replaced by calcium ions through ion exchange. Once the ion exchange is completed, the swelling is further restricted. The resultant suspension will consist of larger particles due to the prevention of the swelling and separation of the clay platelet structure. This leads to improved sedimentation, compression and shear properties. This method is beneficial for both the preservation of the clay in the as-mined, parallel face to face orientated form (i.e. most efficient packing orientation) and the improvement of the characteristics of highly weathered clays in advanced stages of swelling (De Kretser et al, 1997; Nguyen and Boger, 1998; Sofra and Boger, 2000).

Uncontrolled dispersion involves the conditioning of the sodium exchanged clay-water suspension with calcium salts after first contact between the clay and water took place. In most cases, the natural ionic concentration of the process water is not sufficient to suppress the initial swelling of the clay and therefore dispersion occurs leading ultimately to complete separation of the clay platelets. Subsequent addition of calcium ions to the suspension is not particularly effective in reversing the swelling behaviour. In other words, the effect of ion exchange on the properties of montmorillonite clays is small in comparison with the effects of controlling the initial dispersion of the clay (De Kretser et al, 1997; Nguyen and Boger, 1998; Sofra and Boger, 2000).

De Kretser et al (1997) clearly showed the different effects of controlled and uncontrolled dispersion on the yield stress of a montmorillonite clay material, as illustrated in Figure 2.21. It is therefore evident that a clay suspension generated from controlled dispersion could be thickened to higher solids concentrations before the yield stress values started to rise significantly.

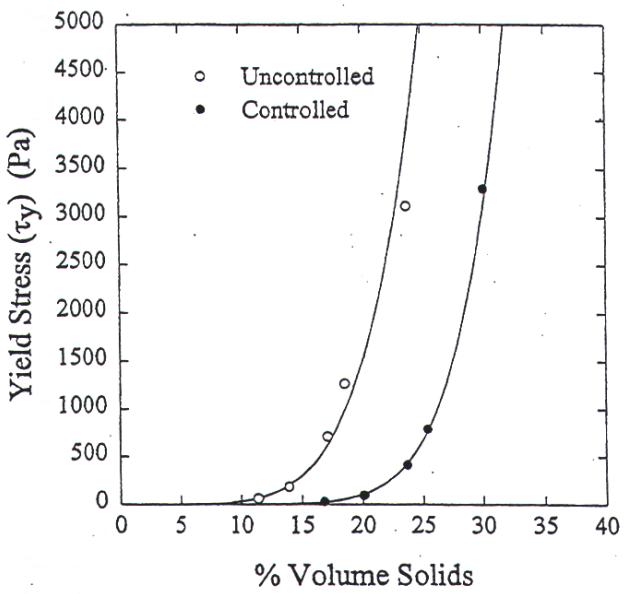

Figure 2.21: Rheological effect of controlled and uncontrolled clay dispersion (De Kretser et al, 1997)

De Kretser et al (1997) further presented a comparison between the sedimentation behaviour between a controlled dispersed simulated montmorillonite clay sample and thickener feed and underflow plant data as part of a case study on coal tailings, represented here in Figure 2.22. The controlled dispersion sample had a higher sedimentation rate and settled to a higher solids concentration than the thickener underflow, yet no flocculant was present in the controlled dispersion sample.

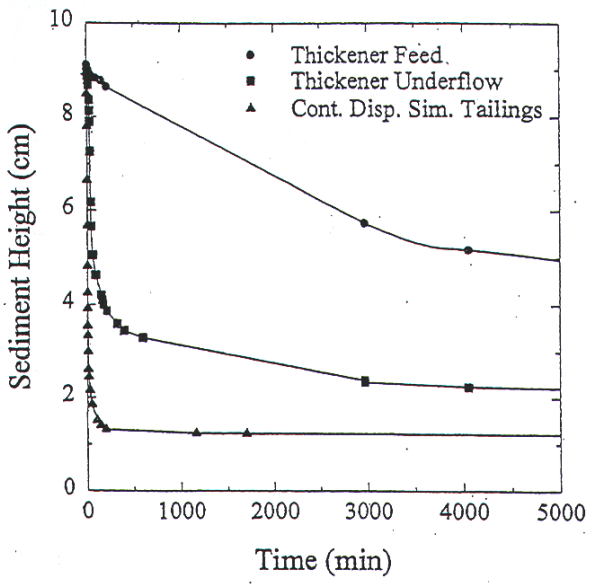

Figure 2.22 : Advanced sedimentation behaviour of controlled clay dispersion (De Kretser et al, 1997)

Practical application of the controlled dispersion effect would be through the maintenance of high ionic concentration levels and the presence of calcium ions in the process water. The possible high cost associated with the large consumption of calcium salts could be balanced by reduced flocculant consumption and improved water recovery (De Kretser et al, 1997).

Kimberlite thickened tailings behavioural model – Vietti (2003b, 2004) proposed quantitative models based on experimental data for the prediction of the colloidal and rheological behaviours of high solids concentration kimberlite thickened tailings. Figure 2.23 presents the rheological behavioural model where the effect of the suspension pH and ion exchanged nature of the clay (expressed as ESP) on the material yield stress is described for a kimberlite clay sample at 41% solids by mass. The yield stress range is colour coded according to the legend in the top right hand corner, i.e. blue referring to low yield stress and orange to high yield stress (Vietti, 2004).

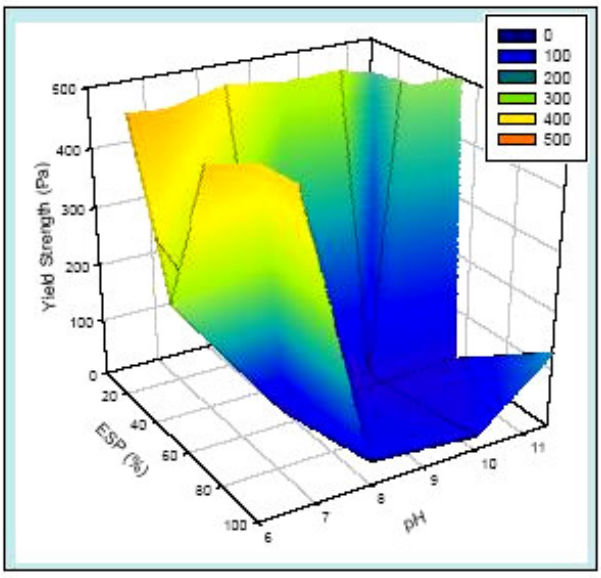

Figure 2.23 : Rheological behavioural model for kimberlite thickened tailings (Vietti, 2004)

Figure 2.24 presents the same behavioural model in terms of mud bed compaction. The mud bed height obtained after 90 hours of free settling is colour coded according to the legend in the top right hand corner, i.e. blue referring to low mud bed height and therefore high compaction, while the opposite counts for orange (Vietti, 2004).

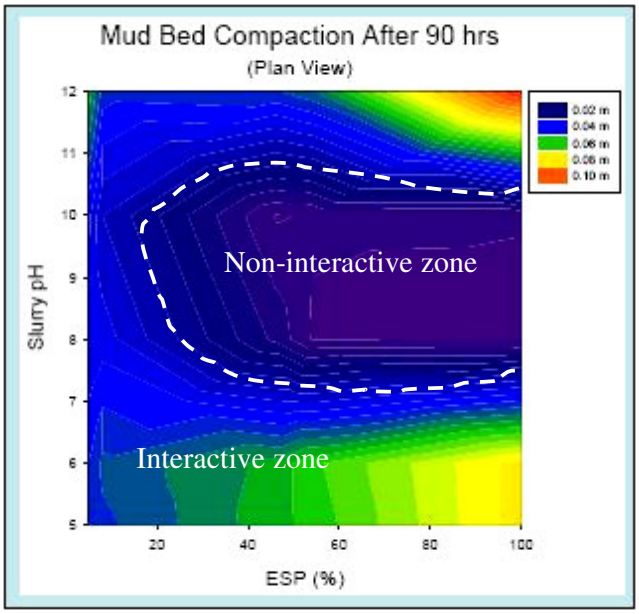

Figure 2.24 : Rheological behavioural model in terms of mud bed compaction (Vietti, 2004)

Distinct particle interaction zones can be identified. The "non-interactive zone" is characterised by limited or no particle interaction, resulting in low yield stress values and a highly compacted mud bed. The "interactive zone", on the other hand is characterised by high yield stress values and a poor to marginally compacted mud bed. The formation of the distinct particle interaction zones can be explained by looking at the main factors that influence the clay surface chemistry characteristics, i.e. suspension ionic concentration, suspension pH and ion exchanged nature of the clay expressed as ESP (Vietti, 2004).

The low yield stress and high mud bed compaction in the non-interactive zone are due to a high degree of dispersion of clay platelets as a result of the dominance of the suspension pH effect. At pH values above 8, electrostatic repulsion between similarly charged face and edge double layers of the clay platelets takes place. This effect is compounded at high ESP values where the enhanced swelling behaviour of sodium exchanged montmorillonite clays leads to complete separation and dispersion of the clay platelets. Upon compaction, the dispersed

clay platelets form a face to face orientated structure as proven by electron microscope studies conducted by Vietti (2004).

The high yield stress and poor to marginal mud bed compaction in the interactive zone are due to a high degree of particle interaction or aggregation. The underlying mechanisms for the particle interaction vary across the interactive zone due to the fact that different factors dominate in different regions within the interactive zone. The suspension pH effect dominates below pH 8 and the ionic concentration effect dominates above pH 11. The dominance of these two effects is best observed at high ESP values. At lower ESP values, the ion exchanged nature of the clay starts to interfere and the resultant better compaction and lower yield stress could probably be ascribed to the reduced swelling behaviour, similar to the effects of controlled dispersion (Vietti, 2004).

At pH values below 8, electrostatic attraction between the oppositely charged face and edge double layers of the clay platelets takes place, leading to the formation of a strong "house of cards" network structure as proven by electron microscope studies conducted by Vietti (2004). This behaviour is observed for a completely sodium exchanged clay in spite of high ESP values and low ionic concentration of the suspension, which ultimately favours dispersion. High pH values, typically above pH 11, are again associated with a high ionic concentration of alkali salts. When the CCC of a salt is exceeded, electrical double layer compression is induced, which allows particles to come close enough to each other for Van der Waals attraction to occur. This behaviour is again observed for a completely sodium exchanged clay in spite of high ESP values and the suspension pH effect, which ultimately favours dispersion (Vietti, 2003b, 2004).

The construction of a rheological behavioural model based on the main factors affecting the clay surface chemistry effects of a particular clay-based thickened tailings material provide the capability to effectively manipulate the flow behaviour of the material to suit the environmental requirements.

2.4 Manipulation of Co-disposed Tailings Rheology

The specific method of co-disposal of tailings under focus in this study is based on the P&TTD concept, i.e. the co-disposal of fine thickened tailings with coarse tailings as discussed in Section 2.1.1. The resultant co-disposed tailings material exhibits complex rheological properties, most of which are not yet fully understood.

In order to make sense of the intricate rheology of co-disposed tailings, a common approach of dividing the material into "vehicle" and "load" components, was adopted. This section starts off with a discussion of the latter and continues to look at the impact of these components and their mixing ratio on the bulk behaviour of co-disposed tailings or other similar materials. Due to the limited research in the area of co-disposed tailings rheology, the literature review was extended into other closely related areas such as the rheology of debris flows or mud flows on mountain slopes, as many similarities exist between these areas.

2.4.1 Vehicle and load components

The concept that high solids concentration slurries exhibiting wide particle size distributions can be divided into "vehicle" and "load" components, first originated out of pipeline flow research on heterogeneous suspensions. The vehicle is defined as the conveying medium or carrier fluid, while the load is defined as the conveyed burden, transported material or carried material (Paterson and Cooke, 2000; Pullum, 2003).

In the case of high solids concentration thickened tailings, the vehicle is often described as a non-Newtonian slurry comprising of fine particles and water (Paterson and Cooke, 2000). Determining the exact particle size, which defines the threshold between vehicle and load components, is a difficult problem. Historically, the vehicle was defined as consisting of all particles smaller than 74 μm. This classification was mainly selected for practical purposes where 74 μm

corresponded to a standard sieve size (Gillies et al, 1991). Later on the 74 μm was rounded up to 75 μm and this became the accepted threshold between vehicle and load components for the transportation of thickened tailings in the P&TTD field.

A similar approach is used in the field of debris flows where the vehicle component is referred to as the initial or interstitial clay-water mixture or the fluid matrix and the load component is referred to as force-free particles (Coussot and Piau, 1995a; O'Brien and Julien, 1988). The particle size threshold between vehicle and load components was defined as 72 μm by O'Brien and Julien (1988), which is in good comparison with the 75 μm used by pipeline flow researchers.

The vehicle is also commonly accepted as the rheologically active part of heterogeneous suspensions. Even though the vehicle is mostly defined as the minus 75 μm fraction, it was shown recently that only particles close to colloidal size, typically smaller than 20 μm, actually influence the rheology of the material (Pullum, 2003).

2.4.2 Co-disposed tailings rheology

The following main factors are used in the rheological manipulation of co-disposed tailings based on the P&TTD concept:

- vehicle characteristics
- load characteristics
- vehicle to load ratio

Vehicle characteristics

In this particular study, the vehicle can be defined as fine thickened tailings. The vehicle characteristics therefore mainly refer to the non-Newtonian rheological characteristics of fine thickened tailings, which are influenced by several factors as discussed in detail in Section 2.3.

As mentioned before, the vehicle is considered as the rheologically active part of co-disposed tailings. Therefore in many instances, the co-disposed tailings rheology is dominated by the vehicle rheology (Paterson and Cooke, 2000). The question if and when the vehicle rheology dominates will be discussed in more detail later on.

Load characteristics

In this particular study, the load can be defined as coarse tailings of which the characteristics are typical of a granular or particulate material. The main factors of interest are therefore the physical characteristics of the coarse particles such as particle size distribution, particle shape, moisture content and mineralogy.

The load is generally not viewed as rheologically active. However, an apparent increase in the co-disposed material yield stress is observed with increasing load fraction (Slatter, 2004). The reason is mainly attributed to the hydrodynamic effects of the coarse particles and the contribution to the overall solids concentration of the co-disposed tailings material. Rheology is a strong function of several parameters, of which the solids concentration is one of the most important (Slatter, 2004). The question if and when the load has a significant impact on the co-disposed tailings rheology will be discussed in more detail later on.

Vehicle to load ratio

The vehicle to load ratio is often defined as a mass or volume percentage ratio. The manipulation of the vehicle to load ratio is instrumental in the design of a co-disposed tailings material with the desired rheological properties as dictated by the surrounding environment.

As the vehicle to load ratio progresses from a maximum where close to the entire material consists of the vehicle component to a minimum where close to the entire material consists of the load component, the bulk material properties undergo a transition from “fluid-like” to “solid-like” behaviour as described by Dunn (2002)

for co-disposed kimberlite tailings in Figure 2.25. The increasing co-disposed material density occurred as a result of decreasing vehicle to load ratio (100:0 to 20:80 in mass %) and increasing solids concentration of the non-Newtonian vehicle component (57-74 mass %). The rheology of the co-disposed material was expressed in terms of a "theoretical yield stress" in Figure 2.25, which refers to the yield stress calculated from the slump height according to the correlation proposed by Pashias et al (1996).

The relationship between yield stress and solids concentration exhibited the typical exponential behaviour at high vehicle to load ratios. However, as the vehicle to load ratio decreased, the yield stress appeared to plateau off, thereby deviating from the typical exponential behaviour (Dunn, 2002).

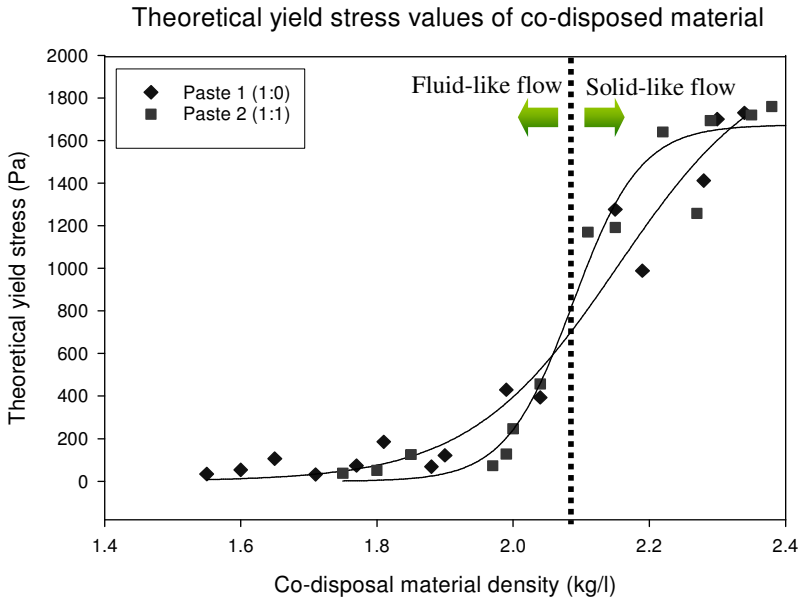

Figure 2.25 : Co-disposed tailings rheology
(Dunn, 2002)

The use of vehicle to load ratios below 50:50 (mass %) are not likely for co-disposal applications based on the P&TTD concept where the combined transportation of the fine thickened tailings and coarse tailings is envisaged. It is

desirable to maintain the "fluid-like" behaviour of co-disposed tailings for efficient pipeline transport and spreading upon deposition. These co-disposed tailings materials are therefore often designed to be statically stable, which mean that the vehicle yield stress is high enough to fully support the load under static conditions, preventing segregation and ensuring that the load is uniformly distributed throughout the vehicle.

Pipeline transport - It was recently shown, however, that such apparently homogeneous materials behave as stratified heterogeneous flows when subjected to periods of prolonged shear as experienced during pumping and pipeline transport, even though they are statically stable. The shear thinning and in many cases thixotropic nature of the non-Newtonian vehicle leads to a breakdown of the inter-particle network structure and therefore a reduction in the yield stress and subsequent ability to support the coarser particles of the load. Under laminar flow conditions, the load often settles out of suspension into a sliding bed of solids, which moves at a slower velocity than the vehicle flowing above the bed. The vehicle rheology plays an important part in keeping the sliding bed from stopping and blocking the pipeline. The more viscous the vehicle, the easier it is to transport the settled bed of load on the bottom of the pipeline. A sufficiently viscous vehicle could impart enough force to the bed when flowing over it to pull the bed along and move it slowly in the direction of flow (Pullum, 2003).

In order to properly design the pipeline transport of co-disposed tailings materials, tests have been developed to investigate the stratification of the vehicle and load components under laminar flow conditions (Cooke, 2001).

It is evident that the manipulation of both the vehicle to load ratio and the vehicle rheology is important to keep the co-disposed tailings material "fluid" enough for pipeline transport, but at the same time viscous enough for efficient two-layer flow. The possibility exists to move the behaviour of the co-disposed tailings material into the "solid" region through the manipulation of the vehicle to load

ratio in order to generate a material suitable for conveying instead of pipeline transport.

Deposition – In terms of the deposition of co-disposed tailings, it is desirable to obtain a decent depositional slope angle with a non-segregating material exhibiting a planar beach profile, similar to the requirements for P&TTD. Robinsky (1999) showed that the slope of a deposit consisting of co-disposed kimberlite slimes and grits increased with decreasing vehicle to load ratio (increasing coarse particle content) and concluded that in order to obtain the same slope, a lesser degree of pre-thickening of the vehicle is required when the load fraction is increased. This enhanced flexibility of co-disposed tailings could be viewed as an ability to accommodate limited process control problems in order to prevent the integrity of the deposit being compromised.

The increase in slope angle with decreasing vehicle to load ratio was also observed by Metago (2002) during large scale deposition tests involving co-thickened and co-disposed kimberlite tailings at De Beers' Finsch Mine (also referred to in Section 2.1.1). However, concave beach profiles and some degree of segregation were observed for the co-disposed tailings. The reason for the segregation of the co-disposed tailings upon deposition was attributed to possible variations in the particle size distribution of the final product. It is the opinion of the author however, that variations in particle size distribution of the vehicle and load components and variations in the vehicle to load ratio were unlikely given the origin of the materials and the specific pilot plant set-up. It is more likely that segregation took place as a result of the proven sensitivity of the vehicle component to shear history and possible variations of the vehicle density (Dunn et al, 2001).

The segregating behaviour of co-disposed kimberlite tailings as a function of the vehicle to load ratio was also investigated by Millar (2004) under static conditions. A segregation boundary was plotted on a ternary diagram, which showed that segregation under static conditions would only become a concern at

very low solids concentrations of the vehicle component. Unfortunately, the main problem of segregation under dynamic conditions still remains.

It is again evident that the manipulation of both the vehicle to load ratio and the vehicle rheology is important to ensure that a material with the desired depositional characteristics is generated. Effects such as static stability and thixotropic strength gain of the vehicle component assist with the development of long term stability of a co-disposed tailings deposit. Although it might be difficult to completely eliminate segregation under dynamic conditions, it could be reduced through manipulation of the vehicle to load ratio and vehicle rheology.

Inference of co-disposed tailings rheology from vehicle to load ratio

In the area of debris flow research, a substantial amount of work has been done on the inference of bulk flow properties from the inspection of the various constituent components (i.e. vehicle and load) and the ratio in which they occur (i.e. vehicle to load ratio). The main drive for this work was the desire to predict the flow behaviour of debris flows without resorting to impractical and expensive laboratory testing of the total material. Most rheological measurement equipment cannot cope with the larger particle sizes typical of debris flows. Therefore indirect methods involving theory and experimental methods involving only the vehicle fraction are often used to estimate the rheological behaviour of debris flows (Ancey and Jorrot, 2001; Coussot et al, 1998; Coussot et al, 1996). Even though from both theoretical and experimental points of view there is still little known about the rheological behaviour of these materials, the findings to date could possibly be applied to co-disposed tailings.

The two main aspects of interest in terms of the inference of co-disposed tailings rheology from the characteristics and mixing ratio of the vehicle and load components, are – (1) the domination of the vehicle rheology and (2) the effect of the load. The discussion in the following paragraphs attempts to represent the findings of the debris flow research in relation to these main aspects of interest.

Domination of vehicle rheology - The specific vehicle to load ratio above which the vehicle rheology dominates the bulk rheological behaviour of the debris flow material, is debatable. The values quoted by workers in the field range from 80:20 to 60:40 (vehicle to load) where the ratio is expressed in terms of volume percentage (O'Brien and Julien, 1988; Coussot and Piau, 1995a; Ancey and Jorrot, 2001).

O'Brien and Julien (1988) found that the effect of adding sand particles to a clay and silt mudflow matrix (minus 72 μm particles) was negligible, provided that the sand concentration remained less than 20% by volume. The viscosity of mudflow materials with a sand concentration less than 20% by volume corresponded closely to the viscosity of the clay and silt fluid matrix. The viscosity of the mixture, however, increased rapidly as a function of volumetric sand concentration at values above 20%.

Coussot and Piau (1995a) observed a similar exponential relationship between yield stress and solids concentration for both the initial clay-water fluid matrix (minus 40 μm) and debris mixtures containing less than 30% by volume of sand (100-200 micron).

Ancey and Jorrot (2001) observed a slight increase in bulk yield stress with the addition of coarse particles (sand, polystyrene or glass particles with a size range of 1-3 mm) to a natural kaolin fluid matrix, at volumetric load fractions below 40%. A sharp increase in the bulk yield stress of the mixture was observed at volumetric load fractions above 40%, with the yield stress tending to infinity when the solids concentration approached the maximum packing concentration.

It seems logical that the addition of small amounts of load to the vehicle could have a negligible effect on the bulk rheology of the mixture. However, the exact point at which the load starts affecting the bulk rheology and where the extent of domination of the vehicle rheology starts decreasing is difficult to determine. Some indication in this regard could be provided by focused experimental work.

Effect of the load - It has been shown experimentally that the addition of coarse particles (load) to the clay-based fluid matrix (vehicle) induced an increase in the bulk yield stress of debris flow material. This effect is negligible where the vehicle rheology dominates, but becomes increasingly pronounced as the load fraction increases. The underlying reasons for this increase in bulk yield stress was investigated by various workers in the field of debris flow research in order to understand the effect of the load on the bulk rheology of the mixture (Ancey and Jorrot, 2001; Coussot et al, 1998; Coussot et al, 1996; Coussot and Piau, 1995a; O'Brien and Julien, 1988).

Initially it was assumed that the vehicle and load fractions acted independently of one another with no interaction between them. Due to the fact that the vehicle is the interstitial fluid, it was assumed that it imparted most of its rheological characteristics to the bulk mixture, similar to the case of non-colloidal particles within a Newtonian fluid. The load was expected to contribute to the rise in bulk viscosity and yield stress mainly through hydrodynamic effects (Ancey and Jorrot, 2001; Slatter, 2004). In other words, as the overall solids concentration increases due to increasing load fraction, a larger number of particles appear within closer proximity to one another, which results in the restriction of their movement past each other. The latter is translated into an increase in resistance to flow (viscosity) and an increase in the minimum shear stress required for the first signs of flow to occur (yield stress).

Colloidal particles, which the vehicle component typically consist of, generally interact with each other through colloidal forces such as Van der Waals attraction and electrical double layer repulsion as discussed in Section 2.3.3. The rheological properties of the vehicle component are therefore strongly linked to the inter-particle network structure and the yield stress is said to be a measure of the strength of this structure. Non-colloidal particles, which the load component typically consist of, generally interact with each other through direct contacts as a result of hydrodynamic forces, frictional forces or collisions. In this case, the yield

stress results from the development of a strong coarse particle network structure (Ancey and Jorrot, 2001; Coussot and Piau, 1995a; Coussot et al, 1996).

As the vehicle to load ratio varies, the bulk yield stress of the mixture is affected to varying degrees by the respective underlying mechanisms discussed in the previous paragraph. At vehicle to load ratios where the vehicle rheology dominates, the bulk yield stress is dictated by colloidal interactions. Small additions of load have no significant effect on the bulk rheology due to the fact that the interstitial fluid lubricates the relative movements of the coarser particles. On the other hand, at vehicle to load ratios where the effect of the load is much more pronounced, the bulk yield stress could be influenced by both colloidal interactions between fine particles and direct contact interactions between coarse particles. The latter is based on the assumption that there is no interaction between the vehicle and load components (Ancey and Jorrot, 2001; Coussot et al, 1996).

However, Ancey and Jorrot (2001) proposed explanations for the existence of interaction between fine and coarse particles from respectively the vehicle and load components, out of their research work. At relatively low load fractions (load volume fraction less than 40%), depletion of colloidal particles per unit volume as a result of load addition, might be sufficient to induce an increase in the bulk yield stress. The coarse particles in effect take up some of the space occupied by the colloidal inter-particle network zones, which might consolidate the inter-particle network structure and lead to an increase in the bulk yield stress. At high load fractions (load volume fraction in excess of 40%), the sharp increase in bulk yield stress with load addition is explained by the fact that the coarse particles (load) are surrounded by a layer of colloidal particles (vehicle), which means that they interact with each other as colloidal particles. It was thought that the coarse particles interact via elastoplastic forces at points of indirect contact due to the fact that the contact points are lubricated by the vehicle component. Yielding of the mixture is therefore a consequence of the breakdown of the indirect (lubricated) contacts between particles (Ancey and Jorrot, 2001).

It is assumed that as the load fraction increases further and the solids concentration approaches the maximum packing concentration, the degree of lubrication between the contacts will decrease, resulting in more direct contacts between particles as discussed earlier and the bulk yield stress will approach infinity.

2.5 Current Status of Identified Knowledge Gap

The identified knowledge gap, as discussed in Section 1.2, refers to the lack of fundamental understanding of the parameters that affect the rheology of a co-disposed tailings material and the extent of their influence. Very few operators have a thorough understanding of their tailings properties and how it could be manipulated to produce specific flow behaviour or depositional characteristics. As a result, very few operators fully exploit the rheological characteristics of their tailings materials in order to minimise the risks associated with tailings disposal.

It is evident from the previous sections that a considerable amount of information is available about the manipulation of clay-based thickened tailings rheology. Currently, only a few people in the P&TTD field have a thorough understanding of this, as can be seen from the same names appearing over and over again on publications in this area. It is believed, however, that due to the availability of published information and an increasing interest by operators to understand the behaviour of their own tailings material, the general level of understanding in the industry is rising.

In contrast to that, relatively little information is available with regard to the manipulation of co-disposed tailings material. The co-disposal of tailings based on the P&TTD concept is not yet widely implemented – most operations considering this kind of co-disposal are still investigating its feasibility through pilot plant evaluations or have implemented it only on a small scale, as discussed in Section 2.1.1. The closely related field of debris flows or mud flows on mountain slopes provided much more information on the extent of influence of various parameters

and the inference of bulk flow properties from the inspection of the characteristics and mixing ratio of the constituent components. Many of these findings could possibly be applied to the rheology of co-disposed tailings.

It is concluded that the general level of understanding by the industry in terms of the manipulation of co-disposed tailings rheology, is currently still very poor, which is clearly one of the barriers for successful implementation of the technology.

3. OBJECTIVES AND SCOPE OF STUDY

The specific objectives and scope of this study are presented in this chapter.

The main purpose of this study is to contribute to the knowledge base of co-disposed tailings rheology and thereby address the current status of the identified knowledge gap, as discussed in Section 2.5.

The overall aim of this study is to gain a better understanding of the relationship between the key tailings material characteristics and the flow behaviour of co-disposed kimberlite tailings upon deposition. A fundamental understanding of this relationship will enable the manipulation and exploitation of the co-disposed tailings rheology for optimal tailings disposal and the minimisation of associated risks.

3.1 Objectives

The main objectives of this study are best understood when phrased as specific questions, which the research work in this study attempted to find answers to. The primary questions addressed by this study are as follows:

- ***What is the relationship between the key material characteristics and the vehicle rheology ?***

  The first part of this study is focussed on understanding how to manipulate the vehicle rheology. This objective relates to understanding how to move the vehicle rheology between the interactive and non-interactive zones as identified by Vietti (2004) and so manipulate the rheological behaviour upon deposition.

- ***What is the relationship between the key material characteristics and the co-disposed tailings rheology ?***

  The second part of this study is focussed on understanding how to manipulate the co-disposed tailings rheology. This objective relates to understanding the extent of the impact of each key material characteristic on the co-disposed tailings rheology and how that could be used to manipulate the rheological behaviour upon deposition.

3.2 Scope

The scope of this study is defined by the following aspects:

- specific method of co-disposal of tailings
- type of tailings material
- research approach
- parameters under consideration

3.2.1 Specific method of co-disposal of tailings

As previously mentioned, the specific method of co-disposal of tailings considered in this study can be described as based on the P&TTD concept, i.e. the co-disposal of fine thickened tailings and coarse tailings. This method of co-disposal refers to the pre-existence of a thickened tailings material, which is combined with coarse tailings for disposal prior to or upon deposition, as shown in Figure 3.1.

The specific configuration of the transportation stage (i.e. separate or combined transportation of the two tailings streams) and the rheological behaviour of the co-disposed tailings during transportation do not form part of the scope of this study. The co-disposed tailings rheology is investigated *upon deposition*, which led to

the assumption that the material flowing onto the deposition site is fully blended and sheared.

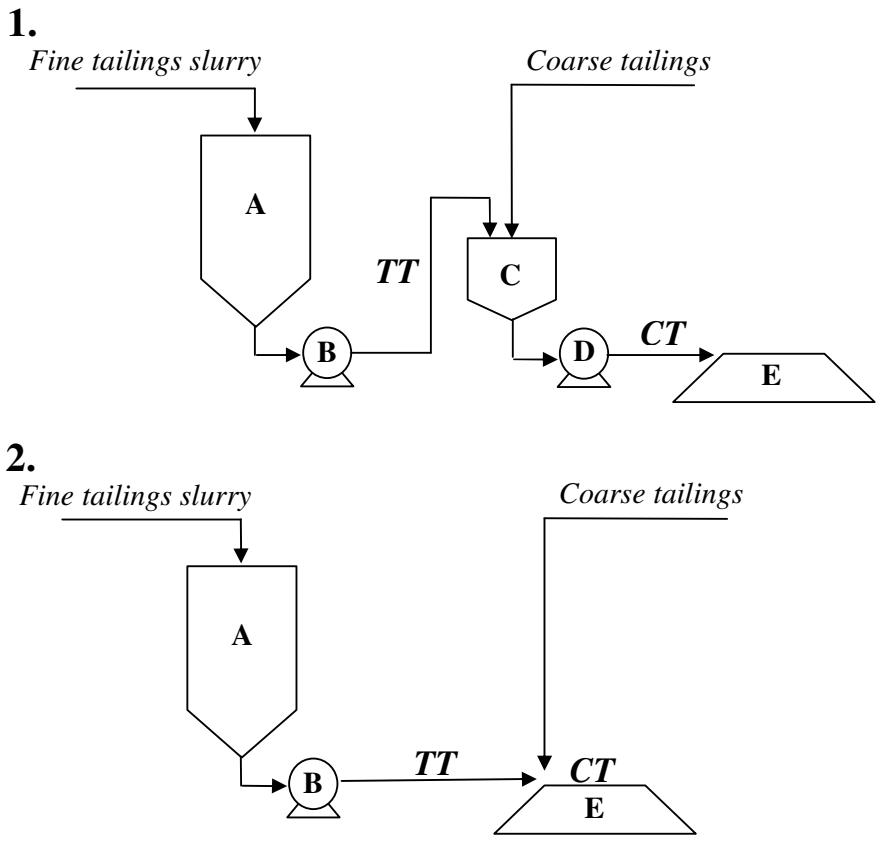

A – High compression thickener

B – Centrifugal or Positive Displacement pumps

C – Mixing hopper

D – Positive displacement or Concrete pumps

E – Deposition site

Figure 3.1 : Co-disposal of tailings based on the P&TTD concept

3.2.2 Type of tailings material

The specific type of tailings material used in this study can be described as montmorillonite clay-based kimberlite tailings sourced from De Beers' Finsch

Mine in the Northern Cape Province of South Africa. Simulated thickened tailings (vehicle), coarse tailings (load) and co-disposed tailings (vehicle + load) samples were manually generated for the specific purpose of this study due to the absence of a full scale co-disposal operation where sampling could be done. The respective material characteristics are discussed in more detail in Section 4.1.

3.2.3 Research approach

The research approach followed in this study was based on fundamental laboratory scale studies. No pilot scale test work was included, mainly due to the time consuming manual preparation of samples.

3.2.4 Parameters under consideration

The parameters under consideration in this study can be divided into input and output parameters. The input parameters refer to all the independent variables that can be manipulated to create a certain response in the output parameters. The output parameters are therefore termed dependent variables.

It is normally possible to identify quite a large number of related input and output parameters for any system, however in most cases only a focussed few are under investigation at a time. The reasons for this are mainly to identify specific interactions between parameters, which are only visible when some parameters are kept constant and also to keep test work manageable and practical.

As discussed under the objectives in Section 3.1, this study was conducted in two parts where the focus of the first part was on the vehicle rheology and that of the second part was on the co-disposed tailings rheology. Therefore in this study, the input parameters refer to the key material characteristics of the vehicle, the load and the co-disposed tailings material, while the output parameters refer to the rheological properties of both the vehicle and the co-disposed tailings material.

In terms of the vehicle rheology, the key material characteristics selected for investigation were the vehicle solids concentration and degree of particle interaction. As a variable input parameter the vehicle solids concentration is fairly easy and straightforward to manipulate. The degree of particle interaction, on the other hand, could be manipulated through a wide range of macroscopic and microscopic effects as discussed in Sections 2.3.2 and 2.3.3. A decision was made to keep the macroscopic particle interaction (i.e. degree of flocculation) constant and rather manipulate the microscopic particle interaction through clay surface chemistry effects. In line with what would be practical on a full scale operation, the suspension pH was then selected as the specific variable input parameter through which the degree of particle interaction was manipulated to vary between interactive and non-interactive behaviour as identified by Vietti (2004). Other material characteristics such as the particle physical characteristics (particle size distribution, mineralogy, ion exchanged nature of the clays) and shear history were kept constant.

In terms of the co-disposed tailings rheology, the key material characteristics selected for investigation were the vehicle rheology and the vehicle to load ratio. The manipulation of the vehicle rheology can be broken down into the two variable input parameters discussed in the previous paragraph, namely vehicle solids concentration and suspension pH. Manipulation of the vehicle to load ratio as a variable input parameter is straightforward when dealt with as a mass percentage ratio. Again, other material characteristics such as the vehicle and load physical characteristics (particle size distribution, mineralogy) and shear history were kept constant.

The yield stress was selected as the key rheological property representing both the vehicle rheology and the co-disposed tailings rheology due to its strong link with the depositional behaviour of thickened tailings. The presence of the yield stress is essential to ensure that the material comes to rest at the required angle of repose for adequate stability and maximum storage capacity. An adequate yield stress also ensures that particle segregation upon deposition is minimised (Boger, 2002).

A decision was made to select two different methods to measure the response of the output parameters (yield stress) and investigate the correlation between these two methods as a secondary objective of this study.

Table 3.1 provides a summary of the various input and output parameters selected for investigation in this study and also indicates which parameters were kept constant to simplify the test work program.

Table 3.1 : Parameters under consideration in this study

INPUT parameters		
	Variable	*Constant*
Vehicle –	solids concentration suspension pH	particle size distribution mineralogy clay ion exchanged state degree of flocculation shear history
Load -		particle size distribution mineralogy
Co-disposed tailings -	vehicle rheology vehicle to load ratio	shear history
OUTPUT parameters		
	Variable	
Vehicle -	yield stress	
Co-disposed tailings -	yield stress	

4. MATERIAL CHARACTERISTICS AND PREPARATION

This chapter presents the characteristics of the raw materials used in this study, the respective preparation procedures for the vehicle, load and co-disposed tailings materials and the procedures for manipulating the selected input parameters under consideration.

4.1 Raw Material Characteristics

Fine and coarse kimberlite tailings, which respectively form the raw material bases of the vehicle and load components, were sampled in dry solids form at De Beers' Finsch Mine in the Northern Cape Province of South Africa. The fine tailings, which could be described as settled dust, were sampled from the floor of the primary stockpile building containing run-of-mine ore, during 2003. The coarse tailings were sampled directly from the main tailings dump during 2000.

The following paragraphs present the characteristics of the vehicle and load component raw materials. Refer to Appendix A for more comprehensive data.

4.1.1 Vehicle

The most important characteristics of the vehicle component raw material (fine kimberlite tailings or dust) are as follows:

- particle size distribution
- mineralogy
- specific gravity

Particle size distribution

The fine tailings were screened at 500 μm to remove any oversize material picked up during the sampling. The minus 500 μm fraction was then used as the basis for the vehicle component. The particle size distribution of the minus 500 μm fraction

was determined using the Microtrac Particle Size Analyser at De Beers' Research Laboratories in Johannesburg and is presented in Figure 4.1. With an average of close to 75% of the particles below 74 μm and more than 99% of the particles below 300 μm, this material was considered as a good approximation of the particle size distribution of a typical vehicle component.

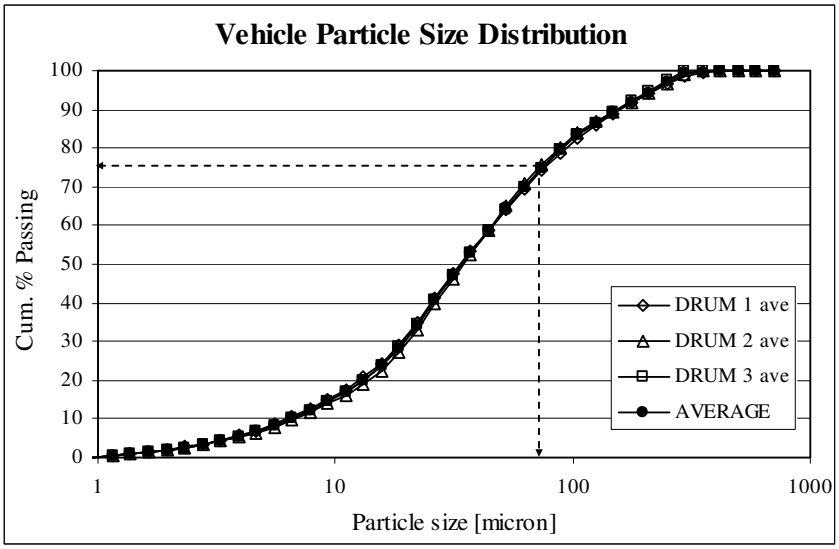

Figure 4.1 : Vehicle particle size distribution

Mineralogy

The mineralogy of the vehicle clay fraction (minus 2 μm) and natural ion exchanged state of the clay were determined by the Institute of Soil, Climate and Water at the Agricultural Research Council in Pretoria. Figure 4.2 shows that the mineralogy of the vehicle clay fraction is dominated by the Smectite group of clays, which is the parent group of the swelling montmorillonite clays. The Exchangeable Sodium Percentage (ESP) of the clay was reported at 32.3%, which indicates a slightly calcium exchanged clay.

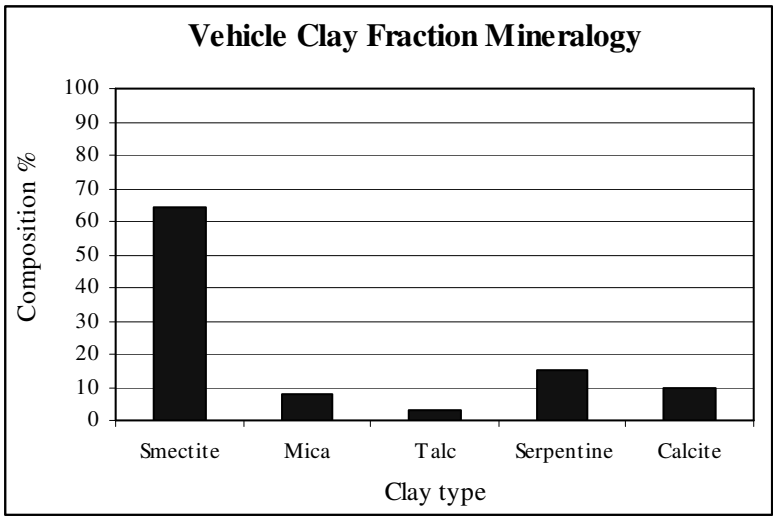

Figure 4.2 : Vehicle clay fraction mineralogy

Specific gravity

The specific gravity of the vehicle component was determined at 2.41 g/cm^3, using the Stereopycnometer at De Beers' Research Laboratories in Johannesburg.

4.1.2 Load

The most important characteristics of the load component raw material (coarse kimberlite tailings) are as follows:

- particle size distribution
- mineralogy
- specific gravity
- void ratio

Particle size distribution

The coarse tailings were screened with a deck of screens consisting of the following sizes – 6.7 mm, 4.0 mm, 2.8 mm, 2.0 mm, 1.4 mm and 1.0 mm. The oversize and undersize material were discarded, resulting in only the minus 6.7

mm plus 1.0 mm fraction been used as the load component. The particle size distribution of this fraction is presented in Figure 4.3.

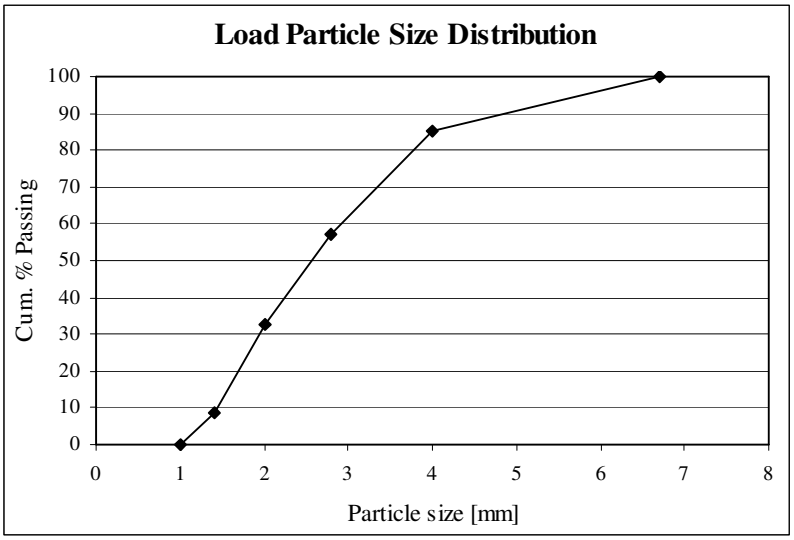

Figure 4.3 : Load particle size distribution

Mineralogy

The mineralogy of the load component was not determined as in the case of the vehicle component. It is therefore only described as kimberlite ore.

Specific gravity

The specific gravity of the load component was determined for each discreet particle size fraction after which the average specific gravity of the load was calculated at 2.59 g/cm^3. Again, the Stereopycnometer at De Beers' Research Laboratories in Johannesburg was used to determine the specific gravity.

Void ratio

The maximum and minimum void ratios of the load component were determined before and after vibration of a sample of the load to obtain the closest particle packing configuration. The maximum void ratio was determined at 0.88, while the minimum void ratio was determined at 0.61.

4.2 Vehicle Preparation

The vehicle dry solids were made into a slurry with distilled water, which was flocculated, settled and sun dried to a high solids concentration thickened tailings material.

The following paragraphs present the procedures that were followed at the various steps in the vehicle preparation program. Refer to Appendix A for more comprehensive data.

4.2.1 Slurry preparation

The vehicle dry solids were added to distilled water in the correct proportions to produce a slurry at a solids concentration of 9% by mass. Distilled water was used in order not to alter the natural ion exchanged state of the clays.

4.2.2 Flocculation and settling

The first step towards efficient flocculation and settling is the selection of an optimum flocculant type and determination of an optimum flocculant dosage according to the standard test procedures presented by Vietti and Dunn (2003b).

Magnafloc E10 was determined as the optimum flocculant type through a test tube flocculant selection trial, while the associated optimum flocculant dosage was determined at 41.5 g/t (grams of flocculant powder per ton of dry solids in the thickener feed stream) through standard beaker tests and one litre cylinder settling tests. The optimum flocculant dosage of 41.5 g/t translated into 16 ml of flocculant solution (0.025% strength) per litre of slurry at a solids concentration of 9% by mass. These conditions yielded a flocculated slurry settling rate of 20 m/h and an acceptable supernatant turbidity.

In order to maintain the degree of flocculation as repeatable as possible, a simple batch procedure was developed for the flocculation and settling of the slurry. Detailed information in regard with the preparation of a typical batch is provided in Table 4.1.

Table 4.1 : Batch preparation for slurry flocculation and settling

FEED SLURRY PREPARATION		
Mass of dry solids	1.61	kg
Volume of water	16.06	litre
% solids of slurry	9.09	%
Mass of slurry	17.67	kg
Volume of slurry	16.67	litre
Density of slurry	1.06	kg/l
FLOCCULATION		
Optimum flocculant	E10	
Flocculant concentration	0.025	%
Actual floc dose	41.51	g/t
Floc dose per litre	16.00	ml
Volume of slurry	16.67	litre
Planned floc dose	266.72	ml
Actual floc dose	267.00	ml
Ave floc flowrate	3.91	ml/s

The following batch procedure was followed to flocculate and settle the vehicle slurry :

- Prepare the vehicle slurry as per Table 4.1 in a 25 litre plastic drum.
- Prepare the flocculant solution as per Table 4.1.
- Stir the slurry with an overhead stirrer.
- Slowly pour in the correct volume of flocculant solution as per Table 4.1, whilst stirring the slurry.
- Switch off the overhead stirrer and allow the slurry to settle under gravity for a period of 2 hours.
- Carefully pour off the supernatant.
- Collect the settled mud bed.

The above batch procedure produced a thickened tailings material in the region of 44% solids by mass and a clear supernatant.

4.2.3 Sun drying

In order to enable simple manipulation of the vehicle solids concentration through dilution during the rheology test work, the settled mud bed collected after flocculation and settling was slowly dried in the sun to reach a high solids concentration in the region of 65-69% solids by mass. This high solids concentration thickened tailings material was considered as the vehicle starting point for the manipulation of the key material characteristics.

The following sun drying procedure was followed to increase the solids concentration of the vehicle thickened tailings material :

- Pour the collected settled mud bed into a flat dish.
- Place the material outside in direct sunlight (or uncovered indoors) to dry out.
- Stir the material frequently by hand to prevent the formation of lumps.
- Continue until a high consistency is reached.

4.3 Load Preparation

The entire sample of load component was screened into the discreet particle size fractions as discussed in Section 4.1. When a particular mass of load component was required for the preparation of a batch of co-disposed tailings material, the load component was constituted out of the correct proportions of the discreet particle size fractions according to the master particle size distribution displayed in Figure 4.3. The main reason for this was to ensure a constant load particle size distribution.

4.4 Co-disposed Material Preparation

The co-disposed tailings material was prepared by mixing the high solids concentration thickened tailings vehicle component with the dry load component in the required vehicle to load ratios. The vehicle to load ratio was defined as a mass percentage ratio to simplify material preparation.

The following procedure was followed to prepare a co-disposed tailings material at a specific vehicle to load ratio:

- Prepare a high solids concentration thickened tailings vehicle through flocculation, settling and sun drying as described in Section 4.2.
- Measure the solids concentration of the vehicle through oven drying.
- Calculate the density of the vehicle from the solids concentration and specific gravity.
- Select an appropriate volume of vehicle based on the volume requirements of the specific rheological measurement technique to be used.
- Calculate the required mass of vehicle from the density and volume.
- Weigh off the required mass of vehicle using a laboratory scale and keep it in a separate sealed container.
- Calculate the total mass of co-disposed tailings from the mass of vehicle and selected vehicle to load mass percentage ratio.
- Calculate the mass of load by subtracting the mass of vehicle from the total mass of co-disposed tailings.
- Calculate the required mass of each discreet particle size fraction of the load according to the load master particle size distribution as described in Section 4.3.
- Weigh off the required mass of each load particle size fraction using a laboratory scale and keep it in a separate container.
- Mix the load particle size fractions thoroughly by hand.
- Add the load component bit by bit to the vehicle component, whilst stirring by hand to aid distribution and mixing.

- Continue until the entire vehicle and load components are thoroughly mixed.

Refer to Appendix B for the equations used in the calculations that form part of the above procedure.

4.5 Manipulation of Variable Input Parameters

The independent variable input parameters of this study, as described in Table 3.1, are the vehicle solids concentration, suspension pH and vehicle to load ratio. The following paragraphs discuss the selection of the range of each input parameter and the procedures that were followed to manipulate these parameters.

4.5.1 Vehicle solids concentration

The vehicle solids concentration range considered in this study was dictated by the desire to observe the output parameter (yield stress) response over a wide range. Overall the vehicle solids concentration was varied between 48-68% solids by mass in order to observe yield stress values over a range of about 40-2000 Pa.

The vehicle solids concentration was manipulated through dilution with distilled water, followed by a mixing period where the dilution water was thoroughly mixed into the material by hand. The solids concentration of the vehicle was measured before and after the addition of the specific dilution volume of distilled water by placing a small sample (about a teaspoon full) of the material in the oven to dry. The solids concentration of the vehicle was then determined as a percentage of the total mass according to Equation B 1 in Appendix B.

In the case of the co-disposed tailings material, the vehicle solids concentration was manipulated through dilution after the addition of the load component. This resulted in the calculation of the vehicle solids concentration due to the fact that the vehicle component could not be isolated again after each dilution for direct solids concentration measurement through oven drying. In order to accurately

calculate the vehicle solids concentration after each dilution, it was necessary to start with a vehicle component of known solids concentration, volume and mass to which a known volume of dilution water was added. The vehicle solids concentration was then calculated according to the equations presented in Appendix C, as the mass of vehicle dry solids remained the same.

For completeness sake, the total solids concentration of the co-disposed tailings material was also calculated as a function of the vehicle solids concentration and the vehicle to load ratio, according to the equations presented in Appendix D.

4.5.2 Suspension pH

The suspension pH range considered in this study was dictated by the desire to manipulate the degree of particle interaction on a microscopic scale between the interactive and non-interactive zones as presented in the kimberlite thickened tailings behavioural model developed by Vietti (2004) and discussed in Section 2.3.3. This model was used as the basis for the selection of the suspension pH range under consideration in this study.

Figure 4.4 shows the three levels of suspension pH considered in this study plotted as points 1, 2 and 3 onto the kimberlite thickened tailings behavioural model in terms of mud bed compaction (Vietti, 2004). The vertical line going through all three the points in Figure 4.4 represents the natural ion exchanged state of the vehicle clay fraction at an ESP of 32%, as reported in Section 4.1.1. The natural pH of the vehicle thickened tailings material produced through flocculation, settling and sun drying was measured at pH 8.6, which is represented by point 2. It is therefore evident from Figure 4.4 that the natural state of the vehicle thickened tailings material clearly falls within the non-interactive zone.

Although the interactive zone represents the entire area around the non-interactive zone, different mechanisms are responsible for the particle interaction in different regions within the interactive zone. As discussed in Section 2.3.3, the suspension

pH effect dominates below pH 8 and the ionic concentration effect dominates above pH 11. The suspension pH range under consideration in this study was therefore selected to cover both these particle interaction mechanisms in the interactive zone. Point 1 represents pH 6 and the point 3 represents pH 11.5.

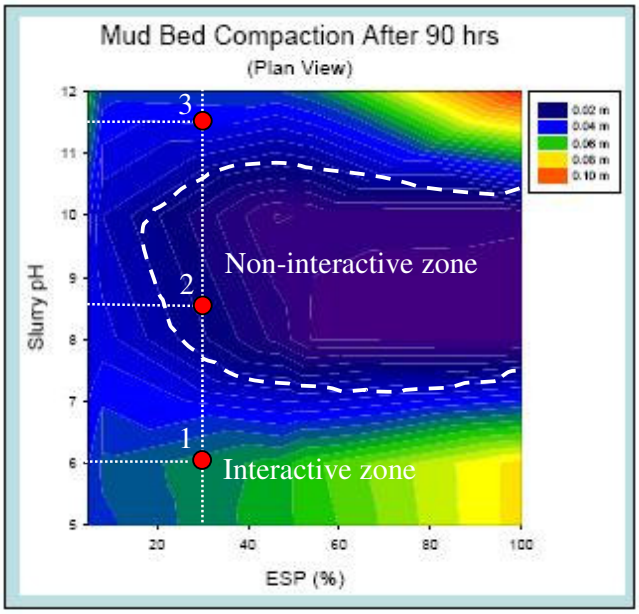

Figure 4.4 : Levels of suspension pH
(Kimberlite thickened tailings behavioural model by Vietti, 2004)

The natural suspension pH was decreased to pH 6 through the addition of hydrochloric acid (HCl) and increased to pH 11.5 through the addition of a solution of sodium hydroxide (NaOH) and calcium hydroxide ($Ca(OH)_2$). The hydrochloric acid was prepared as a 5 molar solution of 33% hydrochloric acid and distilled water as described in Appendix E. The solution of sodium hydroxide and calcium hydroxide was prepared such that the proportion of sodium and calcium ions in solution matches the proportion of these ions on the exchange complex of the vehicle clay fraction so as not to disturb the natural ion exchanged state of the clay. As discussed in Section 2.3.3, the SAR value of a solution is a close approximation of the expected ESP value of the clay at equilibrium (Richards, 1954). The solution of sodium hydroxide and calcium hydroxide was

therefore prepared to have a SAR value equal to the natural ESP value of the vehicle clay fraction, as described in Appendix E.

The suspension pH was modified by adding small amounts of acidic or alkaline solution to the vehicle thickened tailings material, thoroughly mixing the added solution into the material by hand and measuring the resultant pH with a handheld pH meter. This procedure was continued until the desired pH value was observed. In the case of the co-disposed tailings material, the suspension pH of the vehicle component was modified after the addition of the load component.

The suspension pH tended to creep back to the natural pH over time, which necessitated the measurement and adjustment of the pH after each test run during the rheological test work. The dilution effect of the acidic or alkaline solution on the vehicle solids concentration was therefore also taken into account.

4.5.3 Vehicle to load ratio

The vehicle to load ratio range considered in this study was dictated by the desire to generate co-disposed tailings that could still flow upon deposition. As discussed in Section 2.4.2, vehicle to load ratios below 50:50 (mass %) are not likely where it is desirable to maintain the "fluid-like" behaviour of co-disposed tailings. Table 4.2 shows the levels of the vehicle to load ratio considered in this study, expressed as the mass percentage ratio of the vehicle component, in the true sense as a non-Newtonian slurry comprising of the minus 75 μm solid particles and water, and the load component in dry solids form.

Table 4.2 : Levels of vehicle to load ratio

	Levels in mass %			
Vehicle (wet) : Load (dry)	100:0	90:10	70:30	60:40

The vehicle to load ratio was manipulated through the preparation of the co-disposed tailings material as described in Section 4.4. For each vehicle to load ratio a fresh co-disposed tailings sample was prepared. However, due to the fact that the vehicle solids concentration and suspension pH were manipulated after the addition of the load in the case of the co-disposed tailings, its dilution effect on the vehicle component affected the vehicle to load mass percentage ratio as quoted in Table 4.2 slightly. It was therefore decided to express the vehicle to load ratio as a mass percentage ratio based on the dry solids content of the respective vehicle and load components. Table 4.3 shows the levels of the vehicle to load ratio considered in this study, expressed on a dry solids mass percentage basis.

Table 4.3 : Levels of vehicle to load ratio (dry solids basis)

	Levels in mass %			
Vehicle (dry) : Load (dry)	100:0	86:14	60:40	50:50

Although the way in which the vehicle to load ratio is expressed in Table 4.2 simplifies material preparation, it was decided to report all test work results in terms of the vehicle to load ratio expressed on the dry solids basis as presented in Table 4.3 for ease of comparison.

5. MEASUREMENT TECHNIQUES AND EQUIPMENT

This chapter starts off with a general introduction to rheological measurement, followed by a brief overview of yield stress measurement techniques before the focus is turned to the description of the particular yield stress measurement techniques and equipment used in this study.

5.1 General Introduction

The rheological behaviour of a tailings material is typically determined through the measurement of the shear stress–shear rate relationship in a suitable rheometer.

The most common types of rheometers used in the measurement of mineral tailings materials are tube and rotational rheometers (Paterson and Cooke, 2000).

A tube rheometer, also referred to as a capillary rheometer, consists of a straight tube (or pipe) of known diameter through which the material to be tested flows. The basic measurements include the material flow rate and pressure gradient over a known tube length, from which the shear stress and shear rate relationship is inferred (Nguyen and Boger, 1992; Slatter, 2004; Paterson and Cooke, 2000).

A rotational rheometer, also referred to as a bob-in-cup rheometer, consists of two concentric cylinders. The rotating inner cylinder is called the bob and the stationary outer hollow cylinder is called the cup. The material to be tested is placed in the annulus between the two cylinders where it is sheared. The basic measurement is the torque required to rotate the bob at a constant speed. The data analysis involves relating the torque to the shear stress and the speed to the shear rate (Nguyen and Boger, 1992; Slatter, 2004; Paterson and Cooke, 2000).

Several problems are encountered with the use of both these instruments, which often lead to erroneous results. Some of the main problems that are applicable to

the measurement of mineral tailings materials are wall slip, particle segregation and gap size (Vagias, 2003).

Wall slip can be described as the formation of a lubricating layer next to the tube wall or bob surface as a result of particle migration or phase separation. This layer is less viscous than the bulk material and since shearing takes place at this layer, it appears as if the bulk material "slips" along the wall or bob surface, giving rise to an underestimation of the true shear stress. Wall slip can be reduced by roughening the sensor surface (Nguyen and Boger, 1992; Vagias, 2003). Nguyen and Boger (1983) proposed the use of a vane as the rotating body to completely eliminate wall slip problems.

Particle segregation or settling during measurement is a problem that is often encountered in particulate fluids. Particles that accumulate at the bottom of the tube or cup result in a significant increase in flow resistance in the case of the tube rheometer and a significant decrease in flow resistance in the case of the rotational rheometer. In the latter case, the settled particles are not in contact with the sensor and are essentially removed from the measurement, which could lead to the incorrect conclusion of shear thinning or thixotropic effects. Particle segregation could be reduced by using flow through sensor designs (Vagias, 2003; Paterson and Cooke, 2000).

The size of the annular gap in rotational rheometers needs to be greater than 10 times the maximum particle size for accurate results, which means that most commercial rotational rheometers are only capable of measuring materials containing very small particle sizes. A common method to overcome this problem is to widen the gap, however this has drawbacks of its own. When high yield stress materials are measured using a wide gap, the effective gap size (sheared region) might not coincide with the physical gap between the bob and the cup due to the development of a stationary (unsheared) region near the cup wall as a result of the high yield stress. This could lead to erroneous results as the data analysis relating the torque and rotational speed to respectively shear stress and shear rate

is dependent on the gap size determined from the bob and cup dimensions (Vagias, 2003; Slatter, 2004).

In recent years, some large-scale rotational rheometers have been developed in the field of debris flow research in order to enable the measurement of materials containing larger particle sizes including sand and pebbles (Coussot and Piau, 1995b; O'Brien and Julien, 1988). However, these rheometers require large sample volumes in the order of 1 m^3 and are also plagued by the problems of coarse particle segregation and migration (Coussot and Piau, 1995b).

The results obtained from a rheometer are normally described as a rheogram or flow curve and it essentially presents the shear stress-shear rate relationship of the material in question. The rheological behaviour of the material can be identified as Newtonian or non-Newtonian from the shape of the rheogram as indicated by Figure 2.4 in Section 2.2. The specific rheological properties of the material are determined through appropriate rheological model fitting as discussed in Section 2.2.

5.2 Overview of Yield Stress Measurement Techniques

Conventional rheological characterisation of co-disposed tailings and even some types of thickened tailings remains a difficult problem, mainly due to the physical limitations of commercial rheometers and the significant experimental problems experienced with particulate materials. As a result, more attention is devoted lately to the accurate measurement of the yield stress as a key rheological property used in the design and operation of P&TTD systems.

Numerous techniques have been developed for both the indirect and direct measurement of the yield stress based on the general definition of the yield stress as the shear stress limit between flow and non-flow conditions (Nguyen and Boger, 1992). Therefore, the shear stress corresponding to the first evidence of plastic flow can be interpreted as the yield stress (Nguyen and Boger, 1983). Only

the techniques that could possibly be applied to the yield stress measurement of co-disposed tailings are discussed in the following paragraphs.

5.2.1 Indirect measurement techniques

The conventional indirect method of yield stress determination involves the extrapolation of the experimental shear stress-shear rate data to zero shear rate. The shear stress intercept at zero shear rate is taken as the yield stress value. Direct extrapolation of the data is performed or alternatively a suitable rheological model is fitted to the data and the resultant fitted curve extrapolated to zero shear rate. The yield stress value determined through this technique could not be regarded as an absolute material property, due to the fact that its accuracy depends on the applicability of the rheological model to the observed behaviour and the reliability and range of the experimental data available (Nguyen and Boger, 1992; Nguyen and Boger, 1983).

This technique is also dependent on the measurement of the shear stress-shear rate relationship in a rheometer, which might not be applicable to co-disposed tailings due to the reasons discussed earlier. The slump test, on the other hand, has significant potential to be applied as an indirect yield stress measurement technique for co-disposed tailings (Pashias et al, 1996).

Slump test

The slump test, initially developed to determine the flow properties of fresh concrete, has been adopted by the P&TTD field as an indirect yield stress measurement technique for high solids concentration thickened tailings. The slump test involves the filling of a slump container with the material to be tested, removing any air bubbles through tamping, lifting off the container and allowing the material to collapse under its own weight. The slump height is defined as the difference between the height of the container and the height of the slumped material as illustrated in Figure 5.1 where s refers to the slump height and H to the height of the slump container (Pashias et al, 1996; Vietti and Dunn, 2003a).

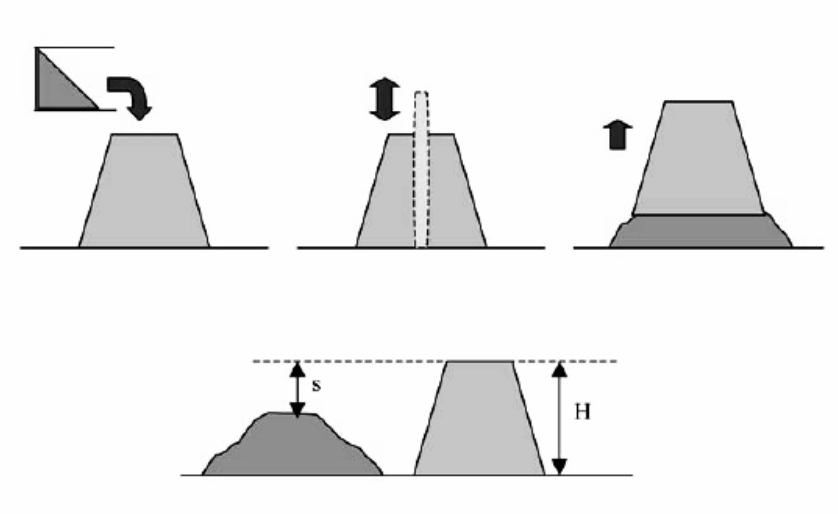

Figure 5.1 : Slump test
(Vietti and Dunn, 2003a)

Historically, a conical geometry was used as the slump container, however Pashias et al (1996) adapted the theoretical analysis relating the slump height to the yield stress to a cylindrical geometry and called it a "50c rheometer" to emphasise the simple and inexpensive nature of this yield stress measurement technique. Recently, Clayton et al (2003) showed that the cylindrical geometry of the slump container more accurately predicted the yield stress than the original conical geometry.

A correlation between slump height and yield stress was developed by Pashias et al (1996) in dimensionless form as described by Equation 5.1.

Equation 5.1 : 50c Rheometer correlation

$$\tau_y^{'} = 0.5 - 0.5\sqrt{s^{'}}$$

Equation 5.2 : Dimensionless slump height

$$s^{'} = s / H$$

Equation 5.3 : Dimensionless yield stress

$$\tau_y^{'} = \tau_y / (\rho g H)$$

where $\tau_y^{'}$ = dimensionless yield stress

s' = dimensionless slump height

s = slump height [m]

H = height of slump container [m]

τ_y = yield stress [Pa]

ρ = material density [kg/m^3]

g = 9.81 [m/s^2]

The slump test has been applied as an indirect yield stress measurement technique with a significant degree of success throughout the P&TTD field and became quite popular as a quick field test (Pashias et al, 1996; Sofra and Boger, 2000; Gawu and Fourie, 2004).

5.2.2 Direct measurement techniques

Direct measurement of the yield stress independently of the basic shear stress – shear rate data can be conducted through one of the following techniques (Nguyen and Boger, 1992; Vagias, 2003):

- vane method
- inclined plane method
- stress relaxation
- stress growth
- creep test
- cone penetration
- immersion of bodies

However, only the vane method and inclined plane method are considered to be applicable to the direct yield stress measurement of co-disposed tailings. The

other methods are either used in conjunction with rotational rheometers, which have obvious physical limitations for co-disposed tailings as discussed before (i.e. stress relaxation, stress growth, creep test) or have questionable accuracies when used in conjunction with highly viscous materials (i.e. cone penetration, immersion of bodies) (Nguyen and Boger, 1992).

Vane test

The problem of wall slip observed in rotational rheometers led to the adaptation of the vane method, originally used in soil mechanics for the measurement of soil shear strength, as a yield stress measurement technique. The vane basically consists of four thin blades arranged at equal angles around a small cylindrical shaft, as illustrated in Figure 5.2. The vane test involves the gentle introduction of the vane into the material until the vane is flush with the material surface or fully immersed. The vane is then slowly rotated at a constant rotational speed and the torque required for maintaining the constant motion of the vane is measured as a function of time. Figure 5.3 shows the typical torque-time curve obtained for yield stress materials (Nguyen and Boger, 1983; Nguyen and Boger, 1992).

The linear behaviour of the first part of the torque-time curve may be attributed to the stretching of the structural bonds of the inter-particle network. The curved part following the linear region of the torque-time curve relates to the gradual breaking of these stretched bonds. When the majority of the bonds have been broken, the inter-particle network structure collapses and the material is said to yield along a cylindrical surface defined by the dimensions of the vane. The latter behaviour is represented by a maximum torque value followed by a rapid decay of torque over time on the torque-time curve. The yield stress can be calculated from the maximum torque value and known vane dimensions according to Equation 5.4 (Nguyen and Boger, 1983; Nguyen and Boger, 1992).

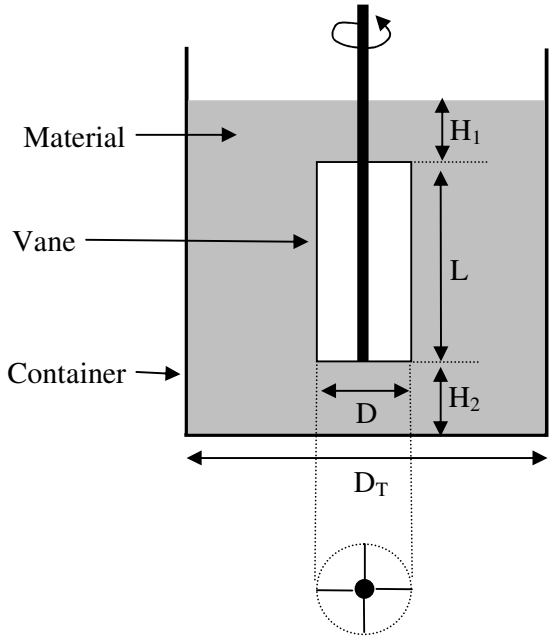

Figure 5.2 : Vane test

(Nguyen and Boger, 1992)

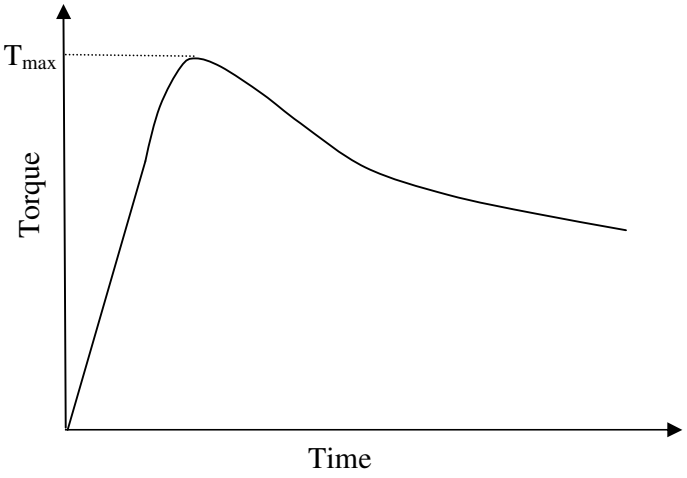

Figure 5.3 : Typical torque-time curve

(Nguyen and Boger, 1983)

Equation 5.4 :

$$\tau_y = T_{\max} / K$$

$$K = \left[\left(\pi D^3\right)/2\right] \times \left[L/D + 1/3\right]$$

where τ_y = yield stress [Pa]

T_{max} = maximum torque [Nm]

D = vane diameter [m]

L = vane length [m]

Accurate yield stress measurement can only be achieved if the vane is rotated at sufficiently low speeds. Nguyen and Boger (1983) suggested that the suitable operating range for vane rotational speeds is in the order of 0.1-8 rpm.

Nguyen and Boger (1985) established the following criteria to minimise interference effects from vane dimensions and rigid boundaries (side walls and bottom of container) as described in Figure 5.2 :

- $L/D < 3.5$
- $D_T/D > 2.0$
- $H_1/D > 1.0$
- $H_2/D > 0.5$

The vane method may be considered superior to other direct yield stress measurement techniques due to the fact that wall slip is eliminated, it operates under static conditions and the vane geometry is such that the material is not significantly disturbed prior to the measurement by the introduction of the vane. It is therefore an attractive method for the study of thixotropic materials that are sensitive to previous shear history (Nguyen and Boger, 1983; Nguyen and Boger, 1992).

Inclined plane test

This technique is based on the static stability of a yield stress material on an inclined plane. It involves an infinitely large plane on which a material of layer thickness H is placed as illustrated in Figure 5.4. The angle of inclination of an initially horizontal plane is increased until a critical angle θ is reached at which the stationary material layer starts to show the first signs of flow (Uhlherr et al, 1999; Nguyen and Boger, 1992).

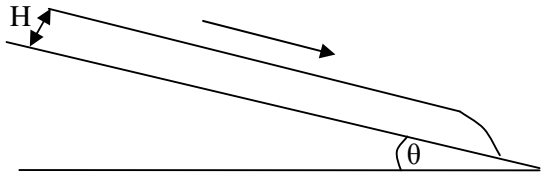

Figure 5.4 : Inclined plane test

The yield stress is then calculated from Equation 5.5 based on a force balance on a differential element of material (Uhlherr et al, 1999; Nguyen and Boger, 1992).

Equation 5.5 :

$$\tau_y = \rho g H \sin\theta$$

where τ_y = yield stress [Pa]

ρ = material density [kg/m^3]

g = 9.81 [m/s^2]

H = material layer thickness [m]

The accuracy of this method depends highly on the accurate measurement of the critical angle of inclination. In the case of thixotropic materials, the time allowed for the material to remain at rest after pouring it onto the plane before the yield stress measurement is conducted, might influence the observed yield stress values. It is therefore essential as with most rheological measurements that a repeatable experimental procedure is developed.

Particle segregation has a seriously negative effect on the accuracy of this method, mainly due to the formation of a region of increased solids concentration at the plane surface. The yield stress, which is a strong function of solids concentration, might then be significantly higher close to the plane surface, resulting in the yield surface not coinciding with the plane surface when the material starts to flow. The effective layer thickness is then unknown and the use of Equation 5.5 is likely to overestimate the actual yield stress (Uhlherr et al, 1999).

5.3 Description of Yield Stress Measurement Equipment

As discussed in Section 3.2.4, the output parameters under consideration in this study are the vehicle component yield stress and the co-disposed tailings material yield stress. The decision to select two different yield stress measurement techniques and to also investigate the correlation between these two methods resulted in the selection of the *vane method* (direct measurement) and *slump test* (indirect measurement) from the potentially applicable yield stress measurement techniques discussed in Section 5.2, to determine the yield stress of both thickened tailings (vehicle) and co-disposed tailings (vehicle + load). The following paragraphs present a description of the specific equipment that was used in this regard.

5.3.1 Vane test equipment

The Paar Physica Rheolab MC1 rotational rheometer was used in conjunction with two steel vane attachments to measure the material yield stress according to the vane method. The dimensions and yield stress measurement range of each of the vanes are presented in Table 5.1. Figure 5.5 shows a picture of the rheometer with both vane attachments.

This rheometer is operated through the US 200 Paar Physica software. The software instructions for use of this rheometer were obtained from Gawu (2004) and are presented in Appendix F.

Table 5.1 : Vane characteristics

	Vane diameter [mm]	*Vane length [mm]*	*Max. yield stress [Pa]*
Medium vane	25	60	745
Small vane	16	22	13 940

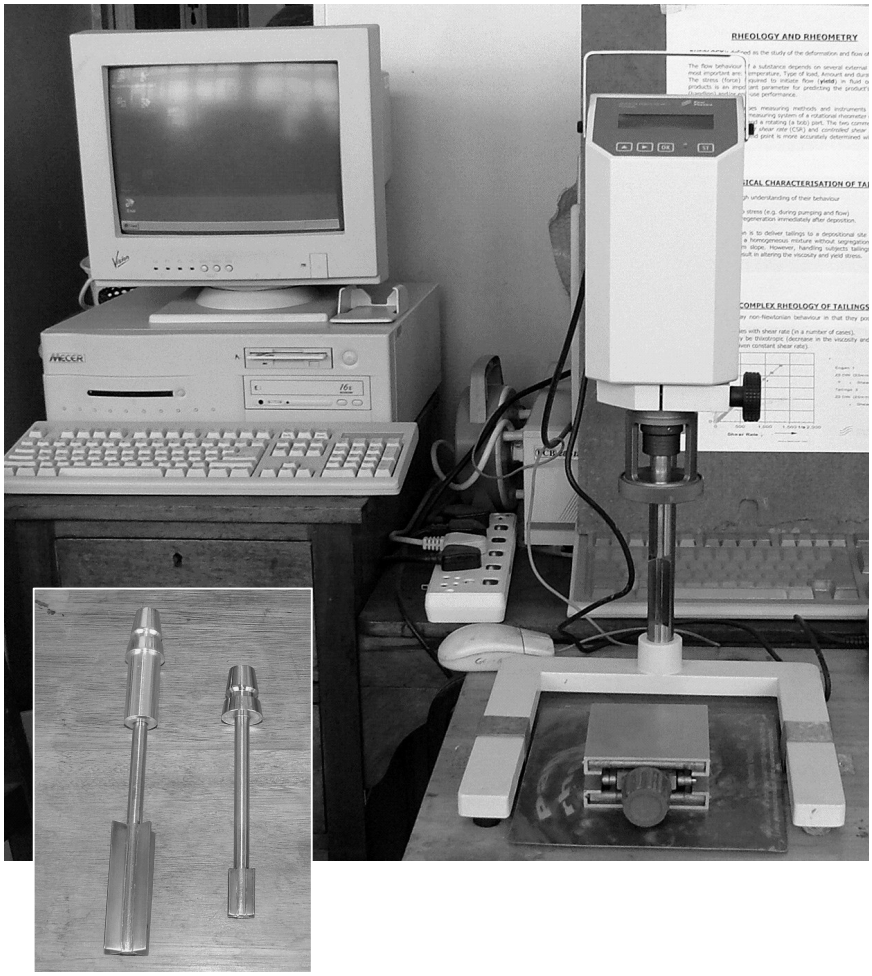

Figure 5.5 : Vane rheometer

5.3.2 Slump test equipment

The slump test was performed using a cylindrical geometry as advised by Pashias et al (1996). Two different sized cylinders were used – a small cylinder was selected as the standard slump test container in this study, while a large cylinder was used for limited test work to investigate the claim by Clayton et al (2003) that the yield stress is predicted more accurately with a taller cylinder. The characteristics of both cylinders are presented in Table 5.2.

Table 5.2 : Slump container characteristics

Slump container	*Material*	*Diameter [mm]*	*Height [mm]*	*Aspect ratio*
Small cylinder	PVC	105	130	1.24
Large cylinder	PVC	186	186	1.00

Besides the slump container, the slump test equipment consists of a slump tray, metal ruler and vernier. The slump tray forms the surface on which the slump test is performed and which is often demarcated with concentric circles to provide an indication of the radial flow distance of the slumped material. The metal ruler is used to provide a horizontal plane representing the height of the slump container from which the slump height is measured. The slump height is measured with a vernier as the distance between the middle point of the slumped material and the height of the slump container, as described in Figure 5.1. Figure 5.6 and Figure 5.7 present the slump test equipment used respectively with the small and large cylinders.

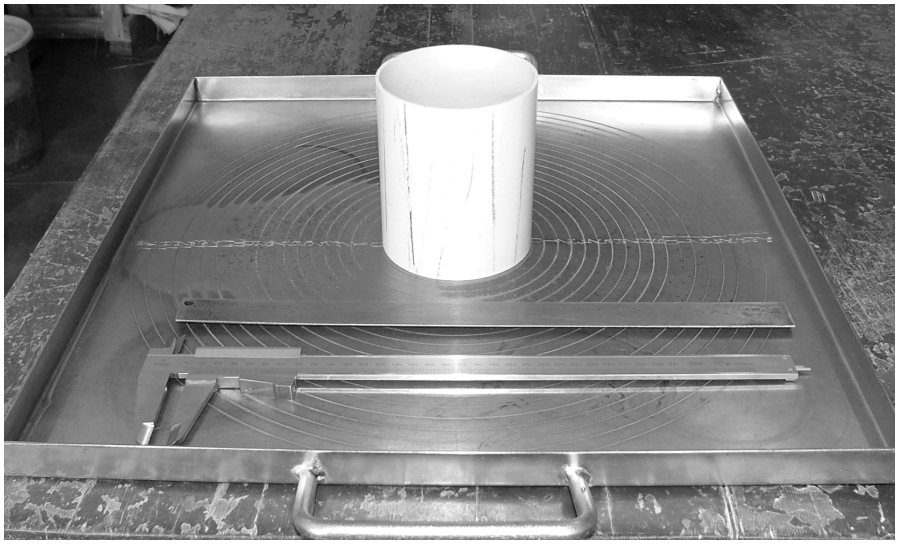

Figure 5.6 : Small slump test equipment

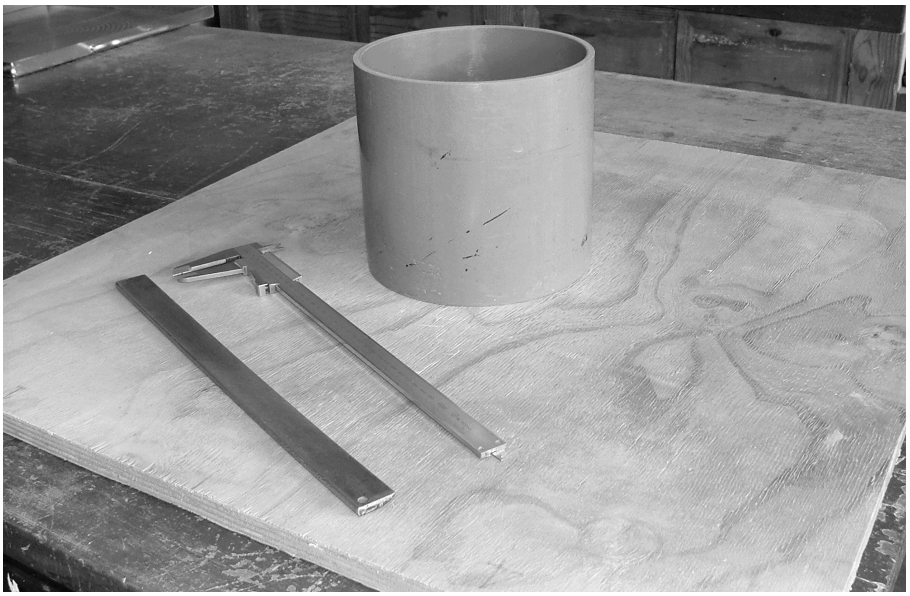

Figure 5.7 : Large slump test equipment

6. EXPERIMENTAL PROCEDURES

This chapter presents the experimental procedures that were followed in the measurement of the output parameters, i.e. vehicle component yield stress and co-disposed material yield stress. The procedures used in the preparation of the test materials and the manipulation of the input parameters, are covered in Chapter 4.

6.1 Preliminary Tests to Establish Experimental Procedures

In order to establish experimental procedures appropriate to the scope of this study, some preliminary test work was conducted to determine the following:

- *Sensitivity of the vehicle rheology to shear history*
  The scope of this study does not include shear history as a variable input parameter (refer to Table 3.1). It is therefore important to keep the shear history constant through the development of repeatable material preparation and experimental procedures.

- *Vane rheometer settings*
  In order to most accurately observe the yield point of a material with the vane method, it is important to select the most suitable settings of the vane rheometer for the specific material under investigation, which in this case is flocculated kimberlite tailings material.

6.1.1 Sensitivity of the vehicle rheology to shear history

The sensitivity of the vehicle rheology to shear history was determined by investigating the influence of the time of shear and the time of recovery on the vehicle rheology.

The vehicle component at the natural pH and a solids concentration in the order of 64-65% (by mass) was used as the test material in this preliminary work. The

response of the vehicle rheology to shear history was assessed through the vehicle yield stress, measured directly with the vane method. The settings of the vane rheometer used in this preliminary test work are presented in Table 6.1.

Table 6.1 : Preliminary settings of vane rheometer

Paar Physica Rheolab MC1 preliminary settings	
Vane size	Medium
Vane immersion	Flush with material surface
Vane rotational speed	0.3 rpm
Number of data points	100
Time per data point	2 s
Test duration	200 s

Influence of time of shear on vehicle rheology

A freshly prepared material was sheared with a handheld kitchen mixer set at a constant maximum speed, for increasing time periods. The material yield stress was measured immediately after each shear interval. No standing time was allowed between test runs, apart from the ±30 seconds it took to move the container and insert the vane for the yield stress measurement.

Figure 6.1 presents the results obtained. A summary of the raw data is provided in Appendix G. It is evident from Figure 6.1 that the material reached its equilibrium state after only 5 minutes of shear. Increasing the time of shear beyond 5 minutes had no significant effect on the yield stress value.

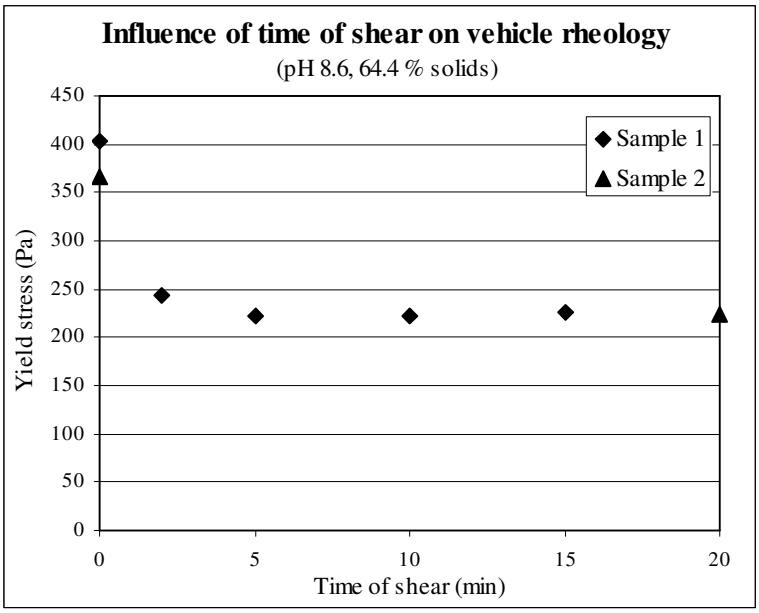

Figure 6.1 : Influence of time of shear on vehicle rheology

The fact that the material reached its equilibrium state after such a short period of shear indicated a somewhat weak inter-particle network structure and therefore possibly a limited degree of particle interaction. It was already established in Section 4.5.2 that the natural state of the vehicle thickened tailings exhibited little to no particle interaction on a microscopic scale due to the combined surface chemistry effects of the suspension pH and ion exchanged nature of the clays. The macroscopic particle interaction provided here by flocculation, was therefore the dominant mechanism holding the inter-particle network structure together. Such a network structure is however, very susceptible to breakdown under shear as the flocculant bonds between particles are generally fairly weak under optimum flocculation conditions. The residual yield stress at the equilibrium state could be attributed to the high solids concentration of the material.

Influence of time of recovery on vehicle rheology

A freshly prepared material was sheared to the equilibrium state using a handheld kitchen mixer set at a constant maximum speed for a period of 5 minutes, after which the vane was left in position and the material allowed to recover at rest in

the absence of shear for a certain time period. This procedure was repeated at increasing recovery times. The recovered yield stress was measured at the end of each recovery period.

Figure 6.2 presents the results obtained. A summary of the raw data is provided in Appendix G. It is evident from Figure 6.2 that the material recovered back to the initial state within about 20 minutes at rest.

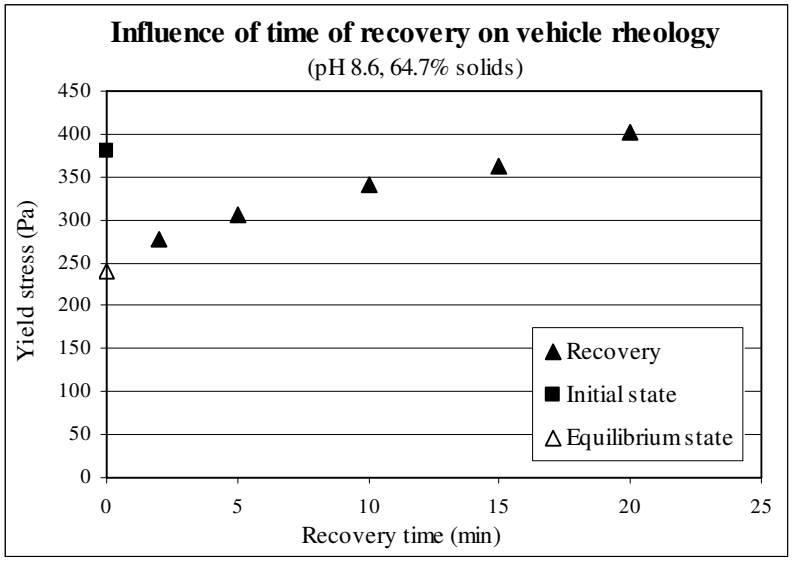

Figure 6.2 : Influence of time of recovery on vehicle rheology

This behaviour is attributed to the reformation of the inter-particle network structure at rest. The increasing yield stress with recovery time could possibly be due to increasing macroscopic particle interaction as a result of the reformation of broken flocculant bonds, as the surface chemistry effects controlling the microscopic particle interaction remained unchanged. When flocculated aggregates are subjected to shear, the flocculant polymer chains bridging between particles are broken. This leads to the exposure of active bonding sites on the polymer chains where particles can attach again and reform into flocculated aggregates. It therefore appears that the more the material is sheared, the more its reformation is induced. This aspect was also observed by Sofra and Boger (2000),

which referred to it as an increase in the structural reformation rate with increasing shear due to an increasing number of bonding sites available.

The fluctuation observed in the torque value over time on the raw data curves obtained in this test work (refer to Appendix G), suggested the continuous breakdown and reformation of flocculant bonds under shear. As the material was allowed to recover at rest in the absence of shear for longer periods of time, more and more flocculant bonds reformed and more flocculated aggregates were generated, leading eventually to a new reformed inter-particle network structure after a recovery period of 20 minutes. The latter exhibited more efficient macroscopic particle interaction than before, possibly due to the re-arrangement and re-attachment of particles and broken flocculant polymer chains, resulting in a yield stress value slightly exceeding that of the material in the initial state. It is believed that an increase in the structural reformation rate was induced during each shear interval.

Yield stress measurement of the recovered material produced torque-time curves exhibiting a sharp peak in torque followed by a rapid drop-off in torque over time (refer to Appendix G). This behaviour indicated that the reformed inter-particle network structure was probably even more susceptible to breakdown under shear than the initial state material.

Conclusion

For thixotropic materials that are highly sensitive to shear history, difficulties might be experienced in ensuring that different materials are in the same structural state for fair comparison. In order to remove the effect of the shear history, rheological test work is often conducted at the material equilibrium state where there is certainty about the structural state of the material (Sofra and Boger, 2000).

Most thixotropic materials also take a considerably longer time to recover than it takes for the inter-particle network structure to breakdown under shear. This

aspect is particularly displayed by the difference in time scales in the red mud example presented in Figure 2.10 in Section 2.3.2 (Nguyen and Boger, 1998).

The preliminary test work showed however, that the flocculated kimberlite thickened tailings, considered in this study as the vehicle component, exhibited relatively high rates of both structural breakdown and reformation. Considering structural breakdown under shear in this study, the material would be subjected to variable amounts of shear during the manipulation of the input parameters mainly due to manual mixing at each dilution or pH modification step as discussed in Section 4.5. It is difficult to control the amount of shear introduced to the material as various degrees of mixing might be required at various times to ensure a thoroughly mixed material. A problem exists in that there is no certainty of the final structural state of the thoroughly mixed material.

It was reasoned then that if the thoroughly mixed material is allowed to recover at rest for a long enough time, the same material structural state would be reached regardless of the amount of shear the material was subjected to in the first place, thereby enabling the fair comparison of different materials. The high rate of structural reformation found in the material used in this study was used to the advantage of this strategy. In order to avoid impractically long recovery times, a time period of 5 minutes was selected as the appropriate recovery period necessary to bring materials subjected to different amounts of shear to the same recovered structural state, thereby keeping the shear history as constant as possible. This resulted in the inclusion of a 5 minute recovery period between test material preparation and yield stress measurement in the experimental procedures.

6.1.2 Vane rheometer settings

The standard settings of the Paar Physica Rheolab MC1 rheometer for yield stress measurement through the vane method are presented in Table 6.1. These settings were successfully used by Gawu and Fourie (2004) on gold, zinc and mineral sands tailings materials.

The shape of the torque-time curves obtained during the preliminary test work described in the previous paragraphs suggested however, that the standard settings on the vane rheometer might not be entirely suitable to flocculated kimberlite tailings. The shape of the torque-time curves presented a problem in that a clear peak or maximum torque value representing the yield point of the material could not always be identified, as displayed by a typical problematic result in Figure 6.3.

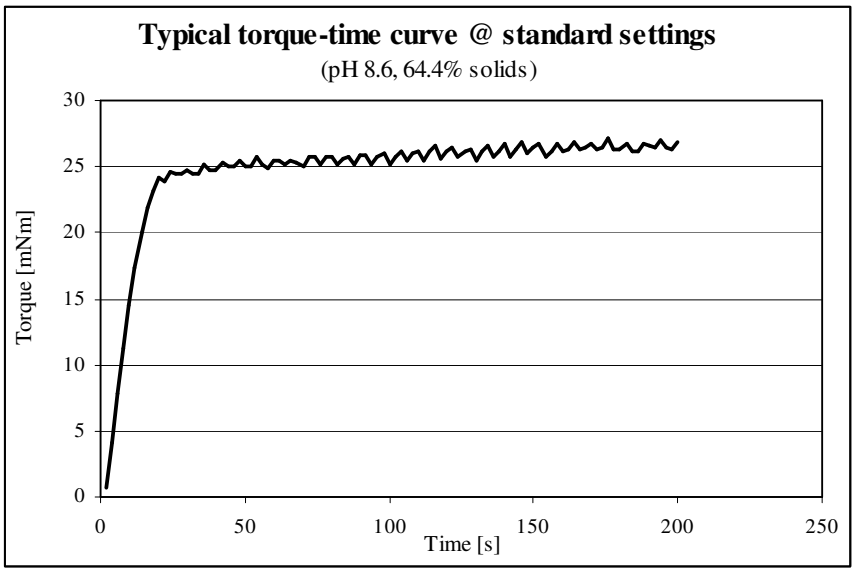

Figure 6.3 : Typical torque-time curve at standard rheometer settings

This prompted an investigation into the vane rheometer settings with particular focus on the vane rotational speed and the software sampling rate used in the generation of the torque curve.

Vane rotational speed

Nguyen and Boger (1983) suggested that the suitable operating range for vane rotational speeds is in the order of 0.1-8 rpm. They acknowledged that in order to minimise unforeseen errors all the vane measurements in their work were carried out at the lowest possible speed of 0.1 rpm. If the rotational speed of the vane is too high, viscous resistance and instrument inertia effects could introduce

significant errors to the measured maximum torque and subsequent calculation of the material yield stress value.

The lowest possible speed of the Paar Physica Rheolab MC1 rheometer is 0.3 rpm according to its operational manual. It was therefore decided to keep the rotational speed of the vane at the standard setting of 0.3 rpm, as it was not physically possible to reduce it any further.

Software sampling rate

The software sampling rate refers to the rate at which the continuously measured torque is sampled to produce a certain number of data points over the duration of the test in order to generate the torque-time curve. The standard software sampling rate is 2 seconds, which results in a test duration of 200 seconds when 100 data points are used, as displayed in Table 6.1.

Sofra (2004) suggested a much higher software sampling rate, which corresponds to a much shorter time period per data point. It might be possible that the true material yield point is not detected due to the "smoothing out" effect of the lower software sampling rate on the measured torque data. Sofra (2004) suggested the use of 400 data points over a period of 1-2 minutes.

The vane rheometer settings presented in Table 6.2 proved to be successful in the accurate detection of the maximum torque value representing the material yield point and are regarded as the most suitable settings for the specific material used in this study. Figure 6.4 displays a typical torque-time curve obtained with the new vane rheometer settings. The maximum torque value (peak) is clearly visible.

Table 6.2 : Most suitable vane rheometer settings

Paar Physica Rheolab MC1 preliminary settings	
Vane size	Small or Medium
Vane immersion	Flush with material surface
Vane rotational speed	0.3 rpm
Number of data points	400
Time per data point	0.3 s
Test duration	120 s

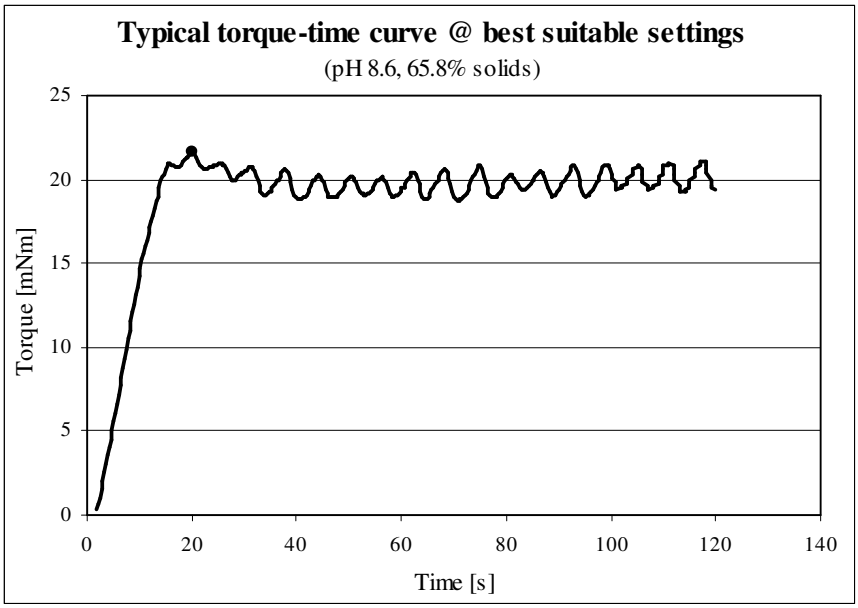

Figure 6.4 : Typical torque-time curve at most suitable rheometer settings

6.2 Experimental Procedures

6.2.1 Direct yield stress measurement with the vane test

This section provides a step by step description of the experimental procedure that was followed in the direct measurement of the yield stress of respectively the vehicle component and the co-disposed tailings material, using the vane method.

- Prepare the test material according to the procedures described in Section 4.2 (vehicle component) and Section 4.4 (co-disposed tailings).
- Set-up the vane rheometer with the settings presented in Table 6.2 using the software instructions described in Appendix F.
- Attach a vane of appropriate size to the rheometer.
- Fill a 500 ml plastic beaker with about 400-450 ml of the test material.
- Manipulate the input parameters to the desired levels according to the procedures described in Section 4.5.
- Tap the beaker on a solid surface to remove any air bubbles and to level the material surface.
- Place the beaker on a laboratory jack directly underneath the vane.
- Insert the vane into the middle of the material by carefully hoisting up the beaker using the laboratory jack until the top of the vane is flushed with the material surface.
- Allow the material to stand like this with the vane inserted for a recovery period of 5 minutes.
- During this time ensure that the vane rheometer is set-up correctly and ready for starting the test.
- Start the vane test immediately after the recovery period.
- Upon completion of the vane test, view the torque-time curve and if satisfactory save the raw data according to the procedure described in Appendix F.
- Lower the beaker using the laboratory jack.
- Remove the vane and clean it.

- Stir the material in the beaker for a few seconds to ensure that it is properly mixed again.
- Repeat each vane test three times in order to calculate an average maximum torque value, which is then converted to yield stress.

6.2.2 Indirect yield stress measurement with the slump test

This section provides a step by step description of the experimental procedure that was followed in the indirect measurement of the yield stress of respectively the vehicle component and the co-disposed tailings material, using the slump test.

- Prepare the test material according to the procedures described in Section 4.2 (vehicle component) and Section 4.4 (co-disposed tailings).
- Set-up the appropriate slump test equipment on a level surface and ensure that the slump cylinder is placed in the middle of the slump tray.
- Manipulate the input parameters to the desired levels according to the procedures described in Section 4.5.
- Fill the slump cylinder to the brim with the test material.
- Remove any air bubbles with the tamping rod.
- Smooth the material surface level with the top of the slump cylinder using the metal ruler.
- Allow the material to stand like this for a recovery period of 5 minutes.
- At the end of the recovery period, immediately pull the slump cylinder straight up, allowing the material to slump under its own weight.
- Place the slump cylinder next to the slumped material on the slump tray without disturbing the slumped material in any way.
- Place the metal ruler over the top of the slump cylinder so that it extends over the slumped material to provide a measure of the cylinder height.
- Measure the slump height as the distance between the top of the slumped material and the top of the slump cylinder, using a vernier. Ensure that this measurement is conducted from the exact middle point of the slumped material.

- Measure the radial flow distance of the slumped material in four directions, i.e. north, south, east and west, using the rings drawn on the surface of the slump tray. If the radial flow distance of the slumped material appears to be significantly unsymmetrical, the test should be repeated.
- Upon completion of these measurements and recording of the data, scoop the material back into the sample storage container.
- Clean the slump cylinder and tray.
- Repeat each slump test three times in order to calculate an average slump height, which is then converted to yield stress.

7. RESULTS AND DISCUSSIONS

This chapter focuses on the presentation of the results obtained in this study and the explanatory discussions around it.

7.1 Vehicle Component

The first part of this study focussed on the manipulation of the vehicle rheology. This objective translated in more specific terms to the determination of the vehicle component yield stress as a function of solids concentration and pH at the natural ion exchanged state of the clays, using two different measurement techniques. The following paragraphs present a summary of the results and observations in this regard. Refer to Appendices H-J for the relevant detailed raw data.

7.1.1 Manipulation of vehicle component yield stress

Figure 7.1 presents the results obtained in the direct and indirect yield stress measurement of the vehicle component with respectively the vane and slump test methods, across the solids concentration and pH ranges considered in this study.

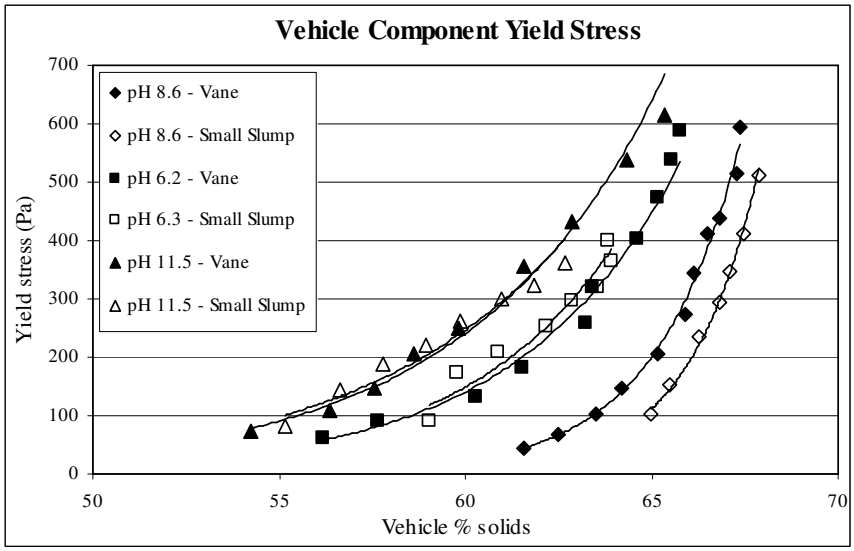

Figure 7.1 : Vehicle component yield stress

Exponential trend

Figure 7.1 displays the typical exponential increase in yield stress with increasing solids concentration as would be expected from a material within the thickened tailings continuum (Jewell, 2002). It is noted that this behaviour is only evident from a much higher solids concentration at pH 8.6 than at the other pH values, thereby allowing the material to reach higher solids concentrations before a significant increase in yield stress is realised.

Exponential trend lines of the form described in Equation 7.1 were fitted to the experimental data points in Figure 7.1. The values of the respective constants and correlation coefficients (R^2 value) of each trend line are presented in Table 7.1.

Equation 7.1 :

$$y = a\, e^{bx}$$

where y = vehicle component yield stress [Pa]

x = vehicle component % solids by mass [%]

a and b = constants

Table 7.1 : Exponential trend line information

pH	*Measurement technique*	*Exponential trend line information*		
		a	b	R^2
8.6	Vane	9E-11	0.4380	0.9972
	Small slump	8E-14	0.5362	0.9935
6.2	Vane	1E-04	0.2313	0.9873
	Small slump	7E-05	0.2420	0.9153
11.5	Vane	2E-03	0.1948	0.9884
	Small slump	4E-03	0.1840	0.9428

Effect of particle interaction

A distinctly different relationship between yield stress and solids concentration is observed in Figure 7.1 for each of the suspension pH values under consideration. The reason for this behaviour is a variation in the degree of particle interaction across suspension pH as identified by Vietti (2004) in his kimberlite thickened tailings behavioural model.

The results presented in Figure 7.1 confirmed the proposed behaviour at the natural ion exchanged state of the clay material (ESP = 32%) considered in this study, as discussed in Section 4.5.2 and presented again for easy reference in Figure 7.2.

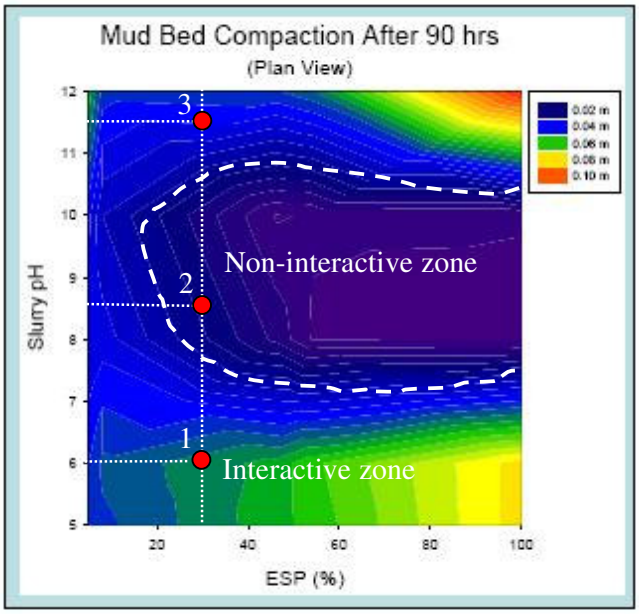

Figure 7.2 : Proposed effect of particle interaction
(Kimberlite thickened tailings behavioural model by Vietti, 2004)

The natural state of the material at pH 8.6 can be described as non-interactive, as a low yield stress indicative of limited to no particle interaction is exhibited. At pH 6.2 and 11.5, a high yield stress indicative of a moderate to high degree of particle interaction is exhibited and the material can therefore be described as interactive.

The degree of particle interaction dictates the strength of the inter-particle network structure and therefore the yield stress (Nguyen and Boger, 1983). The variation in the degree of particle interaction is therefore evident in the significant increase in yield stress when the material is moved from a non-interactive to interactive state at the same solids concentration. Table 7.2 provides a specific example of this behaviour.

Table 7.2 : Vehicle yield stress as a function of pH

Vehicle % solids	*pH*	*Yield stress [Pa]*	*Particle interaction*
62	8.6	56	Non-interactive
62	6.2	169	Interactive
62	11.5	352	Interactive

Vane test observations

The particle interaction effect was also reflected in the shape of the torque-time curves obtained during the vane test work as illustrated by the typical examples in Figure 7.3. The shape of the torque-time curves obtained at pH 6.2 and 11.5 where the material is in the interactive state are similar, but significantly different to that obtained at pH 8.6 where the material is in the non-interactive state.

At pH 6.2 and 11.5, the maximum torque value representing the material yield point, is followed by a steep decline in torque over time. This behaviour is mainly attributed to the progressive destruction of inter-particle bonds under shear. The residual torque value at the end of the test is significantly lower than the maximum torque value, indicating the breakdown of a considerable degree of inter-particle structure under shear. The degree of particle interaction is largely dominated by the microscopic clay surface chemistry effects, which are locked into place by the macroscopic effects of flocculation.

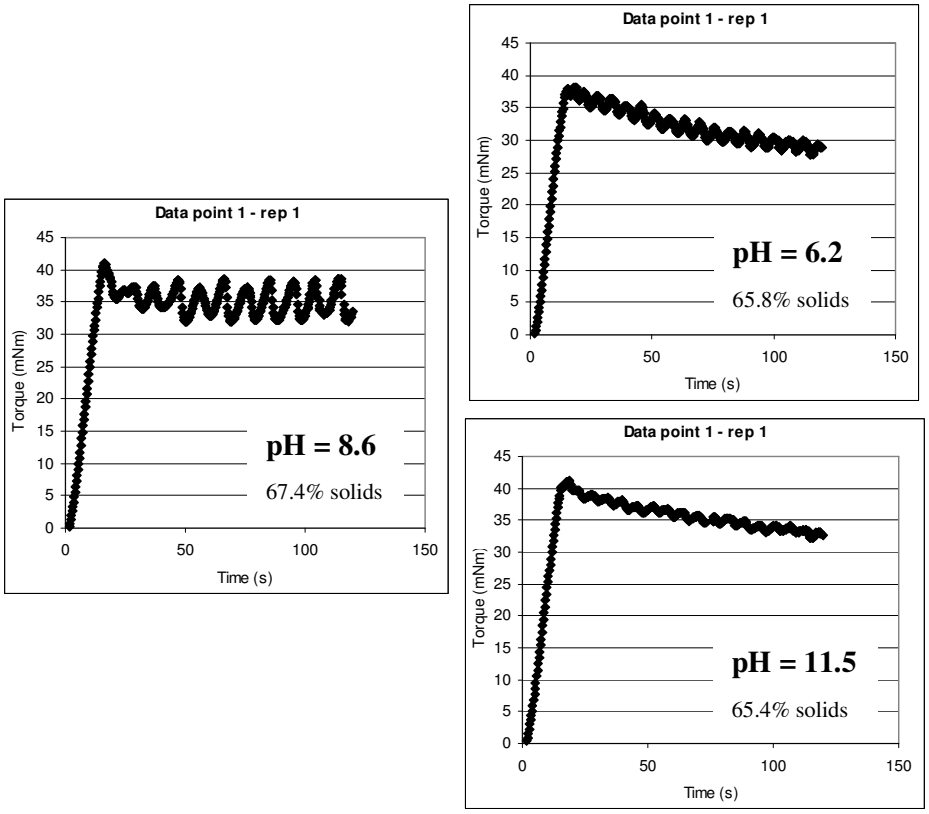

Figure 7.3 : Shape of typical vehicle component torque-time curves

At pH 8.6, the maximum torque value is followed by period of significant fluctuation in the torque value over time. The torque value fluctuated around a residual value close to the maximum torque value, which indicates that only a limited degree of particle interaction was broken down under shear. In this case the degree of particle interaction is largely dominated by the macroscopic effects of flocculation in the absence of microscopic particle interaction due to clay surface chemistry effects. This also explains the more pronounced fluctuation observed in the torque value as a result of the continuous breakdown and reformation of the flocculant bonds under shear.

Slump test observations

Figure 7.4 presents the average radius of the radial flow distance of the slumped material, across the solids concentration and pH ranges considered in this study.

The horizontal broken line in Figure 7.4 presents the radius of the small slump cylinder at 52 mm and indicates the lower limit of the radial flow distance.

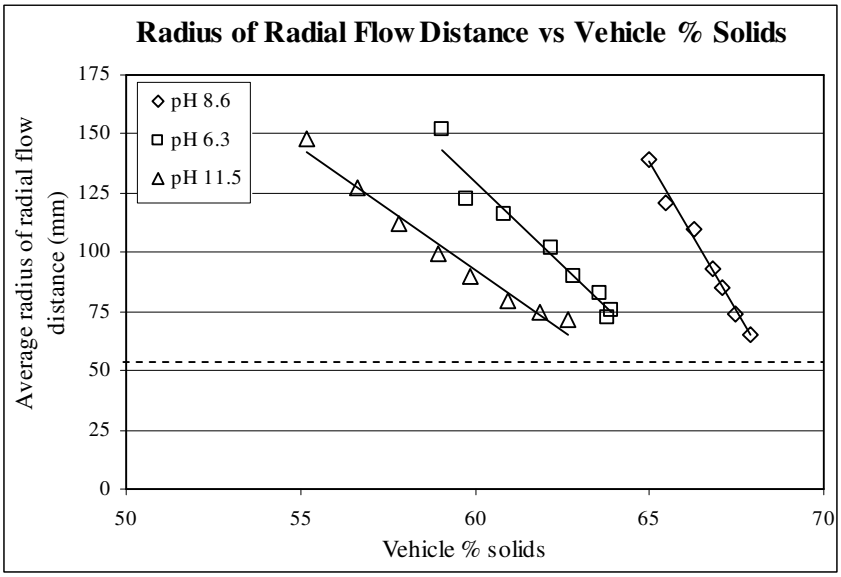

Figure 7.4 : Radius of slumped material radial flow distance

The radial flow distance of the slumped material is obviously closely related to its slump height as illustrated in a typical example in Figure 7.5.

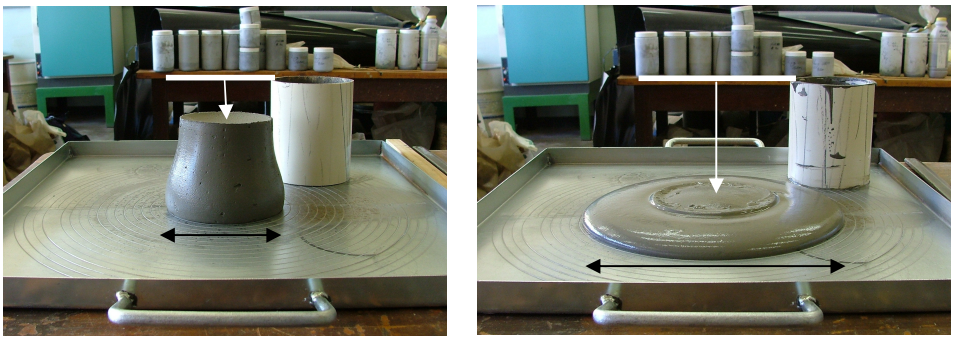

Vehicle – pH 8.6 , 67.9% solids

Vehicle – pH 8.6 , 65.0% solids

Figure 7.5 : Relationship between slump height and radial flow distance

As the vehicle solids concentration increases at a specific pH value, the slump height and radial flow distance decrease. Figure 7.5 shows that the decrease in

average radial flow distance with increasing solids concentration is much steeper at pH 8.6 than at the other pH values. This behaviour corresponds well with a similar steeper increase in yield stress with increasing solids concentration at pH 8.6 in Figure 7.1. This behaviour could be explained due to the fact that limited to no particle interaction is exhibited at pH 8.6, which allows the material to reach high solids concentrations before a significant increase in yield stress is realised. The increase in yield stress is then mainly due to the restriction of particle movement as a result of high solids concentration combined with the effects of flocculation.

Vehicle component design

Figure 7.1 shows that the same yield stress value could be obtained through various combinations of solids concentration and suspension pH. Table 7.3 provides a specific example of this behaviour.

Table 7.3 : Example of input parameter combinations

Yield stress [Pa]	*pH*	*Vehicle % solids*
200	8.6	64.9
200	6.2	62.7
200	11.5	59.1

A major advantage of this behaviour is that it enables the design of a vehicle component with a specific and consistent yield stress value as dictated by the depositional requirements, through appropriate manipulation of the vehicle solids concentration and suspension pH.

7.1.2 Correlation between yield stress measurement techniques

Vane and small slump

Figure 7.1 essentially presents the accuracy of the "50c rheometer correlation" developed by Pashias et al (1996) to link the direct yield stress determined by the vane method with the indirect yield stress determined by the slump test method. The direct and indirect yield stress seemed to correlate well at pH 6.2 and 11.5 where a moderate to high degree of particle interaction occurred. At pH 8.6 where limited to no particle interaction occurred, a poor correlation between the direct and indirect yield stress was observed.

In order to further assess the correlation between the direct and indirect yield stress, the respective exponential trend lines were plotted against each other over a vehicle solids concentration range of 50-70%, as illustrated in Figure 7.6.

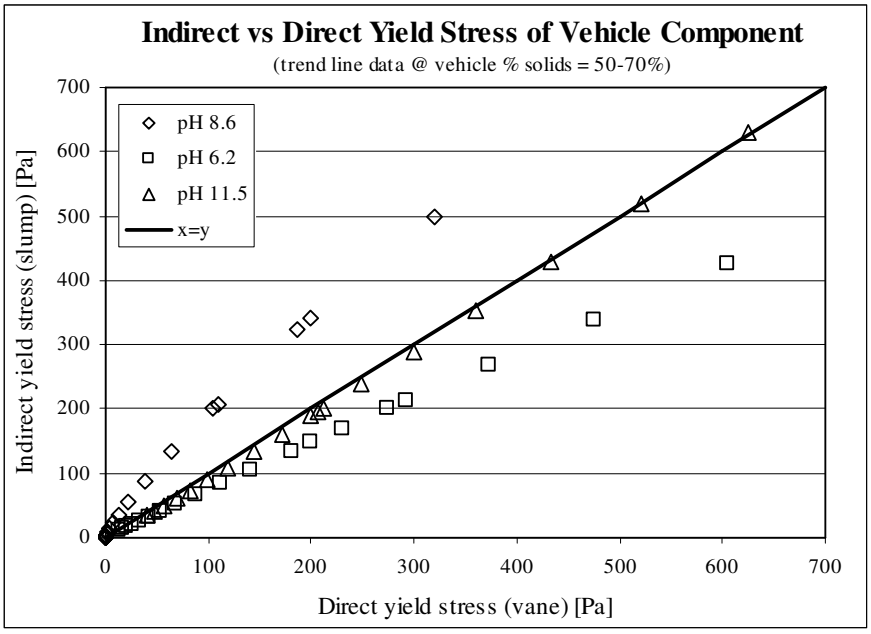

Figure 7.6 : Correlation between direct and indirect vehicle yield stress

Figure 7.6 shows a very good correlation between the direct and indirect yield stress measurement of the vehicle component at pH 11.5. At pH 6.2, the slump

test provided significantly overestimated yield stress values, while at pH 8.6 significantly underestimated yield stress values were obtained with the slump test. The relative error percentage between the exponential trend line data of the direct and indirect vehicle yield stress as presented in Figure 7.6 was calculated according to Equation 7.2. Average values of the absolute relative error percentages are presented in Table 7.4 for the pH values under consideration in this study and over the vehicle solids concentration range at which the fitted exponential trend lines are valid.

Equation 7.2 :

$$Error\ \% = \left((\tau_i - \tau_d) / \tau_d \right) \times 100$$

where τ_i = indirect yield stress determined with the slump test [Pa]

τ_d = direct yield stress determined with the vane test [Pa]

Table 7.4 : Relative error between direct and indirect vehicle yield stress

pH	*Slump cylinder*	*Average relative error %*	*Vehicle % solids range*
8.6	Small	44.8	60-70
6.2	Small	33.1	55-65
11.5	Small	4.8	55-65

Table 7.4 shows that the relative errors between the direct and indirect yield stress at pH 6.2 and 8.6 are significantly large and unacceptable.

Clayton et al (2003) discovered a link between the height of the slump cylinder and the point at which a poor correlation between the vane and slump yield stress measurement techniques became evident. For a slump cylinder with a height of 120 mm, a poor correlation between direct and indirect yield stress was only

observed beyond yield stress values of 500 Pa and for a slump cylinder height of 200 mm, no deviation from the ideal solution was observed. Clayton et al (2003) therefore concluded that a taller slump cylinder provided a more accurate prediction of the material yield stress.

In the light of the findings of Clayton et al (2003), it was therefore expected that a slump cylinder with a height of 130 mm as used in this study, would yield a good correlation between the direct and indirect yield stress measurement techniques at least up to yield stress values of 500 Pa. The results presented in Figure 7.6 only conform to the findings of Clayton et al (2003) at pH 11.5 and not at the other pH values.

A decision was then made to investigate this problem further through additional slump test work on the vehicle component in the non-interactive state at first.

Vane and large slump

A large slump cylinder with a height of 186 mm, as described in Section 5.3.2, was used to investigate the claims of Clayton et al (2003) for a vehicle component in the non-interactive state.

Due to a lack of sample material, fresh samples had to be prepared for the additional work during which several problems were experienced. These are included in the following paragraphs for interest sake.

Even though great care was taken to use the same raw materials and to follow the same sample preparation procedures, the new vehicle component sample exhibited a moderate degree of particle interaction at pH 8.5, similar to what was obtained previously for the vehicle component at pH 6.2, as shown in Figure 7.7. The reason for this behaviour is attributed to the possibility that the natural state of the material might be closer to the borderline between the interactive and non-interactive states than indicated in Figure 7.2, which could cause the material to behave significantly different at slight changes in the suspension pH and ion

exchanged state of the clays (ESP). This material can be altered to a conclusively non-interactive state through an increase in suspension pH and/or exchangeable sodium percentage (ESP).

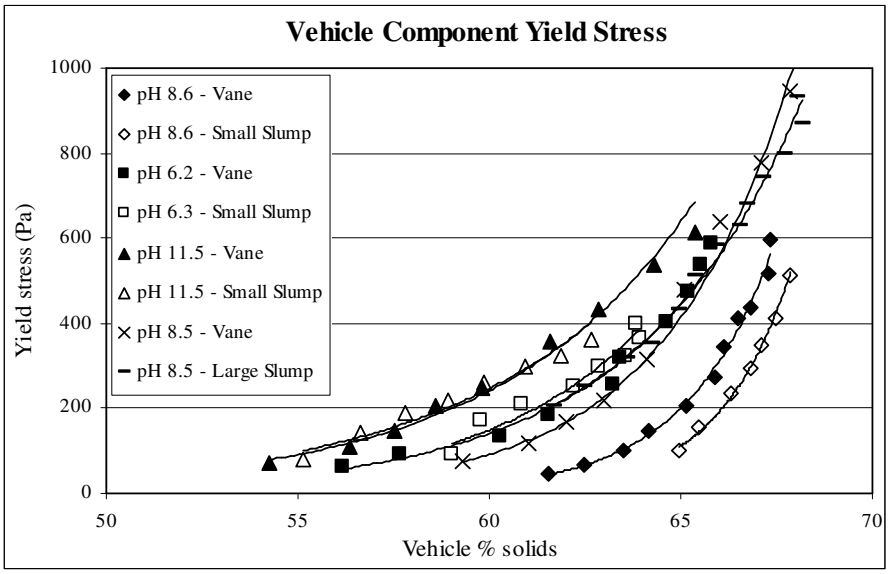

Figure 7.7 : Vehicle component yield stress

Table 7.5 provides information on the exponential trend lines fitted to the experimental data points of the new vehicle component sample, exhibiting interactive behaviour at pH 8.5.

Table 7.5 : Exponential trend line information

pH	*Measurement technique*	*Exponential trend line information*		
		a	b	R^2
8.5	Vane	1E-06	0.3014	0.9946
	Large slump	1E-04	0.2314	0.9933

Although the initial aim of the large slump test work was to investigate the claims of Clayton et al (2003) for a vehicle component in the *non-interactive* state, the

fact that the first newly prepared sample exhibited *interactive* behaviour, provided an opportunity to also investigate these claims for the latter material. This led to the comparison of the results previously obtained with the small slump cylinder for the vehicle component at pH 6.2 and those obtained with the large slump cylinder for the new vehicle component sample at pH 8.5, because both of these materials exhibited interactive behaviour.

Further assessment of the results presented in Figure 7.7 and Table 7.5, made it clear that the accuracy of the correlation between the exponential trend line data of the direct and indirect yield stress of the vehicle in the interactive state, improved only slightly with the use of the larger slump cylinder as displayed in Figure 7.8 and Table 7.6.

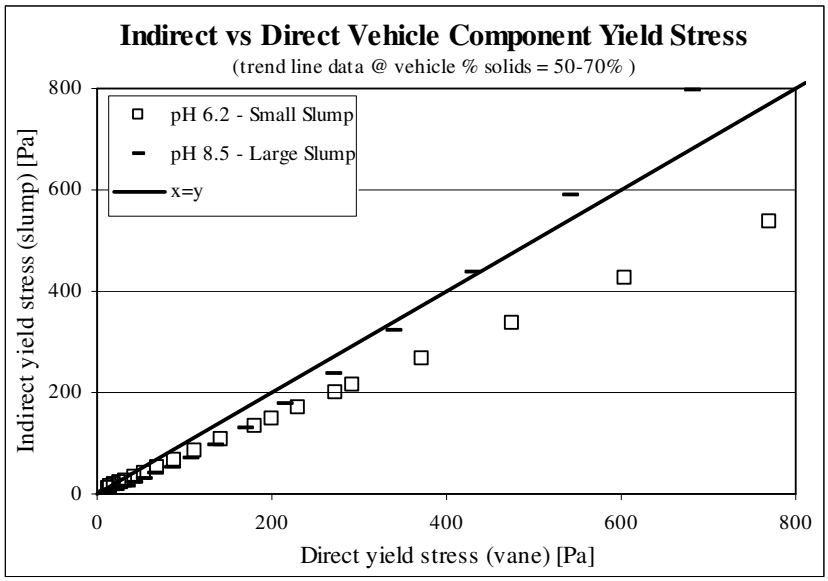

Figure 7.8 : Correlation between direct and indirect vehicle yield stress

Table 7.6 : Relative error between direct and indirect vehicle yield stress

pH	*Slump cylinder*	*Average relative error %*	*Vehicle % solids range*
6.2	Small	33.5	55-65
8.5	Large	20.9	60-70

In an attempt to change the new vehicle component sample from the interactive to non-interactive state, the suspension pH was raised to pH 9.5. Unfortunately, this had no effect on the degree of particle interaction exhibited by the material as illustrated in Figure 7.9. It was concluded then that the ESP of the clay is probably low enough for the suspension pH effect to be overridden by the effect of the ion exchanged nature of the clays, thereby maintaining an interactive state regardless of any change in suspension pH.

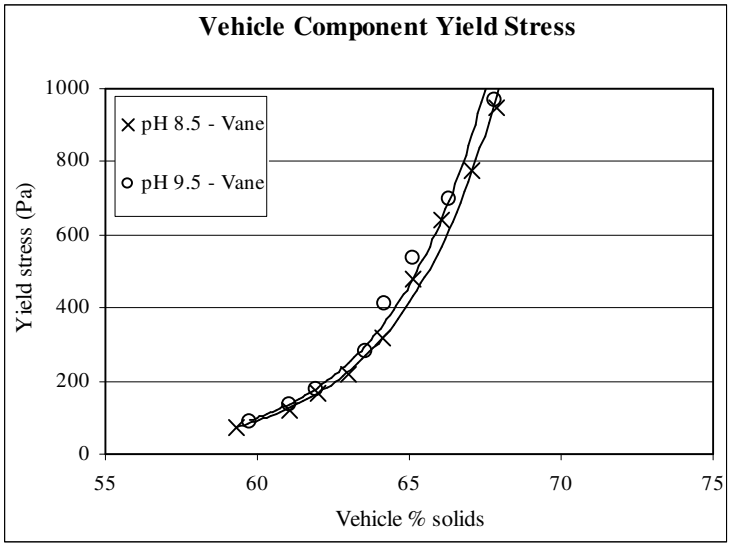

Figure 7.9 : Vehicle component yield stress

In a further attempt to change the new vehicle component sample from the interactive to non-interactive state, the ESP of the material was increased. Fresh material was prepared according to the procedures in Section 4.2, but with the

distilled water used in the slurry preparation step conditioned with 400 mg/l sodium chloride (NaCl) to significantly increase the ESP of the clays. The sodium chloride was added to the water before the dry solids of the vehicle component was mixed in, in order to conduct controlled dispersion of the clay platelets.

Figure 7.10 shows that even with the presumed increase in ESP, the material still behaved as an interactive material when compared to previous results. Upon further investigation it was found that the sodium chloride addition probably exceeded its Critical Coagulation Concentration (CCC). Van Olphen (1977) reports flocculation values (CCC values) for sodium chloride in relation to montmorillonite clays in the sodium and calcium form. Since the purpose of the sodium chloride addition here was to increase the ESP of a largely calcium exchanged clay in order to generate non-interactive behaviour, the sodium chloride CCC range corresponding to calcium exchanged clays as reported by Van Olphen (1977) in milli-equivalents per litre was converted to 58-76 mg/l using Equation E 4 and Equation E 5 in Appendix E. It is therefore clear that the sodium chloride addition of 400 mg/l exceeded its CCC value and induced particle interaction through compression of the electrical double layer around the particles in suspension as a result of high ionic concentration as discussed in Section 2.3.3.

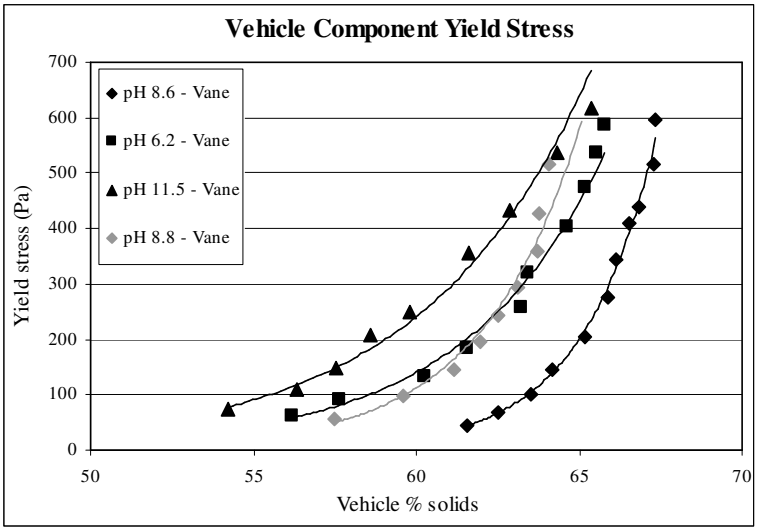

Figure 7.10 : Vehicle component yield stress

In an attempt to lower the ionic concentration of the material, it was washed with distilled water to remove as much of the excess salt as possible. Upon addition of large amounts of distilled water to the material, a highly dispersed slurry was formed, which had to be centrifuged to collect most of the solids before the supernatant containing the excess salt in solution could be decanted.

Figure 7.11 shows that the washed material at pH 8.7 finally behaved as a non-interactive material, similar to what was obtained previously for the vehicle component at pH 8.6.

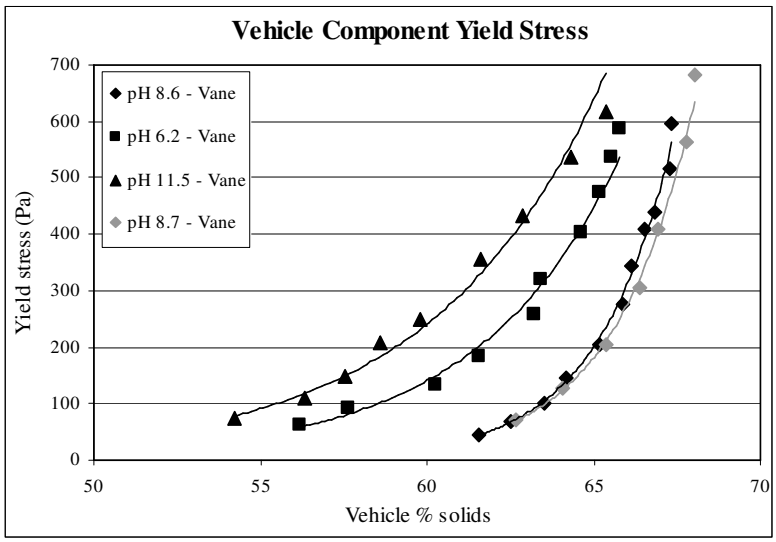

Figure 7.11 : Vehicle component yield stress

Apart from Figure 7.11, the shape of the typical torque-time curve examples presented in Figure 7.12 also show that both these material are in the non-interactive state, exhibiting limited to no particle interaction. This new vehicle component at pH 8.7 was then used in the additional large slump test work to further investigate the claims of Clayton et al (2003) for a vehicle component in the non-interactive state.

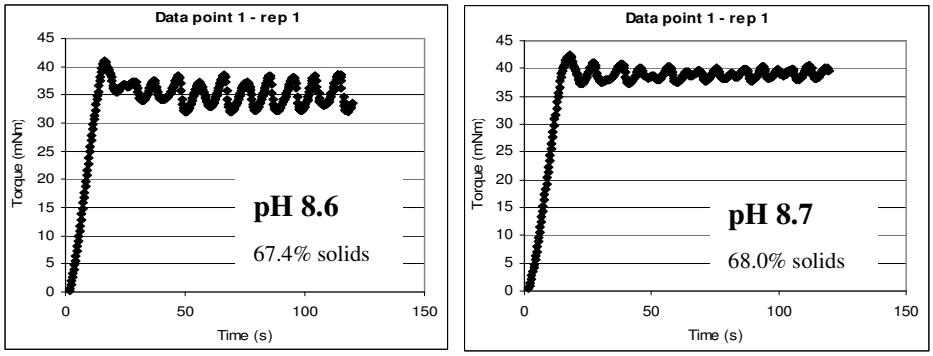

Figure 7.12 : Shape of torque-time curves for a non-interactive vehicle

Figure 7.13 presents the results obtained in the direct yield stress measurement with the vane method and the indirect yield stress measurement with both small and large slump cylinders of the new vehicle component in the non-interactive state at pH 8.7.

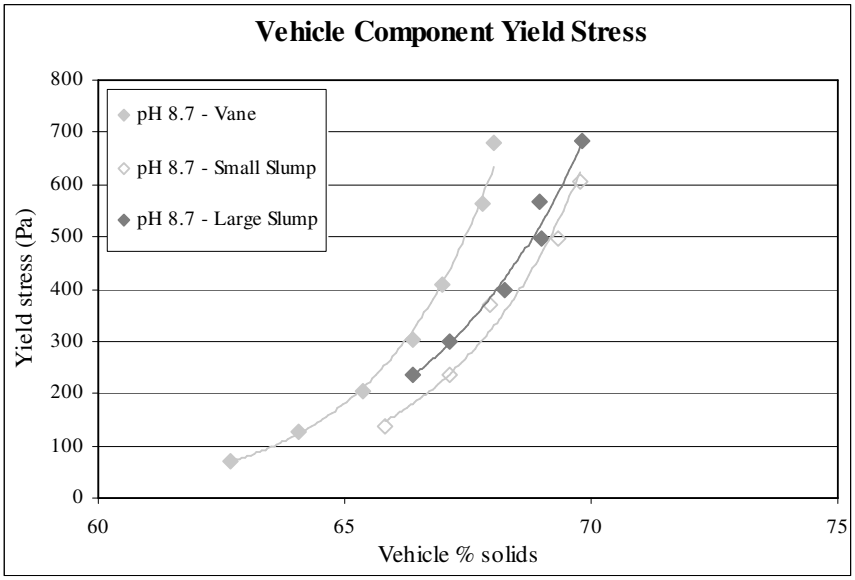

Figure 7.13 : Vehicle component yield stress

Table 7.7 provides information on the exponential trend lines fitted to the experimental data points of the new vehicle component sample, which exhibits non-interactive behaviour at pH 8.7.

Table 7.7 : Exponential trend line information

pH	*Measurement technique*	*Exponential trend line information*		
		a	b	R^2
8.7	Vane	4E-10	0.4139	0.9975
	Small slump	5E-09	0.3649	0.9768
	Large slump	2E-07	0.3116	0.9844

Figure 7.13 shows that the large slump cylinder provided a slightly better correlation with the vane test than was the case for the small slump cylinder, although it still seemed to be poor. Figure 7.14 and Table 7.8 show a slight improvement of the correlation between the exponential trend line data of the direct and indirect vehicle yield stress with the large slump cylinder. However, even with the large slump cylinder the relative error between the direct and indirect yield stress remains unacceptably large.

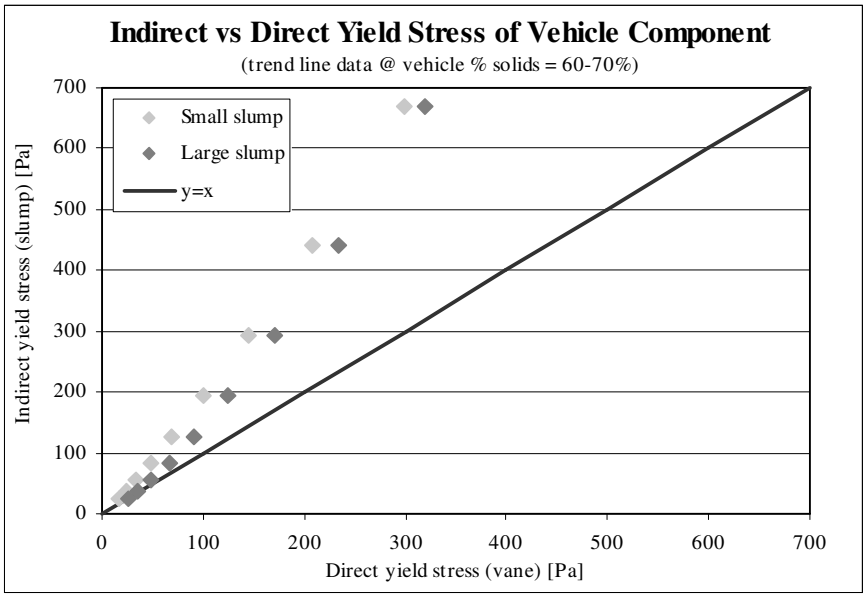

Figure 7.14 : Correlation between direct and indirect vehicle yield stress

Table 7.8 : Relative error between direct and indirect vehicle yield stress

pH	*Slump cylinder*	*Average relative error %*	*Vehicle % solids range*
8.7	Small	47.7	60-70
	Large	33.3	60-70

One of the reasons for the deviation from the results of Clayton et al (2003) could possibly be attributed to the difference in test materials. They used titanium dioxide pigment and a mineral tailings paste sample, the nature of which was not described, in their test work. There is a possibility that these materials contained no swelling montmorillonite clays. The clay fraction of the kimberlite thickened tailings material used in this study consisted of more than 60% Smectite clay, which is the parent group of the montmorillonite clays. These clays exhibit complex surface chemistry effects due to its heterogeneously charged clay particles, which have a significant impact on the configuration and strength of the inter-particle network structure. The rheological behaviour of such materials could be vastly different from those containing homogeneously charged particles or little to no clay.

The fact that the findings of this study indicated a variation in the correlation between the vane and slump test yield stress measurement techniques across suspension pH, could possibly be attributed to differences in the configuration of the clay platelet structure as a result of the particular particle interaction mechanism that dominates at each of the selected suspension pH values. The material is subjected to different types of shearing forces in the vane and slump tests, which may act in different directions. This could possibly lead to the breakdown of different kinds of inter-particle bonds depending on the configuration of the clay platelet structure and the direction of the shearing force.

7.2 Co-disposed Tailings

The second part of this study focussed on the manipulation of the co-disposed tailings rheology. This objective translated in more specific terms to the determination of the yield stress of the co-disposed tailings material (vehicle + load) as a function of the vehicle solids concentration, the suspension pH at the natural ion exchanged state of the clays and the vehicle to load mass percentage ratio, using two different measurement techniques. The following paragraphs present a summary of the results and observations in this regard. Refer to Appendices K-M for the relevant detailed raw data.

7.2.1 Manipulation of co-disposed tailings yield stress

Figure 7.15 presents the results obtained in the direct and indirect yield stress measurement of the co-disposed material with respectively the vane and slump test methods, across the ranges of solids concentration, suspension pH and vehicle to load ratio considered in this study.

Effect of the load

Figure 7.15 shows that the yield stress–solids concentration curve shifts along the x-axis to the right with increasing load percentage. It is evident that the addition of increasing quantities of the load component leads to a significant increase in the total solids concentration of the co-disposed material, which in turn leads to an exponential increase in yield stress.

The shape of the yield stress-solids concentration curves are not significantly affected by the addition of the load component at each pH, which indicates that the load component might not be contributing to the rheologically active part of the material.

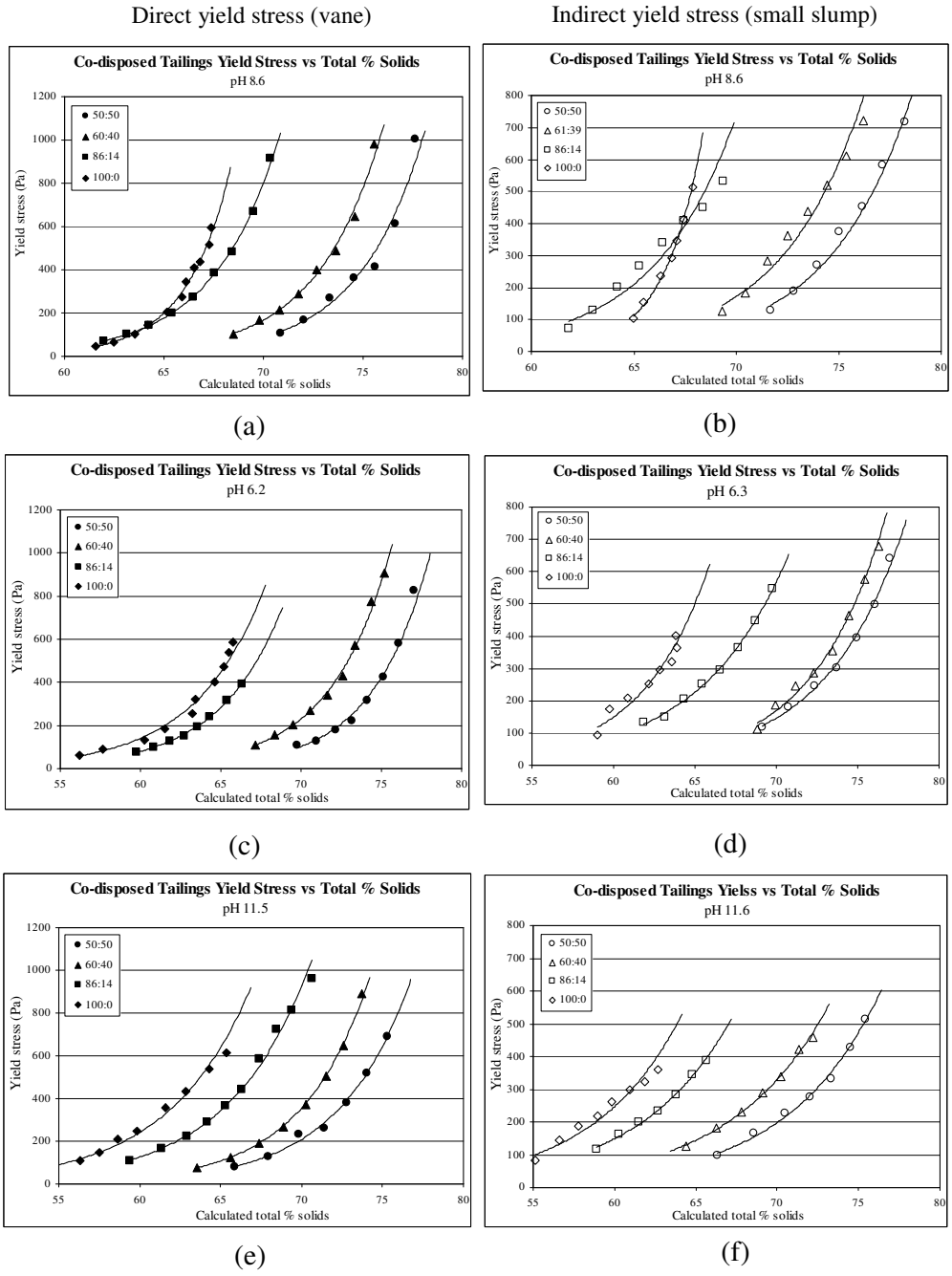

Figure 7.15 : Co-disposed tailings yield stress

(values in legend boxes indicate vehicle to load ratios based on a dry solids basis)

Figure 7.15 (a) shows that at pH 8.6 the yield stress curve representing the 86:14 vehicle to load ratio lies on top of the curve obtained for the vehicle component

only (vehicle to load ratio = 100:0) at yield stress values below about 200 Pa. This behaviour could have been the result of segregation taking place in the measurement container during the 5 minute recovery (standing) period prior to the vane test, which might have caused the vane to move through material that consisted mostly of the vehicle component. Coarse particle segregation is generally a concern at low solids concentrations, however similar behaviour was not observed at the other pH values. The higher degree of particle interaction at pH 6.2 and 11.5 provides a more defined inter-particle network structure, which could possibly have supported the coarse particles of the load component better and largely prevented segregation under static conditions, even at low solids concentrations. The fact that the interactive material exhibited higher yield stress values than the non-interactive material at low solids concentrations, support this view. In the non-interactive state at pH 8.6, the material has no mechanism to support coarser particles and segregation is therefore much more pronounced.

It is interesting to note that the slump test also produced similar results to the above, as shown in Figure 7.15 (b). Although the yield stress-solids concentration curve representing the 86:14 vehicle to load mass percentage ratio is not lying exactly on top of the curve obtained for the vehicle component only, some degree of overlap occurs between the results. The effect of coarse particle segregation would have a more complex impact on the slump test results due to the fact that the segregated material is not removed from the measurement, as in the case of the vane test.

Co-disposed tailings material design

Figure 7.16 presents the co-disposed material yield stress as determined with the vane method, in relation to the vehicle solids concentration. It is evident from Figure 7.16 that the same yield stress value could be obtained through various combinations of vehicle solids concentration, suspension pH and vehicle to load ratio. It is therefore possible to design a co-disposed tailings material with a specific yield stress value through appropriate manipulation of the various input parameters as illustrated by the example in Table 7.9.

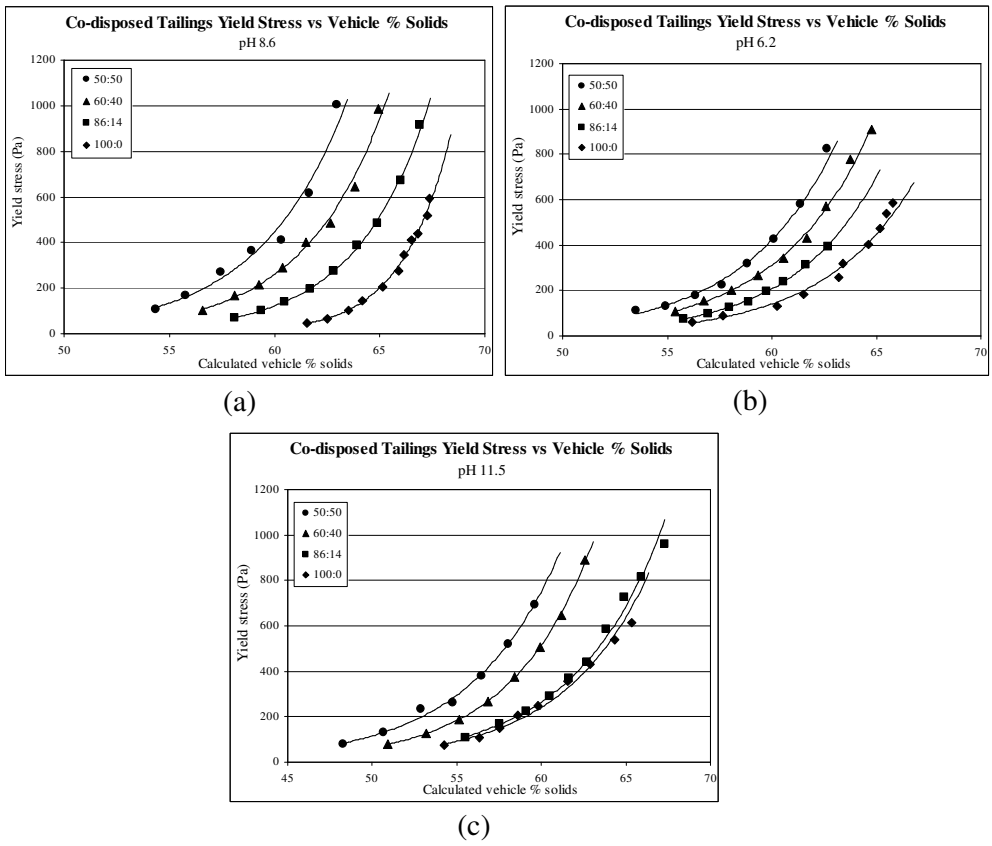

Figure 7.16 : Co-disposed tailings yield stress
(values in legend boxes indicate vehicle to load ratios based on a dry solids basis)

Figure 7.16 shows that decreasing vehicle solids concentrations are required to reach the same co-disposed material yield stress at increasing mass percentage of the load component.

Table 7.9 : Example of input parameter combinations

Co-disposed material yield stress [Pa]	*pH*	*Vehicle : Load mass % ratio*	*Vehicle % solids*
400	8.6	100:0	66.5
		86:14	64.0
		60:40	61.7
		50:50	58.8
400	6.2	100:0	65.7
		86:14	62.7
		60:40	61.0
		50:50	60.1
400	11.5	100:0	62.7
		86:14	62.2
		60:40	58.7
		50:50	56.6

Vane test observations

Irregular shaped torque-time curves were obtained for the co-disposed material, which in some instances complicated the identification of the material yield point. The maximum torque value calculated by the rheometer software did not always prove to represent the material yield point upon inspection of the shape of the torque-time curve. This led to an approach where all the torque-time curves were carefully inspected in order to select the most likely yield point and its associated torque value.

Upon inspection of the shapes of the torque-time curves it became clear that a load addition of 14% by mass did not constitute a significant change in the shape

of the torque-time curve when compared with that obtained for the vehicle component only. The coarser particles of the load, however, led to significant irregularity in the shape of the torque-time curve at load additions exceeding 40% by mass. Figure 7.17 shows a typical example of this observation.

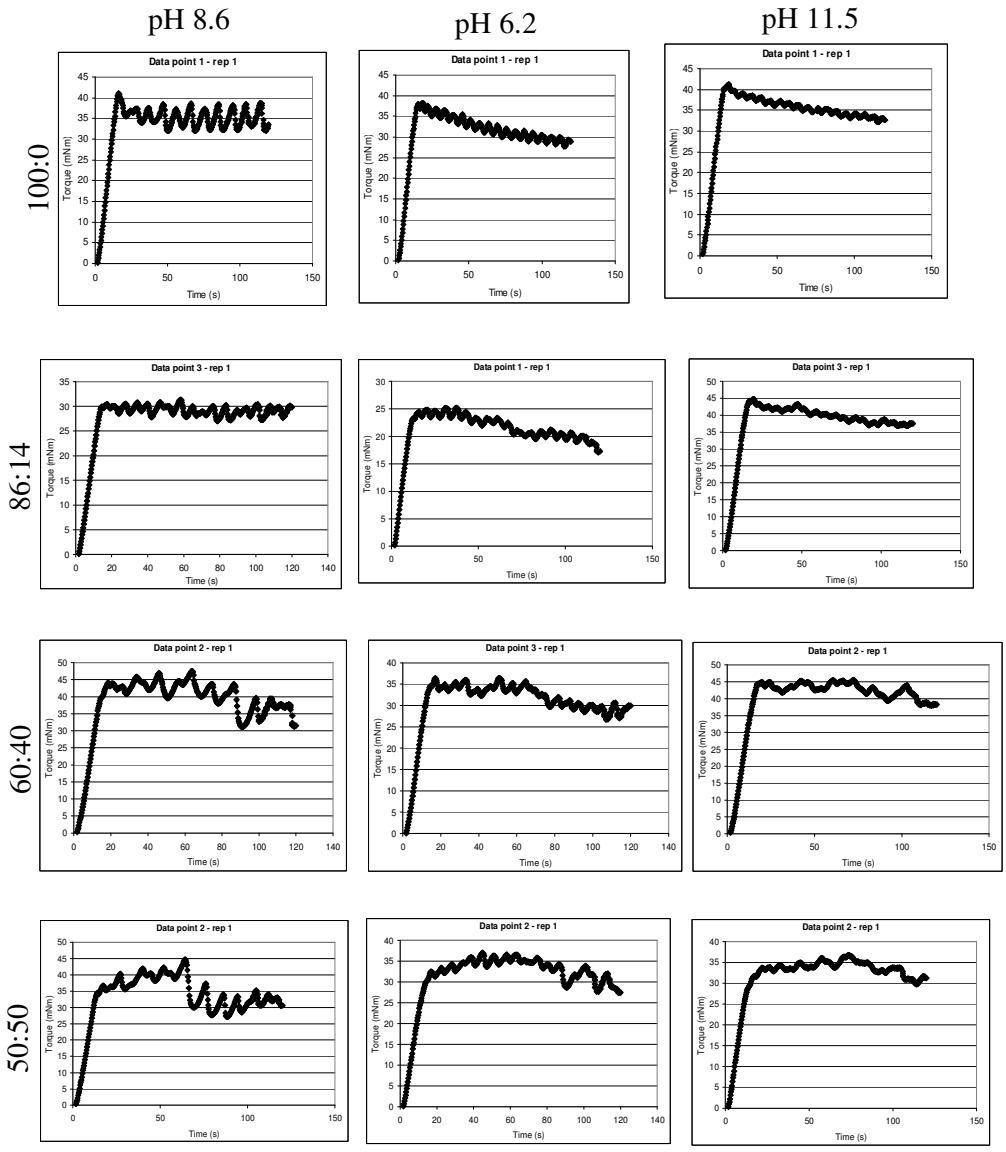

Figure 7.17 : Shape of typical co-disposed material torque-time curves

Slump test observations

Figure 7.18 presents the average radius of the radial flow distance of the slumped material, across the ranges of solids concentration, suspension pH and vehicle to load ratio considered in this study. The horizontal broken lines in Figure 7.18 present the radius of the small slump cylinder at 52 mm and indicate the lower limit of the radial flow distance.

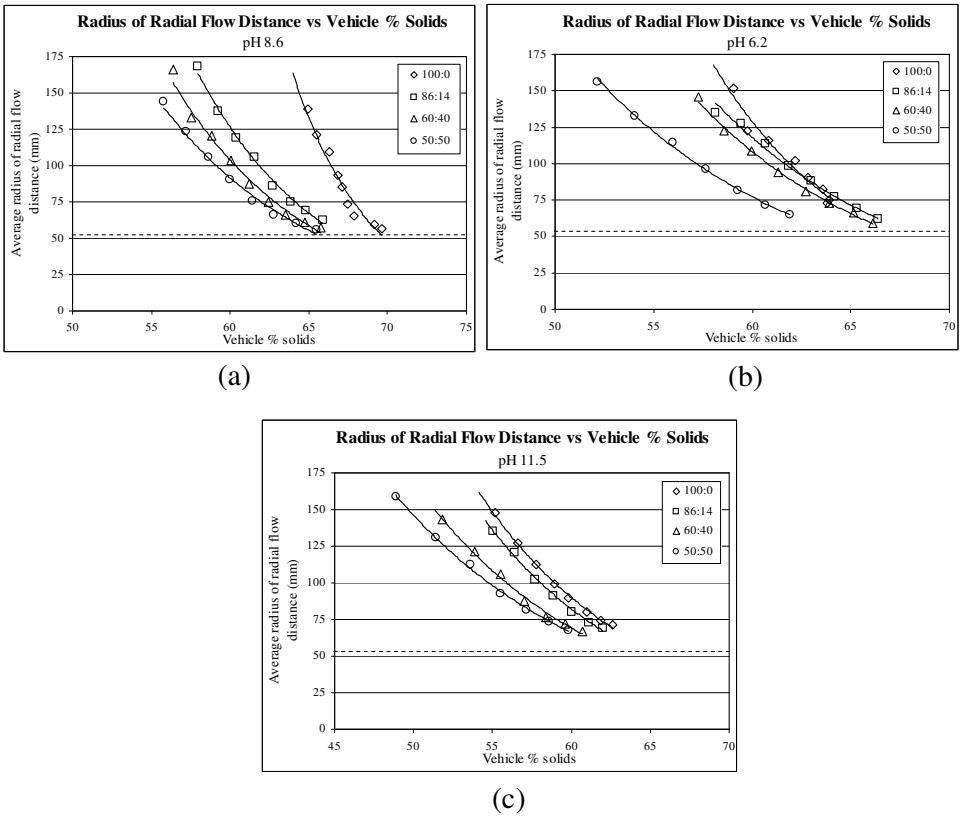

Figure 7.18 : Radius of slumped material radial flow distance

Figure 7.18 shows that for increasing load mass percentage, the average radial flow distance decreases, which corresponds to decreasing slump height. Lower slump heights correspond to higher yield stress values, which were also observed in the vane test results for increasing load addition.

Slump height is often quoted in the P&TTD field to compare different thickened tailings materials. However, both Clayton et al (2003) and Paterson (2002) warned that materials with a similar slump height do not necessarily exhibit similar rheological properties. Clayton et al (2003) particularly states that factors such as particle size distribution and specific gravity have a significant impact on the yield stress value calculated from a given slump height and that care should be taken in the direct comparison of slump heights for different materials.

The findings of this study confirmed the viewpoint of Clayton et al (2003) and Paterson (2002) as shown in the two examples in Table 7.10.

Table 7.10 : Comparison of co-disposed material slump heights

Slump height [mm]	*Yield stress [Pa]*	*pH*	*Vehicle : Load mass %*	*Vehicle % solids*
71.1	270.1	8.6	86:14	61.6
71.1	297.2	6.2	50:50	57.7
74.3	253.7	6.2	86:14	61.9
74.4	272.7	11.5	50:50	55.5

Table 7.10 shows that vastly different yield stress values were obtained for materials exhibiting similar slump heights. In the case of this study, the main factors contributing to the variation in yield stress for similar slump heights are the particle size distribution, which was varied considerably through the vehicle to load ratio, and the suspension pH, which generated significant variation in the degree of particle interaction and the subsequent strength of the inter-particle network structure.

It is therefore not advisable to compare material slump heights if there could be any chance that the materials are not exactly the same in all aspects. The large

number of slump container sizes and shapes only generate more confusion when slump height is quoted alone. Clayton et al (2003) recommend that material yield stress values are compared instead of slump heights, as the yield stress is a unique material property.

7.2.2 Correlation between yield stress measurement techniques

Vane and small slump

Figure 7.19 presents the correlation between the exponential trend line data of the co-disposed material direct and indirect yield stress over a vehicle solids concentration of 50-70%.

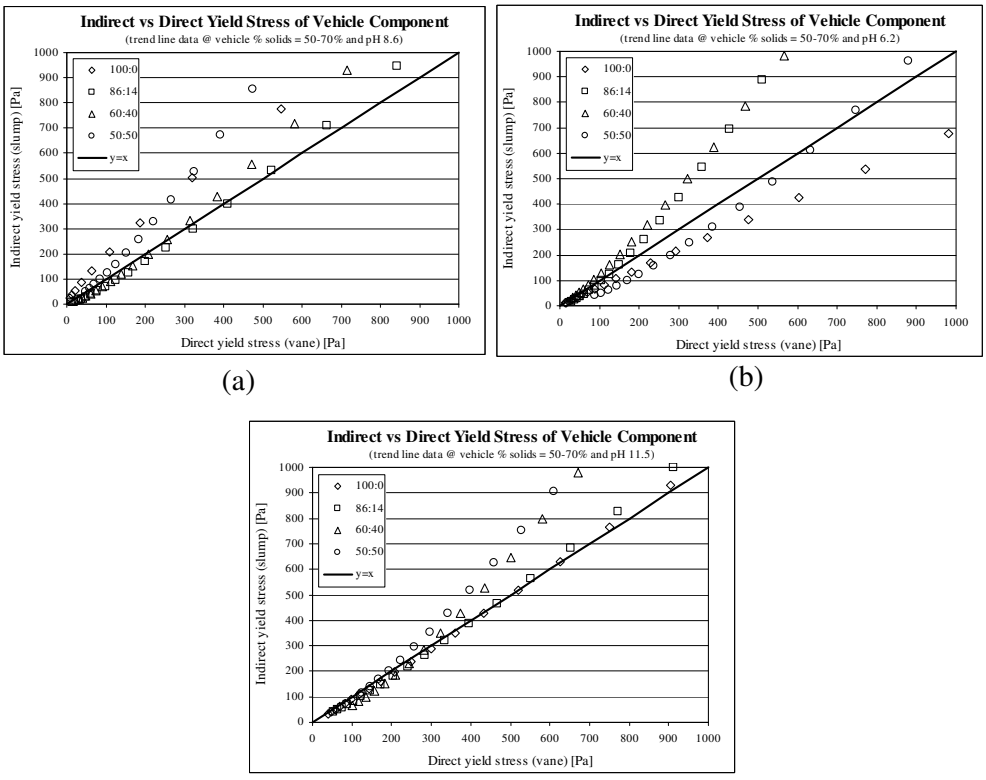

Figure 7.19 : Correlation between direct and indirect co-disposed yield stress

Table 7.11 presents average values of the absolute relative error percentages between the direct and indirect co-disposed material yield stress. The shaded blocks in Table 7.11 indicate an average relative error below 15% with the associated combinations of suspension pH and vehicle to load ratio.

Table 7.11 : Relative error between direct and indirect co-disposed yield stress

pH	*Vehicle : Load ratio*	*Slump cylinder*	*Average relative error %*	*Vehicle % solids range*
8.6	100:0	Small	44.8	60-70
	86:14		26.6	55-65
	60:40		14.1	55-65
	50:50		37.9	55-65
6.2	100:0	Small	33.1	55-65
	86:14		19.0	55-65
	60:40		30.2	55-65
	50:50		23.8	55-65
11.5	100:0	Small	4.8	55-65
	86:14		9.0	55-65
	60:40		21.5	50-60
	50:50		14.1	50-60

The accuracy of the correlation between the direct and indirect yield stress of the co-disposed material varied considerably across the range of input parameters considered in this study. It is evident that the accuracy of the correlation still proves to be the best for a co-disposed material at pH 11.5, similar to what was found with the vehicle component only, as discussed in Section 7.1.2.

The “50c rheometer” correlation developed by Pashias et al (1996) to link the direct yield stress determined by the vane method with the indirect yield stress determined by the slump test method, was developed using materials containing very fine particle sizes, i.e. titanium dioxide, zirconia dioxide and red mud (Pashias et al, 1996). There is some doubt if the correlation would then prove to be accurate for materials containing large amounts of coarse particles (particle sizes up to about 7 mm). The presence of coarse particles definitely has an impact on the flow behaviour of the material as shown by the significant increase in yield stress with increasing load mass percentage in this study.

8. CONCLUSIONS AND RECOMMENDATIONS

The purpose of this chapter is to provide a summary of the main conclusions of this study and to show to what extent the objectives have been reached.

8.1 Vehicle Component

The first objective of this study referred to the development of a fundamental understanding of the relationship between the key material characteristics and the flow behaviour of the vehicle component in order to effectively manipulate its rheological behaviour.

The vehicle component can be described in the context of this study, as a montmorillonite clay based kimberlite thickened tailings material of paste consistency. Therefore, the material characteristics related to the vehicle component were identified as follows :

- Solids concentration
- Suspension pH
- Ion exchanged nature of the clays
- Particle size distribution
- Mineralogy

At full scale operation, the material particle size distribution, mineralogy and ion exchanged nature of the clays are not likely to change significantly on a daily basis. The material mineralogy and ion exchanged nature of the clays are inherent to the ore type that is mined and the quality of the water source that is used. The material particle size distribution is a product of the upstream crushing and screening processes in the mineral processing plant. Besides the fact that these three parameters are more or less constant for long periods of time at full scale operation, it is evident that they are also not easy to manipulate and were therefore kept constant in this study.

The solids concentration and suspension pH were then selected as the key material characteristics for investigation in this study. The material solids concentration is normally determined by the degree of dewatering and therefore thickener performance at full scale operation. Modern thickener control instrumentation enables the manipulation of the material solids concentration. Upon suspension, the material develops a natural suspension pH, which is strongly linked with the ore mineralogy, ion exchanged nature of the clays and quality of the water source. The suspension pH is normally artificially manipulated through the addition of acidic or alkaline solutions to the material.

The effect of the key material characteristics on the flow behaviour of the vehicle component was expressed in this study in terms of the shear yield stress. The yield stress is a unique material rheological property that influences the angle of repose at which the material comes to rest, as well as the degree of particle segregation upon deposition (Boger, 2002).

Solids concentration

It is concluded out of the findings of this study that increasing solids concentration leads to an exponential increase in the vehicle component yield stress. This conclusion is in agreement with the work of Sofra and Boger (2000) as discussed in Section 2.3.2.

The underlying reason for the exponential relationship between the yield stress and solids concentration of the vehicle component is described by Coghill (2003) as due to the restriction of particle movement. As the solids concentration is increased, the liquid volume relative to the solid phase decreases, causing the particles to have less freedom to move past each other. This restriction in particle movement translates to an internal resistance to flow and affects the minimum shear stress required for the first signs of flow to occur, which is the definition of yield stress.

It is also concluded that the vehicle component in the non-interactive state has enhanced compaction abilities. This conclusion is supported by the fact that the vehicle component could reach much higher solids concentrations before a significant increase in yield stress is realised, than is the case for a material in the interactive state. The main reason for the enhanced compaction abilities of the vehicle component in the non-interactive state is the parallel face to face (FF) configuration of the clay platelets.

Suspension pH

It is concluded out of the findings of this study that the suspension pH strongly influences the degree of microscopic particle interaction of the vehicle component. The findings of this study were in agreement with the kimberlite thickened tailings behavioural model developed by Vietti (2004), as discussed in Section 2.3.3.

The behaviour of the vehicle component varied between non-interactive and interactive states depending on the pH of the suspension and the particular particle interaction mechanism that dominated. At pH values in the region of about 8 to 11, the suspension pH effect dominates, which means that no interaction between particles takes place, as a result of electrostatic repulsion between similarly charged clay platelets. Above pH 8, both the clay platelet surfaces and edges are negatively charged. At pH values below 8, the suspension pH effect dominates again, leading to particle interaction as a result of electrostatic attraction between the negatively charged surfaces and positively charged edges of the clay platelets. Below pH 8, the clay platelet edges are positively charged, which results in a "house of card" inter-particle network structure of high mechanical strength. At pH values above 11, the ionic concentration effect dominates, which means that particle interaction takes place as a result of double layer compression enabling the particles to come close enough to each other for Van der Waals attractive forces to have an effect. To reach highly alkaline conditions where the pH exceeds 11, large quantities of concentrated alkaline solutions (i.e. NaOH) are typically added. The increased concentration of cations (i.e. Na^+) in solution leads to an

increased suspension ionic concentration, which overrides the effect of the suspension pH. The result is a high degree of particle interaction and the formation of a mechanically strong inter-particle network structure.

It is concluded that the degree of particle interaction induced by the ionic concentration effect (above pH 11) is much higher than that induced by the suspension pH effect (below pH 8). This conclusion is supported by the difference in yield stress values obtained for these materials.

The degree of particle interaction dictates the strength of the inter-particle network structure and therefore the minimum shear stress required to overcome the material's internal resistance to flow, which is essentially its yield stress (Nguyen and Boger, 1983). The variation in the degree of particle interaction as a result of variation in the suspension pH was therefore clearly observed as a significant increase in yield stress when the vehicle component was moved from the non-interactive to interactive state.

Manipulation of vehicle rheology

It is believed that the first objective of this study has been achieved and that it enables the effective manipulation of the vehicle component yield stress. It is now possible to design the vehicle component to exhibit interactive or non-interactive behaviour and therefore to control its yield stress value to the requirements of the various sub-processes within the P&TTD system.

It would be desirable to transport a non-interactive material with a low yield stress to reduce pumping energy. However, in the presence of larger particles that do not form part of the vehicle component, as is often the case in thickened tailings materials, the yield stress of the vehicle component should be high enough to ensure transportation of the sliding bed of load particles (Pullum, 2003).

On the other hand, it would be desirable to deposit an interactive material with a high yield stress to ensure an appropriate angle of repose for maximum stability

and storage capacity. A high yield stress vehicle component would also largely prevent particle segregation upon deposition (Boger, 2002). It is important though to maintain a balance between the angle of repose and the spreading characteristics of the material upon deposition.

Comparison of yield stress measurement techniques

A secondary objective of this study was to investigate the accuracy of the "50c rheometer" correlation between the direct yield stress measured with the vane method and the indirect yield stress measured with the slump method, as developed by Pashias et al (1996).

It is concluded out of the findings of this study that the slump test only provided an accurate prediction of the vehicle component yield stress in the highly interactive state at pH 11.5. Significant underestimation of the yield stress was obtained with the slump test for a non-interactive vehicle component at pH 8.6, while significant overestimation occurred in the moderate interactive state at pH 6.2.

The use of a taller slump cylinder realised only a very slight improvement of the accuracy of the "50c rheometer" correlation, which means that the findings of Clayton et al (2003), could not be re-created in this study. The reason for this behaviour could possibly be attributed to the varying configuration of the clay platelet structure associated with the different mechanisms of particle interaction across the suspension pH range. It is possible that the internal resistance of the vehicle component to flow might be greater in certain directions than in others due to different types of inter-particle bonds or a certain alignment of the clay platelets. Different yield stress measurement techniques could then produce different results depending on the type and direction of the external shearing force in reference to the possible directional nature of the internal resistance of the material. The "50c rheometer" correlation is probably not taking these effects into account.

8.2 Co-disposed Tailings

The second objective of this study referred to the development of a fundamental understanding of the relationship between the key material characteristics and the flow behaviour of a co-disposed tailings material in order to effectively manipulate its rheological behaviour upon deposition.

The co-disposed tailings material can be described in the context of this study to consist of vehicle and load components. Therefore, the material characteristics related to co-disposed tailings can be divided into the following categories :

- Vehicle characteristics
- Load characteristics
- Vehicle to load ratio

The relationship between the key material characteristics of the vehicle component and its flow behaviour is discussed in Section 8.1 and will not be repeated here.

The load characteristics include aspects such as particle size distribution, mineralogy and moisture content. The mineralogy of the load is inherent to the ore type that is mined, while the particle size distribution and moisture content are dependent on the upstream processes in the mineral processing plant. Since none of these aspects are likely to change frequently during full scale operation, the load characteristics were kept constant for the purpose of this study.

The vehicle to load ratio together with the key material characteristics of the vehicle component, i.e. solids concentration and suspension pH, were then selected for investigation in this study. The vehicle to load ratio was defined as a mass percentage ratio, which translates into the mixing ratio of thickened tailings with coarse tailings prior to or upon deposition during full scale operation.

Again, the effect of the key material characteristics on the flow behaviour of the co-disposed tailings material was expressed in this study in terms of the shear yield stress.

Solids concentration

An increasing load mass percentage leads to a significant increase in the co-disposed material yield stress. The load component mainly affects the co-disposed material yield stress through its contribution to the total solids concentration, which in turn results in an exponential increase in the material yield stress as discussed in Section 8.1.

Suspension pH

The vehicle component in the interactive state exhibits a better ability to support the coarser particles of the load component and prevent segregation under static conditions, even at low solids concentrations. The ability of the vehicle component to transport and support the load becomes important in the transportation and deposition of co-disposed tailings materials.

Vehicle to load ratio

The vehicle to load ratio range considered in this study was selected to maintain the "fluid-like" behaviour of the co-disposed tailings material. As a result, the vehicle to load ratio was manipulated to produce a material that varied between a 100% vehicle component to one consisting of 60% vehicle component (wet) and 40% load component (dry) by mass. However, in the presentation of the results the vehicle to load ratio was expressed as a mass percentage ratio based on the dry solids content of the respective vehicle and load components, which translated into the variation of the vehicle component between 100% and 50% by mass.

Even though the co-disposed tailings material always consisted of a higher mass percentage of vehicle than load in this study, it does not necessarily mean that the vehicle component dominated the rheology of the co-disposed tailings material. It is concluded that the vehicle component only dominated the co-disposed tailings

rheology at a load mass percentage of 14%, in the context of this study. This conclusion is supported by the fact that the shapes of the torque-time curves obtained during the vane test work showed no significant change upon a 14% addition of the load, from those obtained for the vehicle component only. At load mass percentages exceeding 40%, significant irregularities in the shapes of the torque-time curves were observed.

The fact that small additions of load have no significant effect on the bulk rheology of a material has been recognised by Ancey and Jorrot (2001) and Coussot et al (1996). The main reason for this behaviour is that the relative movements of the coarser load particles are lubricated by the vehicle component. However, as the load mass percentage increases, the lubricating effect of the vehicle component decreases.

A well graded load component, such as the material used in this study, would form a much closer particle packing than would be the case for mono-sized particles. The closer particle packing leads to the development of fewer interstitial voids filled with vehicle component. Ancey and Jorrot (2001) suggested a situation where the coarser load particles are coated by a layer of vehicle component material at this point. The degree of lubrication provided by this layer depends on how close the material is to its maximum particle packing concentration. When the latter is approached, direct contacts between particles start to dominate and a strong coarse particle network is formed, which severely restricts the movement of particles past each other. When the maximum particle packing concentration is approached, the bulk material yield stress approaches infinity (Ancey and Jorrot, 2001).

Manipulation of co-disposed tailings rheology

It is believed that the second objective of this study has been achieved to a large extent and that it enables the manipulation of the co-disposed tailings material yield stress. It is now possible to design the co-disposed tailings material to exhibit a yield stress value that suits the depositional requirements of a specific

environment. The ability to manipulate the co-disposed tailings yield stress makes it easier to follow the reverse design sequence for P&TTD systems as proposed by Boger (2002).

Currently, the most practical method of co-disposal of tailings would probably be to transport the vehicle and load components separately to the deposition site and combine them in some sort of mixing stage just before deposition at the desired vehicle to load ratio. This method allows for the manipulation of the suspension pH and vehicle to load ratio during the final mixing stage, while the solids concentration of the vehicle is controlled by upstream thickener performance. The findings of this study showed remarkable flexibility in the manipulation of the various input parameters to produce the same yield stress value. It is therefore possible to maintain a constant yield stress value as required by the environmental depositional requirements through various combinations of the input parameters and so keep the integrity of the deposition site intact.

One of the main benefits of understanding how to manipulate the co-disposed material yield stress is that it can be used to counteract process upsets to a large degree. For instance, variations in vehicle solids concentration due to inconsistent thickener performance during dewatering could be counteracted with changes in the suspension pH and/or vehicle to load ratio to still produce a consistent material yield stress value and angle of repose upon deposition.

It is believed that if the manipulation of co-disposed tailings rheology is fully understood and exploited, successful implementation of the technology would become widespread.

Outstanding issues

Even though the second objective of this study was mostly achieved, the specific effect of the load component on the bulk rheology and when it comes into play are not yet fundamentally understood. This study provided some information in this

regard, which tied in with the research work conducted in the field of debris flows, but it does not provide significantly more insight.

However, it is believed that the point at which the domination of the vehicle rheology starts to decrease and the effect of the load component becomes more pronounced, is unique to each co-disposed tailings material. This particular point could be described as a vehicle to load ratio and it is believed to be dependent on the physical characteristics of the vehicle and load components (i.e. particle size distribution, particle shape, void ratio, etc.) and the efficiency of close particle packing at high solids concentrations.

Comparison of yield stress measurement techniques

As discussed in Section 8.1, a secondary objective of this study was to investigate the accuracy of the "50c rheometer" correlation between vane and slump test measured yield stress as developed by Pashias et al (1996).

A similar conclusion is made for the co-disposed tailings material in that the "50c rheometer" correlation only proved to be accurate for a highly interactive material at pH 11.5. This correlation was developed using materials containing very fine particle sizes and there is therefore some doubt if it would prove to be accurate for materials containing significant quantities of coarse particle such as the co-disposed materials used in this study. Due to the fact that the effect of the load component on the rheology of a co-disposed material is also not generally understood, the probability of it being taken into account in the "50c rheometer" correlation is low.

Initially it was thought that the slump test could be used as an effective method for determining the yield stress of co-disposed materials due to the obvious limitations of conventional rheometers for materials containing large particle sizes and due to its simplicity and practicality as a field test. However, the findings of this study were not promising in this regard.

8.3 Recommendations for Future Work

The following aspects are recommended for future research work :

- *Thixotropic nature of the vehicle rheology as a function of suspension pH*
  In this study the sensitivity of the vehicle rheology to shear history, in other words its thixotropic nature, was only investigated to a limited degree for the vehicle component in the non-interactive state. The shear history was then kept constant through repeatable material preparation and testing procedures in order to remove its effect and reduce the number of input parameters investigated.

  It would be worthwhile however, to investigate if the variation in particle interaction observed across the suspension pH manifests itself in a variation in thixotropic nature for the vehicle component. The different configurations of the clay platelet structure as a result of different particle interaction mechanisms dominating at the different pH values, might not behave the same when subjected to periods of shear and recovery.

- *Accuracy of the "50c rheometer" correlation*
  The "50c rheometer" correlation developed by Pashias et al (1996) links the direct yield stress measured with the vane method with the indirect yield stress measured with the slump test method. The poor accuracy of this correlation obtained in this study for a vehicle component in the non-interactive and moderately interactive states, plus the fact that the claim of Clayton et al (2003) that a taller slump cylinder provides a more accurate prediction of the material yield stress was not achieved in this study, urge further investigation.

  The explanation proposed in this study that the strength, or internal resistance to flow, of the vehicle component inter-particle network structure might be directional, possibly due to different types of inter-particle bonds acting in different directions or a certain alignment of the clay platelets, causing

different yield stress measurement techniques to produce different results based on the type and direction of the external shearing force, require further investigation to find physical proof.

- *Effect of the load on the bulk rheology of the co-disposed material*

  The effect of the load on the bulk rheology of the co-disposed material and when it starts to override the dominance of the vehicle component are a very complex problem and not yet fully understood. Research in the fields of debris flow and pipeline flow contributed to this understanding. However, more fundamental research is required in order to get to a point where the bulk rheology of a co-disposed material can be inferred simply from the characteristics of the individual vehicle and load components.

REFERENCES

Ancey, C. and Jorrot, H. (2001), Yield stress for particle suspensions within a clay dispersion, *Journal of Rheology*, Vol. 45, No.2, pp. 297-319.

Bentel, G. (2002), Chapter 7 : Above ground disposal, *Paste and Thickened Tailings Disposal – A Guide*, Ed Jewell, Fourie and Lord, Australian Centre for Geomechanics, University of Western Australia, Australia.

Boger, D.V. (2000), Exploiting the rheology of mineral tailings, *Proceedings International Seminar on Paste and Thickened Tailings 2000*, Edmonton, Canada.

Boger, D.V. (2002), Chapter 3 : Rheological concepts, *Paste and Thickened Tailings Disposal – A Guide*, Ed Jewell, Fourie and Lord, Australian Centre for Geomechanics, University of Western Australia, Australia.

Boger, D.V. (2003), Why is rheology important ?, *Proceedings First Minerals Processing and Tailings Rheology Workshop*, Australian Centre for Geomechanics and Particulate Fluids Processing Centre, Australia.

Brzezinski, L.S. (2001), Surface disposal of thickened tailings, *Mining Environmental Management*, September, pp. 7-12.

Chambers, R.W. and Plewes, H.D. (2002), Evolving tailings technologies – An overview, *Proceedings International Seminar on Paste and Thickened Tailings 2002*, Santiago, Chile.

Clayton, S.; Grice, T.G.; Boger, D.V. (2003), Analysis of the slump test for on-site yield stress measurement of mineral suspensions, *International Journal of Mineral Processing*, Vol. 70, pp. 3-21.

Coghill, M. (2003), Slurry rheology manipulation, *Proceedings First Minerals Processing and Tailings Rheology Workshop*, Australian Centre for Geomechanics and Particulate Fluids Processing Centre, Australia.

Cooke, R. (2001), Laminar flow settling : the potential for unexpected problems, *Proceedings International Seminar on Paste and Thickened Tailings 2001*, Pilanesberg, South Africa.

Coussot, P. and Piau, J. (1995a), The effect of an addition of force-free particles on the rheological properties of fine suspensions, *Canadian Geotechnical Journal*, Vol.32, pp. 263-270.

Coussot, P. and Piau, J. (1995b), A large-scale field coaxial cylinder rheometer for the study of the rheology of natural coarse suspensions, *Journal of Rheology*, Vol. 39, No. 1, pp. 105-124.

Coussot, P.; Proust, S.; Ancey, C. (1996), Rheological interpretation of deposits of yield stress fluids, *Journal of Non-Newtonian Fluid Mechanics*, Vol. 66, pp. 55-70.

Coussot, P.; Laigle, D.; Arattano, M.; Deganutti, A.; Marchi, L. (1998), Direct determination of rheological characteristics of debris flow, *Journal of Hydraulic Engineering*, Vol. 124, No. 8, pp. 865-868.

De Kretser, R., Scales, P.J., Boger, D.V. (1997), Improving clay-based tailings disposal: case study on coal tailings, *AIChE Journal*, Vol.43, No.7, pp.1894-1903.

Department of Natural Resources and Environment (2002), *Discussion Paper – Tailings Storage Guidelines for Victoria*, State Government of Victoria, Melbourne, Australia.

Dunn, F. (2002), *Preliminary study of some of the slurry characteristics which affect the flow characteristics of a co-disposed product*, Technical Note No. 2002/03/03, De Beers Consolidated Mines, Johannesburg, South Africa.

Dunn, F. (2003a), Chapter 3 : Coagulation and flocculation, *Paste and Thickened Tailings Disposal Handbook*, Ed Vietti and Dunn, Technical Support Services, De Beers Consolidated Mines, Johannesburg, South Africa.

Dunn, F. (2003b), Chapter 4 : Thickening, *Paste and Thickened Tailings Disposal Handbook*, Ed Vietti and Dunn, Technical Support Services, De Beers Consolidated Mines, Johannesburg, South Africa.

Dunn, F., Vietti A.J., Ramulai, S. (2001), *The concept of co-disposal of processed kimberlite products on a pilot plant scale – part 1*, Report No. R2001/06/03, De Beers Consolidated Mines, Johannesburg, South Africa.

Dunn, F. and Vietti, A.J. (2003), The thirsty business of diamond mining, *Proceedings Fourth One Day Seminar on Hydraulic Transport in the Mining Industry*, Hydraulic Conveying Association of South Africa, Johannesburg, South Africa.

Fourie, A.B. (2002a), *Waste disposal as creative geology*, Inaugural lecture, University of Witwatersrand, Johannesburg, South Africa.

Fourie, A.B. (2002b), Thickened tailings : Is it a revolution in the making ?, *Proceedings 4th International Conference on Environmental Geotechnics*, Rio de Janeiro, Brazil, Vol. 2, pp. 977-986.

Fourie, A.B. (2002c), Chapter 4 : Material characterisation, *Paste and Thickened Tailings Disposal – A Guide*, Ed Jewell, Fourie and Lord, Australian Centre for Geomechanics, University of Western Australia, Australia.

Gawu, S.K.Y. (2004), Private communication with Simon Gawu during February 2004.

Gawu, S.K.Y. and Fourie, A.B. (2004), Assessment of the modified slump test as a measure of the yield stress of high density thickened tailings, *Canadian Geotechnical Journal*, Vol. 41, pp. 39-47.

Gillies, R.G.; Shook, C.A.; Wilson, K.C. (1991), An improved two-layer model for horizontal slurry pipeline flow, *Canadian Journal of Chemical Engineering*, Vol. 69, February, pp. 173-178.

Hayley, D. (2000), The future ? What's driving the technology ?, *Proceedings International Seminar on Paste and Thickened Tailings 2000*, Edmonton, Canada.

Helfer, C. (2001a), *The concept of co-disposal of processed kimberlite products on a pilot plant scale – part 2*, Finsch Mine Report, De Beers Consolidate Mines, Johannesburg, South Africa.

Helfer, C. (2001b), Co-disposal of processed kimberlite – The Finsch Mine experience, *Proceedings International Seminar on Paste and Thickened Tailings 2001*, Pilanesberg, South Africa.

Hutcheson, H. (2001), Co-disposal trials for a mineral sands operation, *Proceedings International Seminar on Paste and Thickened Tailings 2001*, Pilanesberg, South Africa.

International Commission on Large Dams (2001), *Tailings Dams – Risk of Dangerous Occurrences*, Bulletin 121, International Commission on Large Dams and United Nations Environment Programme, Paris, France.

Jewell, R. (2000), Deposition and geotechnical characteristics of thickened/paste tailings in the Australian Mining Industry, *Proceedings International Seminar on Paste and Thickened Tailings 2000*, Edmonton, Canada.

Jewell, R. (2002), Chapter 1 : Introduction, *Paste and Thickened Tailings Disposal – A Guide*, Ed Jewell, Fourie and Lord, Australian Centre for Geomechanics, University of Western Australia, Australia.

Jewell, R. (2003), An introduction to thickened tailings applications, *Proceedings International Seminar on Paste and Thickened Tailings 2003*, Melbourne, Australia.

Johnson, S.B., Franks, G.V., Scales, P.J., Boger, D.V., Healy, T.W., (2000), Surface chemistry-rheology relationships in concentrated mineral suspensions, *International Journal of Mineral Processing*, Vol. 58, pp. 267-304.

Johnson, G. and Vietti, A.J. (2003), The design of a co-thickened slimes disposal system for the Kimberley Combined Treatment Plant, *Proceedings International Seminar on Paste and Thickened Tailings 2003*, Melbourne, Australia.

Jones, H. (2002), Chapter 9 : Closure considerations, *Paste and Thickened Tailings Disposal – A Guide*, Ed Jewell, Fourie and Lord, Australian Centre for Geomechanics, University of Western Australia, Australia.

Leduc, M., Bachens, M., Smith, M.E. (2004), Tailings co-disposal and sustainable development, INTERNET. http://technology.infomine.com/leachmine. Cited 09 September 2004.

Lord, T. (2001), Thickened/paste tailings research at Syncrude for oil sands fine tailings, *Proceedings International Seminar on Paste and Thickened Tailings 2001*, Pilanesberg, South Africa.

Lord, T. (2002), Tailings management in the Canadian oil sands industry, *Proceedings International Seminar on Paste and Thickened Tailings 2002*, Santiago, Chile.

Lord, T. (2003), Canadian examples of paste and thickened tailings for surface disposal, *Proceedings International Seminar on Paste and Thickened Tailings 2003*, Melbourne, Australia.

Metago (2002), *Assessment of the geotechnical properties of high compression thickened tailings*, Appendix Report 2, Desktop study into geotechnical aspects of mine waste disposal for slimes, grits and coarse tailings, Project No. 136-006 for De Beers Consolidated Mines, Metago Environmental Engineers, Johannesburg, South Africa.

Millar, M. (2004), *An investigation of the geotechnical characteristics of thickened kimberlite tailings co-disposed with coarse waste*, Project report for De Beers Consolidated Mines, School of Civil and Environmental Engineering, University of Witwatersrand, Johannesburg, South Africa.

Mining, Minerals and Sustainable Development (2002), *Mining for the Future – Appendix A : Large Volume Waste Working Paper*, Report No.31, International Institute for Environment and Development and World Business Council for Sustainable Development, London, United Kingdom.

Morris, P.H. and Williams, D.J. (1997), Co-disposal of washery wastes at Jeebropilly colliery, Queensland, Australia, *Transactions of the Institution of Mining and Metallurgy (Section A : Mining Industry)*, Vol. 106, pp. A25-A29.

Morris, P.H. and Williams, D.J. (1999), Segregation of co-disposed coal mine washery wastes, *CIM Bulletin*, Vol. 92, No. 1035, pp. 72-76.

Nguyen, Q.D. and Boger, D.V. (1983), Yield stress measurement for concentrated suspensions, *Journal of Rheology*, Vol. 27, No. 4, pp. 321-349.

Nguyen, Q.D. and Boger, D.V. (1985), Direct yield stress measurement with the vane method, *Journal of Rheology*, Vol. 29, No. 3, pp. 335-347.
Nguyen, Q.D. and Boger, D.V. (1992), Measuring the flow properties of yield stress fluids, *Annual Review of Fluid Mechanics*, Vol. 24, pp. 47-88.

Nguyen, Q.D. and Boger, D.V. (1998), Application of rheology to solving tailings disposal problems, *International Journal of Mineral Processing*, Vol. 54, pp. 217-233.

O'Brien, J.S. and Julien, P.Y. (1988), Laboratory analysis of mudflow properties, *Journal of Hydraulic Engineering*, Vol. 114, No. 8, pp. 877-887.

Paar Physica, (2002), A little course in rheology - part 1, *Practical Rheology of Polymer Systems*, Course notes, Cape Technikon Rheology Centre and Paar Physica, Johannesburg, South Africa.

Pashias, N.; Summers, J.; Glenister, D.J.; Boger, D.V. (1996), A fifty cent rheometer for yield stress measurement, *Journal of Rheology*, Vol. 40, No. 6, pp. 1179-1189.

Paterson, A. (2002), Is slump a valid measure of the rheological properties of high concentration paste slurries?, *Proceedings 15th International Conference on Slurry Handling and Pipeline Transport,* Banff, Canada.

Paterson, A. and Cooke, R. (2000), *The Design of Slurry Pipeline Systems*, Course notes, Paterson and Cooke Consulting Engineers, Cape Town, South Africa.

Pullum, L. (2003), Pipeline performance, *Proceedings International Seminar on Paste and Thickened Tailings 2003*, Melbourne, Australia.

Regensburg, B, and Tacey, W. (2002), Chapter 2 : Key business issues, *Paste and Thickened Tailings Disposal – A Guide*, Ed Jewell, Fourie and Lord, Australian Centre for Geomechanics, University of Western Australia, Australia.

Rice, S. and Davies, M. (2002), Dewatered tailings for surface tailings management, *Proceedings International Seminar on Paste and Thickened Tailings 2002*, Santiago, Chile.

Richards, L.A. (1954), *Diagnosis and improvement of saline and alkali soils*, Agriculture Handbook No. 60, United States Department of Agriculture, Washington, United States of America.

Robinsky, E.I. (1975), Thickened discharge – A new approach to tailings disposal, *CIM Bulletin*, Vol. 68, No. 764, pp. 47-53.

Robinsky, E.I. (1999), *Thickened Tailings Disposal in the Mining Industry*, Robinsky Associates Ltd., Toronto, Canada.

Robinsky, E.I. (2002), Chapter 10 : Case studies, *Paste and Thickened Tailings Disposal – A Guide*, Ed Jewell, Fourie and Lord, Australian Centre for Geomechanics, University of Western Australia, Australia.

Ruse, B. (2003), Cost implications, *Proceedings International Seminar on Paste and Thickened Tailings 2003*, Melbourne, Australia.

Russell, A.C. (2001), Tools for tailings management, *Engineering and Mining Journal*, Oct., pp. 18-26.

Slatter, P. (2004), The measurement and role of rheology in paste pipelining, *Proceedings International Seminar on Paste and Thickened Tailings 2004*, Cape Town, South Africa.

Sofra, F. (2004), Private communication with Fiona Sofra during March 2004.

Sofra, F. and Boger, D.V. (2000), Exploiting the rheology of mine tailings for dry disposal, *Proceedings Tailings and Mine Waste '00*, Balkema, Rotterdam, pp. 169-180.

Uhlherr, P.H.T.; Fang, T.; Zhou, Z. (1999), Determination of yield stress from initiation of motion on an inclined plane, *Mineral Processing and Extractive Metallurgy Review*, Vol. 20, pp. 93-114.

Vagias, N. (2003), Rheology measurement, *Proceedings First Minerals Processing and Tailings Rheology Workshop*, Australian Centre for Geomechanics and Particulate Fluids Processing Centre, Australia.

Van de Graaff, R. and Paterson, R.A. (2001), Explaining the mysteries of salinity, sodicity, SAR and ESP in on-site practice, *Proceedings On-site '01 Conference – Advancing On-site Wastewater Systems*, Lanfax Laboratories, Armidale, Australia.

Van Olphen, H. (1977), *An Introduction to Clay Colloid Chemistry*, 2nd Edition, John Wiley and Sons, New York, USA.

Van Rensburg, L. and Maboeta, M. (2003), Chapter 8 : Rehabilitation, *Paste and Thickened Tailings Disposal Handbook*, Ed Vietti and Dunn, Technical Support Services, De Beers Consolidated Mines, Johannesburg, South Africa.

Vietti, A.J. (1994), *Clay-water-flocculant interactions*, Report no. E66/005/006, De Beers Consolidated Mines, Johannesburg, South Africa.

Vietti, A.J. (2002), History and evolution of co-disposal technology within the De Beers Group, *De Beers Paste Thickening and Co-disposal Workshop*, DebTech, De Beers Consolidated Mines, Johannesburg, South Africa.

Vietti, A.J. (2003a), Chapter 1 : Development of thickened tailings technology within the De Beers Group, *Paste and Thickened Tailings Disposal Handbook*, Ed Vietti and Dunn, Technical Support Services, De Beers Consolidated Mines, Johannesburg, South Africa.

Vietti, A.J. (2003b), Surface chemistry effects of kimberlitic clay minerals, *Proceedings Fourth One Day Seminar on Hydraulic Transport in the Mining Industry*, Hydraulic Conveying Association of South Africa, Johannesburg, South Africa.

Vietti, A.J. (2004), Know your chemistry – suspension and compaction behaviour of paste, *Proceedings International Seminar on Paste and Thickened Tailings 2004*, Cape Town, South Africa.

Vietti, A.J. and Dunn, F. (2003a), Chapter 5 : Thickened tailings rheology, *Paste and Thickened Tailings Disposal Handbook*, Ed Vietti and Dunn, Technical Support Services, De Beers Consolidated Mines, Johannesburg, South Africa.

Vietti, A.J. and Dunn, F. (2003b), Appendix A : Laboratory test work procedure, *Paste and Thickened Tailings Disposal Handbook*, Ed Vietti and Dunn, Technical Support Services, De Beers Consolidated Mines, Johannesburg, South Africa.

Williams, D.J. and Kuganathan, V. (1992), Co-disposal of fine and coarse grained coal mine washery wastes by combined pumping, *International Journal of Environmental Issues in Minerals and Energy Industry*, Balkema, Rotterdam, pp. 53-58.

Williams, M.P.A. and Seddon, K.D. (1999), Thickened tailings discharge : A review of Australian experience, *Proceedings Tailings and Mine Waste '99*, Balkema, Rotterdam, pp. 125-135.

Williams, M.P.A. (2002), Chapter 10 : Case studies, *Paste and Thickened Tailings Disposal – A Guide*, Ed Jewell, Fourie and Lord, Australian Centre for Geomechanics, University of Western Australia, Australia.

Yong, R.N. and Warkentin, B.P. (1966), *Introduction to Soil Behaviour*, The Macmillian Company, New York, USA.

APPENDIX A : MATERIAL CHARACTERISTICS AND PREPARATION RAW DATA

Table A 1 : Vehicle particle size distribution

	DRUM 1	DRUM 2	DRUM 3	*AVERAGE*
Particle size	**Cum. % Passing**	**Cum. % Passing**	**Cum. % Passing**	**Cum. % Passing**
[micron]				
704.0000	100.000	100.000	100.000	**100.000**
592.0000	100.000	100.000	100.000	**100.000**
497.8000	100.000	100.000	100.000	**100.000**
418.6000	100.000	100.000	100.000	**100.000**
352.0000	99.468	99.760	100.000	**99.743**
296.0000	98.660	99.178	100.000	**99.279**
248.9000	96.645	96.755	97.720	**97.040**
209.3000	94.115	94.130	94.808	**94.351**
176.0000	91.505	91.720	92.053	**91.759**
148.0000	88.825	89.408	89.425	**89.219**
124.5000	85.880	86.900	86.603	**86.461**
104.7000	82.528	83.948	83.318	**83.264**
88.0000	78.660	80.325	79.390	**79.458**
74.0000	74.270	75.920	74.800	**74.997**
62.2300	69.418	70.745	69.670	**69.944**
52.3300	64.275	65.005	64.265	**64.515**
44.0000	58.943	58.925	58.753	**58.873**
37.0000	53.430	52.658	53.130	**53.073**
31.1100	47.595	46.183	47.210	**46.996**
26.1600	41.403	39.570	40.928	**40.633**
22.0000	35.083	33.055	34.495	**34.211**
18.5000	29.245	27.250	28.588	**28.361**
15.5600	24.403	22.573	23.743	**23.573**
13.0800	20.650	19.020	20.035	**19.902**
11.0000	17.660	16.233	17.113	**17.002**
9.2500	15.075	13.853	14.603	**14.510**
7.7780	12.703	11.690	12.300	**12.231**
6.5410	10.525	9.718	10.190	**10.144**
5.5000	8.623	7.995	8.348	**8.322**
4.6250	7.025	6.545	6.798	**6.789**
3.8890	5.690	5.328	5.508	**5.508**
3.2700	4.555	4.283	4.408	**4.415**
2.7500	3.578	3.378	3.468	**3.474**
2.3120	2.738	2.593	2.658	**2.663**
1.9450	2.018	1.918	1.958	**1.964**
1.6350	1.388	1.325	1.348	**1.353**
1.3750	0.835	0.800	0.813	**0.816**
1.1560	0.370	0.355	0.358	**0.361**
0.9720	0.000	0.000	0.000	**0.000**
0.8180	0.000	0.000	0.000	**0.000**

Table A 2 : Vehicle clay fraction mineralogy

Clay type	Composition %
Smectite	64
Mica	8
Talc	3
Serpentine	15
Calcite	10

Table A 3 : Load particle size distribution

Particle size [mm]	Cum. % Passing
1.0	0.0
1.40	8.7
2.00	32.5
2.80	57.2
4.00	85.4
6.70	100.0

Table A 4 : Load specific gravity

Particle size range [mm]	Specific gravity [g/cm3]
-6.7+4.0	2.604
-4.0+2.8	2.592
-2.8+2.0	2.581
-2.0+1.4	2.570
-1.4+1.0	2.593
Average	*2.59*

Table A 5 : Load void ratio

Cylindrical mould					
Diameter of mould	101.7	mm	Volume of mould	939.9	cm^3
Height of mould	115.7	mm	Mass of mould	3776.8	g
Maximum void ratio - before vibration			**Minimum void ratio -** after vibration		
Solids SG	2.59	g/cm^3	Solids SG	2.59	g/cm^3
Mass of solids	1294.6	g	Mass of solids	1515.0	g
Volume of solids	499.8	cm^3	Volume of solids	584.9	cm^3
Volume of voids	440.0	cm^3	Volume of voids	354.9	cm^3
Max void ratio	*0.88*		*Min void ratio*	*0.61*	

Table A 6 : Optimum flocculant selection

	Candidate flocculants			
	Montan	Magnafloc		
	3073	E10	1011	5250
Degree of flocculation	Poor	Good	Fair	Poor
Clarity of supernatant	Poor	Good	Poor	Poor
Optimum flocculant = Magnafloc E10				

Table A 7 : Flocculated slurry settling data

Settling time [min]	Settled distance [mm]
0.000	0.0
0.167	59.5
0.333	118.0
0.500	171.5
0.667	223.0
0.833	240.0
1.000	248.0
2.000	265.5
3.000	272.0
4.000	276.5
5.000	279.0
10.000	287.5
15.000	291.0
20.000	292.5
25.000	294.0
30.000	295.5
Settling rate = 20 m/h	

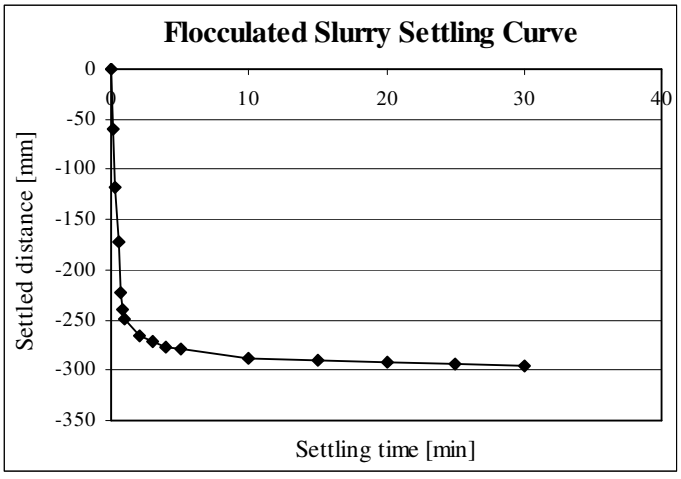

Figure A 1 : Flocculated slurry settling curve

APPENDIX B : PREPARATION OF CO-DISPOSED TAILINGS

The following section presents the equations used in the calculations that form part of the co-disposed tailings preparation procedure described in Section 4.4.

Equation B 1 : Vehicle solids concentration

$$x_{solids} = m_{solids} / m_v \times 100$$

$$m_{solids} = m_{dry} - m_{container}$$

$$m_v = m_{wet} - m_{container}$$

Equation B 2 : Vehicle density

$$\rho_v = \left(SG_v \rho_{liquid}\right) / \left(SG_v + x_{solids}\left(\rho_{liquid} - SG_v\right)\right)$$

Equation B 3 : Vehicle mass

$$m_v = \rho_v / V_v$$

Equation B 4 : Co-disposed tailings mass

$$m_T = m_v / y_v$$

Equation B 5 : Load mass

$$m_l = m_T - m_v$$

where m_i = mass [kg]

x_i = solids mass fraction

SG_i = specific gravity [kg/m^3]

ρ_i = density [kg/l]

V_i = volume [l]

y_i = vehicle or load component mass fraction

and $i = v$: vehicle

$i = l$: load

$i = T$: co-disposed tailings

APPENDIX C : CALCULATION OF VEHICLE SOLIDS CONCENTRATION

The following section presents the equations used in the calculation of the vehicle solids concentration after dilution of the co-disposed tailings material, as described in Section 4.5.1.

Starting point information:

- vehicle solids mass fraction before dilution (x_1)
- vehicle volume before dilution (V_1)
- vehicle mass before dilution (m_1)
- dilution water volume (V_d)

Equation C 1 : Vehicle dry solids mass

$$m_{solids} = x_1 \times m_{v1}$$

Equation C 2 : Volume of water before dilution

$$V_{w1} = m_{w1} = m_{v1} - m_{solids}$$

Equation C 3 : Volume of water after dilution

$$V_{w2} = V_{w1} + V_d = m_{w2}$$

Equation C 4 : Vehicle mass after dilution

$$m_{v2} = m_{solids} + m_{w2}$$

Equation C 5 : Vehicle solids mass fraction after dilution

$$x_2 = m_{solids} / m_{v2}$$

where m_{ij} = mass [kg]

V_{ij} = volume [l]

x_j = solids mass fraction

$i = v$: vehicle $\qquad$ $j = 1$: before dilution

$i = w$: water $\qquad$ $j = 2$: after dilution

APPENDIX D : CALCULATION OF CO-DISPOSED TAILINGS TOTAL SOLIDS CONCENTRATION

The following section presents the equations used in the calculation of the total solids concentration of the co-disposed tailings material, as discussed in Section 4.5.1.

Starting point information in reference to Appendix B:

- vehicle and load component mass fractions (y_v and y_l)
- vehicle mass (m_v)
- vehicle solids mass fraction (x_v)
- load mass (m_l)

Equation D 1 : Vehicle density

$$\rho_v = \left(SG_v \rho_{liquid}\right) / \left(SG_v + x_{solids}\left(\rho_{liquid} - SG_v\right)\right)$$

Equation D 2 : Vehicle volume

$$V_v = m_v / \rho_v$$

Equation D 3 : Load volume

$$V_l = m_l / SG_l$$

Equation D 4 : Co-disposed tailings mass

$$m_T = m_v + m_l$$

Equation D 5 : Co-disposed tailings volume

$$V_T = V_v + V_l$$

Equation D 6 : Co-disposed tailings density

$$\rho_T = m_T / V_T$$

Equation D 7 : Co-disposed tailings specific gravity

$$SG_T = y_v\left(SG_v\right) + y_l\left(SG_l\right)$$

Equation D 8 : Co-disposed tailings total solids mass fraction

$$x_T = \left(SG_T\left(\rho_T - \rho_{liquid}\right)\right) / \left(\rho_T\left(SG_T - \rho_{liquid}\right)\right)$$

where m_i = mass [kg]

x_i = solids mass fraction

SG_i = specific gravity [kg/m^3]

ρ_i = density [kg/l]

V_i = volume [l]

y_i = vehicle or load component mass fraction

and $i = v$: vehicle

$i = l$: load

$i = T$: co-disposed tailings

APPENDIX E : PREPARATION OF ACIDIC AND ALKALINE SOLUTIONS

The following section describes the preparation of a 5 molar solution of 33% hydrochloric acid (HCl). The equations used in the calculations are as follows :

Equation E 1 : Molarity of a solution

$$M = mol / V_{sol}$$

Equation E 2 : Mole of a substance

$$mol = m / MM$$

Equation E 3 : Density of a substance

$$\rho = m / V$$

where M = molarity of a solution [mol/l]

mol = moles of a substance [mol]

V_{sol} = volume of solution [l]

m = mass of a substance [g]

MM = molar mass of a substance [g/mol]

ρ = density of substance [g/cm^3]

V = volume of substance [ml]

According to Table E 1 the 5 molar solution of 33% hydrochloric acid (HCl) was prepared by mixing 158 ml of 33% HCl acid with 1 litre of distilled water.

Table E 1 : Preparation of 5M solution of 33% HCl

PREPARATION OF 5M SOLUTION OF 33% HCl		
Volume of 33% HCl acid	158.0	ml/l
Density of 33% HCl acid	1.1	g/cm3
Mass of 33% HCl acid	179.3	g/l
Atomic weight of H	1.0	
Atomic weight of Cl	35.5	
Molar mass of HCl	36.5	g/mol
Moles of 33% HCl in sol.	4.9	mol/l
Molarity of solution	4.9	mol/l
Concentration of HCl acid	0.33	
Mass of HCl in solution	59.2	g/l
Moles of HCl in sol.	1.6	mol/l

The following section describes the preparation of a solution of sodium hydroxide (NaOH) and calcium hydroxide ($Ca(OH)_2$) with a SAR value matching the natural ESP value of the vehicle clay fraction. The equations used in the calculations, besides Equation E 1 and Equation E 2, are as follows :

Equation E 4 : Equivalent weight of a substance

$$Equivalent\ weight = atomic\ weight / valence$$

Equation E 5 : Milli-equivalent mass of a substance

$$m_{eq} = m / equivalent\ weight$$

Equation E 6 : Sodium Adsorption Ratio (SAR) for only Na^+ and Ca^{2+} cations

$$SAR = \left[Na^+\right] / \sqrt{\left[Ca^{2+}\right]}$$

where m_{eq} = milli-equivalent mass of a substance [meq]

m = mass of a substance [mg]

$[Na^+]$ = concentration of Na^+ ion in solution [meq/l]

$[Ca^{2+}]$ = concentration of Ca^{2+} ion in solution [meq/l]

According to Table E 2 the sodium hydroxide and calcium hydroxide solution was prepared by mixing 40 g NaOH powder and 35.5 g $Ca(OH)_2$ powder in 1 litre of distilled water.

Table E 2 : Preparation of NaOH and $Ca(OH)_2$ solution

PREPARATION OF NaOH AND $Ca(OH)_2$ SOLUTION		
Molarity of NaOH solution	1	mol/l
Moles of NaOH in solution	1	mol/l
Atomic weight of Na	23.0	amu
Atomic weight of O	16.0	amu
Atomic weight of H	1.0	amu
Molar mass of NaOH	40.0	g/mol
Mass of NaOH in solution	40.0	g/l
Mass of Na^+ in solution	23.0	g/l
	22990	mg/l
Equivalent weight of Na^+	23.0	
Milli-equivalent mass of Na^+	1000	meq/l
SAR = ESP	32.3	
Milli-equivalent mass of Ca^{2+}	958.5	meq/l
Atomic weight of Ca	40.1	amu
Equivalent weight of Ca^{2+}	20.0	
Mass of Ca^{2+} in solution	19208	mg/l
	19.2	g/l
Moles of Ca^{2+} in solution	0.5	mol/l
Molarity of $Ca(OH)_2$ solution	0.5	mol/l
Molar mass of $Ca(OH)_2$	74.1	g/mol
Mass of $Ca(OH)_2$ in solution	35.5	g/l

APPENDIX F : US 200 PAAR PHYSICA SOFTWARE INSTRUCTIONS

The following section presents the US 200 Paar Physica software instructions to operate the Paar Physica Rheolab MC1 rheometer for yield stress measurement with the vane method (Gawu, 2004).

- Start the computer
- Double click on the US 200 icon on the desktop
- Click on “File”
- Select “File Assistant”
- Select “Workbook Assistant” and click “OK”
- Select “Time Test / CSR” and click “Finish”
- Many different windows will now open
- Enlarge the “Measurement 1 : Time Test Rotation/CSR” window
- Double click on “MC1+”
- Under “Measuring Systems” select “Vane2(flush)” for the medium vane or “VaneFL100” for the small vane, from the drop down menu and click “OK”
- Double click on “Rotation $\dot{\gamma}$, n”
- Under “Set Variable” select “n speed” from the drop down menu
- Under “Unit” select “rpm” from the drop down menu
- Under “Initial” type in the desired rotational speed of the vane in rpm and click “OK”
- Double click on “1”, the block showing the measurement point information
- Under “Meas. Points” type in the desired number of data points
- Under “Duration” select “Meas. Points” and type in the desired time duration per data point in seconds and click “OK”
- Switch on rheometer
- Press the “OK” key on the rheometer
- Use the arrow keys on the rheometer to select “Remote” and press the “OK” key
- Ensure that the vane is inserted in the sample and that the experimental set-up is ready for the yield stress measurement to start
- Click on the “Start” button in the “Measurement 1” window

- Type in the desired “Data series name for the measurement”, i.e. test or measurement
- Type in the “Sample description”
- Press “Enter” on the keyboard
- Type in the “File name” keeping the .mph extension
- Type in the “Remark” to describe the test series
- Click “Save”
- The test is now running
- After completion of the test, the torque – time raw data is presented in graphical form in the “Diagram 1 : Time Test” window and in tabled form in the “Table 1 : Time Test” window
- If an incorrect variable is displayed on the y-axis of the graph in the “Diagram 1” window, double click on the y-axis and under “Selected Variable” select “Torque” from the drop down menu and click “OK”
- If an incorrect variable is displayed in the table in the “Table 1” window, double click on the variable heading under “Displayed Columns” and under “Selected Variable” select “Torque” from the drop down menu and click “OK”
- Click on “File”
- Select “Save”
- Type in the “File name” keeping the .ctx extension
- Click “Save”

APPENDIX G : PRELIMINARY TEST WORK - RAW DATA SUMMARY

Table G 1 : Influence of shear time on vehicle rheology – raw data

Test file description	*Time of shear (min)*	*Max torque (mNm)*	*Yield stress (Pa)*
Sample 1			
Fredre11 test 2	0	27.1	404.0
Fredre11 test 3	2	16.3	243.0
Fredre11 test 4	5	14.9	222.1
Fredre11 test 5	10	14.9	222.1
Fredre11 test 6	15	15.1	225.1
Sample 2			
Fredre11 test 9	0	24.6	366.7
Fredre11 test 10	20	15.0	223.6

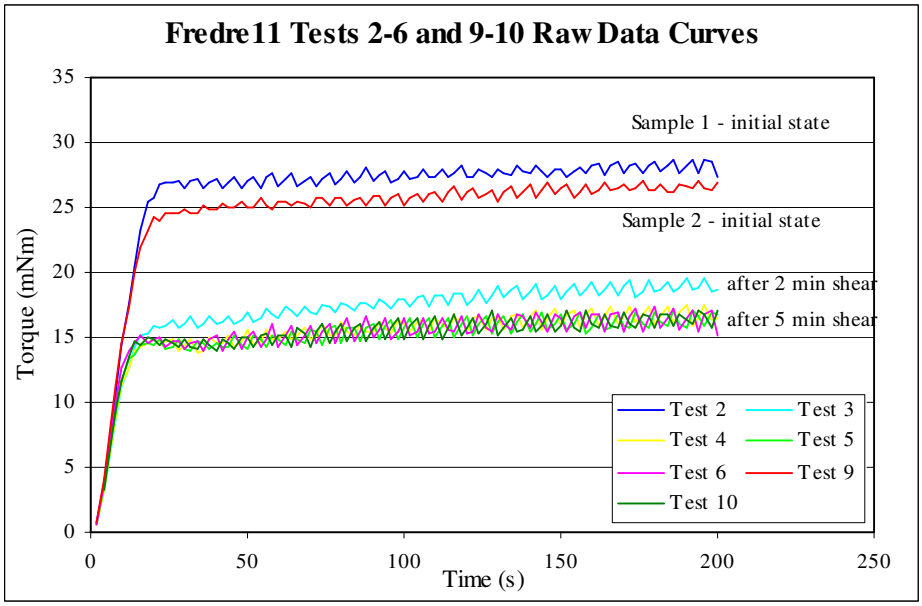

Figure G 1 : Influence of shear time on vehicle rheology – raw data curves

Table G 2 : Influence of recovery time on vehicle rheology – raw data

Test file description	*Time of shear (min)*	*Time of recovery (min)*	*Max torque (mNm)*	*Yield stress (Pa)*
Fredre12 test 1	0	0	25.5	380.1
Fredre12 test 3	5	0	16.1	240.0
Fredre12 test 4	5	2	18.6	277.3
Fredre12 test 5	5	5	20.5	305.7
Fredre12 test 6	5	10	22.8	340.1
Fredre12 test 7	5	15	24.3	362.1
Fredre12 test 8	5	20	26.9	401.0

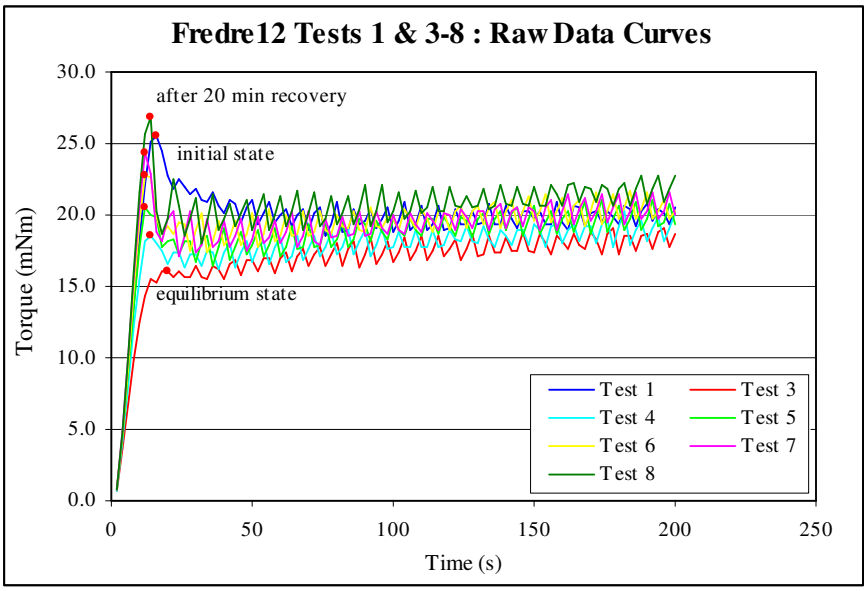

Figure G 2 : Influence of recovery time on vehicle rheology – raw data curves

APPENDIX H : VEHICLE YIELD STRESS - RAW DATA SUMMARY

Table H 1 : Vehicle yield stress - pH 8.6 (non-interactive)

VANE

	measured	*measured*
Data point	*Vehicle*	*Yield stress*
	% solids	*(Pa)*
1	67.4	595.1
2	67.3	516.1
3	66.8	438.1
4	66.5	410.6
5	66.1	345.2
6	65.9	274.7
7	65.2	206.1
8	64.2	145.7
9	63.5	101.5
10	62.5	67.0
11	61.6	45.2

SMALL SLUMP

	measured	*measured*
Data point	*Vehicle*	*Yield stress*
	% solids	*(Pa)*
1	67.9	512.2
2	67.5	413.1
3	67.1	347.5
4	66.8	293.3
5	66.3	236.1
6	65.5	154.4
7	65.0	102.9

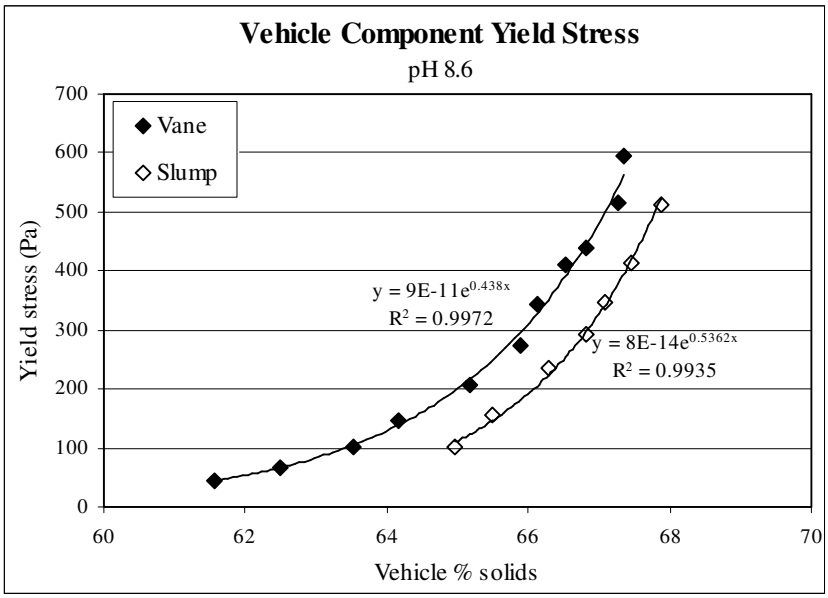

Figure H 1 : Vehicle yield stress - pH 8.6 (non-interactive)

Table H 2 : Vehicle yield stress - pH 6.2 (interactive)

VANE

	measured	*measured*
Data point	*Vehicle*	*Yield stress*
	% solids	*(Pa)*
1	65.8	587.5
2	65.5	537.5
3	65.2	473.6
4	64.6	403.9
5	63.4	320.6
6	63.2	257.5
7	61.5	183.4
8	60.3	132.8
9	57.7	90.8
10	56.2	61.1

SMALL SLUMP

	measured	*measured*
Data point	*Vehicle*	*Yield stress*
	% solids	*(Pa)*
1	63.8	400.8
2	63.9	364.4
3	63.6	321.7
4	62.8	296.8
5	62.2	252.1
6	60.9	209.6
7	59.8	173.3
8	59.0	92.2

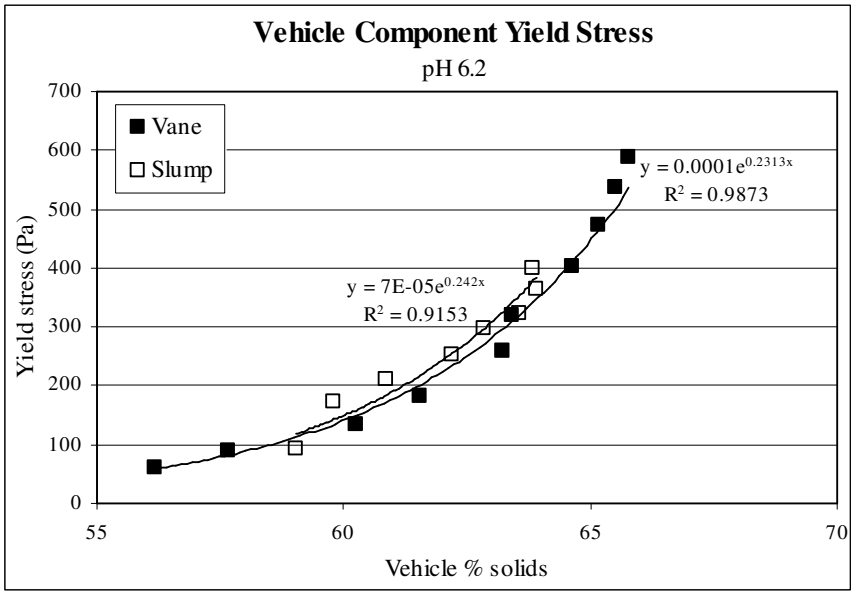

Figure H 2 : Vehicle yield stress - pH 6.2 (interactive)

Table H 3 : Vehicle yield stress - pH 11.5 (interactive)

VANE

	measured	*measured*
Data point	*Vehicle*	*Yield stress*
	% solids	*(Pa)*
1	65.4	615.5
2	64.3	536.8
3	62.9	433.5
4	61.6	356.2
5	59.8	248.6
6	58.6	207.3
7	57.5	148.3
8	56.3	110.1
9	54.2	72.7

SMALL SLUMP

	measured	*measured*
Data point	*Vehicle*	*Yield stress*
	% solids	*(Pa)*
1	62.7	361.1
2	61.8	324.2
3	61.0	299.6
4	59.9	261.9
5	58.9	219.3
6	57.8	188.1
7	56.6	143.1
8	55.2	81.9

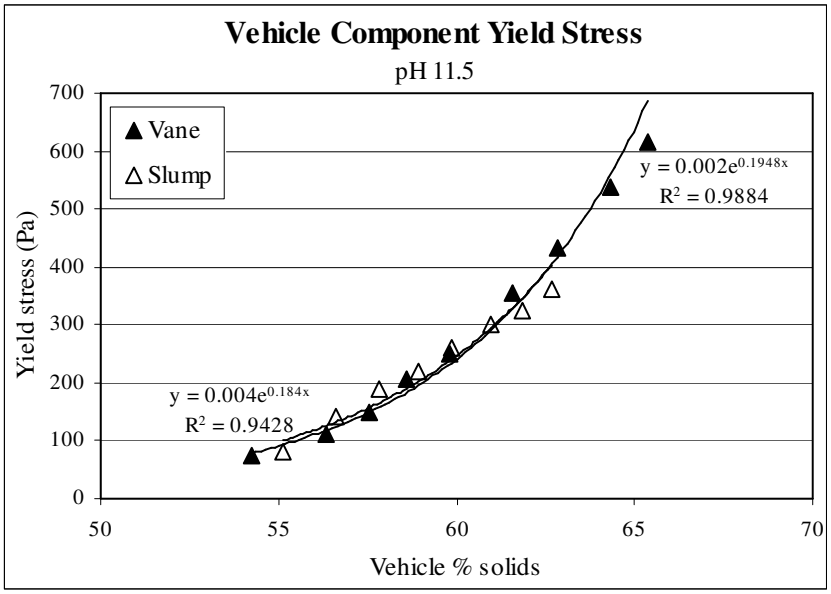

Figure H 3 : Vehicle yield stress - pH 11.5 (interactive)

Table H 4 : Average radius of slumped material radial flow distance

pH = 8.6

Vehicle % solids	*Average radius of radial flow distance (mm)*
67.9	65.6
67.5	73.6
67.1	85.3
66.8	93.0
66.3	109.7
65.5	121.2
65.0	139.3

pH = 6.3

Vehicle % solids	*Average radius of radial flow distance (mm)*
63.8	72.8
63.9	75.3
63.6	82.4
62.8	90.1
62.2	102.0
60.9	115.8
59.8	122.8
59.0	151.7

pH = 11.5

Vehicle % solids	*Average radius of radial flow distance (mm)*
62.7	71.5
61.8	74.5
61.0	79.9
59.9	89.6
58.9	99.1
57.8	112.3
56.6	127.4
55.2	147.6

Additional large slump test work :

Table H 5 : Vehicle yield stress – pH 8.5 (interactive)

VANE

	measured	measured
Data point	*Vehicle*	*Yield stress*
	% solids	*(Pa)*
1	69.0	1268.2
2	67.9	946.1
3	67.1	775.9
4	66.0	639.6
5	65.1	477.3
6	64.1	316.9
7	63.0	219.3
8	62.0	167.4
9	61.0	117.6
10	59.3	73.7

LARGE SLUMP

	measured	measured
Data point	*Vehicle*	*Yield stress*
	% solids	*(Pa)*
1	68.0	932.0
2	68.2	869.2
3	67.7	797.6
4	67.1	744.2
5	66.7	678.6
6	66.5	631.3
7	65.9	582.9
8	65.4	513.7
9	65.0	431.6
10	64.3	354.4
11	63.6	319.2
12	62.5	252.6
13	61.7	204.3

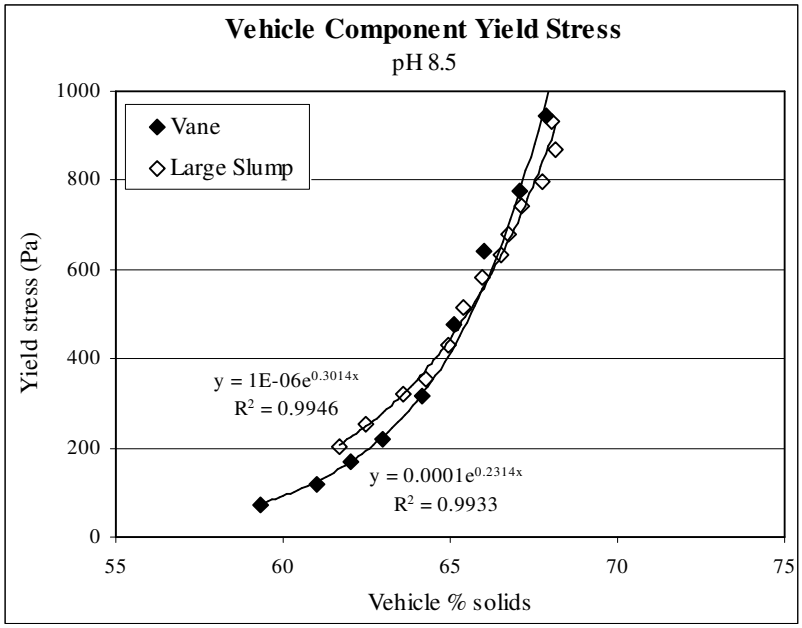

Figure H 4 : Vehicle yield stress – pH 8.5 (interactive)

Table H 6 : Vehicle yield stress – pH 8.7 (non-interactive)

VANE

	measured	*measured*
Data point	*Vehicle*	*Yield stress*
	% solids	*(Pa)*
1	68.0	681.8
2	67.8	563.9
3	67.0	408.7
4	66.4	304.4
5	65.4	205.6
6	64.1	127.0
7	62.7	70.7

SMALL SLUMP

	measured	*measured*
Data point	*Vehicle*	*Yield stress*
	% solids	*(Pa)*
1	69.8	604.7
2	69.3	496.7
3	67.9	371.4
4	67.1	237.6
5	65.8	137.3

LARGE SLUMP

	measured	*measured*
Data point	*Vehicle*	*Yield stress*
	% solids	*(Pa)*
1	69.8	683.4
2	69.0	566.7
3	69.0	498.3
4	68.2	397.3
5	67.1	299.8
6	66.4	234.6

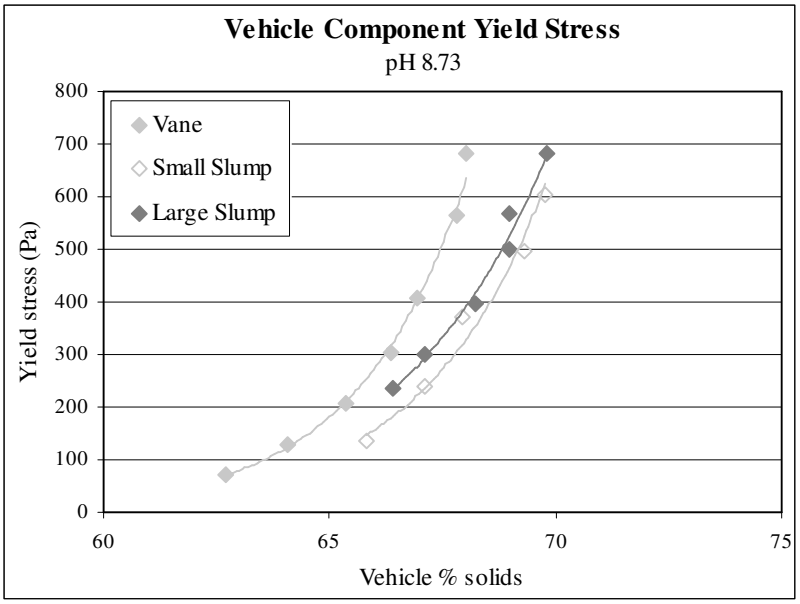

Figure H 5 : Vehicle yield stress – pH 8.7 (non-interactive)

APPENDIX I : VEHICLE YIELD STRESS - RAW DATA SHEETS

Vehicle pH 8.6 - Vane Tests

Date : 07/04/2004

Vane dimensions :			
medium vane	height	0.060	m
	diameter	0.025	m

Rheometer settings :			
	speed	0.3	rpm
	data points	400	
	duration	120	sec

File name :	**Fredre14**
Sample description :	Vehicle pH 8.6 (non-interactive)

Material characteristics :	Type	Vehicle	
	Solids SG	2.41	g/cm^3
	pH	8.6	

Test number	Description	Pan no.	Pan mass (g)	Start mass (g)	Wet mass (g)	End mass (g)	Dry mass (g)	% solids (%)	Density (kg/m^3)	Dilution (ml)	Max Torque (mNm)	Yield stress (Pa)
Test 2	rep 1	11	25.1250	34.0000	8.8750	31.1030	5.9780	67.3577	1650.40	0	41.0923	
Test 3	rep 2										39.3960	
Test 4	rep 3										39.2818	
											39.92	***595.11***
Test 5	rep 1	25	24.3690	27.4520	3.0830	26.4430	2.0740	67.2721	1649.03	4	34.2430	
Test 6	rep 2										34.1433	
Test 7	rep 3										35.4898	
											34.63	***516.13***
Test 8	rep 1	15	24.9460	27.9410	2.9950	26.9470	2.0010	66.8114	1641.73	4	27.0898	
Test 9	rep 2										30.2823	
Test 10	rep 3										30.8083	
											29.39	***438.15***
Test 11	rep 1	7	25.3340	29.1600	3.8260	27.8790	2.5450	66.5186	1637.13	4	26.3903	
Test 12	rep 2										27.5448	
Test 13	rep 3										28.7115	
											27.55	***410.65***
Test 14	rep 1	3	25.2490	27.8090	2.5600	26.9420	1.6930	66.1328	1631.10	7	24.1475	
Test 15	rep 2										21.6978	
Test 16	rep 3										23.6263	
											23.16	***345.19***
Test 17	rep 1	22	24.4390	27.4180	2.9790	26.4020	1.9630	65.8946	1627.40	8.4	17.2970	
Test 18	rep 2										18.3853	
Test 19	rep 3										19.6095	
											18.43	***274.73***
Test 20	rep 1	17	25.2770	28.3770	3.1000	27.2970	2.0200	65.1613	1616.12	10	13.9143	
Test 21	rep 2										13.6040	
Test 22	rep 3										13.9698	
											13.83	***206.14***
Test 23	rep 1	33	27.5980	30.7940	3.1960	29.6490	2.0510	64.1740	1601.17	11	9.4410	
Test 24	rep 2										9.6243	
Test 25	rep 3										10.2505	
											9.77	***145.66***
Test 26	rep 1	43	27.0540	30.6500	3.5960	29.3380	2.2840	63.5150	1591.35	12	6.5710	
Test 27	rep 2										6.8378	
Test 28	rep 3										7.0268	
											6.81	***101.54***
Test 29	rep 1	77	28.3280	33.4820	5.1540	31.5490	3.2210	62.4951	1576.38	13	4.2158	
Test 30	rep 2										4.6205	
Test 31	rep 3										4.6495	
											4.50	***67.01***
Test 32	rep 1	59	24.6530	33.3440	8.6910	30.0030	5.3500	61.5579	1562.87	14	2.8563	
Test 33	rep 2										3.3865	
Test 34	rep 3										2.8473	
											3.03	***45.17***

Vehicle pH 8.6 - Small Slump Tests

Date : 16/04/2004

Slump cylinder : small cylinder

height	0.130	m
diameter	0.105	m
aspect ratio	1.24	
ruler thickness	9	mm

Material characteristics :

Type	Vehicle	
Solids SG	2.41	g/cm^3
pH	8.6	

Test	Description	Pan no.	Pan mass	Start mass	Wet mass	End mass	Dry mass	% solids	Density	Dilution	Slump height	Slump height	Yield stress	Flow distance (rings)				Flow distance radius (mm)				
number			(g)	(g)	(g)	(g)	(g)	(%)	(kg/m^3)	(ml)	incl ruler (mm)	excl ruler (mm)	(Pa)	N	S	E	W	N	S	E	W	*average*
Test 1	rep 1	15	24.9400	30.1720	5.2320	28.4910	3.5510	67.8708	1658.61	40	44.00	35.00		1 start	1 mid	0 mid	1 mid	65.64	70.68	60.38	70.68	66.85
	rep 2										43.20	34.20		1 start	1 start	1 start	1 start	65.64	65.64	65.64	65.64	65.64
	rep 3										43.80	34.80		1 start	1 start	1 start	0 mid	65.64	65.64	65.64	60.38	64.33
												34.67	***512.17***									**65.60**
Test 2	rep 1	14	24.9220	29.8050	4.8830	28.2160	3.2940	67.4585	1652.00	40	57.60	48.60		1 mid	2 mid	1 mid	2 start	70.38	80.73	70.68	75.76	74.39
	rep 2										58.50	49.50		2 start	2 start	2 start	2 start	75.76	75.76	75.76	75.76	75.76
	rep 3										55.30	46.30		1 mid	1 mid	1 mid	1 mid	70.68	70.68	70.68	70.68	70.68
												48.13	***413.08***									**73.61**
Test 3	rep 1	3	25.2410	29.1060	3.8650	27.8340	2.5930	67.0893	1646.13	35	67.40	58.40		3 start	3 mid	2 mid	4 start	85.73	90.38	80.73	95.76	88.15
	rep 2										66.45	57.45		3 mid	2 mid	3 start	2 mid	90.38	80.73	85.73	80.73	84.39
	rep 3										68.00	59.00		2 mid	3 start	2 mid	3 start	80.73	85.73	80.73	85.73	83.23
												58.28	***347.46***									**85.26**
Test 4	rep 1	22	24.4310	30.2850	5.8540	28.3430	3.9120	66.8261	1641.97	35	77.60	68.60		4 mid	3 mid	4 start	4 start	100.78	90.38	95.76	95.76	95.67
	rep 2										75.60	66.60		3 mid	3 mid	3 mid	4 start	90.38	90.38	90.38	95.76	91.73
	rep 3										76.20	67.20		3 mid	3 mid	3 mid	4 start	90.38	90.38	90.38	95.76	91.73
												67.47	***293.34***									**93.04**
Test 5	rep 1	11	25.1190	29.8860	4.7670	28.2790	3.1600	66.2891	1633.54	40	86.40	77.40		5 mid	5 mid	5 start	6 start	111.13	111.13	105.8	115.86	110.98
	rep 2										86.55	77.55		5 mid	5 start	5 start	6 start	111.13	105.8	105.8	115.86	109.65
	rep 3										87.60	78.60		4 mid	5 mid	5 start	6 start	100.78	111.13	105.8	115.86	108.39
												77.85	***236.14***									**109.67**
Test 6	rep 1	25	24.3670	32.4660	8.0990	29.6710	5.3040	65.4896	1621.15	45	105.70	96.70		7 start	7 start	7 start	7 start	125.76	125.76	125.76	125.76	125.76
	rep 2										102.45	93.45		6 start	6 mid	6 mid	7 start	115.86	120.65	120.65	125.76	120.73
	rep 3										101.40	92.40		6 start	6 start	5 mid	7 start	115.86	115.86	111.13	125.76	117.15
												94.18	***154.38***									**121.21**
Test 7	rep 1	33	27.5910	41.1350	13.5440	36.3910	8.8000	64.9734	1613.25	40	114.65	105.65		8 start	8 mid	8 start	9 mid	135.83	140.38	135.83	150.5	140.64
	rep 2										113.90	104.90		8 mid	8 mid	8 mid	8 mid	140.38	140.38	140.38	140.38	140.38
	rep 3										114.70	105.70		7 mid	8 mid	8 start	8 mid	130.83	140.38	135.83	140.38	136.86
												105.42	***102.86***									**139.29**

Vehicle pH 6.2 - Vane Tests

Date : 15/04/2004

Vane dimensions : medium vane			
	height	0.060	m
	diameter	0.025	m

Rheometer settings :			
	speed	0.3	rpm
	data points	400	
	duration	120	sec

File name :	**Fredre15**
Sample description :	Vehicle pH 6.2 (interactive)

Material characteristics :		
Type	Vehicle	
Solids SG	2.41	g/cm^3
pH	6.2	

Test number	Description	Pan no.	Pan mass (g)	Start mass (g)	Wet mass (g)	End mass (g)	Dry mass (g)	% solids (%)	Density (kg/m^3)	Dilution (ml)	Max Torque (mNm)	Yield stress (Pa)	pH before	pH after	pH ave
Vehicle starting point		3	25.2670	31.2290	5.9620	29.3900	4.1230	69.1546	1679.54	0					
Test 2	rep 1	22	24.4550	27.2020	2.7470	26.2620	1.8070	65.7809	1625.64	45 acid	38.2473		6.15	6.42	6.29
Test 3	rep 2										40.3717				
Test 4	rep 3										39.6248				
											39.41	***587.52***			
Test 5	rep 1	17	25.2700	29.5550	4.2850	28.0770	2.8070	65.5076	1621.43	6 acid	35.3170		6.12	6.42	6.27
Test 6	rep 2										36.5350				
Test 7	rep 3										36.3145				
											36.06	***537.45***			
Test 8	rep 1	11	25.1210	28.4580	3.3370	27.2960	2.1750	65.1783	1616.38	5 acid	31.4742		6.12	6.37	6.25
Test 9	rep 2									1 water	32.0008				
Test 10	rep 3										31.8498				
											31.77	***473.64***			
Test 12	rep 1	15	24.9440	28.4800	3.5360	27.2290	2.2850	64.6210	1607.91	5 acid	26.6230		6.16	6.37	6.27
Test 13	rep 2									5 water	26.9700				
Test 14	rep 3										27.7020				
											27.10	***403.93***			
Test 15	rep 1	14	24.9240	27.7940	2.8700	26.7440	1.8200	63.4146	1589.86	4 acid	19.9278		6.10	6.33	6.22
Test 16	rep 2									9 water	22.3500				
Test 17	rep 3										22.2360				
											21.50	***320.55***			
Test 18	rep 1	7	25.2340	28.7520	3.5180	27.4580	2.2240	63.2177	1586.96	3.2 acid	16.4445		6.16	6.33	6.25
Test 19	rep 2									12 water	17.3723				
Test 20	rep 3										18.0030				
											17.27	***257.48***			
Test 21	rep 1	25	24.3680	27.7640	3.3960	26.4580	2.0900	61.5430	1562.66	3.4 acid	11.8215		6.11	6.22	6.17
Test 22	rep 2									16 water	12.3225				
Test 23	rep 3										12.7765				
											12.31	***183.45***			
Test 24	rep 1	33	27.5940	31.6390	4.0450	30.0320	2.4380	60.2719	1544.71	2 acid	8.4088		6.13	6.26	6.20
Test 25	rep 2									17 water	9.1698				
Test 26	rep 3										9.1515				
											8.91	***132.81***			
Test 27	rep 1	23	23.8250	27.5190	3.6940	25.9550	2.1300	57.6611	1509.10	2.4 acid	5.3033		6.12	6.22	6.17
Test 28	rep 2									23 water	6.9100				
Test 29	rep 3										6.0535				
											6.09	***90.76***			
Test 30	rep 1	43	27.0430	34.8370	7.7940	31.4220	4.3790	56.1842	1489.68	2 acid	4.1620		6.15	6.00	6.08
Test 31	rep 2									26 water	4.2103				
Test 32	rep 3										3.9175				
											4.10	***61.06***			

Average pH 6.21

Vehicle pH 6.2 - Small Slump Tests

Date : 19/04/2004

Slump cylinder : small cylinder

height	0.130	m
diameter	0.105	m
aspect ratio	1.24	

ruler thickness	9	mm

Material characteristics :

Type	Vehicle	
Solids SG	2.41	g/cm^3
pH	6.3	

Test	Description	Pan no.	Pan mass	Start mass	Wet mass	End mass	Dry mass	% solids	Density	Dilution	Slump height	Slump height	Yield stress	Flow distance (rings)				Flow distance radius (mm)					pH before	pH after	pH ave
number			(g)	(g)	(g)	(g)	(g)	(%)	(kg/m^3)	(ml)	incl ruler (mm)	excl ruler (mm)	(Pa)	N	S	E	W	N	S	E	W	average			
Test 1	rep 1	7	25.2320	29.4470	4.2150	27.9220	2.6900	63.8197	1595.88	90 acid	57.50	48.50		1 mid	2 start	1 mid	2 mid	70.68	75.76	70.68	80.73	74.46	6.13	6.56	6.35
	rep 2										56.00	47.00		1 mid	1 mid	1 mid	1 mid	70.68	70.68	70.68	70.68	70.68			
	rep 3										57.10	48.10		1 start	2 mid	1 start	2 mid	65.64	80.73	65.64	80.73	73.19			
												47.87	***400.76***									**72.78**			
Test 2	rep 1	25	24.3660	30.7350	6.3690	28.4360	4.0700	63.9033	1597.12	20 acid	64.15	55.15		1 mid	2 mid	2 start	2 start	70.68	80.73	75.76	75.76	75.73	6.14	6.54	6.34
	rep 2										60.30	51.30		1 mid	2 start	2 start	2 start	70.68	75.76	75.76	75.76	74.49			
	rep 3										63.70	54.70		2 start	2 start	1 mid	2 mid	75.76	75.76	70.68	80.73	75.73			
												53.72	***364.38***									**75.32**			
Test 3	rep 1	14	24.9220	29.5030	4.5810	27.8340	2.9120	63.5669	1592.12	23 acid	69.45	60.45		2 mid	2 mid	2 mid	3 mid	80.73	80.73	80.73	90.38	83.14	6.13	6.42	6.28
	rep 2									10 water	69.75	60.75		2 mid	3 start	2 mid	2 mid	80.73	85.73	80.73	80.73	81.98			
	rep 3										70.10	61.10		3 start	2 mid	2 mid	2 mid	85.73	80.73	80.73	80.73	81.98			
												60.77	***321.72***									**82.37**			
Test 4	rep 1	22	24.4310	28.2790	3.8480	26.8490	2.4180	62.8378	1581.38	18 acid	75.00	66.00		3 mid	3 mid	3 start	4 mid	90.38	90.38	85.73	100.78	91.82	6.13	6.43	6.28
	rep 2									25 water	72.90	63.90		3 start	3 mid	3 mid	3 mid	85.73	90.38	90.38	90.38	89.22			
	rep 3										73.60	64.60		3 mid	3 start	3 mid	3 mid	90.38	85.73	90.38	90.38	89.22			
												64.83	***296.84***									**90.08**			
Test 5	rep 1	11	25.1180	29.2620	4.1440	27.6950	2.5770	62.1863	1571.90	19 acid	82.70	73.70		4 mid	4 mid	4 mid	5 start	100.78	100.78	100.78	105.8	102.04	6.08	6.30	6.19
	rep 2									33 water	80.80	71.80		5 start	4 start	5 start	4 mid	105.8	95.76	105.8	100.78	102.04			
	rep 3										82.30	73.30		5 start	4 start	4 mid	5 start	105.8	95.76	100.78	105.8	102.04			
												72.93	***252.13***									**102.04**			
Test 6	rep 1	3	25.2480	33.0090	7.7610	29.9710	4.7230	60.8556	1552.90	13 acid	88.50	79.50		6 start	5 mid	6 mid	6 mid	115.86	111.13	120.65	120.65	117.07	6.15	6.3	6.23
	rep 2									45 water	89.90	80.90		6 start	5 mid	6 start	6 mid	115.86	111.13	115.86	120.65	115.88			
	rep 3										91.30	82.30		6 mid	5 start	6 start	6 start	120.65	105.8	115.86	115.86	114.54			
												80.90	***209.61***									**115.83**			
Test 7	rep 1	15	24.9410	36.6340	11.6930	31.9310	6.9900	59.7794	1537.86	10 acid	96.20	87.20		6 mid	6 mid	6 mid	7 mid	120.65	120.65	120.65	130.83	123.20	6.13	6.43	6.28
	rep 2									40 water	98.50	89.50		6 mid	6 mid	7 start	7 start	120.65	120.65	125.76	125.76	123.21			
	rep 3										96.95	87.95		6 mid	6 mid	6 mid	7 start	120.65	120.65	120.65	125.76	121.93			
												88.22	***173.34***									**122.78**			
Test 8	rep 1	17	25.2680	34.3300	9.0620	30.6180	5.3500	59.0377	1527.67	12 acid	114.20	105.20		9 start	8 mid	9 mid	9 start	145.71	140.38	150.5	145.71	145.58	6.16	6.28	6.22
	rep 2									45 water	114.80	105.80		9 mid	9 mid	10 start	10 start	150.5	150.5	155.04	155.04	152.77			
	rep 3										118.00	109.00		9 mid	10 start	10 mid	10 mid	150.5	155.04	160.56	160.56	156.67			
												106.67	***92.22***									**151.67**			

Average pH 6.27

Vehicle pH 11.5 - Vane Tests

Date : 28/04/2004

Vane dimensions : medium vane			
	height	0.060	m
	diameter	0.025	m

Rheometer settings :			
	speed	0.3	rpm
	data points	400	
	duration	120	sec

File name :	**Fredre16**
Sample description :	Vehicle pH 11.5 (interactive)

Material characteristics :		
Type	Vehicle	
Solids SG	2.41	g/cm^3
pH	11.5	

Test number	Description	Pan no.	Pan mass (g)	Start mass (g)	Wet mass (g)	End mass (g)	Dry mass (g)	% solids (%)	Density (kg/m^3)	Dilution (ml)	Max Torque (mNm)	Yield stress (Pa)	pH before	pH after	pH ave
Vehicle starting point		14	24.9210	29.9950	5.0740	28.2900	3.3690	66.3973	1635.23	0					
Test 2	Rep 1	11	25.1180	28.3490	3.2310	27.2300	2.1120	65.3668	1619.27	13 alkali	41.1638		11.54	10.82	11.18
Test 3	Rep 2										41.6898				
Test 4	Rep 3										41.0225				
											41.29	***615.51***			
Test 6	Rep 1	23	24.8060	28.1320	3.3260	26.9450	2.1390	64.3115	1603.24	5 alkali	36.5723		11.64	11.07	11.36
Test 7	Rep 2									7 water	36.9540				
Test 8	Rep 3										34.5185				
											36.01	***536.85***			
Test 10	Rep 1	21	24.7970	27.6560	2.8590	26.5940	1.7970	62.8541	1581.62	3.6 alkali	28.8700		11.52	11.32	11.42
Test 11	Rep 2									13 water	28.5525				
Test 12	Rep 3										29.8245				
											29.08	***433.51***			
Test 13	Rep 1	19	24.7250	27.4610	2.7360	26.4100	1.6850	61.5863	1563.28	2 alkali	24.6273		11.62	11.47	11.55
Test 14	Rep 2									17 water	23.3608				
Test 15	Rep 3										23.6920				
											23.89	***356.16***			
Test 16	Rep 1	17	25.2670	28.4170	3.1500	27.1510	1.8840	59.8095	1538.28	0.6 alkali	15.6620		11.56	11.49	11.53
Test 17	Rep 2									20 water	16.5820				
Test 18	Rep 3										17.7845				
											16.68	***248.58***			
Test 19	Rep 1	10	24.6810	27.5420	2.8610	26.3580	1.6770	58.6159	1521.93	0.6 alkali	13.7065		11.62	11.49	11.56
Test 20	Rep 2									16 water	14.1508				
Test 21	Rep 3										13.8598				
											13.91	***207.28***			
Test 22	Rep 1	4	23.8800	26.9490	3.0690	25.6460	1.7660	57.5432	1507.53	0.4 alkali	9.7468		11.51	11.5	11.51
Test 23	Rep 2									18 water	10.1325				
Test 24	Rep 3										9.9728				
											9.95	***148.33***			
Test 26	Rep 1	9	23.7960	26.8880	3.0920	25.5380	1.7420	56.3389	1491.69	0.4 alkali	7.3548		11.53	11.5	11.52
Test 27	Rep 2									22 water	7.3845				
Test 28	Rep 3										7.4105				
											7.38	***110.06***			
Test 30	Rep 1	12	24.7500	30.3980	5.6480	27.8130	3.0630	54.2316	1464.75	0.4 alkali	4.8553		11.54	11.51	11.53
Test 31	Rep 2									32 water	4.9303				
Test 32	Rep 3										4.8500				
											4.88	***72.72***			

Average pH *11.46*

Vehicle pH 11.5 - Small Slump Tests

Date : 29/04/2004

Slump cylinder : small cylinder

height	0.130	m
diameter	0.105	m
aspect ratio	1.24	
ruler thickness	9	mm

Material characteristics :

Type	Vehicle	
Solids SG	2.41	g/cm^3
pH	11.5	

Test	Description	Pan no.	Pan mass	Start mass	Wet mass	End mass	Dry mass	% solids	Density	Dilution	Slump height	Slump height	Yield stress	Flow distance (rings)				Flow distance radius (mm)					pH before	pH after	pH ave
number			(g)	(g)	(g)	(g)	(g)	(%)	(kg/m^3)	(ml)	incl ruler (mm)	excl ruler (mm)	(Pa)	N	S	E	W	N	S	E	W	average			
Test 1	Rep 1	23	24.8060	31.5270	6.7210	29.0170	4.2110	62.6544	1578.70	71alkali	62.00	53.0		1 mid	1 mid	1 mid	1 mid	70.68	70.68	70.68	70.68	70.68	11.54	11.34	11.44
	Rep 2									85 water	63.10	54.1		1 start	2 start	1 mid	2 start	65.64	75.76	70.68	75.76	71.96			
	Rep 3										62.60	53.6		1 mid	1 mid	1 start	2 mid	70.68	70.68	65.64	80.73	71.93			
												53.57	***361.09***									**71.52**			
Test 2	Rep 1	19	24.7220	29.8540	5.1320	27.8960	3.1740	61.8472	1567.02	8 alkali	67.70	58.7		2 start	1 mid	1 mid	2 mid	75.76	70.68	70.68	80.73	74.46	11.69	11.21	11.45
	Rep 2									40 water	68.60	59.6		1 start	2 mid	2 start	1 mid	65.64	80.73	75.76	70.68	73.20			
	Rep 3										69.00	60.0		1 mid	2 start	2 start	2 mid	70.68	75.76	75.76	80.73	75.73			
												59.43	***324.19***									**74.47**			
Test 3	Rep 1	21	24.7940	29.6320	4.8380	27.7430	2.9490	60.9549	1554.30	4 alkali	71.40	62.4		2 start	2 mid	2 mid	2 mid	75.76	80.73	80.73	80.73	79.49	11.71	11.54	11.63
	Rep 2									43 water	73.80	64.8		2 mid	2 mid	2 mid	2 mid	80.73	80.73	80.73	80.73	80.73			
	Rep 3										71.95	63.0		1 mid	3 start	2 mid	2 mid	70.68	85.73	80.73	80.73	79.47			
												63.38	***299.64***									**79.90**			
Test 4	Rep 1	14	24.9210	29.7610	4.8400	27.8180	2.8970	59.8554	1538.91	0 alkali	77.95	69.0		3 start	3 mid	3 mid	3 mid	85.73	90.38	90.38	90.38	89.22	11.57	11.55	11.56
	Rep 2									48 water	79.80	70.8		3 mid	3 mid	3 mid	3 mid	90.38	90.38	90.38	90.38	90.38			
	Rep 3										79.15	70.2		3 start	3 mid	3 mid	3 mid	85.73	90.38	90.38	90.38	89.22			
												69.97	***261.95***									**89.61**			
Test 5	Rep 1	10	24.6790	30.0150	5.3360	27.8240	3.1450	58.9393	1526.32	0 alkali	88.60	79.6		4 mid	4 start	4 mid	4 mid	100.78	95.76	100.78	100.78	99.53	11.55	11.48	11.52
	Rep 2									55 water	86.00	77.0		4 mid	3 mid	4 mid	4 mid	100.78	90.38	100.78	100.78	98.18			
	Rep 3										86.80	77.8		4 start	4 mid	4 mid	4 mid	95.76	100.78	100.78	100.78	99.53			
												78.13	***219.27***									**99.08**			
Test 6	Rep 1	4	23.8770	29.6050	5.7280	27.1880	3.3110	57.8038	1511.00	0.8 alkali	91.00	82.0		5 mid	5 mid	5 mid	6 start	111.13	111.13	111.13	115.86	112.31	11.53	11.53	11.53
	Rep 2									55 water	94.75	85.8		5 mid	5 mid	5 mid	6 start	111.13	111.13	111.13	115.86	112.31			
	Rep 3										94.20	85.2		5 mid	5 mid	5 mid	6 start	111.13	111.13	111.13	115.86	112.31			
												84.32	***188.06***									**112.31**			
Test 7	Rep 1	9	23.7910	31.5720	7.7810	28.1980	4.4070	56.6380	1495.59	0 alkali	102.55	93.6		7 mid	6 mid	7 mid	7 mid	130.83	120.65	130.83	130.83	128.29	11.53	11.48	11.51
	Rep 2									65 water	101.50	92.5		7 start	6 mid	7 mid	7 mid	125.76	120.65	130.83	130.83	127.02			
	Rep 3										105.00	96.0		7 mid	6 mid	7 start	7 mid	130.83	120.65	125.76	130.83	127.02			
												94.02	***143.15***									**127.44**			
Test 8	Rep 1	11	25.1170	32.3100	7.1930	29.0840	3.9670	55.1508	1476.38	0.4 alkali	118.50	109.5		10 mid	9 mid	10 start	10 mid	160.56	150.5	155.04	160.56	156.67	11.52	11.47	11.50
	Rep 2									80 water	117.35	108.4		8 mid	8 start	8 mid	9 start	140.38	135.83	140.38	145.71	140.58			
	Rep 3										116.60	107.6		9 start	8 mid	9 start	9 mid	145.71	140.38	145.71	150.5	145.58			
												108.48	***81.89***									**147.61**			

Average pH 11.52

Vehicle pH 8.5 - Vane Tests

Date : 30/07/2004

Vane dimensions :			
medium vane	height	0.060	m
	diameter	0.025	m

Vane dimensions :			
small vane	height	0.022	m
	diameter	0.016	m

File name :	**Fredre29**
Sample description :	New Vehicle pH 8.5 (interactive)

Rheometer settings :

speed	0.3	rpm
data points	400	
duration	120	sec

Material characteristics :

Type	Vehicle
Solids SG	2.41
pH	8.5

Test number	Description	Pan no.	Pan mass (g)	Start mass (g)	Wet mass (g)	End mass (g)	Dry mass (g)	% solids (%)	Density (kg/m^3)	Dilution (ml)	Max Torque (mNm)	Yield stress (Pa)	
Test 3	rep 1	23	24.7930	61.2190	36.4260	49.9380	25.1450	69.0304	***1677.49***	0	14.1295		small vane
Test 4	rep 2										13.1015		
Test 5	rep 3										14.2808		
											13.84	***1268.20***	
Test 6	rep 1	10	24.6720	32.3560	7.6840	29.8870	5.2150	67.8683	***1658.57***	6	10.0848		small vane
Test 7	rep 2										10.3625		
Test 8	rep 3										10.5228		
											10.32	***946.15***	
Test 10	rep 1	4	23.8630	32.3520	8.4890	29.5580	5.6950	67.0868	***1646.09***	10	8.4010		small vane
Test 11	rep 2										8.0542		
Test 12	rep 3										8.9422		
											8.47	***775.90***	
Test 13	rep 1	12	24.7370	32.4680	7.7310	29.8420	5.1050	66.0329	***1629.55***	12	40.6808		medium vane
Test 14	rep 2										44.4135		
Test 15	rep 3										43.6230		
											42.91	***639.56***	
Test 16	rep 1	25	24.3620	30.8510	6.4890	28.5860	4.2240	65.0948	***1615.10***	15	29.6505		medium vane
Test 17	rep 2										33.4760		
Test 18	rep 3										32.9393		
											32.02	***477.33***	
Test 19	rep 1	6	24.5280	30.2070	5.6790	28.1700	3.6420	64.1310	***1600.53***	16	20.5360		medium vane
Test 20	rep 2										21.6720		
Test 21	rep 3										21.5683		
											21.26	***316.89***	
Test 22	rep 1	7	25.2260	31.7410	6.5150	29.3300	4.1040	62.9931	***1583.65***	15	14.7868		medium vane
Test 23	rep 2										14.6268		
Test 24	rep 3										14.7273		
											14.71	***219.32***	
Test 25	rep 1	11	25.1040	31.4400	6.3360	29.0320	3.9280	61.9949	***1569.14***	12	11.0758		medium vane
Test 26	rep 2										11.2593		
Test 27	rep 3										11.3480		
											11.23	***167.36***	
Test 28	rep 1	3	25.2370	33.4520	8.2150	30.2510	5.0140	61.0347	***1555.43***	16	7.9403		medium vane
Test 29	rep 2										7.7223		
Test 30	rep 3										8.0010		
											7.89	***117.58***	
Test 31	rep 1	9	23.7820	34.1010	10.3190	29.9010	6.1190	59.2984	***1531.24***	22	4.9863		medium vane
Test 32	rep 2										4.8455		
Test 33	rep 3										4.9963		
											4.94	***73.68***	

Vehicle pH 8.5 - Large Slump Tests

Date : 28-29/07/2004

Slump cylinder :

height	0.186	m
diameter	0.186	m
aspect ratio	1.00	
ruler thickness	18.5	mm

Material characteristics :

Type	Vehicle	
Solids SG	2.41	g/cm^3
pH	8.5	

Test number	Description	Pan no.	Pan mass (g)	Start mass (g)	Wet mass (g)	End mass (g)	Dry mass (g)	% solids (%)	Density (kg/m^3)	Dilution (ml)	Slump height (mm)	Slump height (mm)	Yield stress (Pa)
Vehicle starting point		7	25.2270	49.6750	24.4480	41.8580	16.6310	68.0260	1661.11				
		4	23.8640	53.0000	29.1360	43.6840	19.8200	68.0258	1661.11				
		13	25.3550	45.1270	19.7720	38.8080	13.4530	68.0407	1661.35				
								68.03	***1661.19***				
Test 1	rep 1				0.0000		0.0000	68.0308	1661.19	0	46.35	27.85	
	rep 2										45.80	27.30	
												27.58	***932.01***
Test 2	rep 1	6	24.5310	37.2840	12.7530	33.2240	8.6930	68.1644	1663.35	80	52.50	34.00	
	rep 2										52.40	33.90	
												33.95	***869.19***
Test 3	rep 1	13	25.3560	38.2980	12.9420	34.1220	8.7660	67.7330	1656.40	60	60.40	41.90	
	rep 2										59.55	41.05	
												41.48	***797.58***
Test 4	rep 1	4	23.8630	37.6150	13.7520	33.0950	9.2320	67.1321	1646.81	70	66.60	48.10	
	rep 2										65.15	46.65	
												47.38	***744.18***
Test 5	rep 1	7	25.2250	39.0620	13.8370	34.4590	9.2340	66.7341	1640.52	70	74.25	55.75	
	rep 2										73.90	55.40	
												55.58	***678.57***
Test 6	rep 1	18	25.0150	37.8140	12.7990	33.5300	8.5150	66.5286	1637.29	75	81.20	62.70	
	rep 2										79.80	61.30	
												62.00	***631.33***
Test 7	rep 1	23	24.7800	40.8880	16.1080	35.4030	10.6230	65.9486	1628.24	80	86.90	68.40	
	rep 2										87.45	68.95	
												68.68	***582.86***
Test 8	rep 1	5	24.6010	37.3230	12.7220	32.9180	8.3170	65.3749	1619.39	90	98.30	79.80	
	rep 2										97.00	78.50	
												79.15	***513.65***
Test 9	rep 1	11	25.1050	44.8030	19.6980	37.9030	12.7980	64.9711	1613.22	105	111.00	92.50	
	rep 2										111.80	93.30	
												92.90	***431.64***
Test 10	rep 1	21	24.7870	39.9300	15.1430	34.5190	9.7320	64.2673	1602.57	125	124.30	105.80	
	rep 2										126.20	107.70	
												106.75	***354.44***
Test 11	rep 1	2	24.5120	37.5310	13.0190	32.7920	8.2800	63.5994	1592.60	155	132.00	113.50	
	rep 2										131.50	113.00	
												113.25	***319.22***
Test 12	rep 1	23	24.8090	38.8800	14.0710	33.6000	8.7910	62.4760	1576.10	170	143.80	125.30	
	rep 2										146.00	127.50	
												126.40	***252.56***
Test 13	rep 1	6	24.5650	45.2280	20.6630	37.3150	12.7500	61.7045	1564.97	180	155.15	136.65	
	rep 2										155.00	136.50	
												136.58	***204.32***

Vehicle pH 8.7 - Vane Tests

Date : 16/08/2004

Vane dimensions : medium vane

height	0.060	m
diameter	0.025	m

Rheometer settings :

speed	0.3	rpm
data points	400	
duration	120	sec

File name :	**Fredre34**
Sample description :	Vehicle pH 8.7 (mod ESP washed)

Material characteristics :

Type	Vehicle
Solids SG	2.41
pH	8.7

Test number	Description	Pan no.	Pan mass (g)	Start mass (g)	Wet mass (g)	End mass (g)	Dry mass (g)	% solids (%)	Density (kg/m^3)	Dilution (ml)	Max Torque (mNm)	Yield stress (Pa)
Test 12	rep 1	61	24.2470	33.4180	9.1710	30.4860	6.2390	68.0297	***1661.17***	13	42.4525	
Test 13	rep 2										46.3408	
Test 14	rep 3										48.4260	
											45.74	***681.81***
Test 15	rep 1	87	27.1770	37.4360	10.2590	34.1330	6.9560	67.8039	***1657.54***	8	36.3403	
Test 16	rep 2										40.3493	
Test 17	rep 3										36.7940	
											37.83	***563.87***
Test 18	rep 1	99	27.6310	37.3220	9.6910	34.1200	6.4890	66.9590	***1644.07***	10	26.4983	
Test 19	rep 2										26.8903	
Test 20	rep 3										28.8745	
											27.42	***408.74***
Test 21	rep 1	118	27.6730	38.7000	11.0270	34.9920	7.3190	66.3734	***1634.86***	10	20.8533	
Test 22	rep 2										20.0895	
Test 23	rep 3										20.3273	
											20.42	***304.44***
Test 24	rep 1	33	27.5970	40.9540	13.3570	36.3290	8.7320	65.3740	***1619.38***	12	13.4380	
Test 25	rep 2										13.8498	
Test 26	rep 3										14.0908	
											13.79	***205.60***
Test 27	rep 1	108	27.4750	46.5120	19.0370	39.6740	12.1990	64.0805	***1599.77***	15	8.6025	
Test 28	rep 2										8.5988	
Test 29	rep 3										8.3600	
											8.52	***127.01***
Test 30	rep 1	17	27.5540	46.2950	18.7410	39.3020	11.7480	62.6861	***1579.16***	17	4.8643	
Test 31	rep 2										4.5948	
Test 32	rep 3										4.7628	
											4.74	***70.66***

Vehicle pH 8.7 - Small Slump Tests

Date : 19/08/2004

Slump cylinder : small cylinder

height	0.130	m
diameter	0.105	m
aspect ratio	1.24	
ruler thickness	9.1	mm

Material characteristics :

Type	Vehicle	
Solids SG	2.41	g/cm^3
pH	8.7	

Test number	Description	Pan no.	Pan mass (g)	Start mass (g)	Wet mass (g)	End mass (g)	Dry mass (g)	% solids (%)	Density (kg/m^3)	Dilution (ml)	Slump height incl ruler (mm)	Slump height excl ruler (mm)	Yield stress (Pa)
Vehicle starting point		33	27.5990	51.4660	23.8670	44.5330	16.9340	70.9515	***1709.72***	0			
Test 1	Rep 1	77	28.3470	39.7200	11.3730	36.2830	7.9360	69.7793	***1689.91***	20	34.65	25.55	
	Rep 2										33.60	24.50	
	Rep 3										34.40	25.30	
												25.12	***604.68***
Test 2	Rep 1	122	27.2710	40.9760	13.7050	36.7700	9.4990	69.3105	***1682.11***	35	47.10	38.00	
	Rep 2										47.50	38.40	
	Rep 3										45.40	36.30	
												37.57	***496.71***
Test 3	Rep 1	105	24.8050	41.5720	16.7670	36.1950	11.3900	67.9311	***1659.58***	40	63.30	54.20	
	Rep 2										66.00	56.90	
	Rep 3										62.60	53.50	
												54.87	***371.39***
Test 4	Rep 1	118	27.6950	43.4510	15.7560	38.2690	10.5740	67.1109	***1646.47***	45	88.00	78.90	
	Rep 2										85.10	76.00	
	Rep 3										88.00	78.90	
												77.93	***237.57***
Test 5	Rep 1	11	27.5850	50.0780	22.4930	42.3890	14.8040	65.8160	***1626.19***	50	106.80	97.70	
	Rep 2										106.30	97.20	
	Rep 3										108.10	99.00	
												97.97	***137.30***

Vehicle pH 8.7 - Large Slump Tests

Date : 18/08/2004

Slump cylinder : large cylinder

height	0.186	m
diameter	0.186	m
aspect ratio	1.00	
ruler thickness	8.6	mm

Material characteristics :

Type	Vehicle	
Solids SG	2.41	g/cm^3
pH	8.7	

Test number	Description	Pan no.	Pan mass (g)	Start mass (g)	Wet mass (g)	End mass (g)	Dry mass (g)	% solids (%)	Density (kg/m^3)	Dilution (ml)	Slump height incl ruler (mm)	Slump height excl ruler (mm)	Yield stress (Pa)
Test 1	Rep 1	122	27.1310	37.4760	10.3450	34.3520	7.2210	69.8018	1690.29	80	64.20	55.60	
	Rep 2										65.30	56.70	
	Rep 3										69.30	60.70	
												57.67	***683.44***
Test 2	Rep 1	105	24.7940	40.2300	15.4360	35.4390	10.6450	68.9622	1676.37	90	82.20	73.60	
	Rep 2										82.90	74.30	
	Rep 3										81.80	73.20	
												73.70	***566.68***
Test 3	Rep 1	77	28.3210	40.4380	12.1170	36.6800	8.3590	68.9857	1676.75	105	92.80	84.20	
	Rep 2										96.10	87.50	
	Rep 3										90.60	82.00	
												84.57	***498.26***
Test 4	Rep 1	87	27.1700	41.8900	14.7200	37.2160	10.0460	68.2473	1664.69	115	111.00	102.40	
	Rep 2										107.85	99.25	
	Rep 3										111.20	102.60	
												101.42	***397.29***
Test 5	Rep 1	11	27.5700	39.9120	12.3420	35.8530	8.2830	67.1123	1646.49	130	128.60	120.00	
	Rep 2										127.50	118.90	
	Rep 3										127.20	118.60	
												119.17	***299.79***
Test 6	Rep 1	2	24.5120	42.9650	18.4530	36.7620	12.2500	66.3849	1635.04	150	141.90	133.30	
	Rep 2										139.90	131.30	
	Rep 3										140.30	131.70	
												132.10	***234.58***

APPENDIX J : VEHICLE VANE TESTS - TORQUE-TIME CURVES

Vehicle – pH 8.6 (non-interactive)

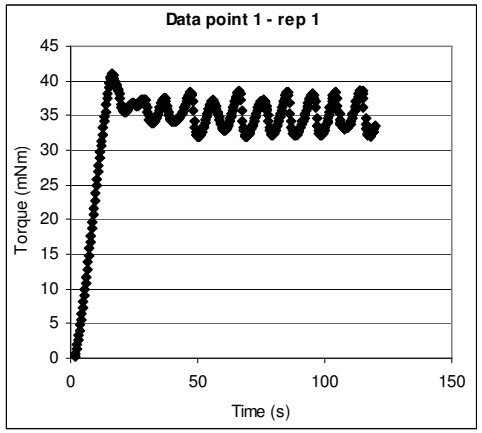

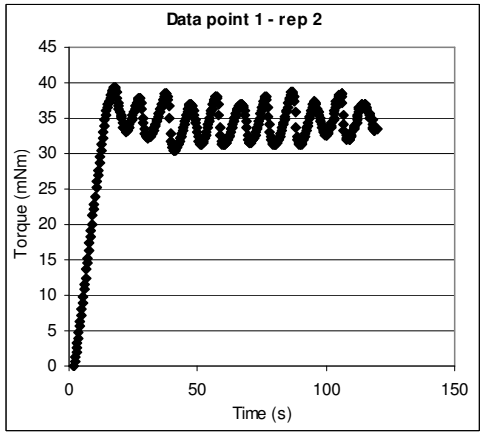

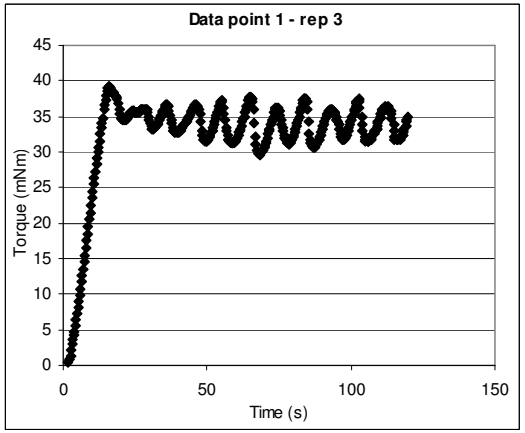

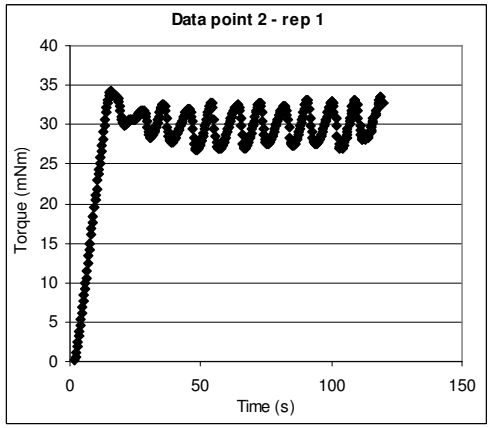

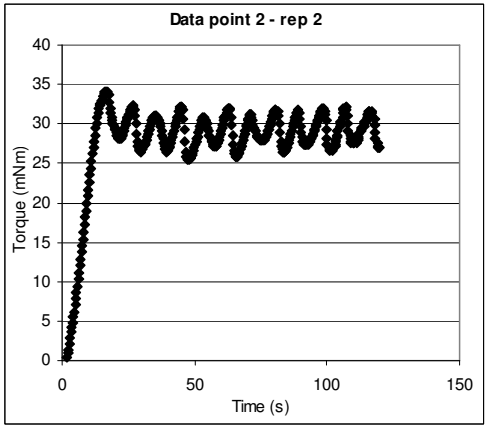

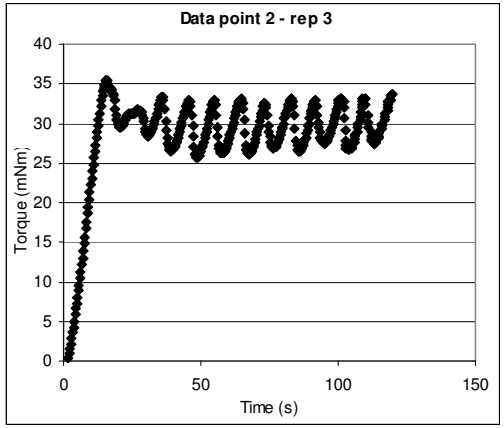

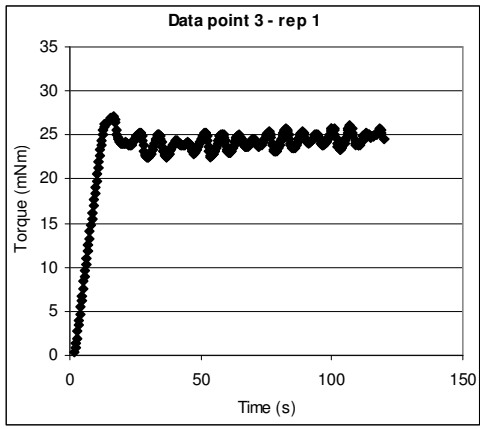
Data point 3 - rep 1
Torque (mNm)
Time (s)
0
5
10
15
20
25
30
35
0
50
100
150

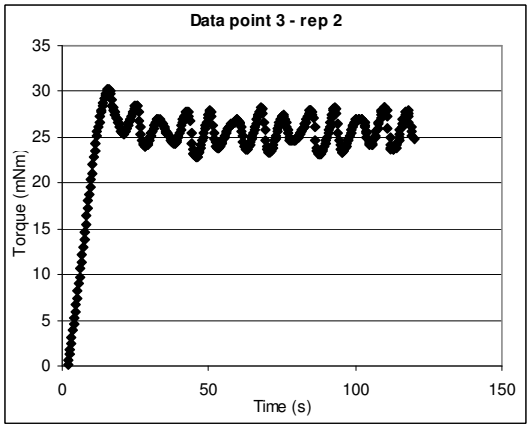
Data point 3 - rep 2
Torque (mNm)
Time (s)
0
5
10
15
20
25
30
35
0
50
100
150

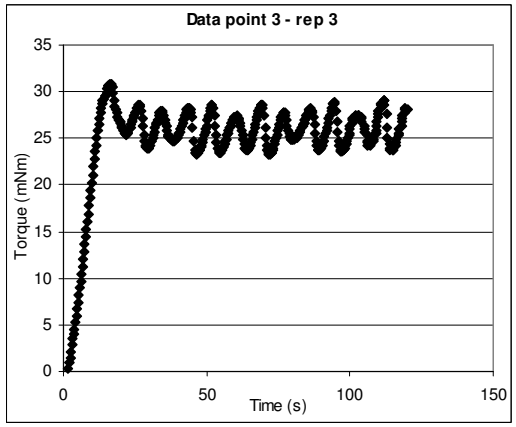
Data point 3 - rep 3
Torque (mNm)
Time (s)
0
5
10
15
20
25
30
35
0
50
100
150

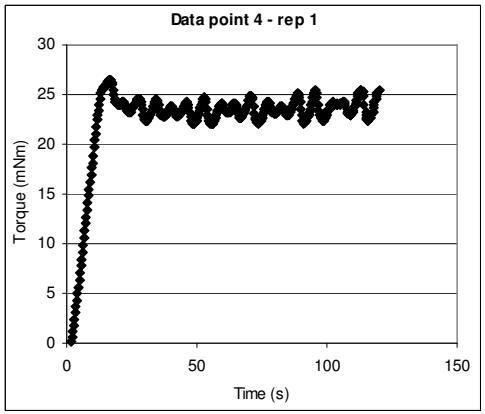
Data point 4 - rep 1
Torque (mNm)
Time (s)
0
5
10
15
20
25
30
0
50
100
150

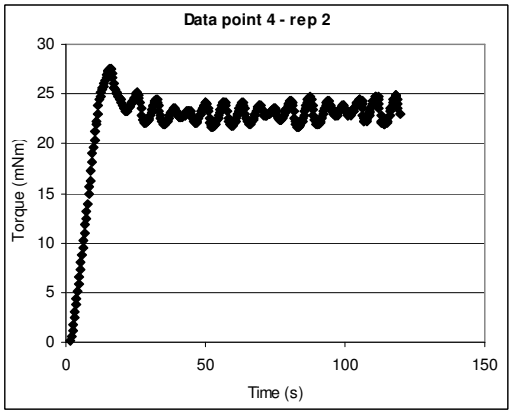
Data point 4 - rep 2
Torque (mNm)
Time (s)
0
5
10
15
20
25
30
0
50
100
150

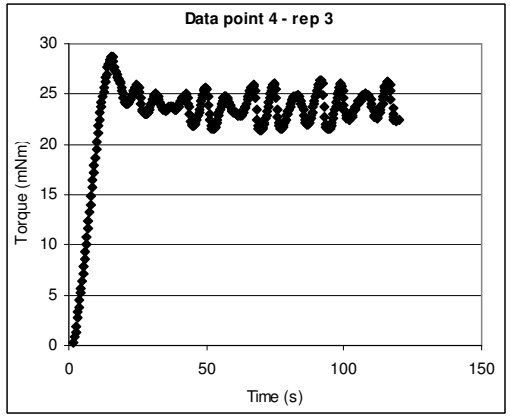
Data point 4 - rep 3
Torque (mNm)
Time (s)
0
5
10
15
20
25
30
0
50
100
150

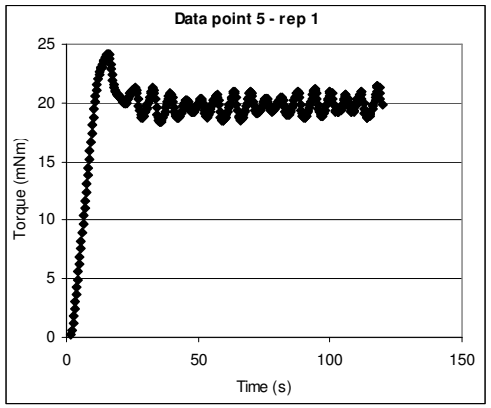
Data point 5 - rep 1
Torque (mNm)
Time (s)
0
5
10
15
20
25
0
50
100
150

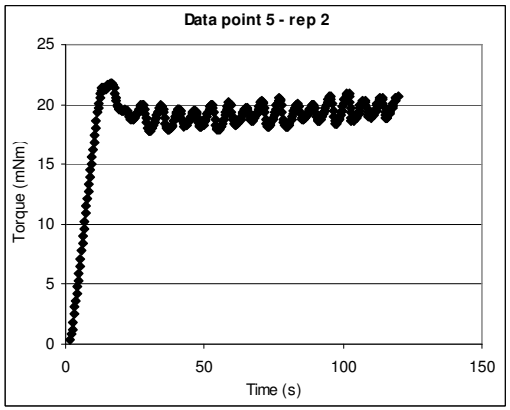
Data point 5 - rep 2
Torque (mNm)
Time (s)
0
5
10
15
20
25
0
50
100
150

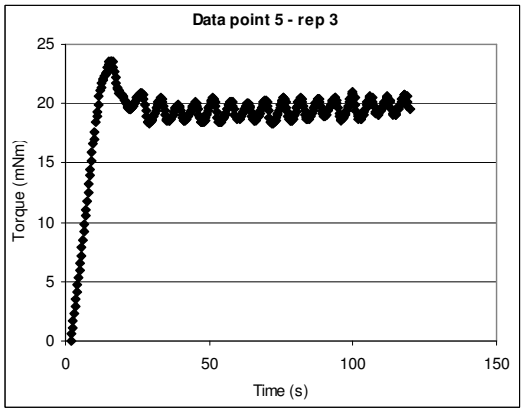
Data point 5 - rep 3
Torque (mNm)
Time (s)
0
5
10
15
20
25
0
50
100
150

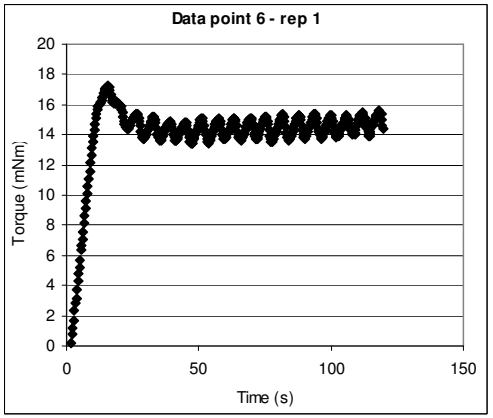
Data point 6 - rep 1
Torque (mNm)
Time (s)
0
2
4
6
8
10
12
14
16
18
20
0
50
100
150

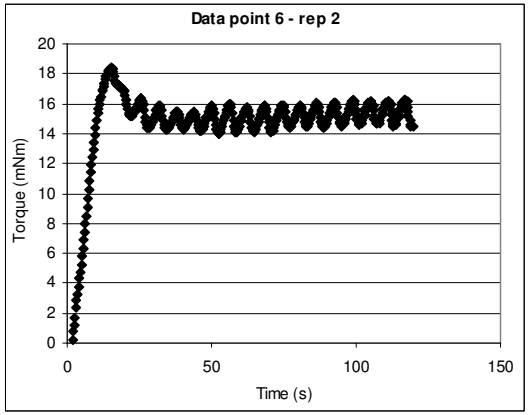
Data point 6 - rep 2
Torque (mNm)
Time (s)
0
2
4
6
8
10
12
14
16
18
20
0
50
100
150

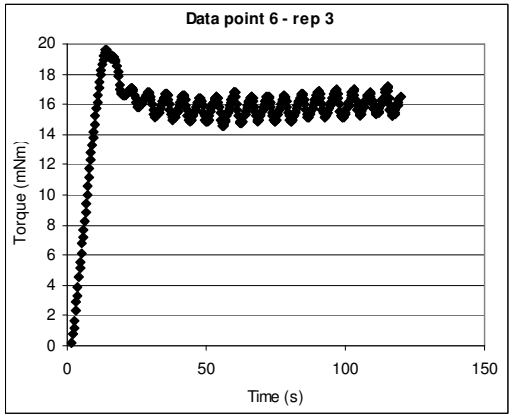
Data point 6 - rep 3
Torque (mNm)
Time (s)
0
2
4
6
8
10
12
14
16
18
20
0
50
100
150

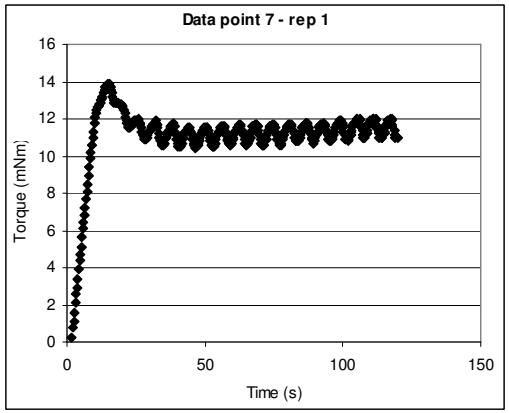
Data point 7 - rep 1
Torque (mNm)
Time (s)
0
2
4
6
8
10
12
14
16
0
50
100
150

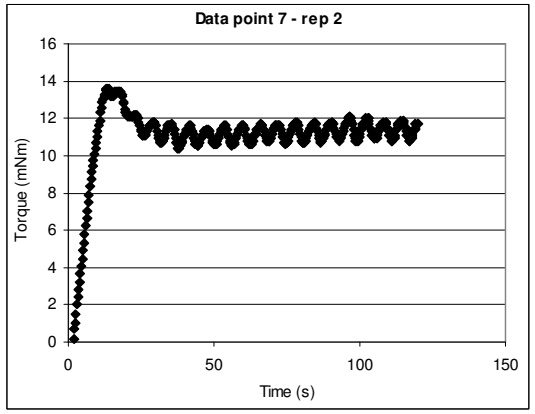
Data point 7 - rep 2
Torque (mNm)
Time (s)
0
2
4
6
8
10
12
14
16
0
50
100
150

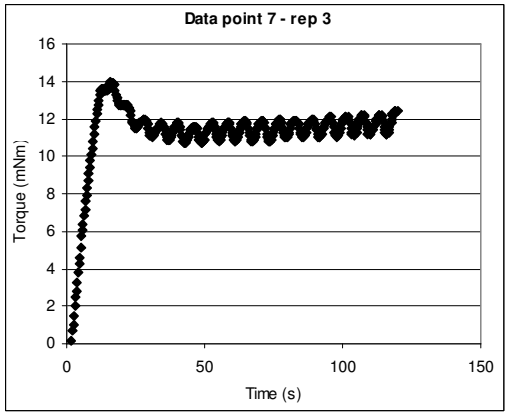
Data point 7 - rep 3
Torque (mNm)
Time (s)
0
2
4
6
8
10
12
14
16
0
50
100
150

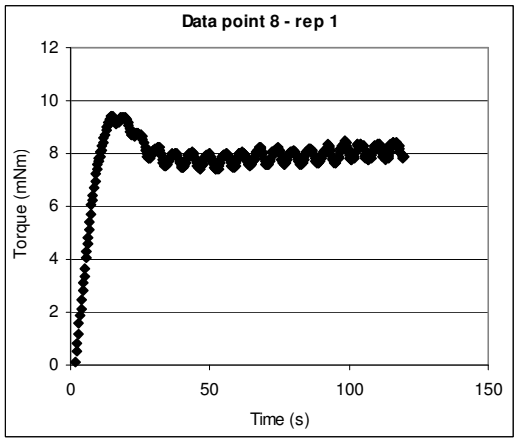
Data point 8 - rep 1
Torque (mNm)
Time (s)
0
2
4
6
8
10
12
0
50
100
150

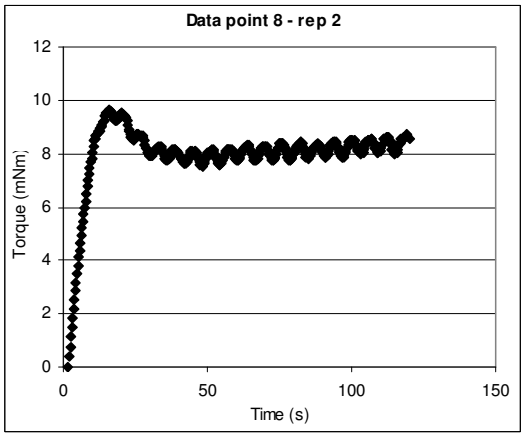
Data point 8 - rep 2
Torque (mNm)
Time (s)
0
2
4
6
8
10
12
0
50
100
150

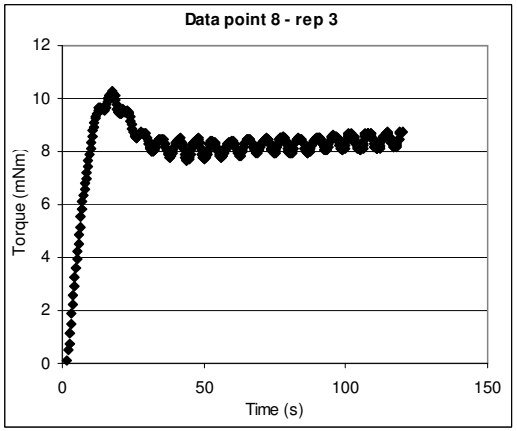
Data point 8 - rep 3
Torque (mNm)
Time (s)
0
2
4
6
8
10
12
0
50
100
150

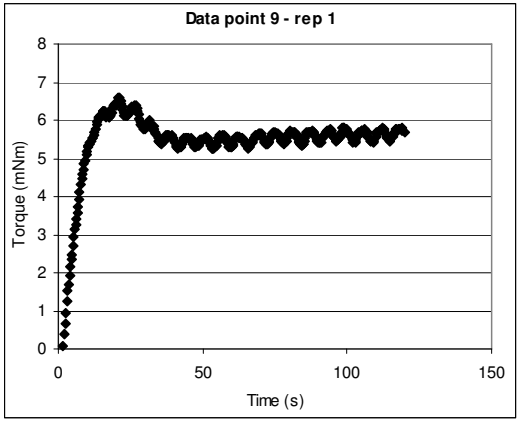
Data point 9 - rep 1
Torque (mNm)
Time (s)
0
1
2
3
4
5
6
7
8
0
50
100
150

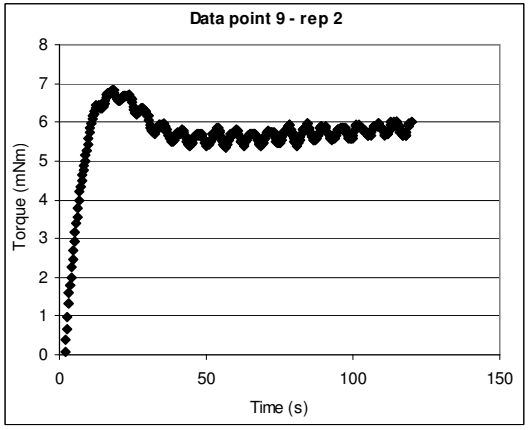
Data point 9 - rep 2
Torque (mNm)
Time (s)
0
1
2
3
4
5
6
7
8
0
50
100
150

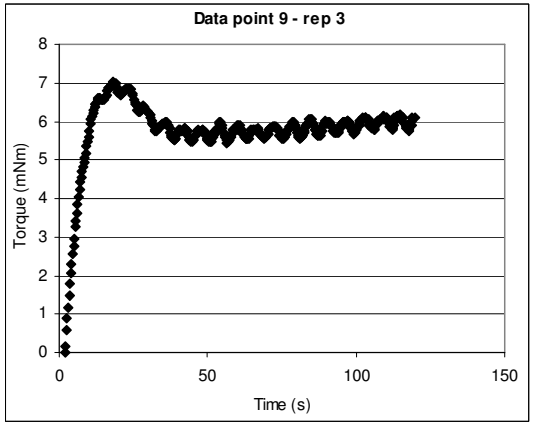
Data point 9 - rep 3
Torque (mNm)
Time (s)
0
1
2
3
4
5
6
7
8
0
50
100
150

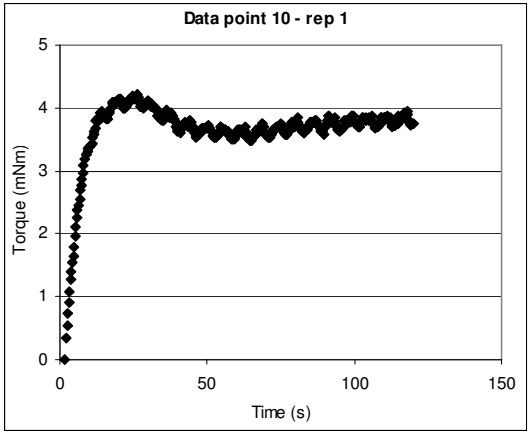
Data point 10 - rep 1
Torque (mNm)
Time (s)
0
1
2
3
4
5
0
50
100
150

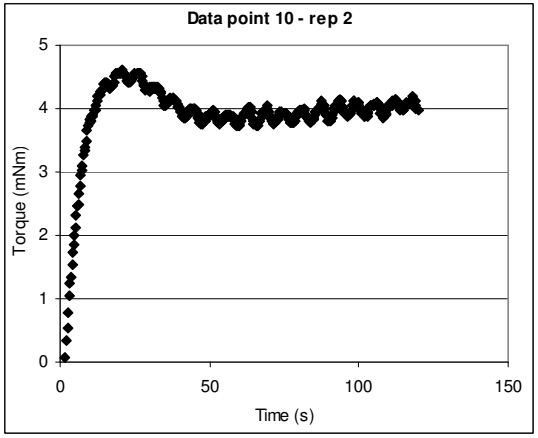
Data point 10 - rep 2
Torque (mNm)
Time (s)
0
1
2
3
4
5
0
50
100
150

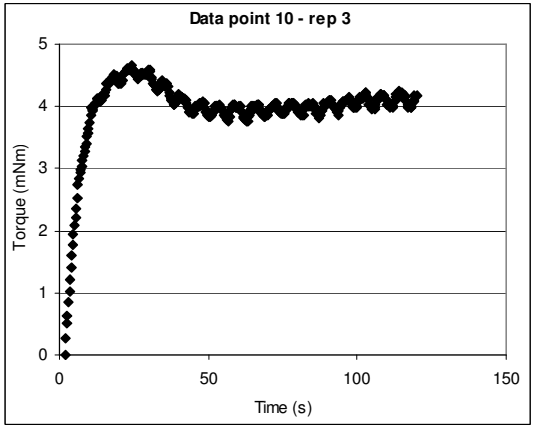
Data point 10 - rep 3
Torque (mNm)
Time (s)
0
1
2
3
4
5
0
50
100
150

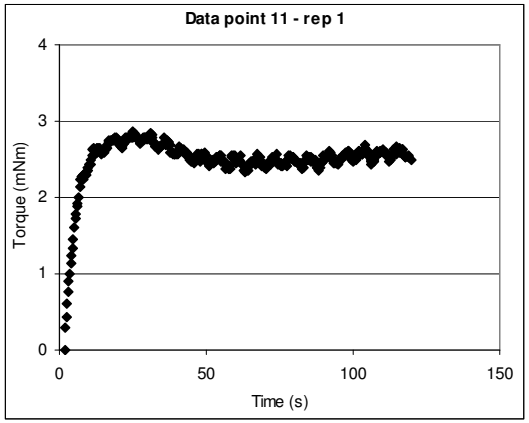
Data point 11 - rep 1
Torque (mNm)
Time (s)
0
1
2
3
4
0
50
100
150

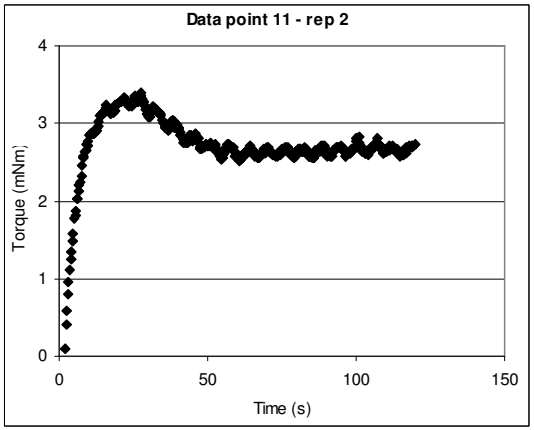
Data point 11 - rep 2
Torque (mNm)
Time (s)
0
1
2
3
4
0
50
100
150

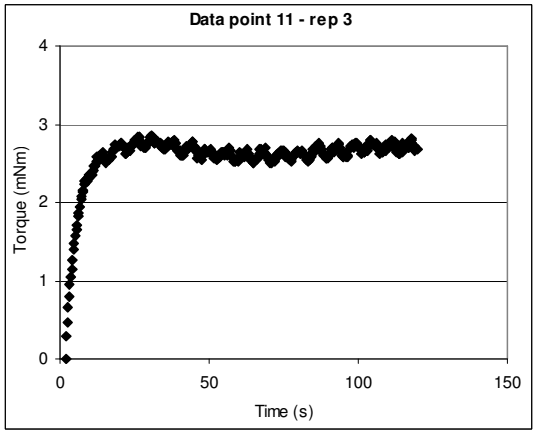
Data point 11 - rep 3
Torque (mNm)
Time (s)
0
1
2
3
4
0
50
100
150

Vehicle – pH 6.2 (interactive)

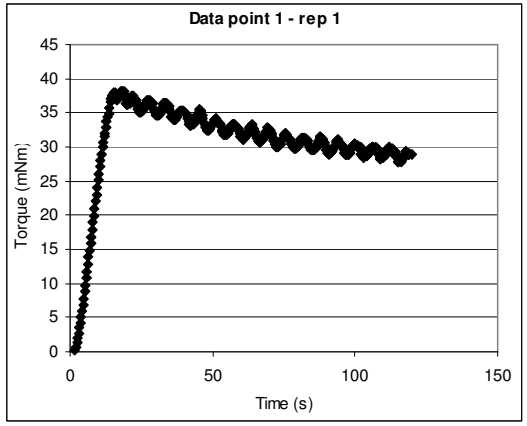

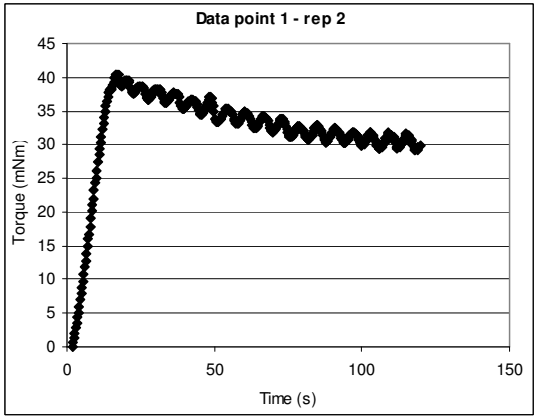

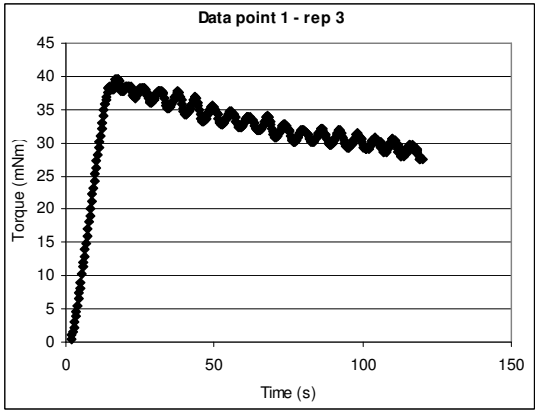

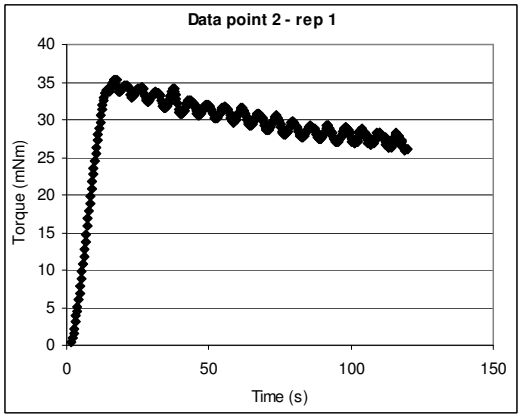

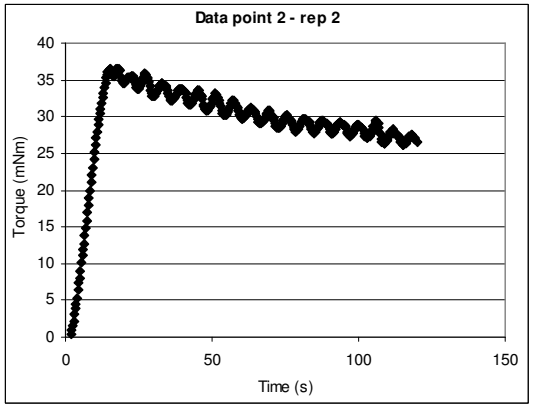

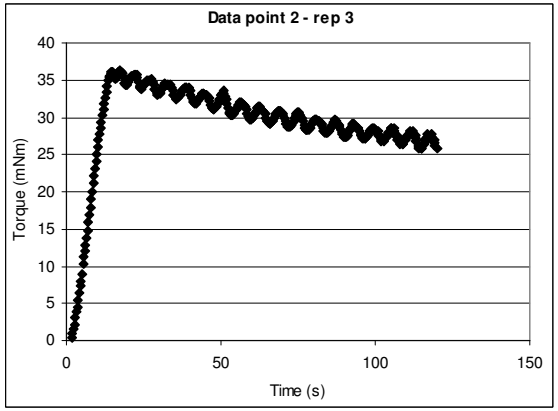

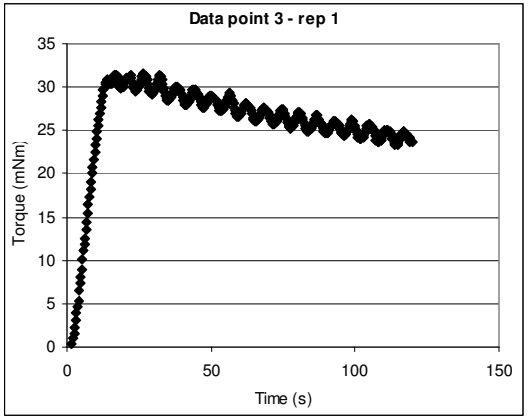
Data point 3 - rep 1
Torque (mNm)
Time (s)
0
5
10
15
20
25
30
35
0
50
100
150

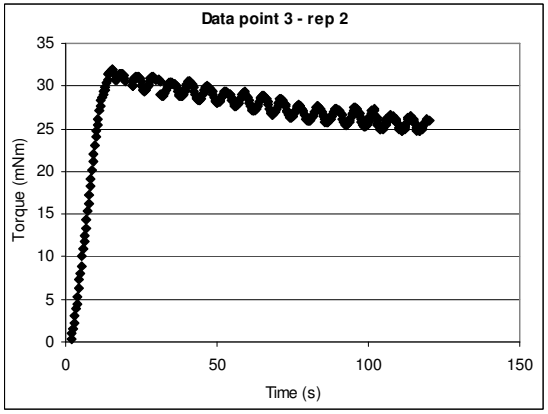
Data point 3 - rep 2
Torque (mNm)
Time (s)
0
5
10
15
20
25
30
35
0
50
100
150

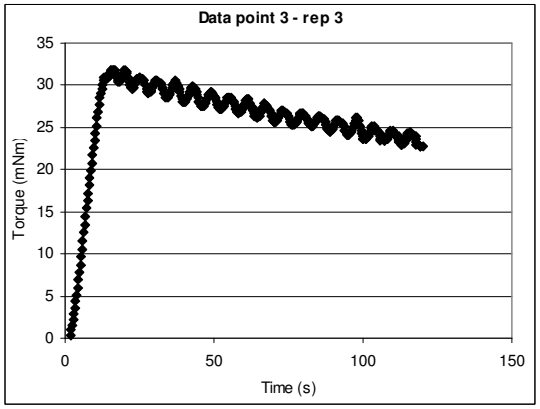
Data point 3 - rep 3
Torque (mNm)
Time (s)
0
5
10
15
20
25
30
35
0
50
100
150

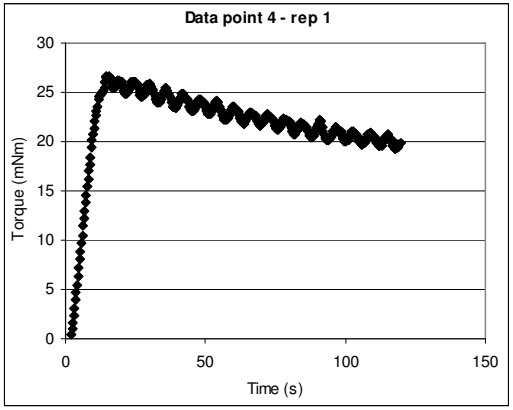
Data point 4 - rep 1
Torque (mNm)
Time (s)
0
5
10
15
20
25
30
0
50
100
150

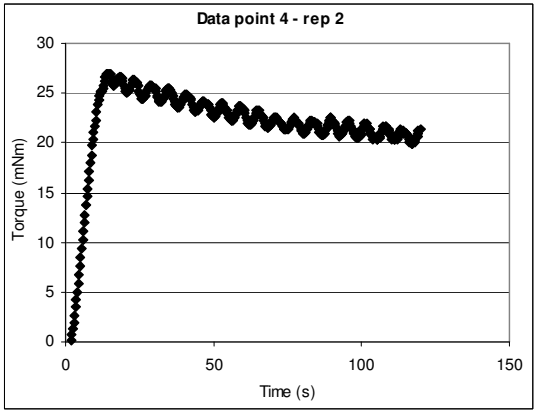
Data point 4 - rep 2
Torque (mNm)
Time (s)
0
5
10
15
20
25
30
0
50
100
150

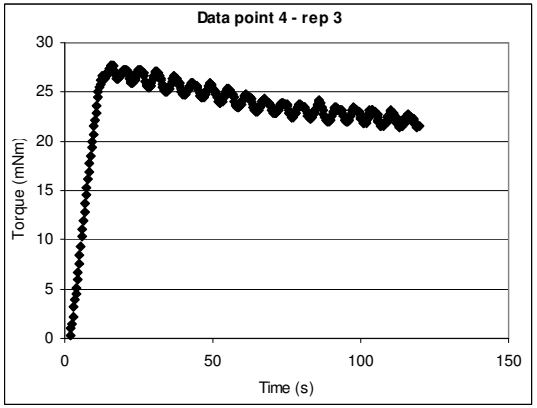
Data point 4 - rep 3
Torque (mNm)
Time (s)
0
5
10
15
20
25
30
0
50
100
150

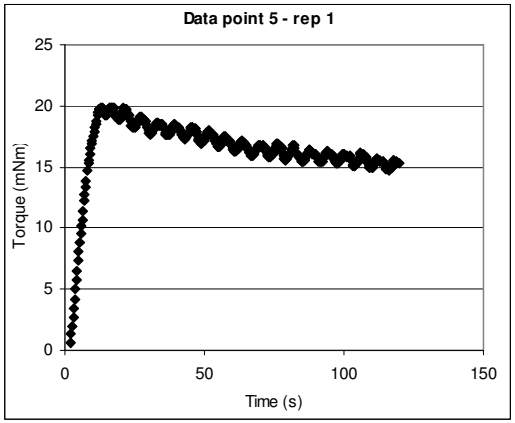
Data point 5 - rep 1
Torque (mNm)
Time (s)
0
5
10
15
20
25
0
50
100
150

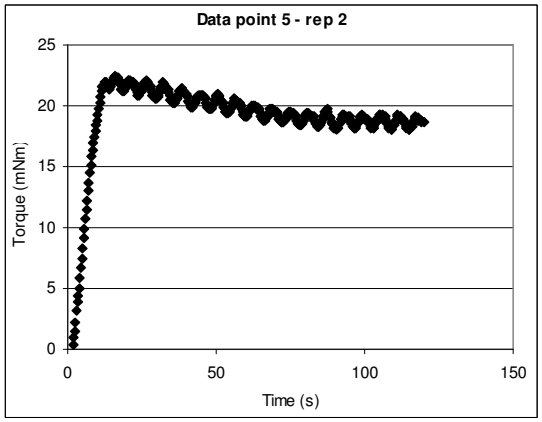
Data point 5 - rep 2
Torque (mNm)
Time (s)
0
5
10
15
20
25
0
50
100
150

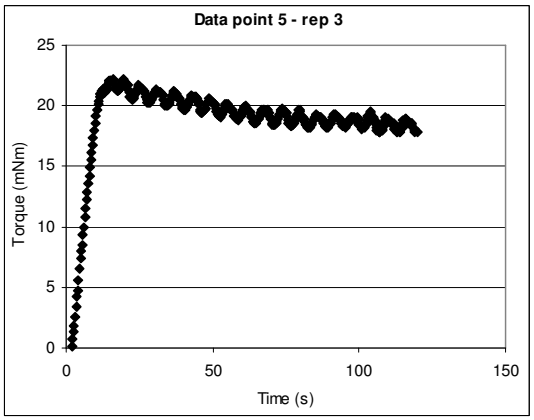
Data point 5 - rep 3
Torque (mNm)
Time (s)
0
5
10
15
20
25
0
50
100
150

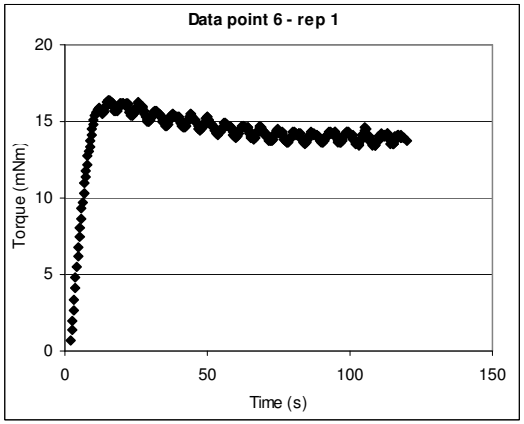
Data point 6 - rep 1
Torque (mNm)
Time (s)
0
5
10
15
20
0
50
100
150

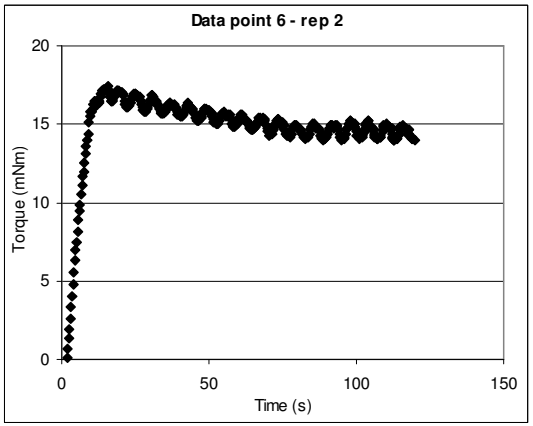
Data point 6 - rep 2
Torque (mNm)
Time (s)
0
5
10
15
20
0
50
100
150

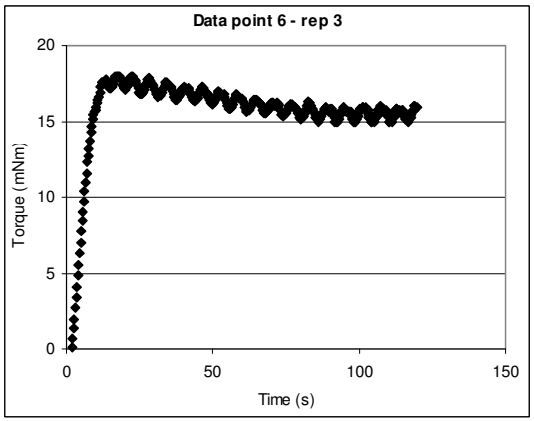
Data point 6 - rep 3
Torque (mNm)
Time (s)
0
5
10
15
20
0
50
100
150

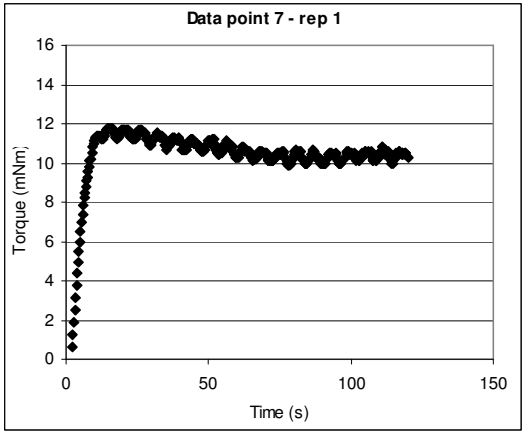
Data point 7 - rep 1
Torque (mNm)
Time (s)
0
2
4
6
8
10
12
14
16
0
50
100
150

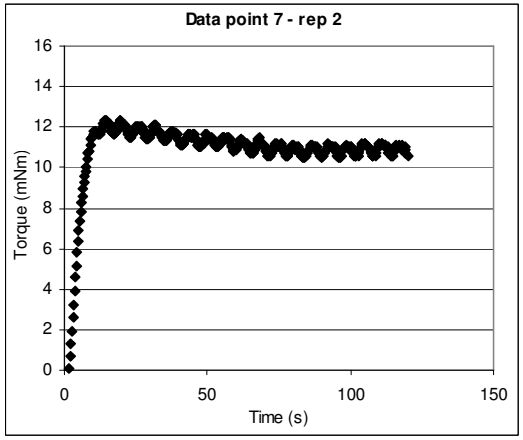
Data point 7 - rep 2
Torque (mNm)
Time (s)
0
2
4
6
8
10
12
14
16
0
50
100
150

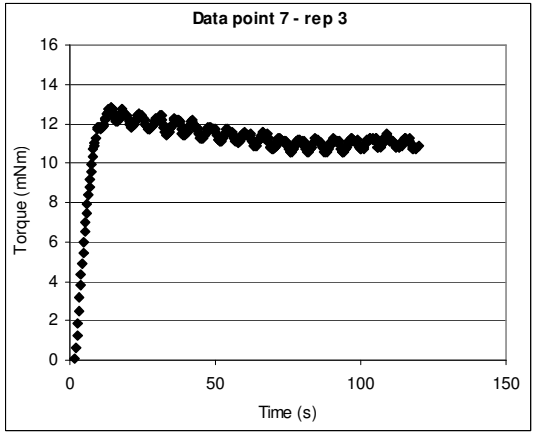
Data point 7 - rep 3
Torque (mNm)
Time (s)
0
2
4
6
8
10
12
14
16
0
50
100
150

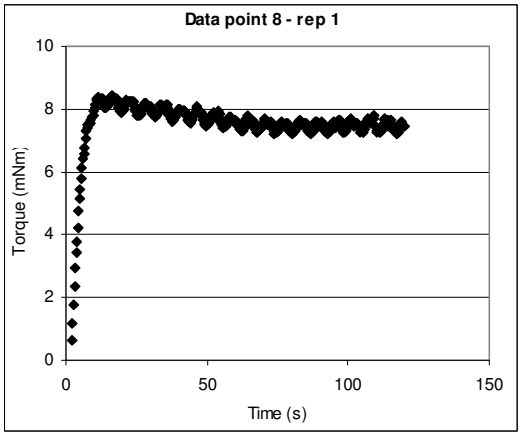
Data point 8 - rep 1
Torque (mNm)
Time (s)
0
2
4
6
8
10
0
50
100
150

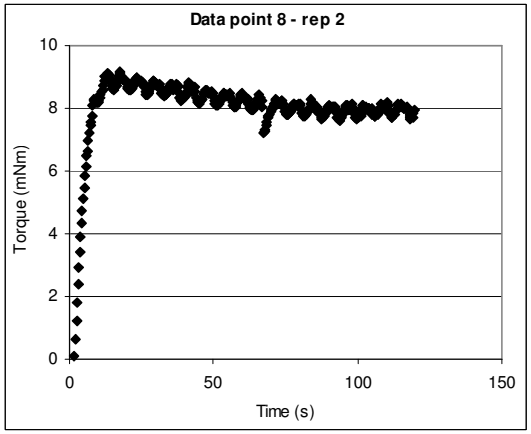
Data point 8 - rep 2
Torque (mNm)
Time (s)
0
2
4
6
8
10
0
50
100
150

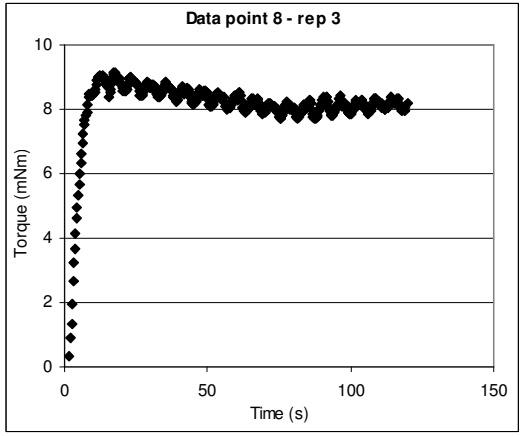
Data point 8 - rep 3
Torque (mNm)
Time (s)
0
2
4
6
8
10
0
50
100
150

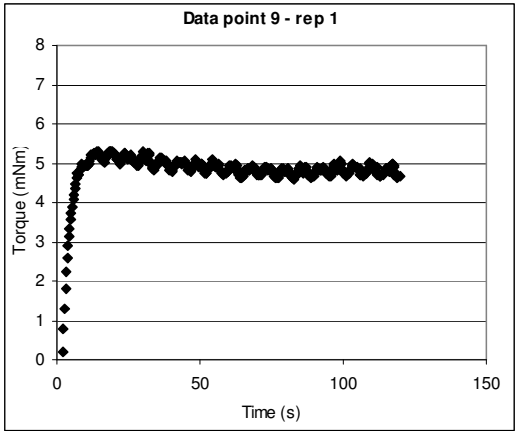
Data point 9 - rep 1
Torque (mNm)
Time (s)
0
1
2
3
4
5
6
7
8
0
50
100
150

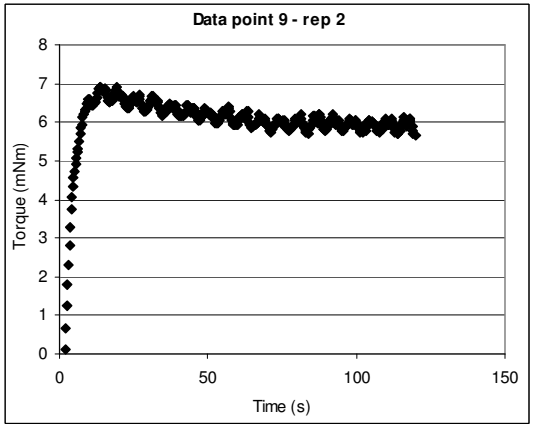
Data point 9 - rep 2
Torque (mNm)
Time (s)
0
1
2
3
4
5
6
7
8
0
50
100
150

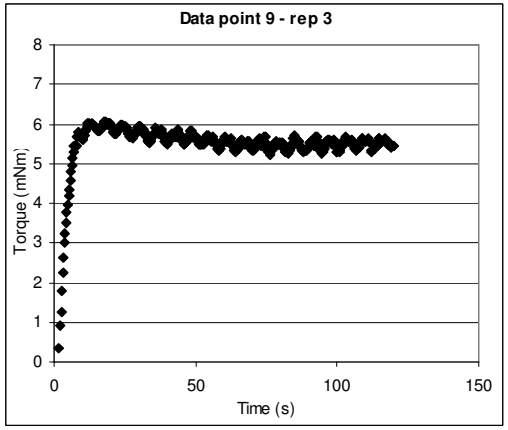
Data point 9 - rep 3
Torque (mNm)
Time (s)
0
1
2
3
4
5
6
7
8
0
50
100
150

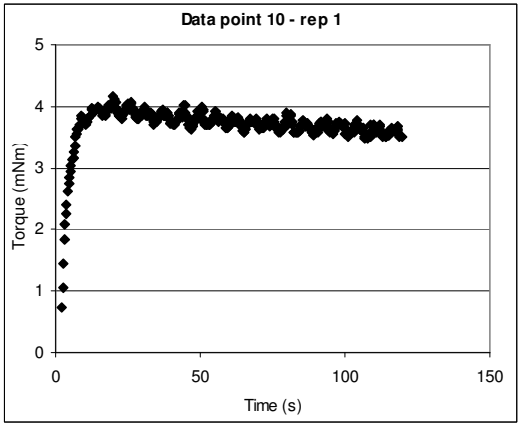
Data point 10 - rep 1
Torque (mNm)
Time (s)
0
1
2
3
4
5
0
50
100
150

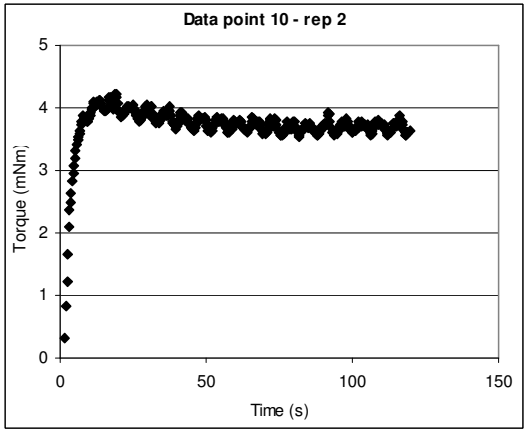
Data point 10 - rep 2
Torque (mNm)
Time (s)
0
1
2
3
4
5
0
50
100
150

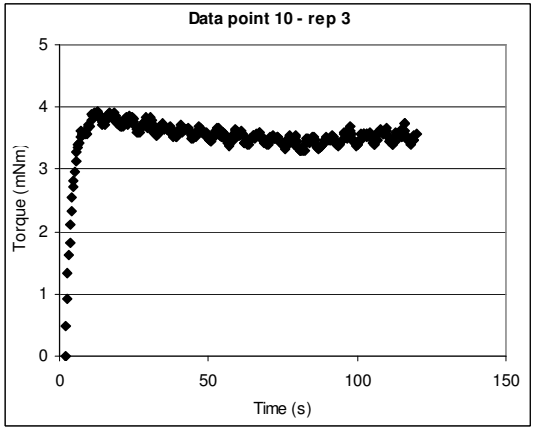
Data point 10 - rep 3
Torque (mNm)
Time (s)
0
1
2
3
4
5
0
50
100
150

Vehicle – pH 11.5 (interactive)

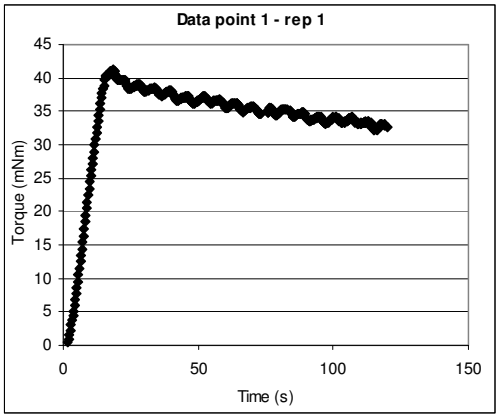

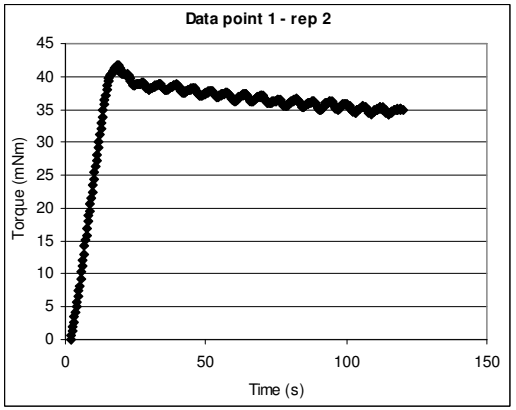

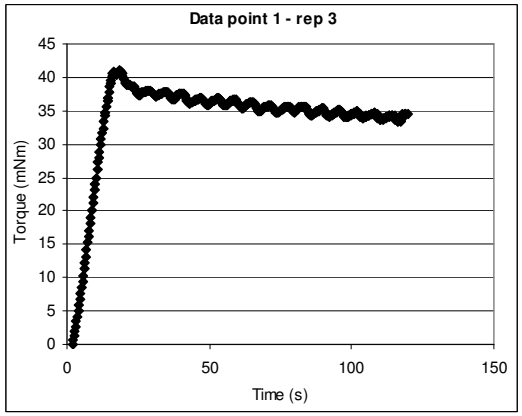

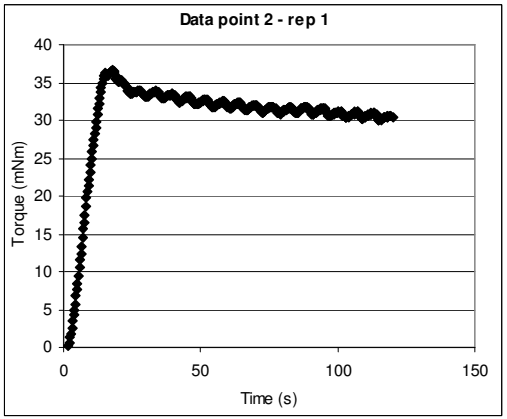

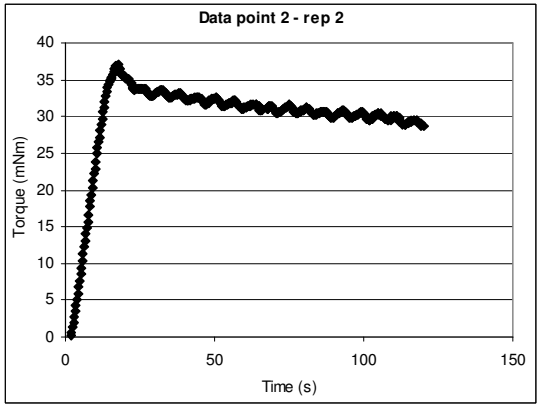

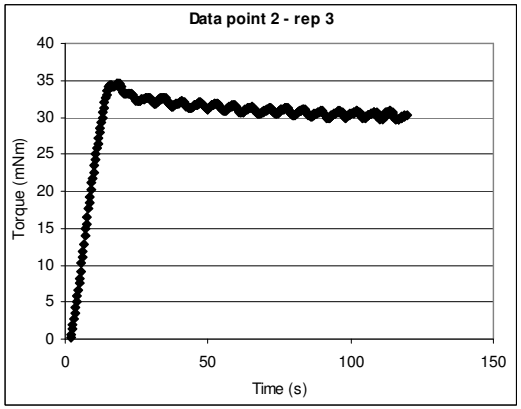

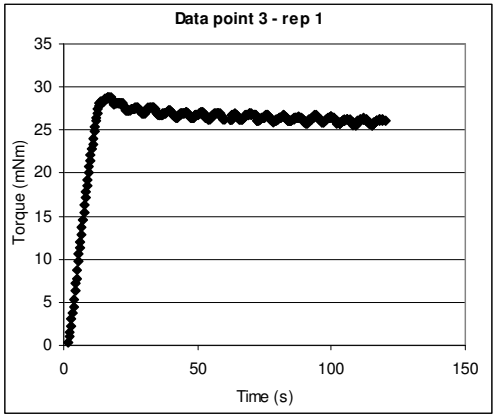
Data point 3 - rep 1
Torque (mNm)
Time (s)
0
5
10
15
20
25
30
35
0
50
100
150

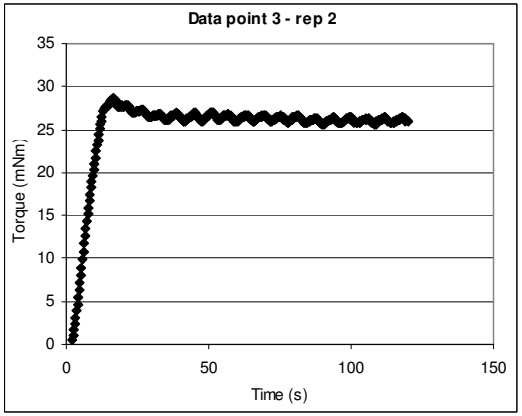
Data point 3 - rep 2
Torque (mNm)
Time (s)
0
5
10
15
20
25
30
35
0
50
100
150

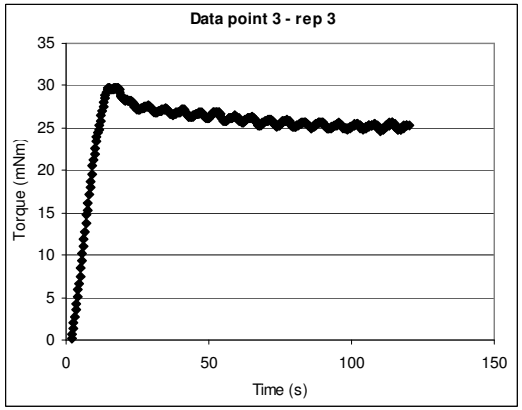
Data point 3 - rep 3
Torque (mNm)
Time (s)
0
5
10
15
20
25
30
35
0
50
100
150

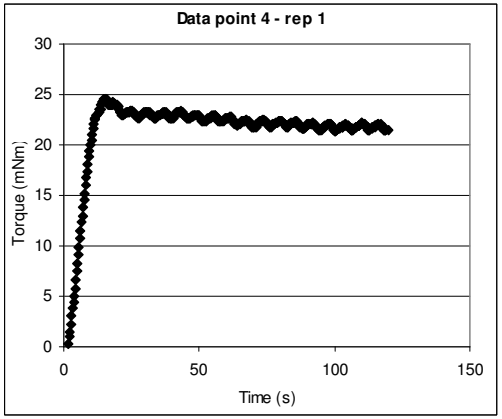
Data point 4 - rep 1
Torque (mNm)
Time (s)
0
5
10
15
20
25
30
0
50
100
150

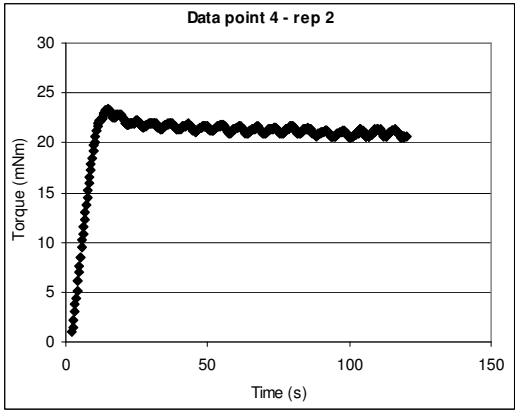
Data point 4 - rep 2
Torque (mNm)
Time (s)
0
5
10
15
20
25
30
0
50
100
150

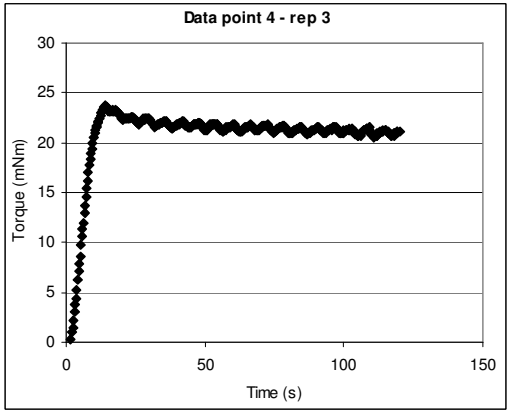
Data point 4 - rep 3
Torque (mNm)
Time (s)
0
5
10
15
20
25
30
0
50
100
150

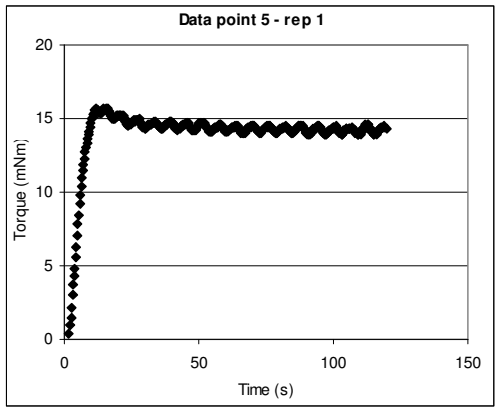
Data point 5 - rep 1
Torque (mNm)
Time (s)
0
5
10
15
20
0
50
100
150

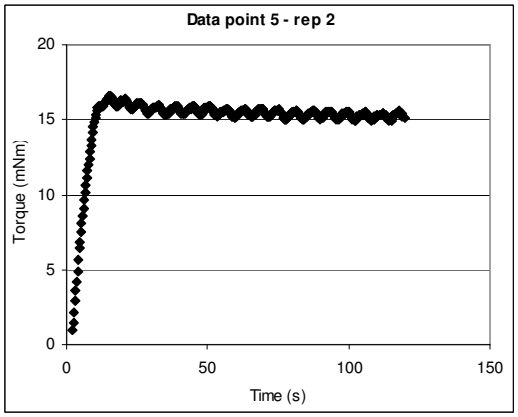
Data point 5 - rep 2
Torque (mNm)
Time (s)
0
5
10
15
20
0
50
100
150

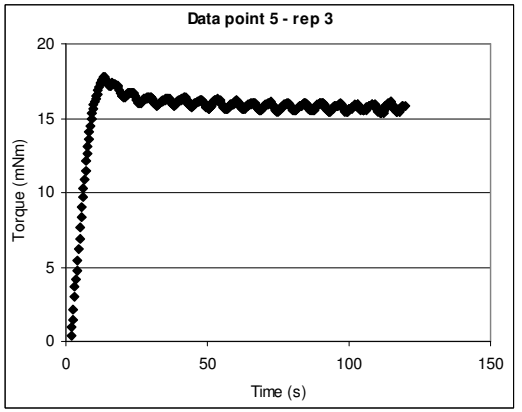
Data point 5 - rep 3
Torque (mNm)
Time (s)
0
5
10
15
20
0
50
100
150

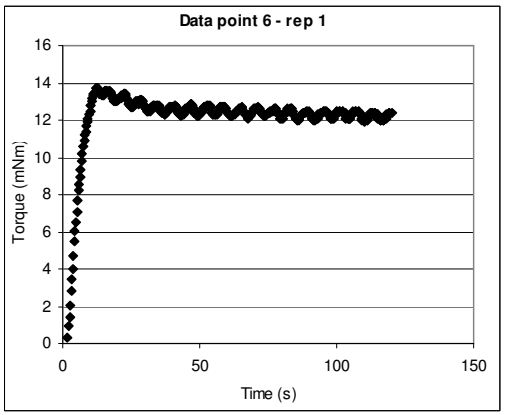
Data point 6 - rep 1
Torque (mNm)
Time (s)
0
2
4
6
8
10
12
14
16
0
50
100
150

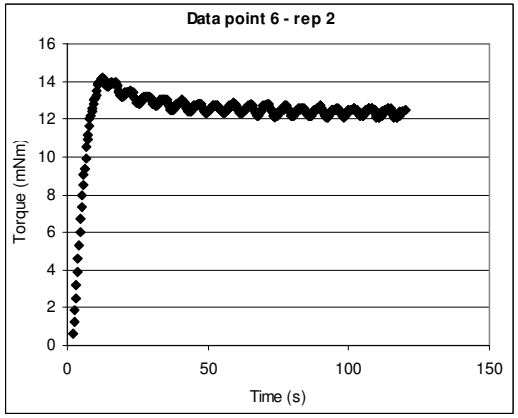
Data point 6 - rep 2
Torque (mNm)
Time (s)
0
2
4
6
8
10
12
14
16
0
50
100
150

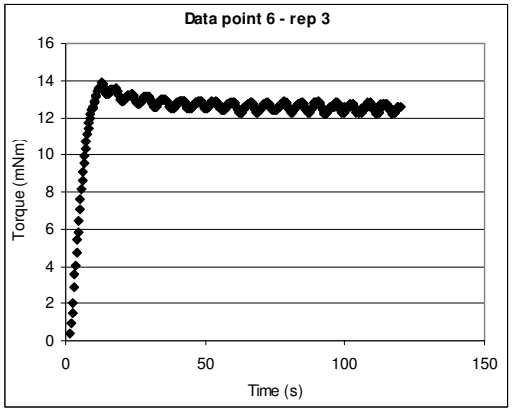
Data point 6 - rep 3
Torque (mNm)
Time (s)
0
2
4
6
8
10
12
14
16
0
50
100
150

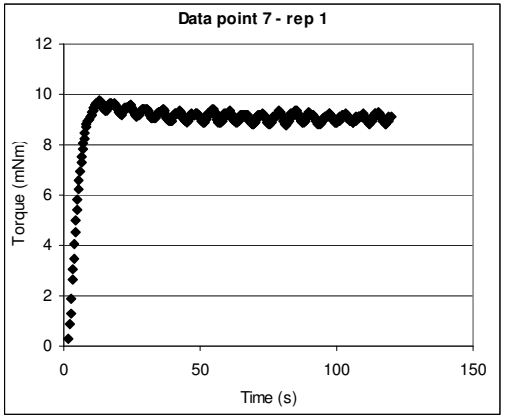
Data point 7 - rep 1
Torque (mNm)
Time (s)
0
2
4
6
8
10
12
0
50
100
150

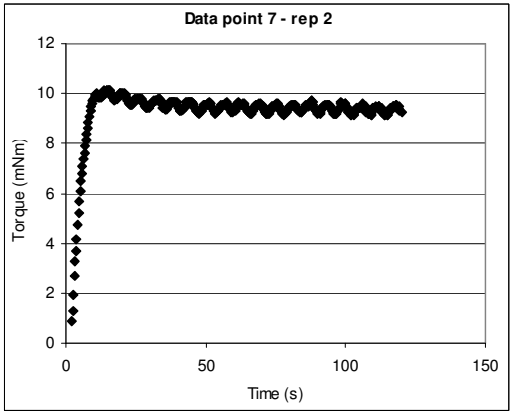
Data point 7 - rep 2
Torque (mNm)
Time (s)
0
2
4
6
8
10
12
0
50
100
150

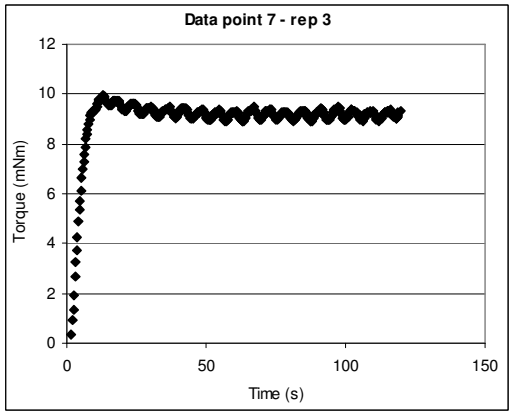
Data point 7 - rep 3
Torque (mNm)
Time (s)
0
2
4
6
8
10
12
0
50
100
150

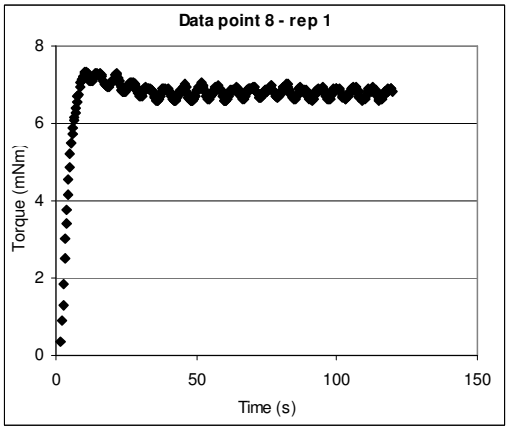
Data point 8 - rep 1
Torque (mNm)
Time (s)
0
2
4
6
8
0
50
100
150

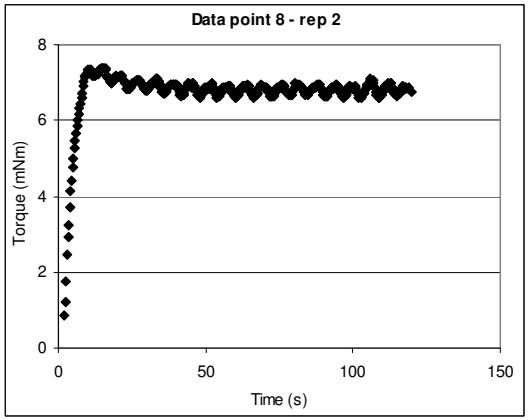
Data point 8 - rep 2
Torque (mNm)
Time (s)
0
2
4
6
8
0
50
100
150

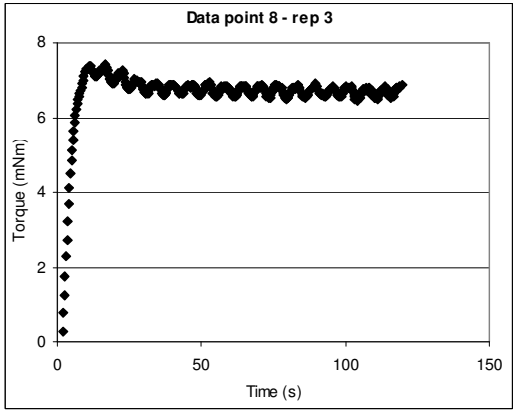
Data point 8 - rep 3
Torque (mNm)
Time (s)
0
2
4
6
8
0
50
100
150

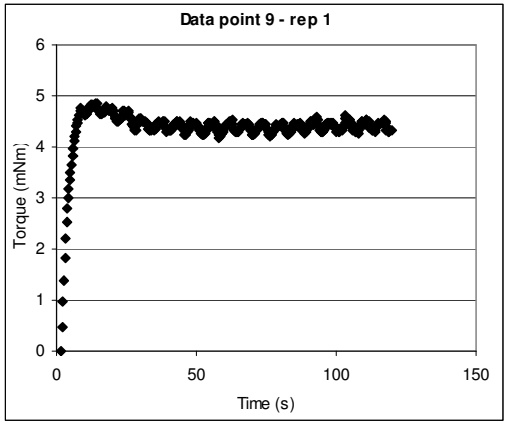
Data point 9 - rep 1
Torque (mNm)
Time (s)
0
1
2
3
4
5
6
0
50
100
150

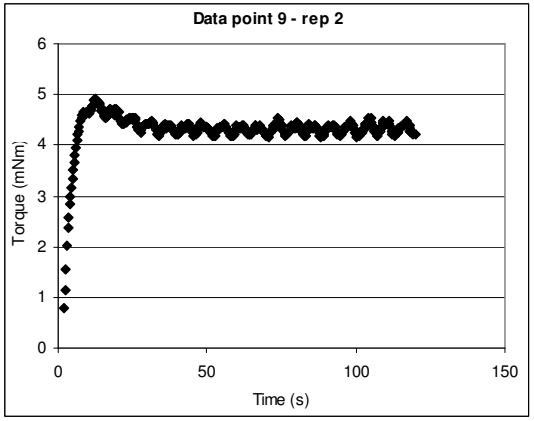
Data point 9 - rep 2
Torque (mNm)
Time (s)
0
1
2
3
4
5
6
0
50
100
150

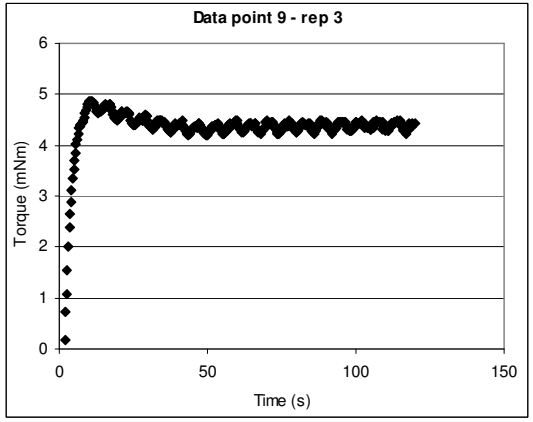
Data point 9 - rep 3
Torque (mNm)
Time (s)
0
1
2
3
4
5
6
0
50
100
150

Vehicle – pH 8.5 (interactive)

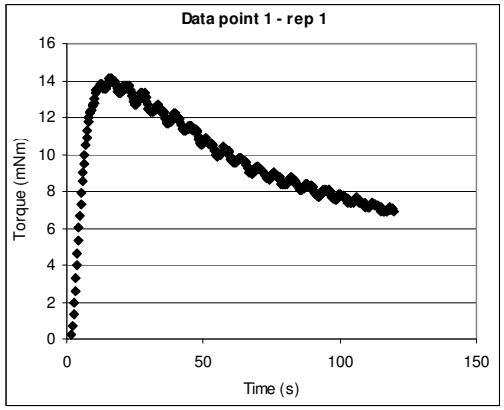

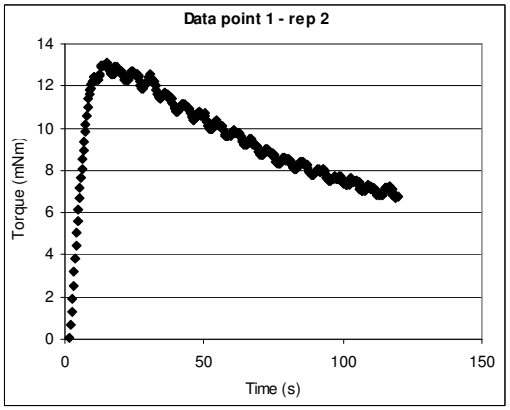

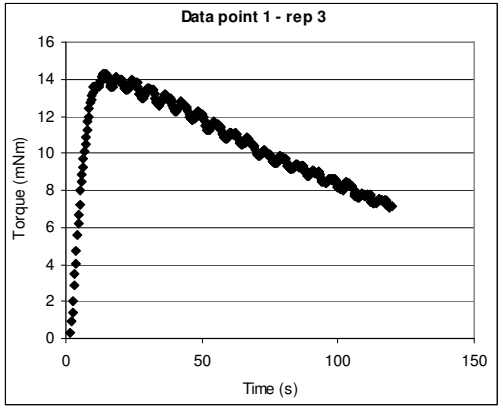

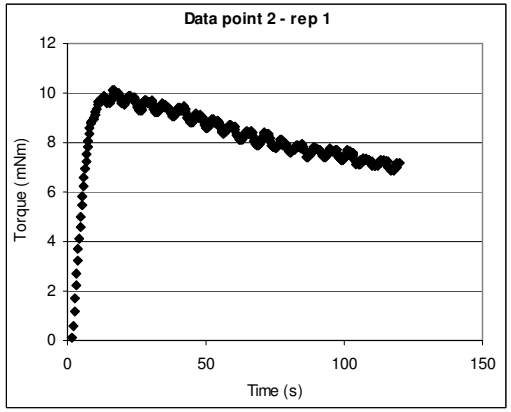

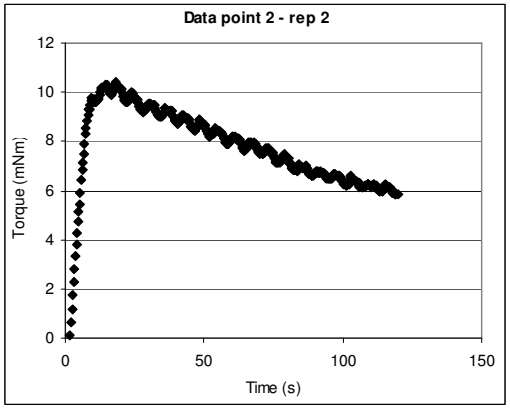

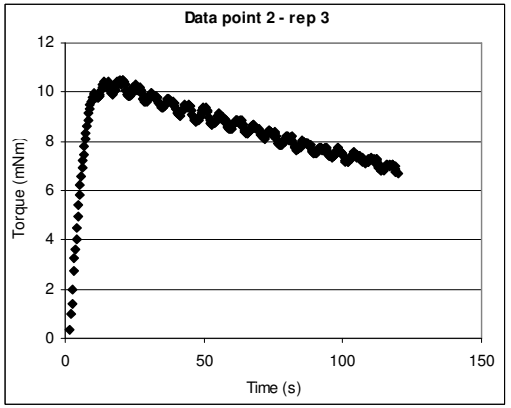

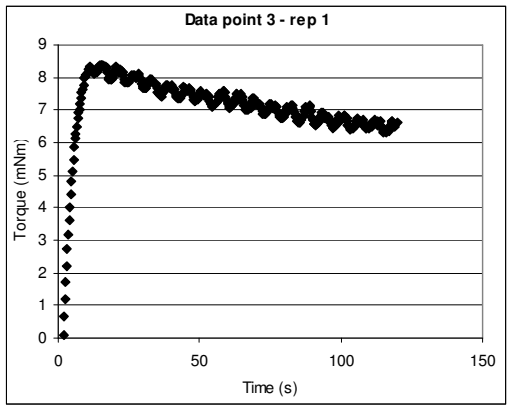
Data point 3 - rep 1
Torque (mNm)
Time (s)
0
1
2
3
4
5
6
7
8
9
0
50
100
150

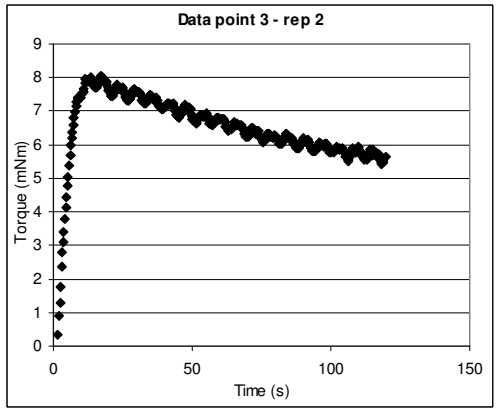
Data point 3 - rep 2
Torque (mNm)
Time (s)
0
1
2
3
4
5
6
7
8
9
0
50
100
150

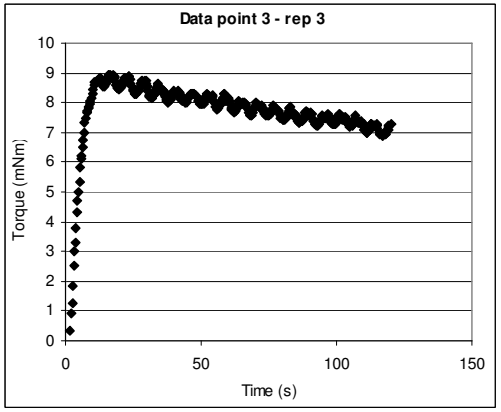
Data point 3 - rep 3
Torque (mNm)
Time (s)
0
1
2
3
4
5
6
7
8
9
10
0
50
100
150

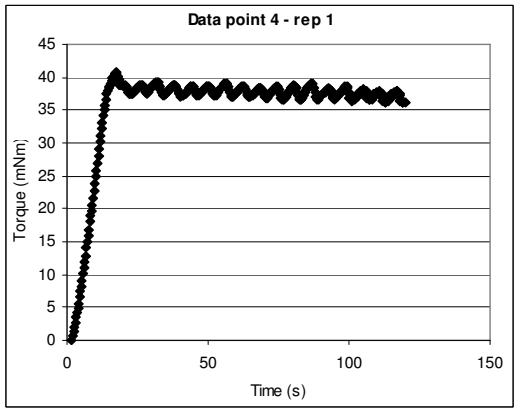
Data point 4 - rep 1
Torque (mNm)
Time (s)
0
5
10
15
20
25
30
35
40
45
0
50
100
150

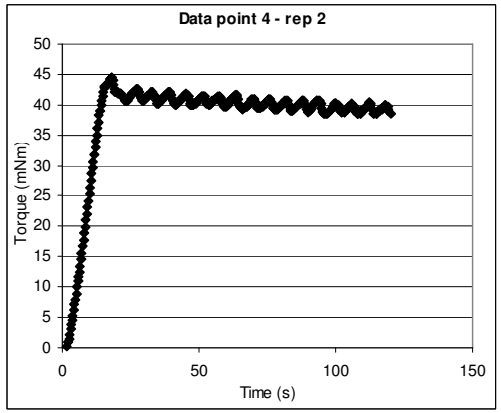
Data point 4 - rep 2
Torque (mNm)
Time (s)
0
5
10
15
20
25
30
35
40
45
50
0
50
100
150

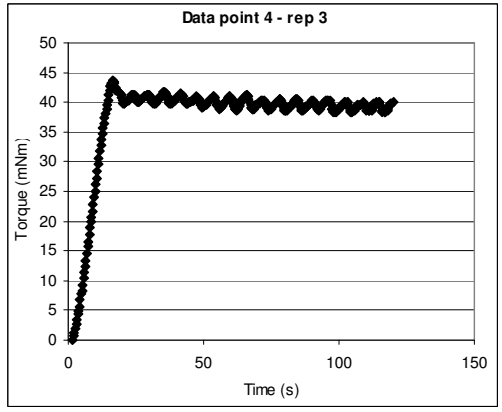
Data point 4 - rep 3
Torque (mNm)
Time (s)
0
5
10
15
20
25
30
35
40
45
50
0
50
100
150

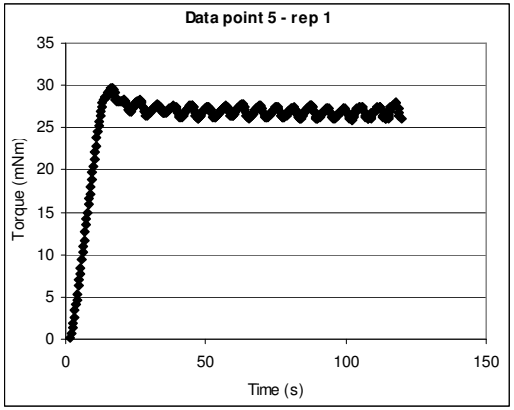
Data point 5 - rep 1
Torque (mNm)
Time (s)
0
5
10
15
20
25
30
35
0
50
100
150

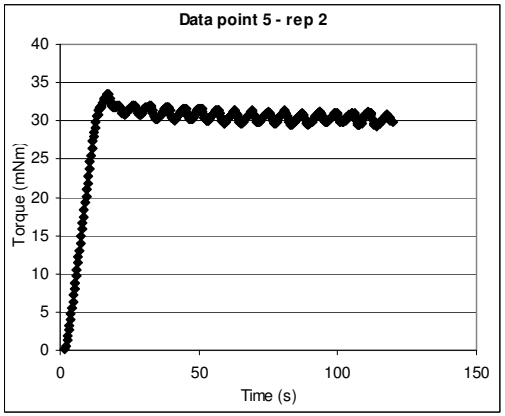
Data point 5 - rep 2
Torque (mNm)
Time (s)
0
5
10
15
20
25
30
35
40
0
50
100
150

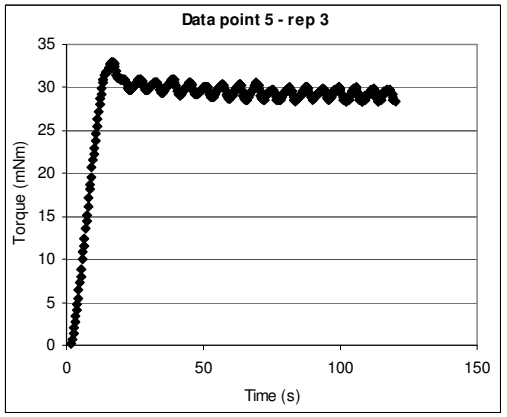
Data point 5 - rep 3
Torque (mNm)
Time (s)
0
5
10
15
20
25
30
35
0
50
100
150

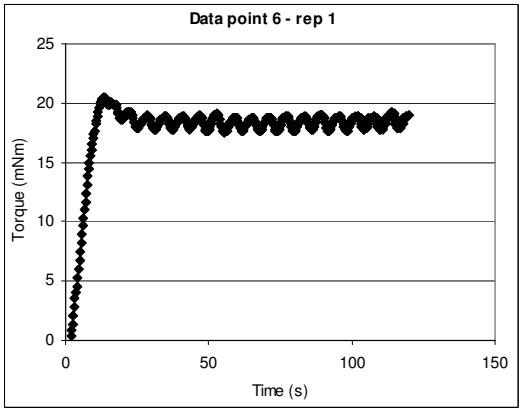
Data point 6 - rep 1
Torque (mNm)
Time (s)
0
5
10
15
20
25
0
50
100
150

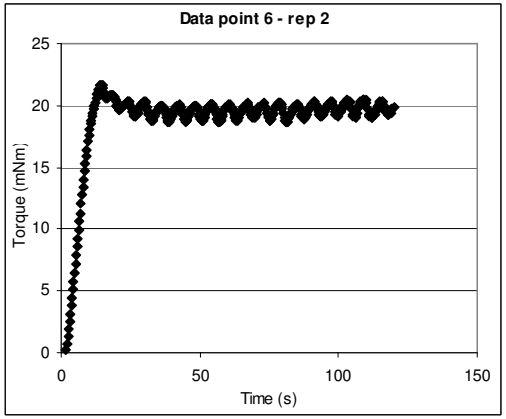
Data point 6 - rep 2
Torque (mNm)
Time (s)
0
5
10
15
20
25
0
50
100
150

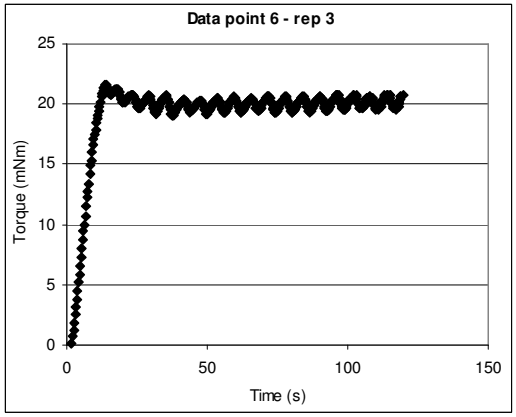
Data point 6 - rep 3
Torque (mNm)
Time (s)
0
5
10
15
20
25
0
50
100
150

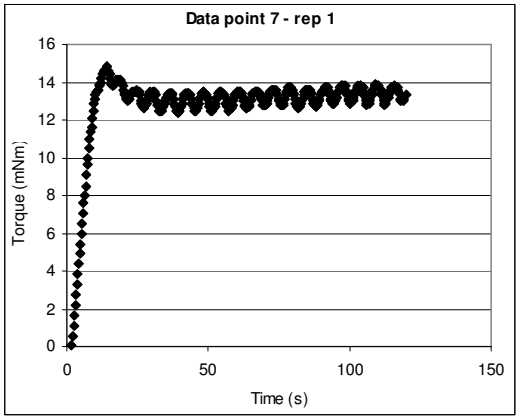
Data point 7 - rep 1
Torque (mNm)
Time (s)
0
2
4
6
8
10
12
14
16
0
50
100
150

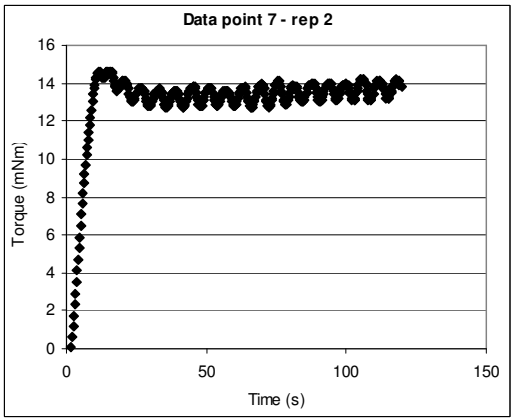
Data point 7 - rep 2
Torque (mNm)
Time (s)
0
2
4
6
8
10
12
14
16
0
50
100
150

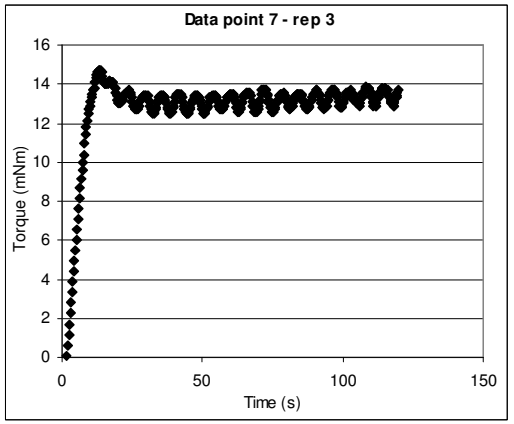
Data point 7 - rep 3
Torque (mNm)
Time (s)
0
2
4
6
8
10
12
14
16
0
50
100
150

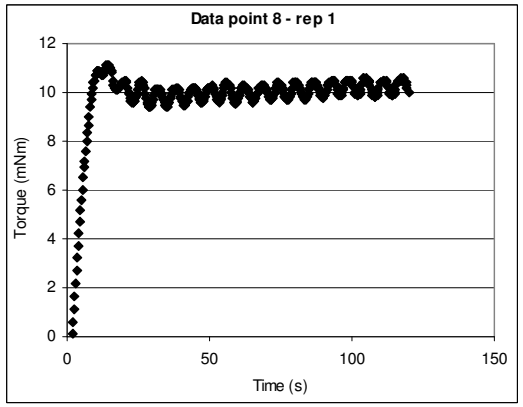
Data point 8 - rep 1
Torque (mNm)
Time (s)
0
2
4
6
8
10
12
0
50
100
150

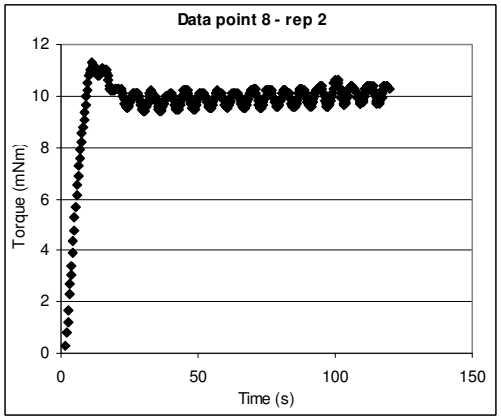
Data point 8 - rep 2
Torque (mNm)
Time (s)
0
2
4
6
8
10
12
0
50
100
150

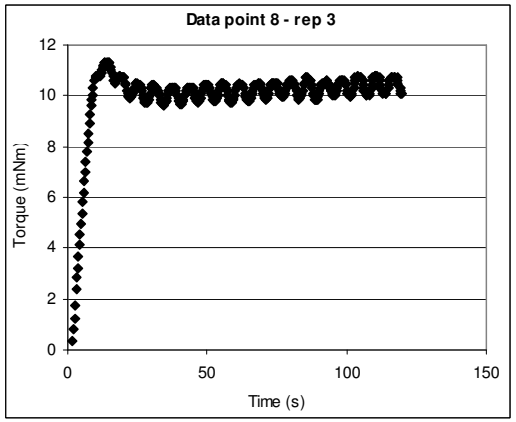
Data point 8 - rep 3
Torque (mNm)
Time (s)
0
2
4
6
8
10
12
0
50
100
150

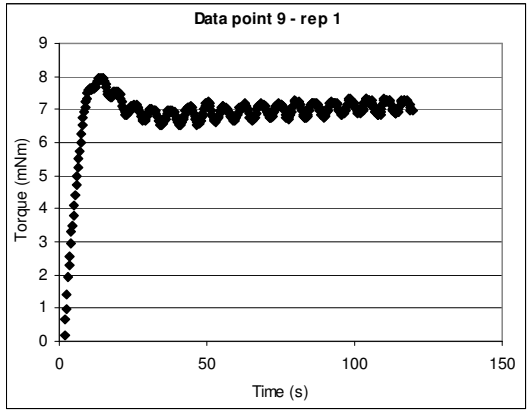
Data point 9 - rep 1
Torque (mNm)
Time (s)
0
1
2
3
4
5
6
7
8
9
0
50
100
150

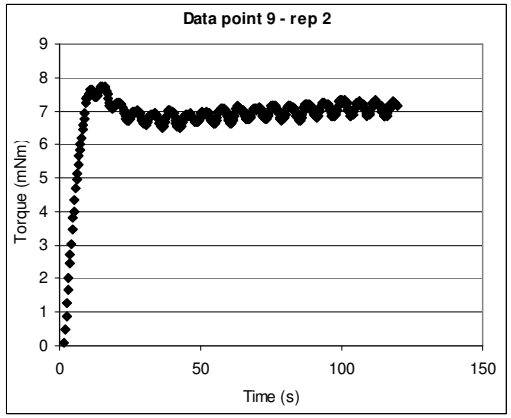
Data point 9 - rep 2
Torque (mNm)
Time (s)
0
1
2
3
4
5
6
7
8
9
0
50
100
150

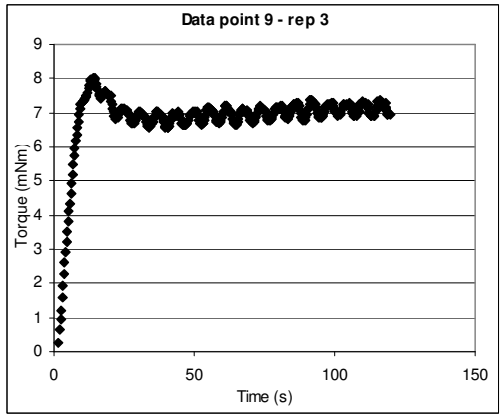
Data point 9 - rep 3
Torque (mNm)
Time (s)
0
1
2
3
4
5
6
7
8
9
0
50
100
150

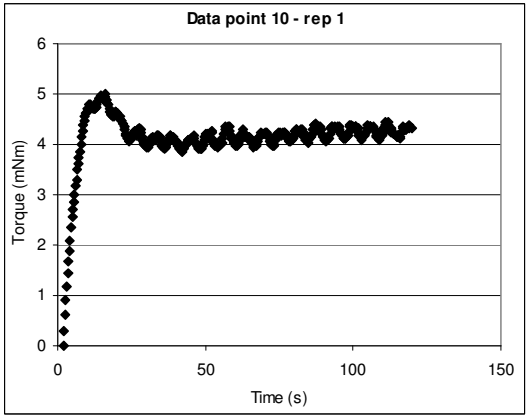
Data point 10 - rep 1
Torque (mNm)
Time (s)
0
1
2
3
4
5
6
0
50
100
150

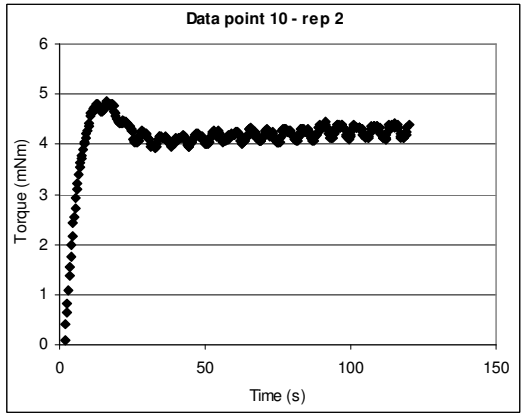
Data point 10 - rep 2
Torque (mNm)
Time (s)
0
1
2
3
4
5
6
0
50
100
150

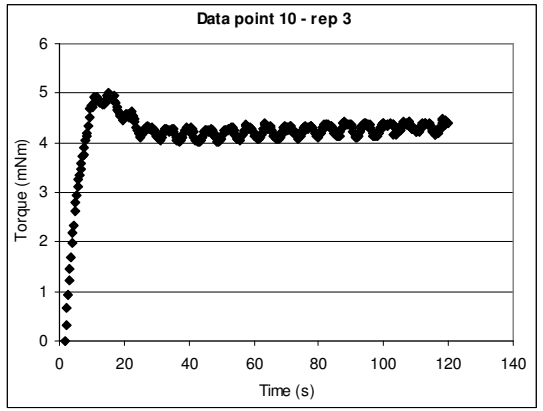
Data point 10 - rep 3
Torque (mNm)
Time (s)
0
1
2
3
4
5
6
0
20
40
60
80
100
120
140

Vehicle – pH 8.7 (non-interactive)

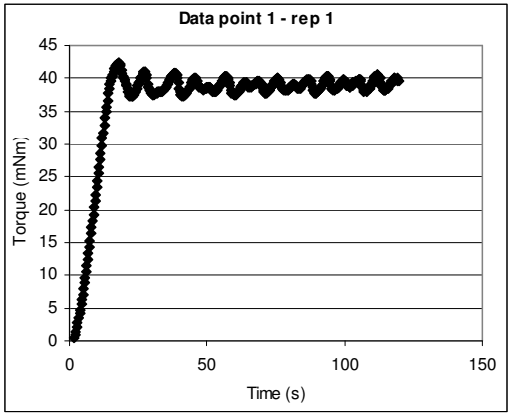

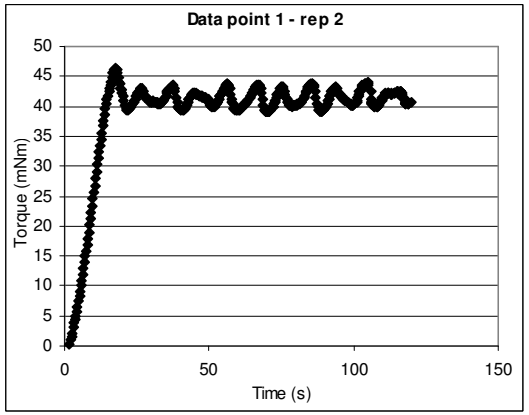

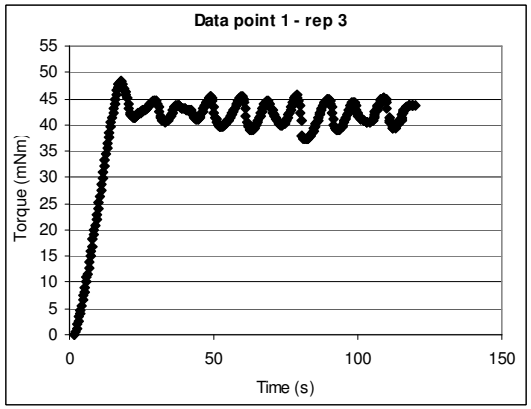

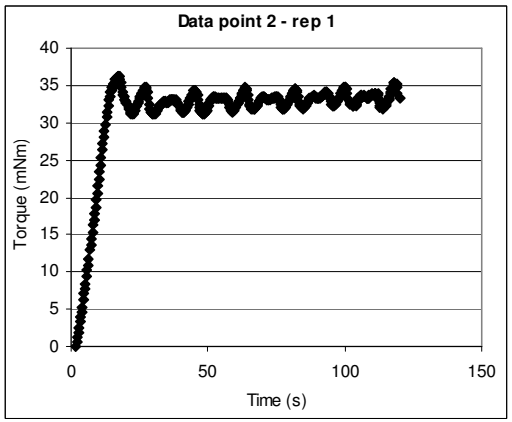

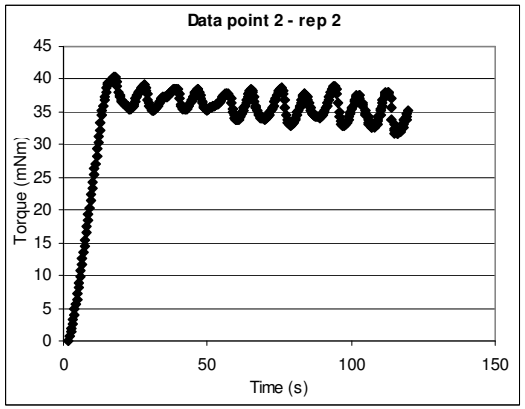

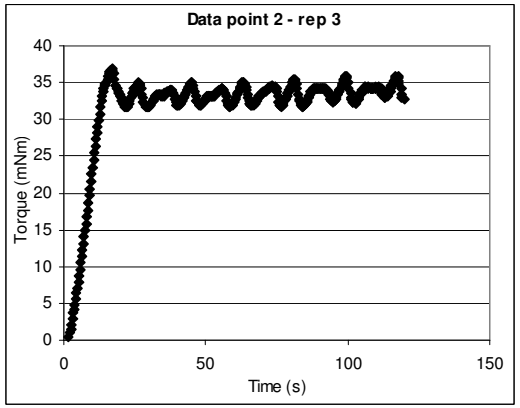

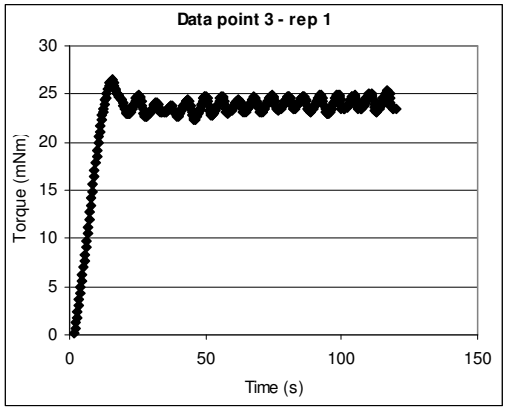
Data point 3 - rep 1
Torque (mNm)
Time (s)
0
5
10
15
20
25
30
0
50
100
150

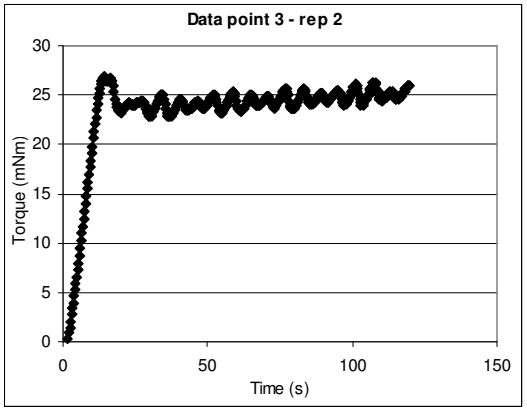
Data point 3 - rep 2
Torque (mNm)
Time (s)
0
5
10
15
20
25
30
0
50
100
150

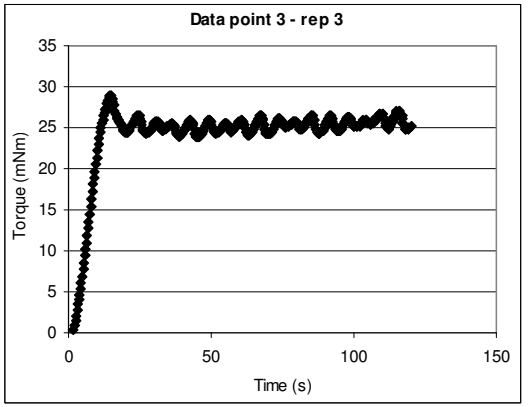
Data point 3 - rep 3
Torque (mNm)
Time (s)
0
5
10
15
20
25
30
35
0
50
100
150

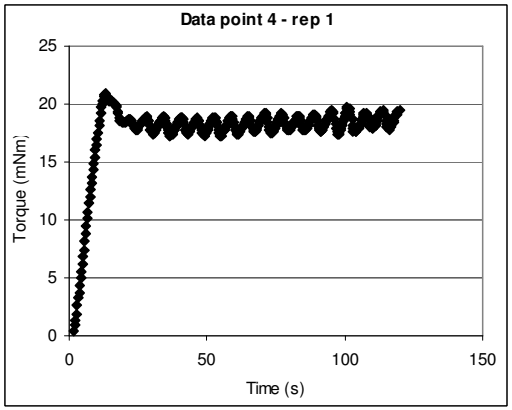
Data point 4 - rep 1
Torque (mNm)
Time (s)
0
5
10
15
20
25
0
50
100
150

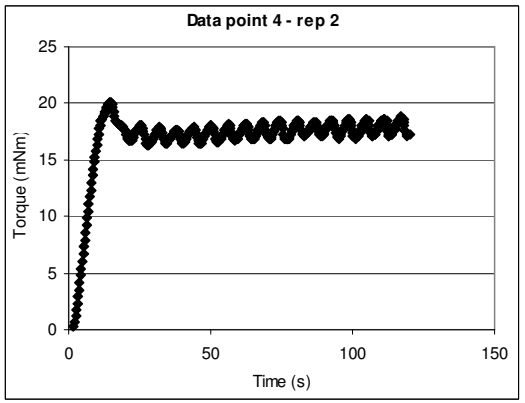
Data point 4 - rep 2
Torque (mNm)
Time (s)
0
5
10
15
20
25
0
50
100
150

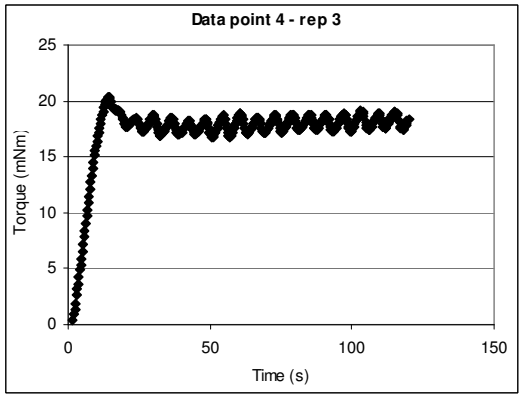
Data point 4 - rep 3
Torque (mNm)
Time (s)
0
5
10
15
20
25
0
50
100
150

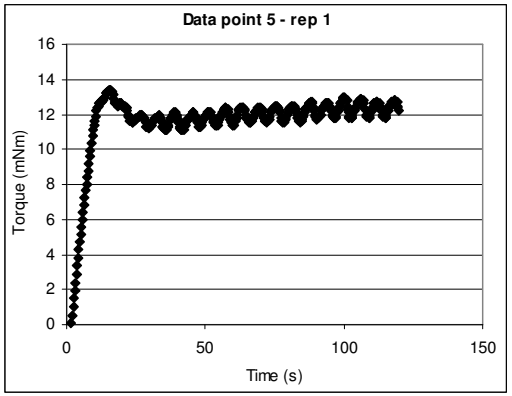
Data point 5 - rep 1
Torque (mNm)
Time (s)
0
2
4
6
8
10
12
14
16
0
50
100
150

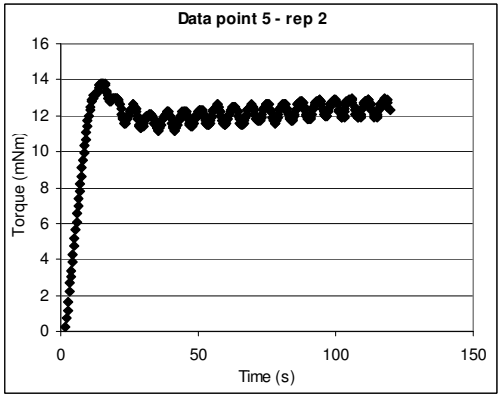
Data point 5 - rep 2
Torque (mNm)
Time (s)
0
2
4
6
8
10
12
14
16
0
50
100
150

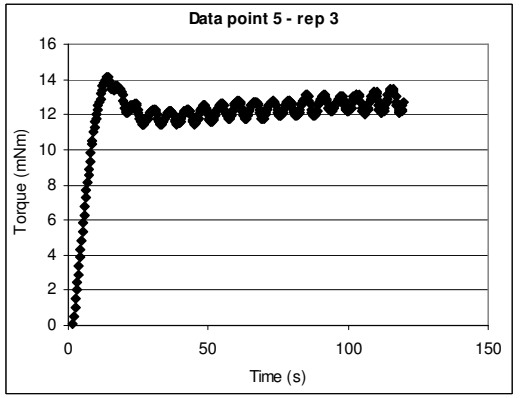
Data point 5 - rep 3
Torque (mNm)
Time (s)
0
2
4
6
8
10
12
14
16
0
50
100
150

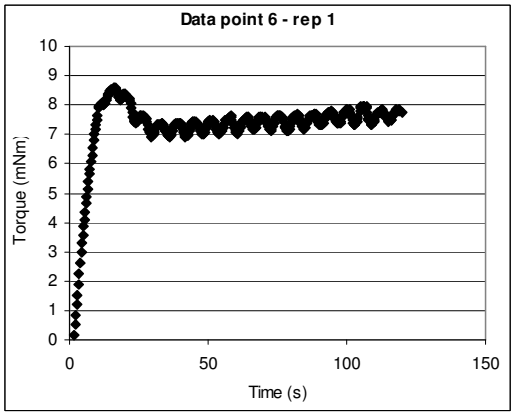
Data point 6 - rep 1
Torque (mNm)
Time (s)
0
1
2
3
4
5
6
7
8
9
10
0
50
100
150

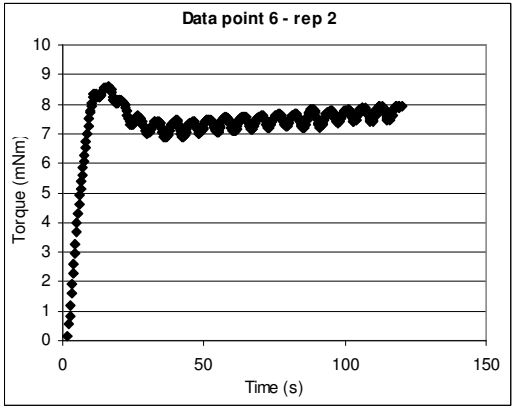
Data point 6 - rep 2
Torque (mNm)
Time (s)
0
1
2
3
4
5
6
7
8
9
10
0
50
100
150

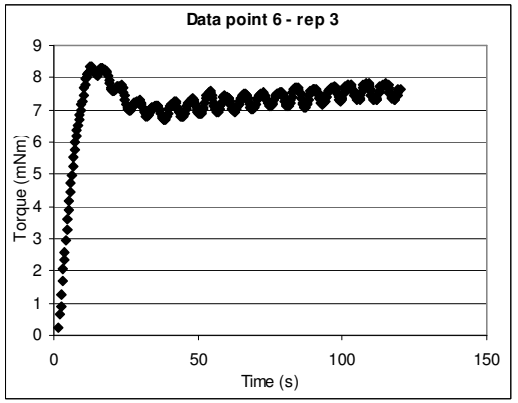
Data point 6 - rep 3
Torque (mNm)
Time (s)
0
1
2
3
4
5
6
7
8
9
0
50
100
150

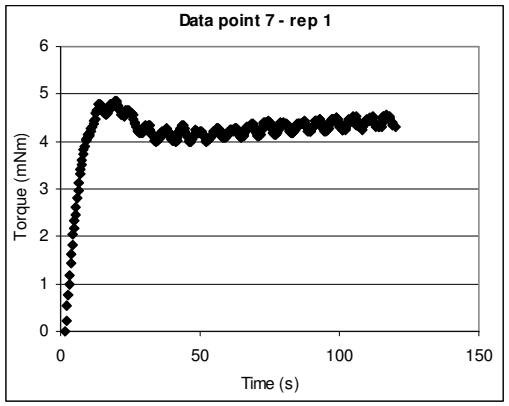
Data point 7 - rep 1
Torque (mNm)
Time (s)
0
1
2
3
4
5
6
0
50
100
150

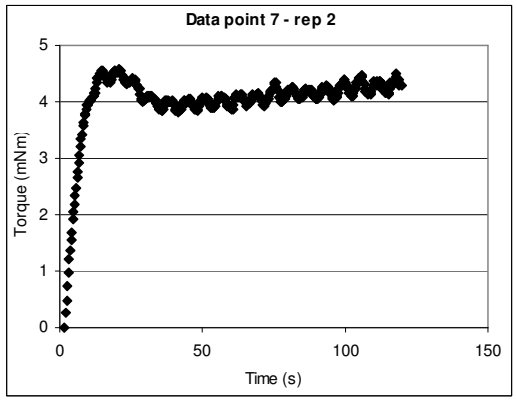
Data point 7 - rep 2
Torque (mNm)
Time (s)
0
1
2
3
4
5
0
50
100
150

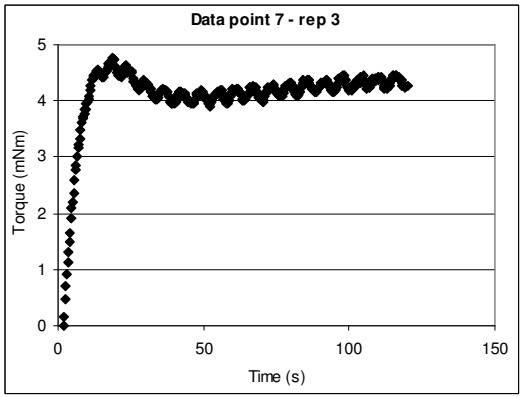
Data point 7 - rep 3
Torque (mNm)
Time (s)
0
1
2
3
4
5
0
50
100
150

APPENDIX K : CO-DISPOSED TAILINGS YIELD STRESS – RAW DATA SUMMARY

Table K 1 : Co-disposed tailings yield stress (pH 8.6, v : l = 86:14 %)

VANE

	calculated	*calculated*	*measured*
Data point	*Vehicle*	*Co-disposed*	*Co-disposed*
	% solids	*% solids*	*yield stress*
			(Pa)
1	66.9	70.4	915.0
2	66.0	69.5	671.3
3	64.9	68.4	484.0
4	63.9	67.5	386.6
5	62.8	66.5	276.3
6	61.7	65.4	197.8
7	60.5	64.2	142.1
8	59.4	63.2	101.7
9	58.1	62.0	70.6

SMALL SLUMP

	calculated	*calculated*	*measured*
Data point	*Vehicle*	*Co-disposed*	*Co-disposed*
	% solids	*% solids*	*yield stress*
			(Pa)
1	65.9	69.4	533.8
2	64.8	68.4	449.3
3	63.8	67.4	408.4
4	62.7	66.4	339.6
5	61.6	65.3	266.7
6	60.4	64.2	201.9
7	59.2	63.0	129.4
8	58.0	61.8	72.4

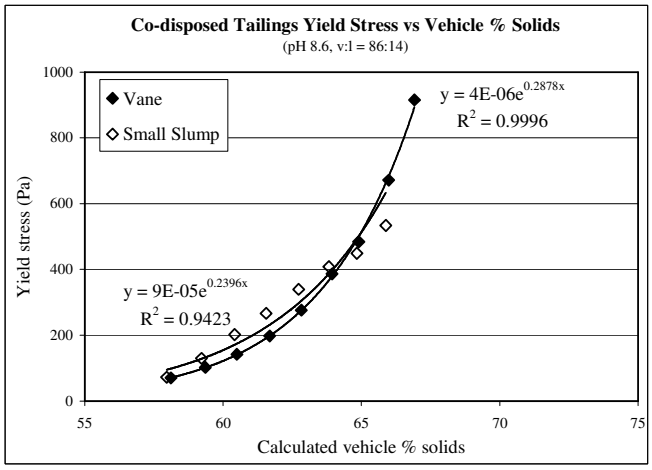

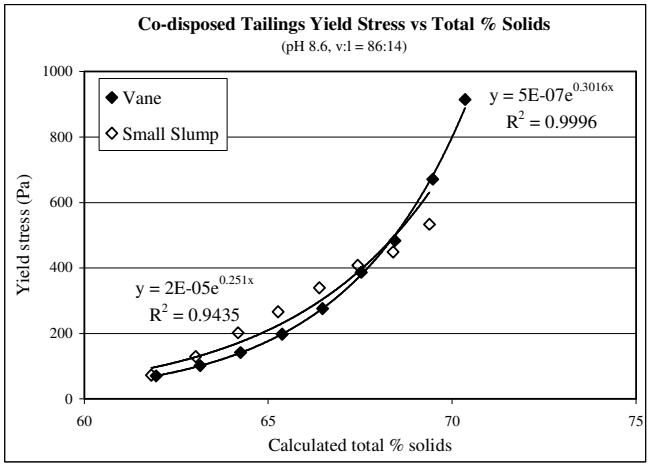

Figure K 1 : Co-disposed tailings yield stress (pH 8.6, v : l = 86:14 %)

Table K 2 : Co-disposed tailings yield stress (pH 8.6, v : l = 60:40 %)

VANE

Data point	calculated Vehicle % solids	calculated Co-disposed % solids	measured Co-disposed yield stress (Pa)
1	64.9	75.5	982.9
2	63.8	74.6	644.4
3	62.6	73.6	486.4
4	61.5	72.7	401.0
5	60.4	71.8	289.7
6	59.3	70.8	215.1
7	58.1	69.8	169.2
8	56.6	68.5	102.4

SMALL SLUMP

Data point	calculated Vehicle % solids	calculated Co-disposed % solids	measured Co-disposed yield stress (Pa)
1	65.8	76.2	722.6
2	64.7	75.4	612.4
3	63.6	74.4	520.6
4	62.4	73.5	437.3
5	61.2	72.5	362.7
6	60.1	71.5	282.7
7	58.8	70.5	183.1
8	57.5	69.3	126.3

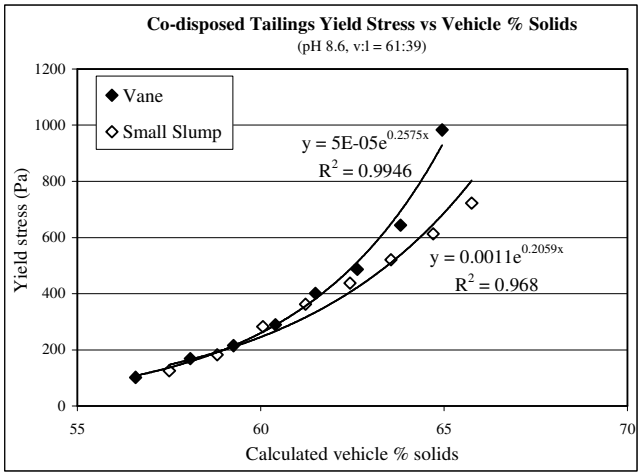

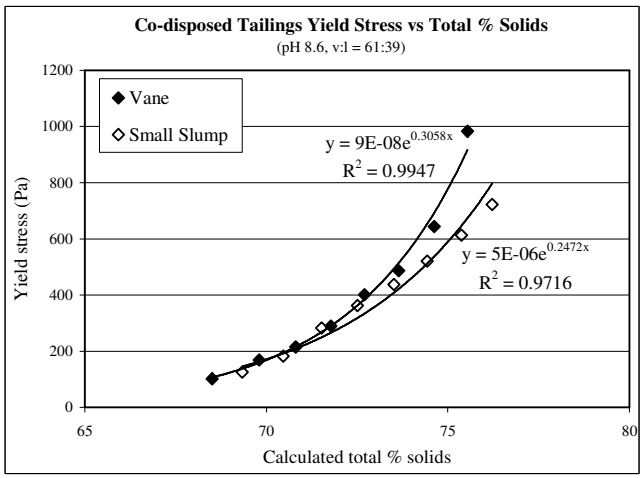

Figure K 2 : Co-disposed tailings yield stress (pH 8.6, v : l = 60:40 %)

Table K 3 : Co-disposed tailings yield stress (pH 8.6, v : l = 50:50 %)

VANE

Data point	calculated Vehicle % solids	calculated Co-disposed % solids	measured Co-disposed yield stress (Pa)
1	63.0	77.6	1005.0
2	61.7	76.6	616.1
3	60.3	75.6	412.4
4	58.9	74.5	362.2
5	57.4	73.3	269.3
6	55.8	72.0	166.9
7	54.4	70.8	108.1

SMALL SLUMP

Data point	calculated Vehicle % solids	calculated Co-disposed % solids	measured Co-disposed yield stress (Pa)
1	65.5	79.2	845.8
2	64.2	78.2	717.0
3	62.8	77.2	582.0
4	61.4	76.1	454.0
5	60.0	75.0	375.2
6	58.6	73.9	270.5
7	57.2	72.8	187.4
8	55.8	71.7	129.1

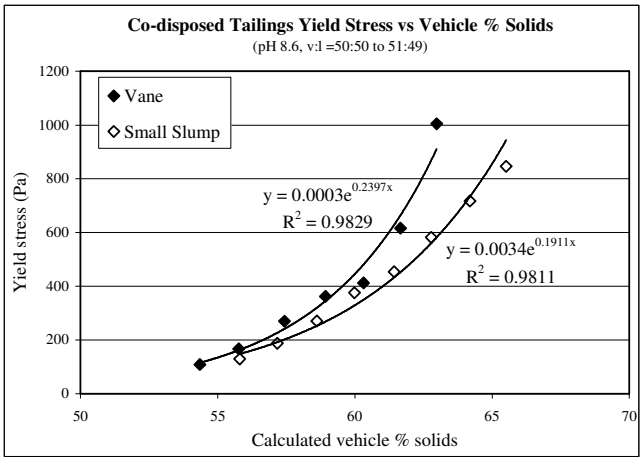

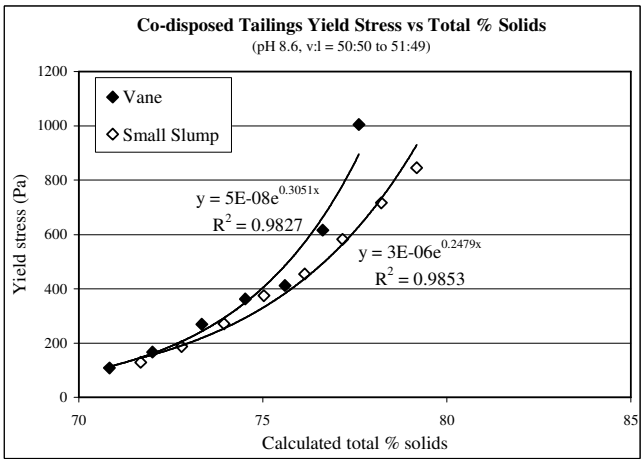

Figure K 3 : Co-disposed tailings yield stress (pH 8.6, v : l = 50:50 %)

Table K 4 : Co-disposed tailings yield stress (pH 6.2, v : l = 86:14 %)

VANE

Data point	Vehicle % solids (calculated)	Co-disposed % solids (calculated)	Co-disposed yield stress (measured)
			(Pa)
1	62.7	66.3	394.0
2	61.6	65.4	316.0
3	60.6	64.3	240.5
4	59.8	63.5	195.8
5	58.9	62.7	151.5
6	58.0	61.8	127.1
7	56.9	60.8	100.6
8	55.8	59.7	74.3

SMALL SLUMP

Data point	Vehicle % solids (calculated)	Co-disposed % solids (calculated)	Co-disposed yield stress (measured)
			(Pa)
1	66.4	69.8	549.1
2	65.3	68.7	447.5
3	64.2	67.6	363.0
4	63.0	66.5	295.7
5	61.9	65.5	251.1
6	60.7	64.3	204.6
7	59.4	63.1	149.2
8	58.2	61.9	132.6

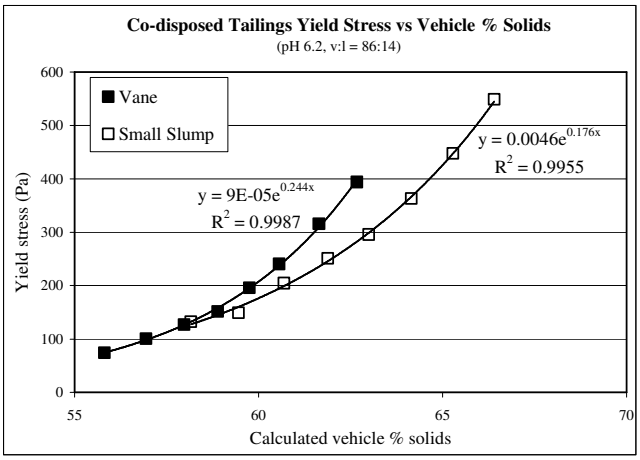

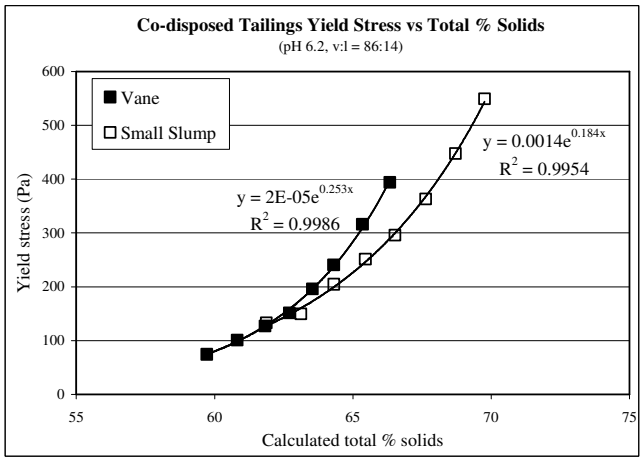

Figure K 4 : Co-disposed tailings yield stress (pH 6.2, v : l = 86:14%)

Table K 5 : Co-disposed tailings yield stress (pH 6.2, v : l = 60:40 %)

VANE

Data point	calculated Vehicle % solids	calculated Co-disposed % solids	measured Co-disposed yield stress (Pa)
1	64.8	75.2	908.6
2	63.8	74.3	777.0
3	62.6	73.4	570.4
4	61.7	72.6	431.3
5	60.6	71.6	341.4
6	59.3	70.6	269.3
7	58.0	69.5	201.7
8	56.8	68.4	156.0
9	55.4	67.1	107.2

SMALL SLUMP

Data point	calculated Vehicle % solids	calculated Co-disposed % solids	measured Co-disposed yield stress (Pa)
1	66.1	76.3	679.7
2	65.1	75.5	576.9
3	63.9	74.4	462.9
4	62.7	73.5	355.8
5	61.3	72.3	285.6
6	60.0	71.1	246.0
7	58.6	70.0	186.6
8	57.3	68.8	111.5

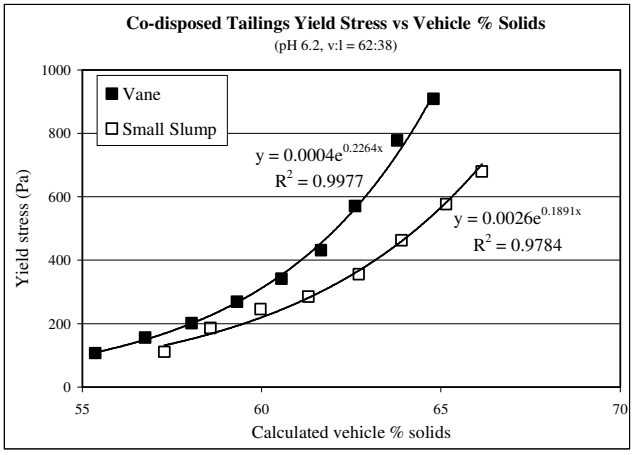

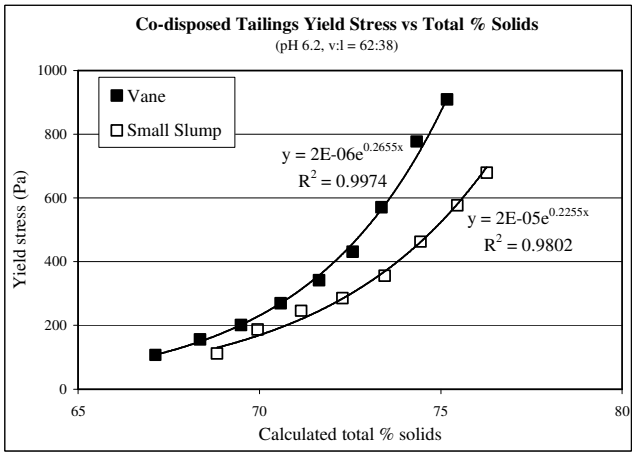

Figure K 5 : Co-disposed tailings yield stress (pH 6.2, v : l = 60:40 %)

Table K 6 : Co-disposed tailings yield stress (pH 6.2, v : l = 50:50 %)

VANE

Data point	calculated Vehicle % solids	calculated Co-disposed % solids	measured Co-disposed yield stress (Pa)
1	62.6	77.0	827.3
2	61.3	76.1	582.8
3	60.1	75.1	424.3
4	58.8	74.1	318.0
5	57.6	73.2	223.6
6	56.4	72.1	177.4
7	54.9	70.9	129.1
8	53.5	69.8	110.8

SMALL SLUMP

Data point	calculated Vehicle % solids	calculated Co-disposed % solids	measured Co-disposed yield stress (Pa)
1	61.9	77.0	642.8
2	60.7	76.0	498.9
3	59.3	75.0	394.1
4	57.7	73.7	303.4
5	56.0	72.4	244.7
6	54.0	70.8	180.5
7	52.1	69.2	119.0

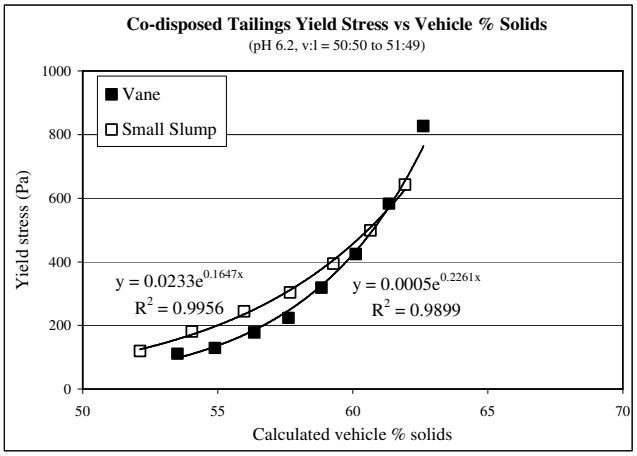

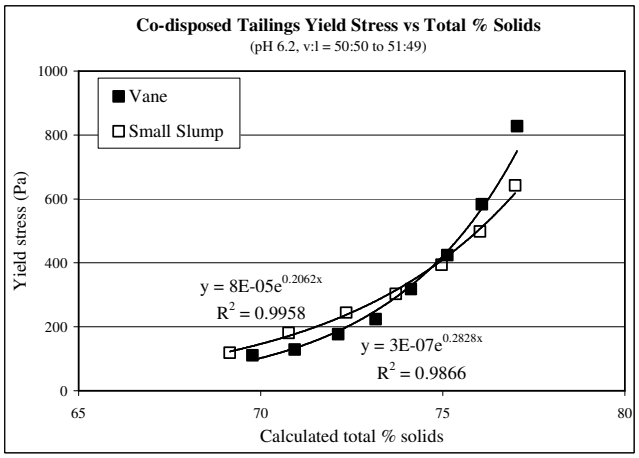

Figure K 6 : Co-disposed tailings yield stress (pH 6.2, v : l = 50:50 %)

Table K 7 : Co-disposed tailings yield stress (pH 11.5, v : l = 86:14 %)

VANE

Data point	calculated Vehicle % solids	calculated Co-disposed % solids	measured Co-disposed yield stress (Pa)
1	67.3	70.6	961.4
2	65.9	69.4	814.3
3	64.9	68.4	725.9
4	63.8	67.4	585.8
5	62.7	66.3	442.2
6	61.7	65.3	368.7
7	60.5	64.2	289.2
8	59.1	62.9	223.6
9	57.6	61.4	168.4
10	55.5	59.4	108.6

SMALL SLUMP

Data point	calculated Vehicle % solids	calculated Co-disposed % solids	measured Co-disposed yield stress (Pa)
1	62.0	65.7	387.0
2	61.1	64.8	343.6
3	60.0	63.8	283.4
4	58.9	62.7	234.5
5	57.7	61.5	198.5
6	56.4	60.3	163.3
7	55.0	58.9	116.3

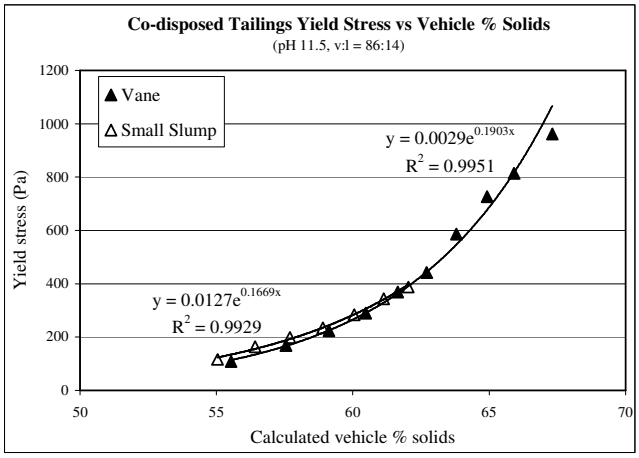

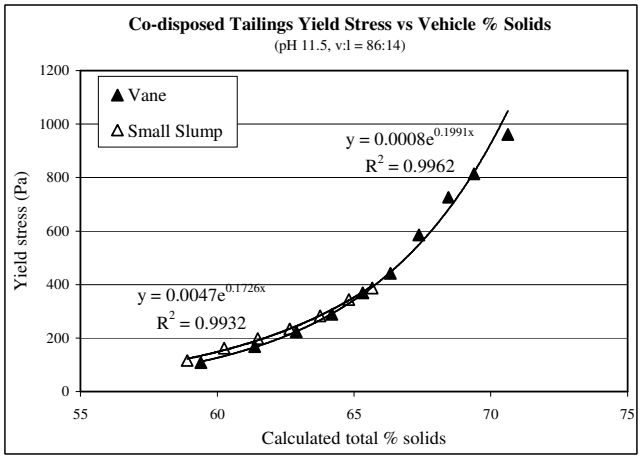

Figure K 7 : Co-disposed tailings yield stress (pH 11.5, v : l = 86:14 %)

Table K 8 : Co-disposed tailings yield stress (pH 11.5, v : l = 60:40 %)

VANE

	calculated	*calculated*	*measured*
Data point	*Vehicle*	*Co-disposed*	*Co-disposed*
	% solids	*% solids*	*yield stress*
			(Pa)
1	62.6	73.7	888.6
2	61.2	72.6	646.4
3	59.9	71.5	506.8
4	58.4	70.2	373.2
5	56.8	68.9	266.3
6	55.1	67.4	189.3
7	53.2	65.6	126.2
8	50.9	63.5	77.9

SMALL SLUMP

	calculated	*calculated*	*measured*
Data point	*Vehicle*	*Co-disposed*	*Co-disposed*
	% solids	*% solids*	*yield stress*
			(Pa)
1	60.7	72.2	457.3
2	59.6	71.3	421.1
3	58.4	70.2	338.9
4	57.0	69.1	287.7
5	55.6	67.8	231.7
6	53.8	66.3	182.7
7	51.8	64.4	126.8

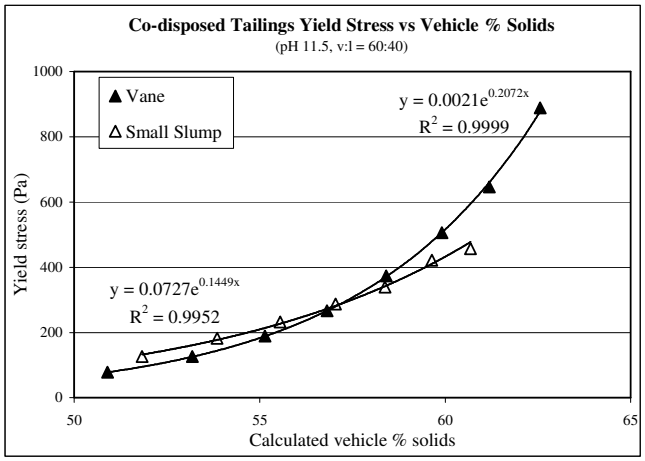

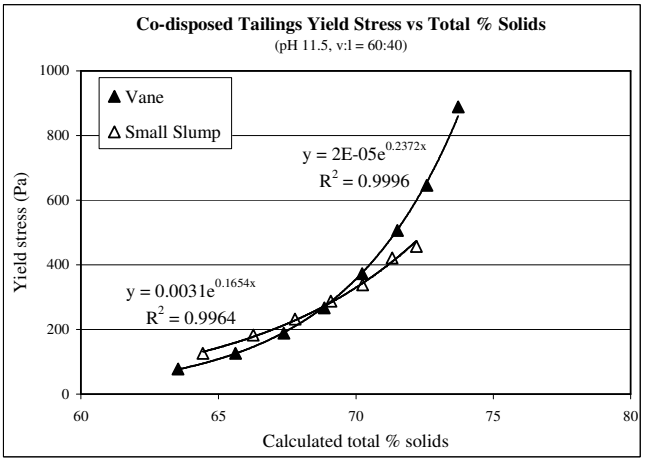

Figure K 8 : Co-disposed tailings yield stress (pH 11.5, v : l = 60:40 %)

Table K 9 : Co-disposed tailings yield stress (pH 11.5, v : l = 50:50 %)

VANE

Data point	calculated Vehicle % solids	calculated Co-disposed % solids	measured Co-disposed yield stress (Pa)
1	59.6	75.3	691.8
2	58.0	74.0	521.2
3	56.4	72.8	378.6
4	54.7	71.4	260.9
5	52.9	69.8	233.5
6	50.7	68.0	129.7
7	48.3	65.9	80.2

SMALL SLUMP

Data point	calculated Vehicle % solids	calculated Co-disposed % solids	measured Co-disposed yield stress (Pa)
1	59.8	75.4	514.9
2	58.6	74.5	429.0
3	57.2	73.3	332.7
4	55.5	72.0	276.5
5	53.6	70.5	228.8
6	51.4	68.6	166.9
7	48.9	66.3	97.7

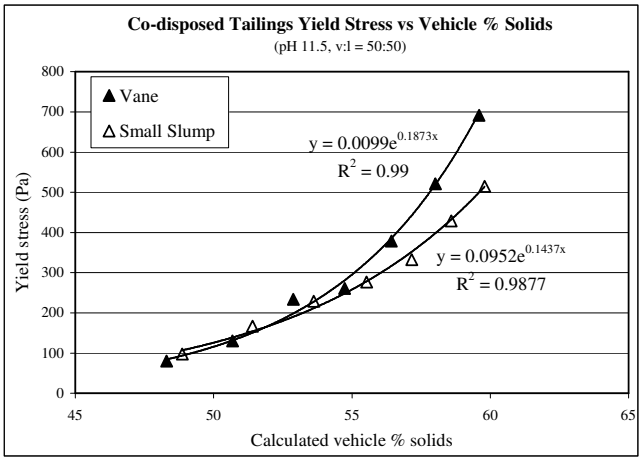

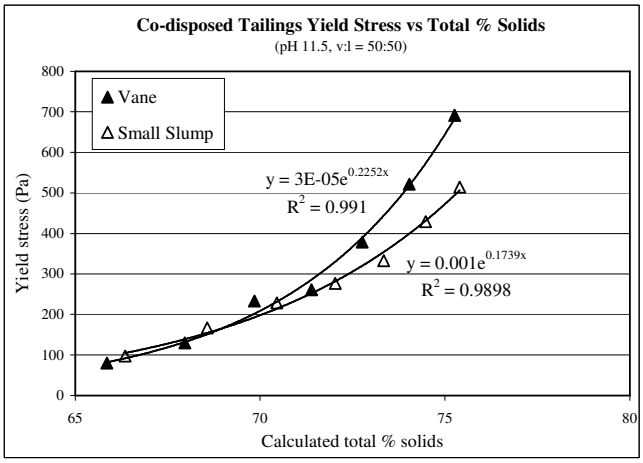

Figure K 9 : Co-disposed tailings yield stress (pH 11.5, v : l = 50:50 %)

APPENDIX L : CO-DISPOSED TAILINGS YIELD STRESS – RAW DATA SHEETS

Co-disposed Tailings - Vane tests

pH = 8.6
vehicle (wet) : load (dry) = 90:10
vehicle (dry) : load (dry) = 86:14

Date : 12/05/2004

Vane dimensions :			
medium vane	height	0.060	m
	diameter	0.025	m

Vane dimensions :			
small vane	height	0.022	m
	diameter	0.016	m

File name :	**Fredre21**
Sample description :	Co-disposed tails pH 8.6 (86:14)

Rheometer settings :

speed	0.3	rpm
data points	400	
duration	120	sec

Material characteristics :

Type	Vehicle	Load	
Solids SG	2.41	2.59	g/cm^3

Type	Co-disposed tails
pH	8.6
vehicle : load	86:14

dry solids mass basis

Test number	Description	Pan no.	Pan mass (g)	Start mass (g)	Wet mass (g)	End mass (g)	Dry mass (g)	% solids (%)	Density (kg/l)	Dilution (ml)	Vehicle volume (litre)	Load mass (kg)
Vehicle starting point		22	27.136	35.5490	8.4130	32.7620	5.6260	66.8727	1.6427	0	0.4300	0.0785
		23	23.826	32.3240	8.4980	29.5140	5.6880	66.9334	1.6437			
		33	27.593	37.9760	10.3830	34.5450	6.9520	66.9556	1.6440			
								66.9206	***1.6435***			

from Dilution sheet

		Dry solids Vehicle mass (kg)	Dry solids Load mass (kg)		Dry solids Vehicle mass %	Dry solids Load mass %
		0.4729	**0.0785**		**85.8**	**14.2**

Test number	Description	Dilution (ml)	Vehicle volume (litre)	Vehicle % solids (%)	Vehicle density (kg/l)	Vehicle mass (kg)	Load mass (kg)	Co-disposed mass (kg)	New vehicle mass %	New load mass %	Load volume (litre)	Co-disposed volume (litre)	Co-disposed density (kg/l)	Co-disposed SG (kg/l)	Co-disposed % solids	Max Torque (mNm)	Yield stress (Pa)	
Test 2	Rep 1	0	0.4300	66.9206	1.6435	0.7067	**0.0785**	0.7852	90.0000	10.0000	0.0303	0.4603	1.7058	2.4280	70.35	8.8700		
Test 3	Rep 2															10.6000		
Test 5	Rep 3															10.7000		
																10.06	***914.96***	small vane
Test 6	Rep 1	10	0.4400	65.9869	1.6288	0.7167	**0.0785**	0.7952	90.1258	9.8742	0.0303	0.4703	1.6908	2.4278	69.47	43.6000		
Test 7	Rep 2															47.0000		
Test 8	Rep 3															44.5000		
																45.03	***671.28***	medium vane
Test 9	Rep 1	12	0.4520	64.9002	1.6121	0.7287	**0.0785**	0.8072	90.2725	9.7275	0.0303	0.4823	1.6736	2.4275	68.44	30.3000		
Test 10	Rep 2															33.4000		
Test 12	Rep 3															33.7000		
																32.47	***483.96***	medium vane
Test 13	Rep 1	11	0.4630	63.9351	1.5976	0.7397	**0.0785**	0.8182	90.4033	9.5967	0.0303	0.4933	1.6586	2.4273	67.53	26.0000		
Test 14	Rep 2															26.1000		
Test 15	Rep 3															25.7000		
																25.93	***386.57***	medium vane
Test 16	Rep 1	13	0.4760	62.8308	1.5813	0.7527	**0.0785**	0.8312	90.5534	9.4466	0.0303	0.5063	1.6417	2.4270	66.48	19.0000		
Test 17	Rep 2															18.1000		
Test 18	Rep 3															18.5000		
																18.53	***276.26***	medium vane
Test 19	Rep 1	14	0.4900	61.6835	1.5647	0.7667	**0.0785**	0.8452	90.7099	9.2901	0.0303	0.5203	1.6244	2.4267	65.38	13.1000		
Test 20	Rep 2															13.5000		
Test 21	Rep 3															13.2000		
																13.27	***197.76***	medium vane
Test 22	Rep 1	15	0.5050	60.4998	1.5479	0.7817	**0.0785**	0.8602	90.8719	9.1281	0.0303	0.5353	1.6069	2.4264	64.25	9.6100		
Test 23	Rep 2															9.7700		
Test 24	Rep 3															9.2100		
																9.53	***142.06***	medium vane
Test 25	Rep 1	15	0.5200	59.3607	1.5321	0.7967	**0.0785**	0.8752	91.0283	8.9717	0.0303	0.5503	1.5904	2.4261	63.15	6.6800		
Test 26	Rep 2															6.8800		
Test 27	Rep 3															6.9000		
																6.82	***101.66***	medium vane
Test 28	Rep 1	17	0.5370	58.1205	1.5152	0.8137	**0.0785**	0.8922	91.1993	8.8007	0.0303	0.5673	1.5727	2.4258	61.95	4.4200		
Test 29	Rep 2															5.0400		
Test 30	Rep 3															4.7400		
																4.73	***70.56***	medium vane

Co-disposed Tailings - Slump tests

pH = 8.6

vehicle (wet) : load (dry) = 90:10

vehicle (dry) : load (dry) = 86:14

Date : 18/05/2004

Slump cylinder : small cylinder

height	0.130	m
diameter	0.105	m
aspect ratio	1.24	
ruler thickness	9	mm

Material characteristics :

Type	Vehicle	Load	
Solids SG	2.41	2.59	g/cm^3

Type	Co-disposed tails
pH	8.6
vehicle : load	86:14

dry solids mass basis

Test number	Description	Pan no.	Pan mass (g)	Start mass (g)	Wet mass (g)	End mass (g)	Dry mass (g)	% solids (%)	Density (kg/l)	Dilution (ml)	Vehicle volume (litre)	Load mass (kg)
Vehicle starting point		8	24.768	42.8460	18.0780	36.8240	12.0560	66.6888	1.6398	0	1.5000	0.2733
		22	24.438	36.0070	11.5690	32.1570	7.7190	66.7214	1.6403			
		25	24.365	41.2550	16.8900	35.6200	11.2550	66.6371	1.6390			
								66.6824	***1.6397***			

	Dry solids Vehicle mass (kg)	Dry solids Load mass (kg)
from Dilution sheet	**1.6401**	**0.2733**

	Dry solids Vehicle mass %	Dry solids Load mass %
	85.7	**14.3**

Test number	Description	Dilution (ml)	Vehicle volume (litre)	Vehicle % solids (%)	Vehicle density (kg/l)	Vehicle mass (kg)	Load mass (kg)	Co-disposed mass (kg)	New vehicle mass %	New load mass %	Load volume (litre)	Co-disposed volume (litre)	Co-disposed density (kg/l)	Co-disposed SG (kg/l)	Co-disposed % solids	Slump height incl ruler (mm)	Slump height excl ruler (mm)	Yield stress (Pa)	Flow distance N	Flow distance S	Flow distance E	Flow distance W	Flow distance radius (mm) N	Flow distance radius (mm) S	Flow distance radius (mm) E	Flow distance radius (mm) W	*average*
Test 1	Rep 1	30	1.5300	65.8789	1.6272	2.4896	**0.2733**	2.7628	90.1086	9.8914	0.1055	1.6355	1.6893	2.4278	69.38	42.20	33.20		0 start	1 mid	0 mid	1 start	55.56	70.68	60.38	65.64	63.07
	Rep 2															40.70	31.70		0 start	1 mid	0 mid	1 start	55.56	70.68	60.38	65.64	63.07
	Rep 3															43.60	34.60		0 mid	0 mid	0 start	1 start	60.38	60.38	55.56	65.64	60.49
																	33.17	**533.81**									**62.21**
Test 2	Rep 1	40	1.5700	64.8372	1.6112	2.5296	**0.2733**	2.8028	90.2498	9.7502	0.1055	1.6755	1.6728	2.4276	68.40	52.05	43.05		1 start	1 mid	1 mid	1 mid	65.64	70.68	70.68	70.68	69.42
	Rep 2															53.80	44.80		0 mid	2 start	0 mid	2 mid	60.38	75.76	60.38	80.73	69.31
	Rep 3															52.10	43.10		0 mid	2 mid	1 start	1 mid	60.38	80.73	65.64	70.68	69.36
																	43.65	**449.26**									**69.36**
Test 3	Rep 1	40	1.6100	63.8279	1.5960	2.5696	**0.2733**	2.8428	90.3869	9.6131	0.1055	1.7155	1.6571	2.4273	67.44	57.90	48.90		1 mid	2 mid	2 start	2 start	70.68	80.73	75.76	75.76	75.73
	Rep 2															57.20	48.20		1 mid	2 mid	1 mid	2 mid	70.68	80.73	70.68	80.73	75.71
	Rep 3															59.00	50.00		1 mid	2 start	2 start	2 start	70.68	75.76	75.76	75.76	74.49
																	49.03	**408.37**									**75.31**
Test 4	Rep 1	45	1.6550	62.7293	1.5798	2.6146	**0.2733**	2.8878	90.5367	9.4633	0.1055	1.7605	1.6403	2.4270	66.39	67.45	58.45		2 mid	3 mid	3 start	3 mid	80.73	90.38	85.73	90.38	86.81
	Rep 2															68.35	59.35		2 mid	3 mid	2 start	4 start	80.73	90.38	75.76	95.76	85.66
	Rep 3															69.40	60.40		2 mid	3 start	3 start	3 mid	80.73	85.73	85.73	90.38	85.64
																	59.40	**339.55**									**86.04**
Test 5	Rep 1	50	1.7050	61.5522	1.5628	2.6646	**0.2733**	2.9378	90.6978	9.3022	0.1055	1.8105	1.6227	2.4267	65.27	80.10	71.10		4 mid	5 mid	5 start	5 mid	100.8	111.13	105.8	111.1	107.21
	Rep 2															80.40	71.40		4 mid	5 start	5 start	5 mid	100.8	105.8	105.8	111.1	105.88
	Rep 3															81.70	72.70		4 mid	5 start	4 mid	5 mid	100.8	105.8	100.8	111.1	104.62
																	71.73	**266.67**									**105.90**
Test 6	Rep 1	50	1.7550	60.4185	1.5468	2.7146	**0.2733**	2.9878	90.8535	9.1465	0.1055	1.8605	1.6059	2.4265	64.18	94.15	85.15		5 mid	6 mid	6 mid	6 mid	111.1	120.65	120.7	120.7	118.27
	Rep 2															91.00	82.00		6 mid	5 mid	6 mid	6 mid	120.7	111.13	120.7	120.7	118.27
	Rep 3															93.55	84.55		6 mid	6 start	6 mid	7 start	120.7	115.86	120.7	125.8	120.73
																	83.90	**201.91**									**119.09**
Test 7	Rep 1	55	1.8100	59.2187	1.5301	2.7696	**0.2733**	3.0428	91.0188	8.9812	0.1055	1.9155	1.5885	2.4262	63.03	108.00	99.00		7 mid	7 mid	9 start	8 mid	130.8	130.83	145.7	140.4	136.94
	Rep 2															108.70	99.70		7 mid	8 start	8 mid	8 mid	130.8	135.83	140.4	140.4	136.86
	Rep 3															107.35	98.35		7 mid	8 mid	8 mid	8 mid	130.8	140.38	140.4	140.4	137.99
																	99.02	**129.42**									**137.26**
Test 8	Rep 1	55	1.8650	57.9630	1.5131	2.8220	**0.2733**	3.0953	91.1709	8.8291	0.1055	1.9705	1.5708	2.4259	61.82	121.00	112.00		11 start	11 mid	11 mid	11 mid	164.9	169.96	170	170	168.69
	Rep 2																										
	Rep 3																										
																	112.00	**72.41**									**168.69**

Co-disposed Tailings - Vane tests

pH = 8.6
vehicle (wet) : load (dry) = 70:30
vehicle (dry) : load (dry) = 61:39

Date : 11/05/2004

Vane dimensions :			
medium vane	height	0.060	m
	diameter	0.025	m

Vane dimensions :			
small vane	height	0.022	m
	diameter	0.016	m

Rheometer settings :			
	speed	0.3	rpm
	data points	400	
	duration	120	sec

Material characteristics :			
	Type	Vehicle	Load
	Solids SG	2.41	2.59

File name :	**Fredre20**
Sample description :	Co-disposed tails pH 8.6 (61:39)

Type	Co-disposed tails
pH	8.6
vehicle : load	61:39

dry solids mass basis

Test number	Description	Pan no.	Pan mass (g)	Start mass (g)	Wet mass (g)	End mass (g)	Dry mass (g)	% solids (%)	Density (kg/l)	Dilution (ml)	Vehicle volume (litre)	Load mass (kg)
Vehicle starting point		22	27.136	35.5490	8.4130	32.7620	5.6260	66.8727	1.6427	0	0.4000	0.2817
		23	23.826	32.3240	8.4980	29.5140	5.6880	66.9334	1.6437			
		33	27.593	37.9760	10.3830	34.5450	6.9520	66.9556	1.6440			
								66.9206	***1.6435***			

						Dry solids Vehicle mass (kg)	Dry solids Load mass (kg)		Dry solids Vehicle mass %	Dry solids Load mass %							
				from Dilution sheet		**0.4399**	**0.2817**		**61.0**	**39.0**							
Test number	Description	Dilution (ml)	Vehicle volume (litre)	Vehicle % solids (%)	Vehicle density (kg/l)	Vehicle mass (kg)	Load mass (kg)	Co-disposed mass (kg)	New vehicle mass %	New load mass %	Load volume (litre)	Co-disposed volume (litre)	Co-disposed density (kg/l)	Co-disposed SG (kg/l)	Co-disposed % solids	Max Torque (mNm)	Yield stress (Pa)	
Test 10	Rep 1	20	0.4200	64.9448	1.6128	0.6774	**0.2817**	0.9591	70.6256	29.3744	0.1088	0.5288	1.8138	2.4629	75.54	10.9000		
Test 11	Rep 2															11.8000		
Test 12	Rep 3															9.7100		
																10.80	***982.89***	small vane
Test 15	Rep 1	12	0.4320	63.8143	1.5958	0.6894	**0.2817**	0.9711	70.9886	29.0114	0.1088	0.5408	1.7958	2.4622	74.62	44.1000		
Test 16	Rep 2															41.9000		
Test 18	Rep 3															43.7000		
																43.23	***644.45***	medium vane
Test 19	Rep 1	13	0.4450	62.6332	1.5784	0.7024	**0.2817**	0.9841	71.3718	28.6282	0.1088	0.5538	1.7771	2.4615	73.65	29.4000		
Test 20	Rep 2															35.4000		
Test 22	Rep 3															33.1000		
																32.63	***486.44***	medium vane
Test 23	Rep 1	13	0.4580	61.4950	1.5620	0.7154	**0.2817**	0.9971	71.7450	28.2550	0.1088	0.5668	1.7593	2.4609	72.70	25.8000		
Test 24	Rep 2															27.2000		
Test 25	Rep 3															27.7000		
																26.90	***400.98***	medium vane
Test 26	Rep 1	13	0.4710	60.3975	1.5465	0.7284	**0.2817**	1.0101	72.1087	27.8913	0.1088	0.5798	1.7423	2.4602	71.78	20.0000		
Test 27	Rep 2															18.8000		
Test 28	Rep 3															19.5000		
																19.43	***289.68***	medium vane
Test 29	Rep 1	14	0.4850	59.2585	1.5307	0.7424	**0.2817**	1.0241	72.4900	27.5100	0.1088	0.5938	1.7248	2.4595	70.81	13.9000		
Test 30	Rep 2															14.3000		
Test 31	Rep 3															15.1000		
																14.43	***215.15***	medium vane
Test 32	Rep 1	15	0.5000	58.0849	1.5148	0.7574	**0.2817**	1.0391	72.8871	27.1129	0.1088	0.6088	1.7069	2.4588	69.80	9.7600		
Test 33	Rep 2															11.4000		
Test 34	Rep 3															12.9000		
																11.35	***169.24***	medium vane
Test 35	Rep 1	20	0.5200	56.5905	1.4950	0.7774	**0.2817**	1.0591	73.3991	26.6009	0.1088	0.6288	1.6844	2.4579	68.50	7.3600		
Test 36	Rep 2															7.2400		
Test 37	Rep 3															6.0100		
																6.87	***102.41***	medium vane

Co-disposed Tailings - Slump tests

pH = 8.6

vehicle (wet) : load (dry) = 70:30

vehicle (dry) : load (dry) = 61:39

Date : 19/05/2004

Slump cylinder : small cylinder

height	0.130	m
diameter	0.105	m
aspect ratio	1.24	
ruler thickness	9	mm

Material characteristics :

Type	Vehicle	Load	
Solids SG	2.41	2.59	g/cm^3

Type	Co-disposed tails
pH	8.6
vehicle : load	61:39

dry solids mass basis

Test number	Description	Pan no.	Pan mass (g)	Start mass (g)	Wet mass (g)	End mass (g)	Dry mass (g)	% solids (%)	Density (kg/l)	Dilution (ml)	Vehicle volume (litre)	Load mass (kg)
Vehicle starting point		8	24.768	42.8460	18.0780	36.8240	12.0560	66.6888	1.6398	0	1.3000	0.9135
		22	24.438	36.0070	11.5690	32.1570	7.7190	66.7214	1.6403			
		25	24.365	41.2550	16.8900	35.6200	11.2550	66.6371	1.6390			
								66.6824	***1.6397***			

	Dry solids Vehicle mass (kg)	Dry solids Load mass (kg)		Dry solids Vehicle mass %	Dry solids Load mass %
from Dilution sheet	**1.4214**	**0.9135**		**60.9**	**39.1**

Test number	Description	Dilution (ml)	Vehicle volume (litre)	Vehicle % solids (%)	Vehicle density (kg/l)	Vehicle mass (kg)	Load mass (kg)	Co-disposed mass (kg)	New vehicle mass %	New load mass %	Load volume (litre)	Co-disposed volume (litre)	Co-disposed density (kg/l)	Co-disposed SG (kg/l)	Co-disposed % solids	Slump height incl ruler (mm)	Slump height excl ruler (mm)	Yield stress (Pa)	Flow distance N	Flow distance S	Flow distance E	Flow distance W	Flow distance radius (mm) N	Flow distance radius (mm) S	Flow distance radius (mm) E	Flow distance radius (mm) W	*average*
Test 1	Rep 1	30	1.3300	65.7569	1.6253	2.1616	**0.9135**	3.0752	70.2927	29.7073	0.3527	1.6827	1.8275	2.4635	76.22	27.20	18.20		0 start	0 mid	0 start	0 mid	55.56	60.38	55.56	60.38	57.97
	Rep 2															28.30	19.30		0 start	0 start	0 start	0 mid	55.56	55.56	55.56	60.38	56.77
	Rep 3															28.00	19.00		0 start	0 mid	0 start	0 mid	55.56	60.38	55.56	60.38	57.97
																	18.83	***722.61***									**57.57**
Test 2	Rep 1	35	1.3650	64.7092	1.6092	2.1966	**0.9135**	3.1102	70.6270	29.3730	0.3527	1.7177	1.8106	2.4629	75.38	37.55	28.55		0 start	1 start	0 mid	1 start	55.56	65.64	60.38	65.64	61.81
	Rep 2															37.70	28.70		0 start	1 start	0 mid	0 mid	55.56	65.64	60.38	60.38	60.49
	Rep 3															38.00	29.00		0 start	1 start	0 mid	1 start	55.56	65.64	60.38	65.64	61.81
																	28.75	***612.39***									**61.37**
Test 3	Rep 1	40	1.4050	63.5519	1.5919	2.2366	**0.9135**	3.1502	70.9999	29.0001	0.3527	1.7577	1.7922	2.4622	74.43	47.10	38.10		1 start	1 mid	0 mid	1 mid	65.64	70.68	60.38	70.68	66.85
	Rep 2															49.70	40.70		0 mid	1 mid	1 start	1 mid	60.38	70.68	65.64	70.68	66.85
	Rep 3															46.10	37.10		0 mid	1 mid	1 start	1 start	60.38	70.68	65.64	65.64	65.59
																	38.63	***520.55***									**66.43**
Test 4	Rep 1	40	1.4450	62.4353	1.5755	2.2766	**0.9135**	3.1902	71.3636	28.6364	0.3527	1.7977	1.7746	2.4615	73.51	57.60	48.60		1 mid	2 start	1 mid	2 mid	70.68	75.76	70.68	80.73	74.46
	Rep 2															58.00	49.00		1 mid	2 mid	1 mid	2 mid	70.68	80.73	70.68	80.73	75.71
	Rep 3															58.50	49.50		1 mid	2 mid	2 start	2 start	70.68	80.73	75.76	75.76	75.73
																	49.03	***437.31***									**75.30**
Test 5	Rep 1	45	1.4900	61.2251	1.5581	2.3216	**0.9135**	3.2352	71.7619	28.2381	0.3527	1.8427	1.7556	2.4608	72.50	68.60	59.60		3 start	4 start	4 mid	3 start	85.73	95.76	100.78	85.73	92.00
	Rep 2															68.65	59.65		2 mid	3 mid	3 start	3 mid	80.73	90.38	85.73	90.38	86.81
	Rep 3															68.30	59.30		2 mid	3 start	3 mid	2 mid	80.73	85.73	90.38	80.73	84.39
																	59.52	***362.68***									**87.73**
Test 6	Rep 1	45	1.5350	60.0609	1.5418	2.3666	**0.9135**	3.2802	72.1493	27.8507	0.3527	1.8877	1.7376	2.4601	71.52	82.70	73.70		5 start	4 mid	5 start	5 mid	105.8	100.78	105.8	111.13	105.88
	Rep 2															81.90	72.90		4 start	5 mid	4 mid	5 mid	95.76	111.13	100.78	111.13	104.70
	Rep 3															79.10	70.10		4 mid	4 mid	4 mid	4 mid	100.78	100.78	100.78	100.78	100.78
																	72.23	***282.71***									**103.79**
Test 7	Rep 1	50	1.5850	58.8182	1.5247	2.4166	**0.9135**	3.3302	72.5674	27.4326	0.3527	1.9377	1.7186	2.4594	70.46	96.80	87.80		6 mid	6 mid	7 start	7 start	120.65	120.65	125.76	125.76	123.21
	Rep 2															100.70	91.70		6 start	6 mid	6 mid	6 mid	115.86	120.65	120.65	120.65	119.45
	Rep 3															100.40	91.40		6 start	6 mid	6 mid	6 mid	115.86	120.65	120.65	120.65	119.45
																	90.30	***183.11***									**120.70**
Test 8	Rep 1	55	1.6400	57.5093	1.5071	2.4716	**0.9135**	3.3852	73.0131	26.9869	0.3527	1.9927	1.6988	2.4586	69.33	103.00	94.00		8 mid	7 start	8 mid	7 mid	140.38	125.76	140.38	130.83	134.34
	Rep 2															106.00	106.0		7 mid	7 mid	8 start	8 start	130.83	130.83	135.83	135.83	133.33
	Rep 3															104.70	104.7		7 mid	7 mid	8 start	7 mid	130.83	130.83	135.83	130.83	132.08
																	101.57	***126.30***									**133.25**

Co-disposed Tailings - Vane tests

pH = 8.6
vehicle (wet) : load (dry) = 60:40
vehicle (dry) : load (dry) = 50:50

Date : 13/05/2004

Vane dimensions : medium vane			
height	0.060	m
diameter	0.025	m

Vane dimensions : small vane			
height	0.022	m
diameter	0.016	m

File name :	**Fredre22**
Sample description :	Co-disposed tails pH 8.6 (50:50)

Rheometer settings :

speed	0.3	rpm
data points	400	
duration	120	sec

Material characteristics :

Type	Vehicle	Load	
Solids SG	2.41	2.59	g/cm^3

Type	Co-disposed tails
pH	8.6
vehicle : load	50:50 dry solids mass basis

Test number	Description	Pan no.	Pan mass (g)	Start mass (g)	Wet mass (g)	End mass (g)	Dry mass (g)	% solids (%)	Density (kg/l)	Dilution (ml)	Vehicle volume (litre)	Load mass (kg)
Vehicle starting point		22	27.136	35.5490	8.4130	32.7620	5.6260	66.8727	1.6427	0	0.3500	0.3835
		23	23.826	32.3240	8.4980	29.5140	5.6880	66.9334	1.6437			
		33	27.593	37.9760	10.3830	34.5450	6.9520	66.9556	1.6440			
								66.9206	***1.6435***			

						Dry solids Vehicle mass (kg)	Dry solids Load mass (kg)		Dry solids Vehicle mass %	Dry solids Load mass %							
				from Dilution sheet		**0.3849**	**0.3835**		**50.1**	**49.9**							
Test number	Description	Dilution (ml)	Vehicle volume (litre)	Vehicle % solids (%)	Vehicle density (kg/l)	Vehicle mass (kg)	Load mass (kg)	Co-disposed mass (kg)	New vehicle mass %	New load mass %	Load volume (litre)	Co-disposed volume (litre)	Co-disposed density (kg/l)	Co-disposed SG (kg/l)	Co-disposed % solids	Max Torque (mNm)	Yield stress (Pa)	
Test 15	Rep 1	36	0.3860	62.9790	1.5834	0.6112	**0.3835**	0.9947	61.4477	38.5523	0.1481	0.5341	1.8625	2.4794	77.61	9.3400		
Test 16	Rep 2															11.4000		
Test 17	Rep 3															12.4000		
																11.05	***1005.03***	small vane
Test 20	Rep 1	13	0.3990	61.6674	1.5644	0.6242	**0.3835**	1.0077	61.9451	38.0549	0.1481	0.5471	1.8420	2.4785	76.63	40.3000		
Test 21	Rep 2															41.4000		
Test 22	Rep 3															42.3000		
																41.33	***616.12***	medium vane
Test 23	Rep 1	14	0.4130	60.3146	1.5453	0.6382	**0.3835**	1.0217	62.4665	37.5335	0.1481	0.5611	1.8210	2.4776	75.60	26.7000		
Test 24	Rep 2															28.4000		
Test 25	Rep 3															27.9000		
																27.67	***412.41***	medium vane
Test 26	Rep 1	15	0.4280	58.9296	1.5262	0.6532	**0.3835**	1.0367	63.0096	36.9904	0.1481	0.5761	1.7996	2.4766	74.52	23.4000		
Test 28	Rep 2															24.000		
Test 29	Rep 3															25.5000		
																24.30	***362.22***	medium vane
Test 30	Rep 1	17	0.4450	57.4348	1.5061	0.6702	**0.3835**	1.0537	63.6064	36.3936	0.1481	0.5931	1.7767	2.4755	73.34	18.2000		
Test 31	Rep 2															17.6000		
Test 32	Rep 3															18.4000		
																18.07	***269.31***	medium vane
Test 33	Rep 1	20	0.4650	55.7705	1.4843	0.6902	**0.3835**	1.0737	64.2843	35.7157	0.1481	0.6131	1.7514	2.4743	72.00	10.8000		
Test 34	Rep 2															11.7000		
Test 35	Rep 3															11.1000		
																11.20	***166.95***	medium vane
Test 36	Rep 1	18	0.4830	54.3530	1.4663	0.7082	**0.3835**	1.0917	64.8732	35.1268	0.1481	0.6311	1.7299	2.4732	70.83	7.3900		
Test 37	Rep 2															6.6500		
Test 38	Rep 3															7.7200		
																7.25	***108.12***	medium vane

Co-disposed Tailings - Slump tests

pH = 8.6

vehicle (wet) : load (dry) = 60:40

vehicle (dry) : load (dry) = 51:49

Date : 27/05/2003

Slump cylinder : small cylinder

height	0.130	m
diameter	0.105	m
aspect ratio	1.24	
ruler thickness	9	mm

Material characteristics :

Type	Vehicle	Load	
Solids SG	2.41	2.59	g/cm^3

Type	Co-disposed tails
pH	8.6
vehicle : load	51:49

dry solids mass basis

Test number	Description	Pan no.	Pan mass (g)	Start mass (g)	Wet mass (g)	End mass (g)	Dry mass (g)	% solids (%)	Density (kg/l)	Dilution (ml)	Vehicle volume (litre)	Load mass (kg)
Vehicle starting point		22	24.432	38.7830	14.3510	34.3630	9.9310	69.2008	1.6803	0	1.1000	1.2326
		17	25.251	40.7490	15.4980	35.9860	10.7350	69.2670	1.6814			
								69.2339	***1.6808***			

from Dilution sheet

						Dry solids Vehicle mass (kg)	Dry solids Load mass (kg)		Dry solids Vehicle mass %	Dry solids Load mass %																
						1.2801	**1.2326**		**50.9**	**49.1**																
Test number	Description	Dilution (ml)	Vehicle volume (litre)	Vehicle % solids (%)	Vehicle density (kg/l)	Vehicle mass (kg)	Load mass (kg)	Co-disposed mass (kg)	New vehicle mass %	New load mass %	Load volume (litre)	Co-disposed volume (litre)	Co-disposed density (kg/l)	Co-disposed SG (kg/l)	Co-disposed % solids	Slump height incl ruler (mm)	Slump height excl ruler (mm)	Yield stress (Pa)	Flow distance N	Flow distance S	Flow distance E	Flow distance W	Flow distance radius (mm) N	Flow distance radius (mm) S	Flow distance radius (mm) E	Flow distance radius (mm) W	average
Test 1	Rep 1	105	1.2050	65.5134	1.6215	1.9539	**1.2326**	3.1866	61.3180	38.6820	0.4759	1.6809	1.8957	2.4796	79.18	23.30	14.30		0 start	0 start	0 start	0 start	55.56	55.56	55.56	55.56	55.56
	Rep 2															20.35	11.35		0 start	0 start	0 start	0 start	55.56	55.56	55.56	55.56	55.56
	Rep 3															18.70	9.70		0 start	0 start	0 start	0 mid	55.56	55.56	55.56	60.38	56.77
																	11.78	***845.80***									**55.96**
Test 2	Rep 1	40	1.2450	64.1991	1.6016	1.9939	**1.2326**	3.2265	61.7976	38.2024	0.4759	1.7209	1.8749	2.4788	78.22	31.80	22.80		0 mid	0 mid	0 mid	0 mid	60.38	60.38	60.38	60.38	60.38
	Rep 2															30.70	21.70		0 start	1 start	0 mid	0 mid	55.56	65.64	60.38	60.38	60.49
	Rep 3															27.20	18.20		0 start	0 mid	0 mid	0 mid	55.56	60.38	60.38	60.38	59.18
																	20.90	***717.03***									**60.02**
Test 3	Rep 1	45	1.2900	62.7822	1.5806	2.0389	**1.2326**	3.2715	62.3230	37.6770	0.4759	1.7659	1.8526	2.4778	77.16	40.75	31.75		0 mid	2 start	1 start	1 mid	60.38	75.76	65.64	70.68	68.12
	Rep 2															43.30	34.30		0 mid	1 mid	0 mid	1 mid	60.38	70.68	60.38	70.68	65.53
	Rep 3															43.60	34.60		0 mid	1 mid	0 mid	1 mid	60.38	70.68	60.38	70.68	65.53
																	33.55	***581.98***									**66.39**
Test 4	Rep 1	45	1.3350	61.4265	1.5610	2.0839	**1.2326**	3.3165	62.8343	37.1657	0.4759	1.8109	1.8314	2.4769	76.14	54.40	45.40		1 mid	2 mid	1 mid	2 mid	70.68	80.73	70.68	80.73	75.71
	Rep 2															60.90	51.90		1 mid	2 mid	1 mid	2 mid	70.68	80.73	70.68	80.73	75.71
	Rep 3															57.70	48.70		1 mid	2 mid	1 mid	2 mid	70.68	80.73	70.68	80.73	75.71
																	48.67	***454.01***									**75.71**
Test 5	Rep 1	50	1.3850	59.9872	1.5407	2.1339	**1.2326**	3.3665	63.3862	36.6138	0.4759	1.8609	1.8091	2.4759	75.03	66.00	57.00		2 mid	4 mid	3 mid	4 mid	80.73	100.8	90.38	100.78	93.17
	Rep 2															68.80	59.80		3 mid	3 mid	3 start	3 mid	90.38	90.38	85.73	90.38	89.22
	Rep 3															70.07	61.07		3 start	3 mid	3 start	3 mid	85.73	90.38	85.73	90.38	88.06
																	59.29	***375.21***									**90.15**
Test 6	Rep 1	50	1.4350	58.6138	1.5219	2.1839	**1.2326**	3.4165	63.9221	36.0779	0.4759	1.9109	1.7879	2.4749	73.95	82.75	73.75		4 mid	5 mid	5 start	5 mid	100.8	111.1	105.8	111.13	107.21
	Rep 2															84.65	75.65		4 mid	5 mid	5 start	5 start	100.8	111.1	105.8	105.8	105.88
	Rep 3															86.80	77.80		4 mid	5 start	4 mid	5 mid	100.8	105.8	100.8	111.13	104.62
																	75.73	***270.53***									**105.90**
Test 7	Rep 1	55	1.4900	57.1739	1.5026	2.2389	**1.2326**	3.4715	64.4937	35.5063	0.4759	1.9659	1.7659	2.4739	72.80	100.65	91.65		6 mid	6 mid	7 start	7 mid	120.7	120.7	125.8	130.83	124.47
	Rep 2															98.35	89.35		6 start	7 start	6 mid	7 mid	115.9	125.8	120.7	130.83	123.28
	Rep 3															99.30	90.30		6 mid	6 mid	7 start	6 mid	120.7	120.7	125.8	120.65	121.93
																	90.43	***187.45***									**123.23**
Test 8	Rep 1	55	1.5450	55.8031	1.4847	2.2939	**1.2326**	3.5265	65.0474	34.9526	0.4759	2.0209	1.7450	2.4729	71.68	106.30	97.30		7 mid	10 start	8 mid	10 mid	130.8	155	140.4	160.56	146.70
	Rep 2															112.20	103.20		8 mid	8 mid	8 mid	9 mid	140.4	140.4	140.4	150.5	142.91
	Rep 3															113.60	104.60		9 start	8 start	8 mid	9 start	145.7	135.8	140.4	145.71	141.91
																	101.70	***129.10***									**143.84**

Co-disposed Tailings - Vane tests

pH = 6.2
vehicle (wet) : load (dry) = 90:10
vehicle (dry) : load (dry) = 86:14

Date : 21/05/2004

Vane dimensions : medium vane			
height	0.060	m
diameter	0.025	m

Vane dimensions : small vane			
height	0.022	m
diameter	0.016	m

File name :	Fredre23
Sample description :	Co-disposed tails pH 6.2 (86:14)

Rheometer settings :

speed	0.3	rpm
data points	400	
duration	120	sec

Material characteristics :

Type	Vehicle	Load	
Solids SG	2.41	2.59	g/cm^3

Type	Co-disposed tails
pH	6.2
vehicle : load	86:14

dry solids mass basis

Test number	Description	Pan no.	Pan mass (g)	Start mass (g)	Wet mass (g)	End mass (g)	Dry mass (g)	% solids (%)	Density (kg/l)	Dilution (ml)	Vehicle volume (litre)	Load mass (kg)
Vehicle starting point		8	24.768	42.8460	18.0780	36.8240	12.0560	66.6888	1.6398	0	0.4100	0.0747
		22	24.438	36.0070	11.5690	32.1570	7.7190	66.7214	1.6403			
		25	24.365	41.2550	16.8900	35.6200	11.2550	66.6371	1.6390			
								66.6824	***1.6397***			

						Dry solids Vehicle mass (kg)	Dry solids Load mass (kg)		Dry solids Vehicle mass %	Dry solids Load mass %									
				from Dilution sheet		**0.4483**	**0.0747**		**85.7**	**14.3**									
Test number	Description	Dilution (ml)	Vehicle volume (litre)	Vehicle % solids (%)	Vehicle density (kg/l)	Vehicle mass (kg)	Load mass (kg)	Co-disposed mass (kg)	New vehicle mass %	New load mass %	Load volume (litre)	Co-disposed volume (litre)	Co-disposed density (kg/l)	Co-disposed SG (kg/l)	Co-disposed % solids	Max Torque (mNm)	Yield stress (Pa)	pH before	pH after	pH ave	
Test 2	Rep 1	43 acid	0.4530	62.6737	1.5790	0.7153	**0.0747**	0.7900	90.5443	9.4557	0.0288	0.4818	1.6395	2.4270	66.34	24.8000		6.11	6.64	6.38	medium vane
Test 3	Rep 2															26.4000					
Test 4	Rep 3															28.1000					
																26.43	***394.02***				
Test 5	Rep 1	12 acid	0.4650	61.6396	1.5640	0.7273	**0.0747**	0.8020	90.6858	9.3142	0.0288	0.4938	1.6240	2.4268	65.35	20.9000		6.04	6.43	6.24	medium vane
Test 6	Rep 2															21.0000					
Test 7	Rep 3															21.7000					
																21.20	***316.01***				
Test 8	Rep 1	9 acid	0.4780	60.5571	1.5487	0.7403	**0.0747**	0.8150	90.8344	9.1656	0.0288	0.5068	1.6080	2.4265	64.31	15.7000		6.14	6.47	6.31	medium vane
Test 9	Rep 2	4 water														16.5000					
Test 10	Rep 3															16.2000					
																16.13	***240.49***				
Test 11	Rep 1	6 acid	0.4880	59.7500	1.5375	0.7503	**0.0747**	0.8250	90.9455	9.0545	0.0288	0.5168	1.5962	2.4263	63.54	13.4000		6.14	6.33	6.24	medium vane
Test 12	Rep 2	4 water														13.1000					
Test 13	Rep 3															12.9000					
																13.13	***195.77***				
Test 14	Rep 1	5 acid	0.4990	58.8866	1.5256	0.7613	**0.0747**	0.8360	91.0646	8.9354	0.0288	0.5278	1.5838	2.4261	62.71	10.2000		6.10	6.25	6.18	medium vane
Test 15	Rep 2	6 water														10.2000					
Test 16	Rep 3															10.1000					
																10.17	***151.55***				
Test 17	Rep 1	4 acid	0.5110	57.9728	1.5133	0.7733	**0.0747**	0.8480	91.1911	8.8089	0.0288	0.5398	1.5708	2.4259	61.82	8.5100		6.11	6.26	6.19	medium vane
Test 18	Rep 2	8 water														8.5600					
Test 19	Rep 3															8.5000					
																8.52	***127.05***				
Test 20	Rep 1	4 acid	0.5250	56.9419	1.4996	0.7873	**0.0747**	0.8620	91.3341	8.6659	0.0288	0.5538	1.5564	2.4256	60.82	6.8300		6.11	6.25	6.18	medium vane
Test 21	Rep 2	10 water														6.5600					
Test 22	Rep 3															6.8600					
																6.75	***100.62***				
Test 23	Rep 1	4 acid	0.5410	55.8077	1.4848	0.8033	**0.0747**	0.8780	91.4921	8.5079	0.0288	0.5698	1.5407	2.4253	59.72	5.0300		6.03	6.21	6.12	medium vane
Test 24	Rep 2	12 water														5.0500					
Test 25	Rep 3															4.8800					
																4.99	***74.33***				

Ave. pH *6.23*

Co-disposed Tailings - Slump tests

pH = 6.3

vehicle (wet) : load (dry) = 90:10

vehicle (dry) : load (dry) = 86:14

Date : 01/06/2004

Slump cylinder : small cylinder

height	0.130	m
diameter	0.105	m
aspect ratio	1.24	
ruler thickness	9	mm

Material characteristics :

Type	Vehicle	Load	
Solids SG	2.41	2.59	g/cm^3

Type	Co-disposed tails
pH	6.3
vehicle : load	86:14

dry solids mass basis

Test number	Description	Pan no.	Pan mass (g)	Start mass (g)	Wet mass (g)	End mass (g)	Dry mass (g)	% solids (%)	Density (kg/l)	Dilution (ml)	Vehicle volume (litre)	Load mass (kg)
Vehicle starting point		17	25.250	49.8500	24.6000	42.2800	17.0300	69.2276	1.6807	0	1.5000	0.2800
		18	25.020	52.4460	27.4260	43.9820	18.9620	69.1388	1.6793			
		25	24.367	49.0070	24.6400	41.4040	17.0370	69.1437	1.6794			
								69.1700	***1.6798***			

from Dilution sheet

Dry solids Vehicle mass (kg)	Dry solids Load mass (kg)
1.7429	**0.2800**

Dry solids Vehicle mass %	Dry solids Load mass %
86.2	**13.8**

Test number	Description	Dilution (ml)	Vehicle volume (litre)	Vehicle % solids (%)	Vehicle density (kg/l)	Vehicle mass (kg)	Load mass (kg)	Co-disposed mass (kg)	New vehicle mass %	New load mass %	Load volume (litre)	Co-disposed volume (litre)	Co-disposed density (kg/l)	Co-disposed SG (kg/l)	Co-disposed % solids	Slump height incl ruler (mm)	Slump height excl ruler (mm)	Yield stress (Pa)	Flow distance N	Flow distance S	Flow distance E	Flow distance W	Flow distance radius (mm) N	Flow distance radius (mm) S	Flow distance radius (mm) E	Flow distance radius (mm) W	average	pH before	pH after	pH ave
Test 1	Rep 1	105 acid	1.6050	66.4029	1.6353	2.6247	**0.2800**	2.9047	90.3615	9.6385	0.1081	1.7131	1.6956	2.4273	69.76	41.40	32.40		0 start	1 start	0 mid	1 start	55.56	65.64	60.38	65.64	61.81	6.25	6.74	6.50
	Rep 2															39.90	30.90		0 mid	0 mid	0 start	1 mid	60.38	60.38	55.56	70.68	61.75			
	Rep 3															40.40	31.40		0 start	0 mid	0 mid	2 start	55.56	60.38	55.56	75.76	61.82			
																31.57	***549.14***										**61.79**			
Test 2	Rep 1	35 acid	1.6500	65.2836	1.6180	2.6697	**0.2800**	2.9497	90.5085	9.4915	0.1081	1.7581	1.6778	2.4271	68.70	45.50	45.50		1 start	1 mid	1 start	2 start	65.64	70.68	65.64	75.76	69.43	6.18	6.61	6.40
	Rep 2	10 water														52.40	43.40		0 mid	2 start	1 start	2 start	60.38	75.76	65.64	75.76	69.39			
	Rep 3															52.35	43.35		0 mid	1 mid	0 mid	2 mid	60.38	70.68	60.38	80.73	68.04			
																	44.08	***447.52***									**68.95**			
Test 3	Rep 1	32 acid	1.6970	64.1542	1.6009	2.7167	**0.2800**	2.9967	90.6574	9.3426	0.1081	1.8051	1.6601	2.4268	67.63	63.00	54.00		1 start	3 start	1 mid	3 start	65.64	85.73	70.68	85.73	76.95	6.28	6.57	6.43
	Rep 2	15 water														66.40	57.40		2 start	2 start	2 start	2 start	75.76	75.76	75.76	75.76	75.76			
	Rep 3															66.30	57.30		2 start	2 mid	2 start	2 mid	75.76	80.73	75.76	80.73	78.25			
																	56.23	***362.99***									**76.98**			
Test 4	Rep 1	35 acid	1.7470	62.9948	1.5837	2.7667	**0.2800**	3.0467	90.8107	9.1893	0.1081	1.8551	1.6423	2.4265	66.53	76.70	67.70		2 mid	4 start	3 mid	3 mid	80.73	95.76	90.38	90.38	89.31	6.16	6.46	6.31
	Rep 2	15 water														74.95	65.95		2 start	4 start	2 mid	3 mid	75.76	95.76	80.73	90.38	85.66			
	Rep 3															76.50	67.50		3 start	3 mid	4 start	3 start	85.73	90.38	95.76	85.73	89.40			
																	67.05	***295.74***									**88.12**			
Test 5	Rep 1	30 acid	1.7970	61.8766	1.5674	2.8167	**0.2800**	3.0967	90.9591	9.0409	0.1081	1.9051	1.6255	2.4263	65.46	85.70	76.70		4 mid	4 mid	4 mid	4 mid	100.8	100.8	100.8	100.8	100.78	6.06	6.34	6.20
	Rep 2	20 water														82.30	73.30		3 mid	4 mid	4 start	5 start	90.38	100.8	95.76	105.8	98.18			
	Rep 3															83.25	74.25		3 mid	4 mid	3 mid	4 mid	90.38	100.8	90.38	100.8	95.58			
																	74.75	***251.11***									**98.18**			
Test 6	Rep 1	20 acid	1.8520	60.6915	1.5506	2.8717	**0.2800**	3.1517	91.1169	8.8831	0.1081	1.9601	1.6079	2.4260	64.32	92.20	83.20		6 start	5 mid	6 mid	6 start	115.9	111.1	120.7	115.9	115.88	6.14	6.32	6.23
	Rep 2	35 water														92.75	83.75		5 mid	5 mid	6 start	6 start	111.1	111.1	115.9	115.9	113.50			
	Rep 3															92.25	83.25		5 mid	5 mid	5 mid	6 start	111.1	111.1	111.1	115.9	112.31			
																	83.40	***204.62***									**113.89**			
Test 7	Rep 1	15 acid	1.9120	59.4494	1.5333	2.9317	**0.2800**	3.2117	91.2828	8.7172	0.1081	2.0201	1.5899	2.4257	63.12	103.90	94.90		7 mid	7 start	7 mid	7 mid	130.8	125.8	130.8	130.8	129.56	6.16	6.37	6.27
	Rep 2	45 water														103.45	94.45		6 mid	6 mid	7 mid	7 mid	120.7	120.7	130.8	130.8	125.74			
	Rep 3																													
																	94.68	***149.15***									**127.65**			
Test 8	Rep 1	15 acid	1.9770	58.1599	1.5158	2.9967	**0.2800**	3.2767	91.4558	8.5442	0.1081	2.0851	1.5715	2.4254	61.88	108.75	99.75		7 mid	8 start	8 mid	8 mid	130.8	135.8	140.4	140.4	136.86	6.14	6.38	6.26
	Rep 2	50 water														105.20	96.20		7 mid	7 mid	7 mid	8 mid	130.8	130.8	130.8	140.4	133.22			
	Rep 3																													
																	97.98	***132.65***									**135.04**			

Ave. pH 6.32

Co-disposed Tailings - Vane tests

pH = 6.2
vehicle (wet) : load (dry) = 70:30
vehicle (dry) : load (dry) = 62:38

Date : 25/05/2004

Vane dimensions : medium vane			
	height	0.060	m
	diameter	0.025	m

Vane dimensions : small vane			
	height	0.022	m
	diameter	0.016	m

File name :	**Fredre24**
Sample description :	Co-disposed tails pH 6.2 (62:38)

Rheometer settings :

speed	0.3	rpm
data points	400	
duration	120	sec

Material characteristics :

Type	Vehicle	Load	
Solids SG	2.41	2.59	g/cm^3

Type	Co-disposed tails
pH	6.2
vehicle : load	62:38 dry solids mass basis

Test number	Description	Pan no.	Pan mass (g)	Start mass (g)	Wet mass (g)	End mass (g)	Dry mass (g)	% solids (%)	Density (kg/l)	Dilution (ml)	Vehicle volume (litre)	Load mass (kg)
Vehicle starting point		18	25.017	43.7840	18.7670	38.0120	12.9950	69.2439	1.6810	0	0.3500	0.2521
		6	24.538	47.1370	22.5990	40.1680	15.6300	69.1624	1.6797			
								69.2031	***1.6803***			

						Dry solids Vehicle mass (kg)	Dry solids Load mass (kg)		Dry solids Vehicle mass %	Dry solids Load mass %										
					from Dilution sheet	**0.4070**	**0.2521**		**61.8**	**38.2**										
Test number	Description	Dilution (ml)	Vehicle volume (litre)	Vehicle % solids (%)	Vehicle density (kg/l)	Vehicle mass (kg)	Load mass (kg)	Co-disposed mass (kg)	New vehicle mass %	New load mass %	Load volume (litre)	Co-disposed volume (litre)	Co-disposed density (kg/l)	Co-disposed SG (kg/l)	Co-disposed % solids	Max Torque (mNm)	Yield stress (Pa)	pH before	pH after	pH ave	
Test 3	Rep 1	40 acid	0.3900	64.7961	1.6106	0.6281	**0.2521**	0.8802	71.3634	28.6366	0.0973	0.4873	1.8062	2.4615	75.17	9.3300		6.05	6.63	6.34	small vane
Test 4	Rep 2															9.1300					
Test 5	Rep 3															11.5000					
																9.99	***908.59***				
Test 6	Rep 1	10 acid	0.4000	63.7807	1.5953	0.6381	**0.2521**	0.8902	71.6851	28.3149	0.0973	0.4973	1.7899	2.4610	74.34	7.3200		6.03	6.49	6.26	small vane
Test 8	Rep 2															8.4800					
Test 9	Rep 3															9.8200					
																8.54	***776.97***				
Test 10	Rep 1	9 acid	0.4120	62.6034	1.5780	0.6501	**0.2521**	0.9022	72.0617	27.9383	0.0973	0.5093	1.7713	2.4603	73.36	36.4000		6.06	6.39	6.23	medium vane
Test 11	Rep 2	3 water														36.6000					
Test 12	Rep 3															41.8000					
																38.27	***570.41***				
Test 13	Rep 1	5 acid	0.4220	61.6550	1.5643	0.6601	**0.2521**	0.9122	72.3680	27.6320	0.0973	0.5193	1.7565	2.4597	72.57	27.4000		6.03	6.33	6.18	medium vane
Test 14	Rep 2	5 water														30.6000					
Test 15	Rep 3															28.8000					
																28.93	***431.29***				
Test 16	Rep 1	4 acid	0.4340	60.5542	1.5487	0.6721	**0.2521**	0.9242	72.7268	27.2732	0.0973	0.5313	1.7394	2.4591	71.64	23.2000		6.05	6.30	6.18	medium vane
Test 17	Rep 2	8 water														21.2000					
Test 18	Rep 3															24.3000					
																22.90	***341.35***				
Test 19	Rep 1	4 acid	0.4480	59.3186	1.5315	0.6861	**0.2521**	0.9382	73.1338	26.8662	0.0973	0.5453	1.7204	2.4584	70.59	16.8000		6.07	6.27	6.17	medium vane
Test 20	Rep 2	10 water														18.5000					
Test 21	Rep 3															18.9000					
																18.07	***269.31***				
Test 22	Rep 1	3 acid	0.4630	58.0495	1.5143	0.7011	**0.2521**	0.9532	73.5565	26.4435	0.0973	0.5603	1.7011	2.4576	69.49	11.4000		6.07	6.21	6.14	medium vane
Test 23	Rep 2	12 water														15.8000					
Test 24	Rep 3															13.4000					
																13.53	***201.73***				
Test 25	Rep 1	3 acid	0.4790	56.7543	1.4971	0.7171	**0.2521**	0.9692	73.9931	26.0069	0.0973	0.5763	1.6817	2.4568	68.36	10.2000		6.02	6.18	6.10	medium vane
Test 26	Rep 2	13 water														10.2000					
Test 27	Rep 3															11.0000					
																10.47	***156.02***				
Test 28	Rep 1	2 acid	0.4970	55.3646	1.4791	0.7351	**0.2521**	0.9872	74.4673	25.5327	0.0973	0.5943	1.6610	2.4560	67.13	6.7200		6.08	6.20	6.14	medium vane
Test 29	Rep 2	16 water														6.9500					
Test 30	Rep 3															7.9100					
																7.19	***107.23***				
																			Ave. pH	*6.19*	

Co-disposed Tailings - Slump tests

pH = 6.4

vehicle (wet) : load (dry) = 70:30

vehicle (dry) : load (dry) = 62:38

Date : 02/06/2004

Slump cylinder :

small cylinder

height	0.130	m
diameter	0.105	m
aspect ratio	1.24	
ruler thickness	9	mm

Material characteristics :

Type	Vehicle	Load	
Solids SG	2.41	2.59	g/cm^3

Type	Co-disposed tails
pH	6.4
vehicle : load	62:38

dry solids mass basis

Test number	Description	Pan no.	Pan mass (g)	Start mass (g)	Wet mass (g)	End mass (g)	Dry mass (g)	% solids (%)	Density (kg/l)	Dilution (ml)	Vehicle volume (litre)	Load mass (kg)
Vehicle starting point		17	25.250	49.8500	24.6000	42.2800	17.0300	69.2276	1.6807	0	1.3000	0.9359
		18	25.020	52.4460	27.4260	43.9820	18.9620	69.1388	1.6793			
		25	24.367	49.0070	24.6400	41.4040	17.0370	69.1437	1.6794			
								69.1700	***1.6798***			

from Dilution sheet

	Dry solids Vehicle mass (kg)	Dry solids Load mass (kg)
	1.5105	**0.9359**

	Dry solids Vehicle mass %	Dry solids Load mass %
	61.7	**38.3**

Test number	Description	Dilution (ml)	Vehicle volume (litre)	Vehicle % solids (%)	Vehicle density (kg/l)	Vehicle mass (kg)	Load mass (kg)	Co-disposed mass (kg)	New vehicle mass %	New load mass %	Load volume (litre)	Co-disposed volume (litre)	Co-disposed density (kg/l)	Co-disposed SG (kg/l)	Co-disposed % solids	Slump height incl ruler (mm)	Slump height excl ruler (mm)	Yield stress (Pa)	Flow distance N	Flow distance S	Flow distance E	Flow distance W	Flow distance radius (mm) N	Flow distance radius (mm) S	Flow distance radius (mm) E	Flow distance radius (mm) W	*average*	pH before	pH after	pH ave
Test 1	Rep 1	100 acid	1.4000	66.1412	1.6312	2.2837	**0.9359**	3.2196	70.9318	29.0682	0.3613	1.7613	1.8279	2.4623	76.27	34.00	25.00		0 start	1 mid	0 mid	0 mid	55.56	70.68	60.38	60.38	61.75	6.16	6.80	6.48
	Rep 2															31.00	22.00		0 start	0 mid	0 start	0 mid	55.56	60.38	55.56	60.38	57.97			
	Rep 3															30.00	21.00		0 start	0 start	0 start	0 mid	55.56	55.56	55.56	60.38	56.77			
																	22.67	***679.70***									**58.83**			
Test 2	Rep 1	25 acid	1.4350	65.1428	1.6158	2.3187	**0.9359**	3.2546	71.2444	28.7556	0.3613	1.7963	1.8118	2.4618	75.46	42.20	33.20		0 mid	1 mid	0 start	2 start	60.38	70.68	55.56	75.76	65.60	6.27	6.71	6.49
	Rep 2	10 water														40.00	31.00		0 mid	1 start	0 mid	2 start	60.38	65.64	60.38	75.76	65.54			
	Rep 3															42.80	33.80		0 mid	1 mid	1 start	1 mid	60.38	70.68	65.64	70.68	66.85			
																	32.67	***576.94***									**65.99**			
Test 3	Rep 1	20 acid	1.4800	63.9026	1.5971	2.3637	**0.9359**	3.2996	71.6366	28.3634	0.3613	1.8413	1.7920	2.4611	74.44	52.80	43.80		1 mid	2 start	2 start	1 mid	70.68	75.76	75.76	70.68	73.22	6.25	6.62	6.44
	Rep 2	25 water														56.10	47.10		1 start	2 mid	1 mid	2 start	65.64	80.73	70.68	75.76	73.20			
	Rep 3															56.40	47.40		1 mid	1 mid	1 mid	2 start	70.68	70.68	70.68	75.76	71.95			
																	46.10	***462.92***									**72.79**			
Test 4	Rep 1	15 acid	1.5250	62.7088	1.5795	2.4087	**0.9359**	3.3446	72.0182	27.9818	0.3613	1.8863	1.7731	2.4604	73.46	68.30	59.30		2 mid	3 start	2 mid	3 start	80.73	85.73	80.73	85.73	83.23	6.18	6.61	6.40
	Rep 2	30 water														72.70	63.70		2 mid	2 mid	2 mid	2 mid	80.73	80.73	80.73	80.73	80.73			
	Rep 3															69.45	60.45		2 start	2 mid	2 mid	2 mid	75.76	80.73	80.73	80.73	79.49			
																	61.15	***355.85***									**81.15**			
Test 5	Rep 1	25 acid	1.5800	61.3089	1.5593	2.4637	**0.9359**	3.3996	72.4709	27.5291	0.3613	1.9413	1.7512	2.4596	72.28	80.50	71.50		3 start	5 start	4 start	4 start	85.73	105.8	95.76	95.76	95.76	6.29	6.51	6.40
	Rep 2	30 water														81.20	72.20		3 mid	4 mid	3 mid	4 mid	90.38	100.8	90.38	100.8	95.58			
	Rep 3															81.65	72.65		3 mid	3 start	3 mid	4 start	90.38	85.73	90.38	95.76	90.56			
																	72.12	***285.58***									**93.97**			
Test 6	Rep 1	20 acid	1.6350	59.9701	1.5405	2.5187	**0.9359**	3.4546	72.9092	27.0908	0.3613	1.9963	1.7305	2.4588	71.15	87.05	78.05		4 mid	5 mid	5 mid	5 mid	100.8	111.1	111.1	111.1	108.54	6.22	6.47	6.35
	Rep 2	35 water														87.80	78.80		5 start	5 mid	5 mid	5 mid	105.8	111.1	111.1	111.1	109.80			
	Rep 3															88.00	79.00		5 start	5 start	5 mid	5 mid	105.8	105.8	111.1	111.1	108.47			
																	78.62	***245.95***									**108.94**			
Test 7	Rep 1	15 acid	1.6950	58.5748	1.5214	2.5787	**0.9359**	3.5146	73.3716	26.6284	0.3613	2.0563	1.7092	2.4579	69.95	100.80	91.80		6 mid	6 mid	6 mid	7 start	120.7	120.7	120.7	125.8	121.93	6.25	6.46	6.36
	Rep 2	45 water														96.50	87.50		6 mid	6 mid	7 start	7 start	120.7	120.7	125.8	125.8	123.21			
	Rep 3															97.90	88.90		6 mid	6 mid	7 start	7 start	120.7	120.7	125.8	125.8	123.21			
																	89.40	***186.64***									**122.78**			
Test 8	Rep 1	18 acid	1.7530	57.2863	1.5041	2.6367	**0.9359**	3.5726	73.8039	26.1961	0.3613	2.1143	1.6897	2.4572	68.83	112.00	103.00		8 mid	9 start	9 mid	10 start	140.4	145.7	150.5	155	147.91	6.16	6.44	6.30
	Rep 2	40 water														116.80	107.80		8 mid	9 start	10 start	9 mid	140.4	145.7	155	150.5	147.91			
	Rep 3															112.00	103.00		7 mid	8 mid	9 start	9 start	130.8	140.4	145.7	145.7	140.66			
																	104.60	***111.51***									**145.49**			

Ave.pH *6.40*

Co-disposed Tailings - Vane tests

pH = 6.2
vehicle (wet) : load (dry) = 60:40
vehicle (dry) : load (dry) = 51:49

Date : 26/05/2004

Vane dimensions : medium vane			
height	0.060	m
diameter	0.025	m

Vane dimensions : small vane			
height	0.022	m
diameter	0.016	m

File name :	Fredre25
Sample description :	Co-disposed tails pH 6.2 (51:49)

Rheometer settings :

speed	0.3	rpm
data points	400	
duration	120	sec

Material characteristics :

Type	Vehicle	Load	
Solids SG	2.41	2.59	g/cm^3

Type	Co-disposed tails
pH	6.2
vehicle : load	51:49

dry solids mass basis

Test number	Description	Pan no.	Pan mass (g)	Start mass (g)	Wet mass (g)	End mass (g)	Dry mass (g)	% solids (%)	Density (kg/l)	Dilution (ml)	Vehicle volume (litre)	Load mass (kg)
Vehicle starting point		22	24.432	38.7830	14.3510	34.3630	9.9310	69.2008	1.6803	0	0.3100	0.3474
		17	25.251	40.7490	15.4980	35.9860	10.7350	69.2670	1.6814			
								69.2339	***1.6808***			

	Dry solids Vehicle mass (kg)	Dry solids Load mass (kg)		Dry solids Vehicle mass %	Dry solids Load mass %
from Dilution sheet	**0.3608**	**0.3474**		**50.9**	**49.1**

Test number	Description	Dilution (ml)	Vehicle volume (litre)	Vehicle % solids (%)	Vehicle density (kg/l)	Vehicle mass (kg)	Load mass (kg)	Co-disposed mass (kg)	New vehicle mass %	New load mass %	Load volume (litre)	Co-disposed volume (litre)	Co-disposed density (kg/l)	Co-disposed SG (kg/l)	Co-disposed % solids	Max Torque (mNm)	Yield stress (Pa)	pH before	pH after	pH ave	
Test 5	Rep 1	55 acid	0.3650	62.6237	1.5783	0.5761	**0.3474**	0.9234	62.3824	37.6176	0.1341	0.4991	1.8501	2.4777	77.04	8.7200		6.06	6.41	6.24	small vane
Test 6	Rep 2															8.4600					
Test 7	Rep 3															10.1000					
																9.09	***827.31***				
Test 8	Rep 1	5 acid	0.3770	61.3458	1.5598	0.5881	**0.3474**	0.9354	62.8650	37.1350	0.1341	0.5111	1.8302	2.4768	76.07	37.0000		5.96	6.41	6.19	medium vane
Test 10	Rep 2	7 water														38.3000					
Test 11	Rep 3															42.0000					
																39.10	***582.83***				
Test 12	Rep 1	3 acid	0.3890	60.1190	1.5426	0.6001	**0.3474**	0.9474	63.3353	36.6647	0.1341	0.5231	1.8111	2.4760	75.13	25.5000		6.12	6.37	6.25	medium vane
Test 13	Rep 2	9 water														29.4000					
Test 14	Rep 3															30.5000					
																28.47	***424.33***				
Test 15	Rep 1	3 acid	0.4020	58.8442	1.5250	0.6131	**0.3474**	0.9604	63.8316	36.1684	0.1341	0.5361	1.7915	2.4751	74.13	19.6000		6.07	6.34	6.21	medium vane
Test 16	Rep 2	10 water														22.2000					
Test 17	Rep 3															22.2000					
																21.33	***318.00***				
Test 18	Rep 1	3 acid	0.4150	57.6223	1.5086	0.6261	**0.3474**	0.9734	64.3146	35.6854	0.1341	0.5491	1.7727	2.4742	73.16	15.4000		6.09	6.24	6.17	medium vane
Test 19	Rep 2	10 water														15.5000					
Test 20	Rep 3															14.1000					
																15.00	***223.59***				
Test 21	Rep 1	2 acid	0.4290	56.3619	1.4920	0.6401	**0.3474**	0.9874	64.8206	35.1794	0.1341	0.5631	1.7535	2.4733	72.14	11.9000		6.11	6.24	6.18	medium vane
Test 22	Rep 2	12 water														12.0000					
Test 23	Rep 3															11.8000					
																11.90	***177.38***				
Test 24	Rep 1	1 acid	0.4460	54.9037	1.4732	0.6571	**0.3474**	1.0044	65.4160	34.5840	0.1341	0.5801	1.7314	2.4723	70.94	8.9100		6.18	6.27	6.23	medium vane
Test 25	Rep 2	16 water														8.9700					
Test 26	Rep 3															8.1100					
																8.66	***129.14***				
Test 27	Rep 1	1 acid	0.4630	53.5190	1.4559	0.6741	**0.3474**	1.0214	65.9916	34.0084	0.1341	0.5971	1.7106	2.4712	69.78	7.9500		6.24	6.30	6.27	medium vane
Test 28	Rep 2	16 water														7.0900					
Test 29	Rep 3															7.2500					
																7.43	***110.75***				

Ave. pH *6.21*

Co-disposed Tailings - Slump tests

pH = 6.4

vehicle (wet) : load (dry) = 60:40

vehicle (dry) : load (dry) = 50:50

Date : 10/06/2004

Slump cylinder : small cylinder

height	0.130	m
diameter	0.105	m
aspect ratio	1.24	
ruler thickness	9.2	mm

Material characteristics :

Type	Vehicle	Load	
Solids SG	2.41	2.59	g/cm^3

Type	Co-disposed tails
pH	6.4
vehicle : load	50:50

dry solids mass basis

Test number	Description	Pan no.	Pan mass (g)	Start mass (g)	Wet mass (g)	End mass (g)	Dry mass (g)	% solids (%)	Density (kg/l)	Dilution (ml)	Vehicle volume (litre)	Load mass (kg)
Vehicle starting point		20	25.116	36.5050	11.3890	32.6000	7.4840	65.7125	1.6246	0	1.1000	1.1918
		23	24.789	35.9880	11.1990	32.1560	7.3670	65.7827	1.6257			
								65.7476	***1.6251***			

	Dry solids Vehicle mass (kg)	Dry solids Load mass (kg)		Dry solids Vehicle mass %	Dry solids Load mass %
from Dilution sheet	**1.1753**	**1.1918**		**49.7**	**50.3**

Test number	Description	Dilution (ml)	Vehicle volume (litre)	Vehicle % solids (%)	Vehicle density (kg/l)	Vehicle mass (kg)	Load mass (kg)	Co-disposed mass (kg)	New vehicle mass %	New load mass %	Load volume (litre)	Co-disposed volume (litre)	Co-disposed density (kg/l)	Co-disposed SG (kg/l)	Co-disposed % solids	Slump height incl ruler (mm)	Slump height excl ruler (mm)	Yield stress (Pa)	Flow distance N	Flow distance S	Flow distance E	Flow distance W	Flow distance radius (mm) N	Flow distance radius (mm) S	Flow distance radius (mm) E	Flow distance radius (mm) W	pH before	pH after	pH ave
Test 1	rep 1	70 acid	1.2100	61.9364	1.5683	1.8976	**1.1918**	3.0894	61.4242	38.5758	0.4601	1.6701	1.8498	2.4794	76.99	37.90	28.70		0 mid	1 start	0 mid	1 mid	60.38	65.64	60.38	70.68	64.27	6.11	6.90	6.51
	rep 2	40 water														35.50	26.30		0 mid	1 mid	0 mid	1 mid	60.38	70.68	60.38	70.68	65.53			
	rep 3															35.20	26.00		1 mid	0 mid	0 mid	1 mid	70.68	60.38	60.38	70.68	65.53			
																	27.00	***642.79***									**65.11**			
Test 2	rep 1	25 acid	1.2500	60.6578	1.5501	1.9376	**1.1918**	3.1294	61.9173	38.0827	0.4601	1.7101	1.8299	2.4785	76.03	49.80	40.60		1 mid	1 mid	1 mid	2 start	70.68	70.68	70.68	75.76	71.95	6.21	6.80	6.51
	rep 2	15 water														53.00	43.80		1 mid	1 mid	0 mid	2 mid	70.68	70.68	60.38	80.73	70.62			
	rep 3															52.90	43.70		1 mid	1 mid	1 mid	2 start	70.68	70.68	70.68	75.76	71.95			
																	42.70	***498.85***									**71.51**			
Test 3	rep 1	25 acid	1.2950	59.2811	1.5310	1.9826	**1.1918**	3.1744	62.4571	37.5429	0.4601	1.7551	1.8086	2.4776	74.97	66.50	57.30		2 start	3 start	2 start	3 mid	75.76	85.73	75.76	90.38	81.91	6.07	6.61	6.34
	rep 2	20 water														64.55	55.35		3 start	2 mid	2 start	3 start	85.73	80.73	75.76	85.73	81.99			
	rep 3															65.85	56.65		3 start	2 start	2 start	3 mid	85.73	75.76	75.76	90.38	81.91			
																	56.43	***394.12***									**81.93**			
Test 4	rep 1	20 acid	1.3500	57.6810	1.5094	2.0376	**1.1918**	3.2294	63.0966	36.9034	0.4601	1.8101	1.7841	2.4764	73.71	77.80	68.60		4 start	4 mid	3 mid	5 start	95.76	100.8	90.38	105.8	98.18	6.16	6.58	6.37
	rep 2	35 water														80.25	71.05		4 start	3 mid	3 mid	5 start	95.76	90.38	90.38	105.8	95.58			
	rep 3															79.60	70.40		4 mid	3 mid	3 start	4 mid	100.8	90.38	85.73	100.8	94.42			
																	70.02	***303.38***									**96.06**			
Test 5	rep 1	17 acid	1.4120	55.9777	1.4870	2.0996	**1.1918**	3.2914	63.7917	36.2083	0.4601	1.8721	1.7581	2.4752	72.35	89.30	80.10		6 start	5 mid	6 start	6 mid	115.9	111.1	115.9	120.7	115.88	6.23	6.49	6.36
	rep 2	45 water														89.65	80.45		5 mid	5 mid	5 mid	6 mid	111.1	111.1	111.1	120.7	113.51			
	rep 3															87.30	78.10		6 mid	5 mid	6 start	5 mid	120.7	111.1	115.9	111.1	114.69			
																	79.55	***244.72***									**114.69**			
Test 6	rep 1	20 acid	1.4870	54.0471	1.4624	2.1746	**1.1918**	3.3664	64.5984	35.4016	0.4601	1.9471	1.7289	2.4737	70.77	100.90	91.70		7 mid	7 mid	8 start	8 start	130.8	130.8	135.8	135.8	133.33	6.15	6.46	6.31
	rep 2	55 water														100.60	91.40		7 mid	7 start	8 start	8 mid	130.8	125.8	135.8	140.4	133.20			
	rep 3															99.20	90.00		7 mid	6 mid	8 mid	8 start	130.8	120.7	140.4	135.8	131.92			
																	91.03	***180.48***									**132.82**			
Test 7	rep 1	20 acid	1.5670	52.1294	1.4388	2.2546	**1.1918**	3.4464	65.4201	34.5799	0.4601	2.0271	1.7001	2.4722	69.15	115.90	106.70		10 mid	10 mid	10 mid	11 mid	160.6	160.6	160.6	170	162.91	6.20	6.42	6.31
	rep 2	60 water														110.10	100.90		9 start	9 mid	9 mid	10 mid	145.7	150.5	150.5	160.6	151.82			
	rep 3															111.00	101.80		9 mid	9 start	10 mid	10 mid	150.5	145.7	160.6	160.6	154.33			
																	103.13	***119.04***									**156.35**			

Ave. pH *6.39*

Co-disposed Tailings - Vane tests

pH = 11.5
vehicle (wet) : load (dry) = 90:10
vehicle (dry) : load (dry) = 86:14

Date : 31/05/2004

Vane dimensions : medium vane			
height	0.060	m
diameter	0.025	m

Vane dimensions : small vane			
height	0.022	m
diameter	0.016	m

File name :	**Fredre26**
Sample description :	Co-disposed tails pH 11.5 (86:14)

Rheometer settings :

speed	0.3	rpm
data points	400	
duration	120	sec

Material characteristics :

Type	Vehicle	Load	
Solids SG	2.41	2.59	g/cm^3

Type	Co-disposed tails
pH	11.5
vehicle : load	86:14

dry solids mass basis

Test number	Description	Pan no.	Pan mass (g)	Start mass (g)	Wet mass (g)	End mass (g)	Dry mass (g)	% solids (%)	Density (kg/l)	Dilution (ml)	Vehicle volume (litre)	Load mass (kg)
Vehicle starting point		17	25.250	49.8500	24.6000	42.2800	17.0300	69.2276	1.6807	0	0.4100	0.0765
		18	25.020	52.4460	27.4260	43.9820	18.9620	69.1388	1.6793			
		25	24.367	49.0070	24.6400	41.4040	17.0370	69.1437	1.6794			
								69.1700	***1.6798***			

						Dry solids Vehicle mass (kg)	Dry solids Load mass (kg)		Dry solids Vehicle mass %	Dry solids Load mass %									
					from Dilution sheet	**0.4764**	**0.0765**		**86.2**	**13.8**									
Test number	Description	Dilution (ml)	Vehicle volume (litre)	Vehicle % solids (%)	Vehicle density (kg/l)	Vehicle mass (kg)	Load mass (kg)	Co-disposed mass (kg)	New vehicle mass %	New load mass %	Load volume (litre)	Co-disposed volume (litre)	Co-disposed density (kg/l)	Co-disposed SG (kg/l)	Co-disposed % solids	Max Torque (mNm)	Yield stress (Pa)	pH before	pH after	pH ave	
Test 2	Rep 1	19 alkali	0.4290	67.3130	1.6497	0.7077	**0.0765**	0.7842	90.2423	9.7577	0.0295	0.4585	1.7103	2.4276	70.62	10.4000		11.70	11.11	11.41	small vane
Test 3	Rep 2															10.4000					
Test 4	Rep 3															10.9000					
																10.57	***961.36***				
Test 8	Rep 1	5 alkali	0.4320	65.9159	1.6277	0.7032	**0.0765**	0.7797	90.1855	9.8145	0.0295	0.4615	1.6893	2.4277	69.39	9.6600		11.65	11.52	11.59	small vane
Test 9	Rep 2	10 water														8.4800					
Test 10	Rep 3															8.7100					
																8.95	***814.27***				
Test 11	Rep 1	11 water	0.4430	64.9277	1.6126	0.7144	**0.0765**	0.7909	90.3243	9.6757	0.0295	0.4725	1.6737	2.4274	68.45	44.7000		11.51	11.43	11.47	medium vane
Test 12	Rep 2															49.9000					
Test 13	Rep 3															51.5000					
																48.70	***725.93***				
Test 14	Rep 1	1 alkali	0.4560	63.7973	1.5955	0.7276	**0.0765**	0.8041	90.4832	9.5168	0.0295	0.4855	1.6561	2.4271	67.37	39.3000		11.68	11.49	11.59	medium vane
Test 15	Rep 2	12 water														38.7000					
Test 16	Rep 3															39.9000					
																39.30	***585.81***				
Test 17	Rep 1	13 water	0.4690	62.7056	1.5794	0.7408	**0.0765**	0.8173	90.6368	9.3632	0.0295	0.4985	1.6393	2.4269	66.33	29.9000		11.52	11.41	11.47	medium vane
Test 18	Rep 2															28.6000					
Test 19	Rep 3															30.5000					
																29.67	***442.22***				
Test 20	Rep 1	0.6 alkali	0.4820	61.6507	1.5642	0.7539	**0.0765**	0.8305	90.7855	9.2145	0.0295	0.5115	1.6234	2.4266	65.32	23.4000		11.57	11.45	11.51	medium vane
Test 21	Rep 2	12.4 water														25.8000					
Test 22	Rep 3															25.0000					
																24.73	***368.68***				
Test 23	Rep 1	0.6 alkali	0.4970	60.4767	1.5476	0.7691	**0.0765**	0.8457	90.9511	9.0489	0.0295	0.5265	1.6061	2.4263	64.19	19.0000		11.59	11.46	11.53	medium vane
Test 24	Rep 2	14.4 water														19.8000					
Test 25	Rep 3															19.4000					
																19.40	***289.18***				
Test 26	Rep 1	0.4 alkali	0.5150	59.1256	1.5289	0.7874	**0.0765**	0.8639	91.1420	8.8580	0.0295	0.5445	1.5864	2.4259	62.89	15.3000		11.60	11.49	11.55	medium vane
Test 27	Rep 2	17.6 water														15.1000					
Test 28	Rep 3															14.6000					
																15.00	***223.59***				
Test 29	Rep 1	0.6 alkali	0.5370	57.5541	1.5077	0.8096	**0.0765**	0.8861	91.3644	8.6356	0.0295	0.5665	1.5641	2.4255	61.37	11.4000		11.65	11.53	11.59	medium vane
Test 30	Rep 2	21.4 water														11.2000					
Test 31	Rep 3															11.3000					
																11.30	***168.44***				
Test 32	Rep 1	30 water	0.5670	55.5410	1.4814	0.8399	**0.0765**	0.9165	91.6501	8.3499	0.0295	0.5965	1.5363	2.4250	59.40	7.2900		11.57	11.52	11.55	medium vane
Test 33	Rep 2															7.4900					
Test 34	Rep 3															7.0800					
																7.29	***108.62***				

Ave. pH 11.52

Co-disposed Tailings - Slump tests

pH = 11.6

vehicle (wet) : load (dry) = 90:10

vehicle (dry) : load (dry) = 86:14

Date : 03/06/2004

Slump cylinder : small cylinder

height	0.130	m	
diameter	0.105	m	
aspect ratio	1.24		
ruler thickness	9	mm	

Material characteristics :

Type	Vehicle	Load	
Solids SG	2.41	2.59	g/cm^3

Type	Co-disposed talls
pH	11.6
vehicle : load	86:14

dry solids mass basis

Test number	Description	Pan no.	Pan mass (g)	Start mass (g)	Wet mass (g)	End mass (g)	Dry mass (g)	% solids (%)	Density (kg/l)	Dilution (ml)	Vehicle volume (litre)	Load mass (kg)
Vehicle starting point		9	23.789	60.7150	36.9260	48.8580	25.0690	***67.8898***	***1.6589***	0	1.5000	0.2765

						Dry solids Vehicle mass (ko)	Dry solids Load mass (kg)		Dry solids Vehicle mass %	Dry solids Load mass %																							
						from Dilution sheet																										
Test number	Description	Dilution (ml)	Vehicle volume (litre)	Vehicle % solids (%)	Vehicle density (kg/l)	Vehicle mass (kg)	Load mass (kg)	Co-disposed mass (kg)	New vehicle mass %	New load mass %	Load volume (litre)	Co-disposed volume (litre)	Co-disposed density (kg/l)	Co-disposed SG (kg/l)	Co-disposed % solids	Slump height incl ruler (mm)	Slump height excl ruler (mm)	Yield stress (Pa)	Flow distance N	Flow distance S	Flow distance E	Flow distance W	Flow distance radius (mm) N	Flow distance radius (mm) S	Flow distance radius (mm) E	Flow distance radius (mm) W	average	pH before	pH after	pH ave
Test 1	Rep 1	75 alkali	1.7350	62.0316	1.5697	2.7234	**0.2765**	2.9999	90.7834	9.2166	0.1068	1.8418	1.6288	2.4266	65.67	57.20	48.20		0 mid	1 mid	0 mid	2 mid	60.38	70.68	60.38	80.73	68.04	11.80	11.34	11.57
	Rep 2	160 water										61.50	52.50					1 start	0 mid	2 start	0 mid	65.64	60.38	75.76	60.38	65.54			
	Rep 3											62.10	53.10					1 start	2 mid	1 start	2 mid	65.64	80.73	65.64	80.73	73.19			
													51.27	***387.02***													**68.92**			
Test 2	Rep 1	10 alkali	1.7750	61.1337	1.5568	2.7634	**0.2765**	3.0399	90.9046	9.0954	0.1068	1.8818	1.6154	2.4264	64.81	68.30	59.30		1 start	2 start	1 start	2 mid	65.64	75.76	65.64	80.73	71.94	11.79	11.49	11.64
	Rep 2	30 water										66.00	57.00					1 start	1 mid	0 mid	3 start	65.64	70.68	60.38	85.73	70.61			
	Rep 3											66.20	57.20					1 mid	2 mid	1 start	3 start	70.68	80.73	65.64	85.73	75.70			
													57.83	***343.65***													**72.75**			
Test 3	Rep 1	5 alkali	1.8250	60.0472	1.5416	2.8134	**0.2765**	3.0899	91.0518	8.9482	0.1068	1.9318	1.5995	2.4261	63.76	75.10	66.10		1 mid	3 start	2 mid	2 mid	70.68	85.73	80.73	80.73	79.47	11.84	11.54	11.69
	Rep 2	45 water										77.30	68.30					2 mid	2 mid	2 start	2 mid	80.73	80.73	75.76	80.73	79.49			
	Rep 3											78.30	69.30					2 mid	2 mid	2 mid	2 mid	80.73	80.73	80.73	80.73	80.73			
													67.90	***283.40***													**79.90**			
Test 4	Rep 1	55 water	1.8800	58.8958	1.5257	2.8684	**0.2765**	3.1449	91.2083	8.7917	0.1068	1.9868	1.5829	2.4258	62.65	85.25	76.25		3 start	4 mid	3 mid	4 start	85.73	100.8	90.38	95.76	93.16	11.55	11.50	11.53
	Rep 2											85.90	76.90					3 mid	3 mid	3 mid	3 mid	90.38	90.38	90.38	90.38	90.38			
	Rep 3											86.00	77.00					3 mid	3 mid	3 mid	3 mid	90.38	90.38	90.38	90.38	90.38			
													76.72	***234.53***													**91.31**			
Test 5	Rep 1	1 alkali	1.9400	57.6891	1.5095	2.9284	**0.2765**	3.2049	91.3729	8.6271	0.1068	2.0468	1.5658	2.4255	61.49	93.10	84.10		4 mid	4 mid	4 mid	5 start	100.8	100.8	100.8	105.8	102.04	11.57	11.47	11.52
	Rep 2	59 water										91.20	82.20					4 mid	4 mid	4 mid	5 start	100.8	100.8	100.8	105.8	102.04			
	Rep 3											93.40	84.40					5 start	4 mid	4 mid	5 start	105.8	100.8	100.8	105.8	103.29			
													83.57	***198.47***													**102.45**			
Test 6	Rep 1	1 alkali	2.0060	56.4176	1.4927	2.9944	**0.2765**	3.2709	91.5470	8.4530	0.1068	2.1128	1.5482	2.4252	60.25	100.60	91.60		6 start	6 mid	6 mid	7 mid	115.9	120.7	120.7	130.8	122.90	11.55	11.47	11.51
	Rep 2	65 water										99.70	90.70					6 start	6 mid	6 mid	6 mid	115.9	120.7	120.7	120.7	119.45			
	Rep 3											98.70	89.70					6 start	6 mid	6 mid	7 start	115.9	120.7	120.7	125.8	120.73			
													90.67	***163.28***													**120.73**			
Test 7	Rep 1	1 alkali	2.0810	55.0390	1.4750	3.0694	**0.2765**	3.3459	91.7365	8.2635	0.1068	2.1878	1.5294	2.4249	58.91	110.45	101.45		8 mid	8 mid	8 mid	8 mid	140.4	140.4	140.4	140.4	140.38	11.54		11.54
	Rep 2	74 water										110.50	101.50					7 mid	7 mid	7 mid	8 mid	130.8	130.8	130.8	140.4	133.22			
	Rep 3											108.90	99.90					7 mid	7 mid	7 mid	8 mid	130.8	130.8	130.8	140.4	133.22			
													100.95	***116.33***													**135.61**			

Ave. pH *11.57*

Co-disposed Tailings - Vane tests

pH = 11.5

vehicle (wet) : load (dry) = 70:30

vehicle (dry) : load (dry) = 60:40

Date : 04/06/2004

Vane dimensions :			
medium vane	height	0.060	m
	diameter	0.025	m

Vane dimensions :			
small vane	height	0.022	m
	diameter	0.016	m

File name :	**Fredre27**
Sample description :	Co-disposed tails pH 11.5 (60:40)

Rheometer settings :

speed	0.3	rpm
data points	400	
duration	120	sec

Material characteristics :

Type	Vehicle	Load	
Solids SG	2.41	2.59	g/cm^3

Type	Co-disposed tails
pH	11.5
vehicle : load	60:40

dry solids mass basis

Test	Description	Pan no.	Pan mass	Start mass	Wet mass	End mass	Dry mass	% solids	Density	Dilution	Vehicle volume	Load mass
number			(g)	(g)	(g)	(g)	(g)	(%)	(kg/l)	(ml)	(litre)	(kg)
Vehicle starting point		9	23.7900	55.9490	32.1590	44.8910	21.1010	65.6146	1.6231	0	0.3500	0.2438
		7	25.2330	69.3220	44.0890	54.2770	29.0440	65.8758	1.6271			
								65.7452	***1.6251***			

from Dilution sheet

						Dry solids Vehicle mass (kg) **0.3591**	Dry solids Load mass (kg) **0.2438**		Dry solids Vehicle mass % **59.6**	Dry solids Load mass % **40.4**										
Test	Description	Dilution	Vehicle volume	Vehicle % solids	Vehicle density	Vehicle mass	Load mass	Co-disposed mass	New vehicle	New load	Load volume	Co-disposed volume	Co-disposed density	Co-disposed SG	Co-disposed % solids	Max Torque	Yield stress	pH before	pH after	pH ave	
number		(ml)	(litre)	(%)	(kg/l)	(kg)	(kg)	(kg)	mass %	mass %	(litre)	(litre)	(kg/l)	(kg/l)		(mNm)	(Pa)				
Test 5	Rep 1	19 alkali	0.3640	62.5557	1.5773	0.5741	**0.2438**	0.8179	70.1959	29.8041	0.0941	0.4581	1.7853	2.4636	74.04	9.3500		11.96	11.50	11.73	small vane
Test 6	Rep 2	10 water														9.3500					
Test 7	Rep 3															10.6000					
																9.77	***888.57***				
Test 8	Rep 1	0.4 alkali	0.3774	61.1842	1.5575	0.5878	**0.2438**	0.8316	70.6868	29.3132	0.0941	0.4715	1.7636	2.4628	72.90	44.9000		11.54	11.25	11.40	medium vane
Test 9	Rep 2	13 water														42.9000					
Test 10	Rep 3															42.3000					
																43.37	***646.43***				
Test 11	Rep 1	1 alkali	0.3904	59.9099	1.5397	0.6011	**0.2438**	0.8449	71.1471	28.8529	0.0941	0.4845	1.7437	2.4619	71.82	31.2000		11.54	11.25	11.40	medium vane
Test 12	Rep 2	12 water														35.1000					
Test 13	Rep 3															35.7000					
																34.00	***506.81***				
Test 14	Rep 1	2 alkali	0.4064	58.4126	1.5192	0.6174	**0.2438**	0.8612	71.6935	28.3065	0.0941	0.5005	1.7205	2.4610	70.54	24.8000		11.77	11.41	11.59	medium vane
Test 15	Rep 2	14 water														25.4000					
Test 16	Rep 3															24.9000					
																25.03	***373.15***				
Test 17	Rep 1	1.4 alkali	0.4244	56.8151	1.4979	0.6357	**0.2438**	0.8795	72.2831	27.7169	0.0941	0.5185	1.6961	2.4599	69.16	18.6000		11.80	11.50	11.65	medium vane
Test 18	Rep 2	16.6 water														16.8000					
Test 19	Rep 3															18.2000					
																17.87	***266.32***				
Test 20	Rep 1	20 water	0.4444	55.1396	1.4762	0.6560	**0.2438**	0.8998	72.9092	27.0908	0.0941	0.5385	1.6709	2.4588	67.68	11.8000		11.51	11.43	11.47	medium vane
Test 21	Rep 2															13.3000					
Test 22	Rep 3															13.0000					
																12.70	***189.31***				
Test 23	Rep 1	1 alkali	0.4694	53.1792	1.4517	0.6814	**0.2438**	0.9252	73.6520	26.3480	0.0941	0.5635	1.6418	2.4574	65.91	8.9900		11.59	11.46	11.53	medium vane
Test 24	Rep 2	24 water														8.0600					
Test 25	Rep 3															8.3400					
																8.46	***126.16***				
Test 26	Rep 1	0.6 alkali	0.5010	50.8922	1.4240	0.7134	**0.2438**	0.9572	74.5333	25.4667	0.0941	0.5951	1.6084	2.4558	63.81	4.7900		11.60	11.53	11.57	medium vane
Test 27	Rep 2	31 water														5.4700					
Test 28	Rep 3															5.4200					
																5.23	***77.91***				

Ave. pH *11.54*

Co-disposed Tailings - Slump tests

pH ~ 11.5

vehicle (wet) : load (dry) ~ 70:30

vehicle (dry) : load (dry) ~ 60:40

Date : 08/06/2004

Slump cylinder : small cylinder

height	0.130	m
diameter	0.105	m
aspect ratio	1.24	
ruler thickness	9.2	mm

Material characteristics :

Type	Vehicle	Load	
Solids SG	2.41	2.59	g/cm^3

Type	Co-disposed tails
pH	11.5
vehicle : load	60:40

dry solids mass basis

Test number	Description	Pan no.	Pan mass (g)	Start mass (g)	Wet mass (g)	End mass (g)	Dry mass (g)	% solids (%)	Density (kg/l)	Dilution (ml)	Vehicle volume (litre)	Load mass (kg)
Vehicle starting point		20	25.1140	57.4650	32.3510	46.2810	21.1670	65.4292	1.6202	0	1.3000	0.9028
		22	24.4290	47.4410	23.0120	39.4930	15.0640	65.4615	1.6207			
		14	24.9150	59.5320	34.6170	47.5640	22.6490	65.4274	1.6202			
								65.4394	***1.6204***			

from Dilution sheet

						Dry solids Vehicle mass (kg)	Dry solids Load mass (kg)		Dry solids Vehicle mass %	Dry solids Load mass %																							
						1.3785	**0.9028**		**60.4**	**39.6**																							
Test number	Description	Dilution (ml)	Vehicle volume (litre)	Vehicle % solids (%)	Vehicle density (kg/l)	Vehicle mass (kg)	Load mass (kg)	Co-disposed mass (kg)	New vehicle mass %	New load mass %	Load volume (litre)	Co-disposed volume (litre)	Co-disposed density (kg/l)	Co-disposed SG (kg/l)	Co-disposed % solids	Slump height incl ruler (mm)	Slump height excl ruler (mm)	Yield stress (Pa)	Flow distance N	Flow distance S	Flow distance E	Flow distance W	Flow distance radius (mm) N	Flow distance radius (mm) S	Flow distance radius (mm) E	Flow distance radius (mm) W	*average*	pH before	pH after	pH ave
Test 1	Rep 1	65 alkali	1.4650	60.6859	1.5505	2.2715	**0.9028**	3.1743	71.5594	28.4406	0.3486	1.8136	1.7503	2.4612	72.20	54.20	45.00		0 start	1 mid	0 start	2 mid	55.56	70.68	55.56	80.73	65.63	12.02	11.18	11.60
	Rep 2	100 water														54.90	45.70		0 mid	1 mid	0 start	2 mid	60.38	70.68	55.56	80.73	66.84			
	Rep 3															54.65	45.45		0 mid	2 start	0 mid	2 mid	60.38	75.76	60.38	80.73	69.31			
																	45.38	***457.35***									**67.26**			
Test 2	Rep 1	10 alkali	1.5050	59.6357	1.5359	2.3115	**0.9028**	3.2143	71.9133	28.0867	0.3486	1.8536	1.7341	2.4606	71.32	60.00	50.80		1 mid	1 mid	0 mid	3 start	70.68	70.68	60.38	85.73	71.87	11.82	11.39	11.61
	Rep 2	30 water														60.05	50.85		1 mid	1 mid	0 mid	2 mid	70.68	70.68	60.38	80.73	70.62			
	Rep 3															57.35	48.15		2 start	1 start	0 mid	3 mid	75.76	65.64	60.38	90.38	73.04			
																	49.93	***421.14***									**71.84**			
Test 3	Rep 1	5 alkali	1.5550	58.3730	1.5186	2.3615	**0.9028**	3.2643	72.3435	27.6565	0.3486	1.9036	1.7148	2.4598	70.24	70.90	61.70		1 mid	1 mid	1 start	3 mid	70.68	70.68	65.64	90.38	74.35	11.79	11.43	11.61
	Rep 2	45 water														73.10	63.90		2 mid	2 start	1 mid	2 mid	80.73	75.76	70.68	80.73	76.98			
	Rep 3															69.65	60.45		2 mid	2 start	1 mid	3 start	80.73	75.76	70.68	85.73	78.23			
																	62.02	***338.86***									**76.52**			
Test 4	Rep 1	2 alkali	1.6100	57.0444	1.5009	2.4165	**0.9028**	3.3193	72.8018	27.1982	0.3486	1.9586	1.6947	2.4590	69.09	78.95	69.75		3 start	3 mid	2 mid	4 start	85.73	90.38	80.73	95.76	88.15	11.75	11.41	11.58
	Rep 2	53 water														78.00	68.80		3 mid	2 mid	3 start	3 mid	90.38	80.73	85.73	90.38	86.81			
	Rep 3															80.95	71.75		3 start	3 mid	2 mid	4 start	85.73	90.38	80.73	95.76	88.15			
																	70.10	***287.72***									**87.70**			
Test 5	Rep 1	1 alkali	1.6750	55.5502	1.4815	2.4815	**0.9028**	3.3843	73.3242	26.6758	0.3486	2.0236	1.6724	2.4580	67.78	88.70	79.50		5 start	4 mid	4 mid	5 mid	150.8	100.8	100.8	111.1	115.87	11.5	11.39	11.45
	Rep 2	64 water														89.90	80.70		4 mid	4 mid	4 mid	4 mid	100.8	100.8	100.8	100.8	100.78			
	Rep 3															88.25	79.05		4 mid	4 mid	4 mid	5 start	100.8	100.8	100.8	105.8	102.04			
																	79.75	***231.74***									**106.23**			
Test 6	Rep 1	1.4 alkali	1.7534	53.8489	1.4600	2.5599	**0.9028**	3.4627	73.9282	26.0718	0.3486	2.1020	1.6474	2.4569	66.27	96.30	87.10		6 start	7 start	6 mid	7 start	115.9	125.8	120.7	125.8	122.01	11.48	11.38	11.43
	Rep 2	77 water														97.20	88.00		6 start	6 mid	6 mid	7 start	115.9	120.7	120.7	125.8	120.73			
	Rep 3															100.60	91.40		6 mid	6 start	7 start	6 mid	120.7	115.9	125.8	120.7	120.73			
																	88.83	***182.66***									**121.16**			
Test 7	Rep 1	2 alkali	1.8534	51.8244	1.4351	2.6599	**0.9028**	3.5627	74.6600	25.3400	0.3486	2.2020	1.6180	2.4556	64.43	109.80	100.60		8 mid	9 start	9 start	10 star	140.4	145.7	145.7	155	146.71	11.52	11.38	11.45
	Rep 2	98 water														109.20	100.00		9 start	8 mid	8 mid	9 start	145.7	140.4	140.4	145.7	143.05			
	Rep 3															109.00	99.80		8 mid	8 mid	8 mid	8 mid	140.4	140.4	140.4	140.4	140.38			
																	100.13	***126.75***									**143.38**			

Ave. pH *11.53*

Co-disposed Tailings - Vane tests

pH = 11.5
vehicle (wet) : load (dry) = 60:40
vehicle (dry) : load (dry) = 50:50

Date : 07/06/2004

Vane dimensions : medium vane			
	height	0.060	m
	diameter	0.025	m

Vane dimensions : small vane			
	height	0.022	m
	diameter	0.016	m

File name :	**Fredre28**
Sample description :	Co-disposed tails pH 11.5 (50:50)

Rheometer settings :

speed	0.3	rpm
data points	400	
duration	120	sec

Material characteristics :

Type	Vehicle	Load	
Solids SG	2.41	2.59	g/cm^3

Type	Co-disposed tails
pH	11.5
vehicle : load	50:50

dry solids mass basis

Test number	Description	Pan no.	Pan mass (g)	Start mass (g)	Wet mass (g)	End mass (g)	Dry mass (g)	% solids (%)	Density (kg/l)	Dilution (ml)	Vehicle volume (litre)	Load mass (kg)
Vehicle starting point		20	25.1140	57.4650	32.3510	46.2810	21.1670	65.4292	1.6202	0	0.3100	0.3349
		22	24.4290	47.4410	23.0120	39.4930	15.0640	65.4615	1.6207			
		14	24.9150	59.5320	34.6170	47.5640	22.6490	65.4274	1.6202			
								65.4394	***1.6204***			

						Dry solids Vehicle mass (kg)	Dry solids Load mass (kg)		Dry solids Vehicle mass %	Dry solids Load mass %									
					from Dilution sheet	**0.3287**	**0.3349**		**49.5**	**50.5**									
Test number	Description	Dilution (ml)	Vehicle volume (litre)	Vehicle % solids (%)	Vehicle density (kg/l)	Vehicle mass (kg)	Load mass (kg)	Co-disposed mass (kg)	New vehicle mass %	New load mass %	Load volume (litre)	Co-disposed volume (litre)	Co-disposed density (kg/l)	Co-disposed SG (kg/l)	Co-disposed % solids	Max Torque (mNm)	Yield stress (Pa)	pH before	pH after	pH ave	
Test 8	Rep 1	21.2 alkali	0.3592	59.6017	1.5354	0.5515	**0.3349**	0.8864	62.2202	37.7798	0.1293	0.4885	1.8145	2.4780	75.26	7.7800		11.56	11.41	11.49	small vane
Test 9	Rep 2	28 water														6.9900					
Test 10	Rep 3															8.0400					
																7.60	***691.75***				
Test 11	Rep 1	0.4 alkali	0.3742	58.0236	1.5139	0.5665	**0.3349**	0.9014	62.8489	37.1511	0.1293	0.5035	1.7903	2.4769	74.03	34.3000		11.51	11.33	11.42	medium vane
Test 12	Rep 2	14.6 water														36.1000					
Test 13	Rep 3															34.5000					
																34.97	***521.22***				
Test 14	Rep 1	1 alkali	0.3902	56.4299	1.4929	0.5825	**0.3349**	0.9174	63.4969	36.5031	0.1293	0.5195	1.7659	2.4757	72.76	23.7000		11.64	11.42	11.53	medium vane
Test 15	Rep 2	15 water														26.0000					
Test 16	Rep 3															26.5000					
																25.40	***378.62***				
Test 17	Rep 1	0.6 alkali	0.4082	54.7385	1.4711	0.6005	**0.3349**	0.9354	64.1993	35.8007	0.1293	0.5375	1.7403	2.4744	71.39	17.0000		11.59	11.40	11.50	medium vane
Test 18	Rep 2	17.4 water														18.1000					
Test 19	Rep 3															17.4000					
																17.50	***260.86***				
Test 20	Rep 1	1 alkali	0.4292	52.8890	1.4481	0.6215	**0.3349**	0.9564	64.9854	35.0146	0.1293	0.5585	1.7124	2.4730	69.85	14.3000		11.65	11.46	11.56	medium vane
Test 21	Rep 2	20 water														15.3000					
Test 22	Rep 3															17.4000					
																15.67	***233.53***				
Test 23	Rep 1	1 alkali	0.4562	50.6871	1.4216	0.6485	**0.3349**	0.9834	65.9468	34.0532	0.1293	0.5855	1.6796	2.4713	67.96	8.5300		11.66	11.52	11.59	medium vane
Test 24	Rep 2	26 water														9.0600					
Test 25	Rep 3															8.5200					
																8.70	***129.73***				
Test 26	Rep 1	32 water	0.4882	48.3036	1.3939	0.6805	**0.3349**	1.0154	67.0200	32.9800	0.1293	0.6175	1.6444	2.4694	65.86	4.4900		11.50	11.50	11.50	medium vane
Test 27	Rep 2															5.7400					
Test 28	Rep 3															5.9100					
																5.38	***80.20***				

Ave. pH 11.51

Co-disposed Tailings - Slump tests

pH = 11.6
vehicle (wet) : load (dry) = 60:40
vehicle (dry) : load (dry) = 50:50

Date : 09/06/2004

Slump cylinder :
small cylinder

height	0.130	m
diameter	0.105	m
aspect ratio	1.24	
ruler thickness	9.2	mm

Material characteristics :

Type	Vehicle	Load	
Solids SG	2.41	2.59	g/cm^3

Type	Co-disposed tails
pH	11.6
vehicle : load	50:50

dry solids mass basis

Test number	Description	Pan no.	Pan mass (g)	Start mass (g)	Wet mass (g)	End mass (g)	Dry mass (g)	% solids (%)	Density (kg/l)	Dilution (ml)	Vehicle volume (litre)	Load mass (kg)
Vehicle starting point		20	25.112	37.9600	12.8480	33.5250	8.4130	65.4810	1.6210	0	1.1000	1.1889
		23	24.800	40.8940	16.0940	35.3440	10.5440	65.5151	1.6215			
								65.4981	***1.6213***			

	Dry solids Vehicle mass (kg)	Dry solids Load mass (kg)		Dry solids Vehicle mass %	Dry solids Load mass %
from Dilution sheet	**1.1681**	**1.1889**		**49.6**	**50.4**

Test number	Description	Dilution (ml)	Vehicle volume (litre)	Vehicle % solids (%)	Vehicle density (kg/l)	Vehicle mass (kg)	Load mass (kg)	Co-disposed mass (kg)	New vehicle mass %	New load mass %	Load volume (litre)	Co-disposed volume (litre)	Co-disposed density (kg/l)	Co-disposed SG (kg/l)	Co-disposed % solids	Slump height incl ruler (mm)	Slump height excl ruler (mm)	Yield stress (Pa)	Flow distance N	Flow distance S	Flow distance E	Flow distance W	Flow distance radius (mm) N	Flow distance radius (mm) S	Flow distance radius (mm) E	Flow distance radius (mm) W	average	pH before	pH after	pH ave
Test 1	Rep 1	60 alkali	1.2700	59.7979	1.5381	1.9534	**1.1889**	3.1424	62.1640	37.8360	0.4591	1.7291	1.8174	2.4781	75.40	48.45	39.25		1 start	1 start	0 start	3 start	65.64	65.64	55.56	85.73	68.14	12.05	11.37	11.71
	Rep 2	110 water														49.25	40.05		0 start	1 mid	0 mid	2 mid	55.56	70.68	60.38	80.73	66.84			
	Rep 3															50.60	41.40		1 start	1start	0 start	3 start	65.64	65.64	55.56	85.73	68.14			
																	40.23	***514.92***									***67.71***			
Test 2	Rep 1	5 alkali	1.3100	58.5980	1.5217	1.9934	**1.1889**	3.1824	62.6395	37.3605	0.4591	1.7691	1.7989	2.4772	74.47	59.25	50.05		0 mid	2 mid	1 mid	2 mid	60.38	80.73	70.68	80.73	73.13	11.63	11.33	11.48
	Rep 2	35 water														60.30	51.10		1 mid	1 mid	1 mid	2 mid	70.68	70.68	70.68	80.73	73.19			
	Rep 3															61.20	52.00		1 start	2 mid	2 mid	1 mid	65.64	80.73	80.73	70.68	74.45			
																	51.05	***428.96***									**73.59**			
Test 3	Rep 1	5 alkali	1.3600	57.1642	1.5025	2.0434	**1.1889**	3.2324	63.2175	36.7825	0.4591	1.8191	1.7769	2.4762	73.34	73.10	63.90		2 mid	3 start	1 mid	3 mid	80.73	85.73	70.68	90.38	81.88	11.77	11.29	11.53
	Rep 2	45 water														75.10	65.90		2 mid	2 mid	2 start	3 mid	80.73	80.73	75.76	90.38	81.90			
	Rep 3															74.30	65.10		2 mid	2 mid	2 start	3 mid	80.73	80.73	75.76	90.38	81.90			
																	64.97	***332.73***									**81.89**			
Test 4	Rep 1	5 alkali	1.4200	55.5336	1.4813	2.1034	**1.1889**	3.2924	63.8878	36.1122	0.4591	1.8791	1.7521	2.4750	72.03	81.10	71.90		4 start	3 mid	3 start	4 mid	95.76	90.38	85.73	100.8	93.16	11.75	11.37	11.56
	Rep 2	55 water														83.60	74.40		3 mid	3 mid	3 mid	4 start	90.38	90.38	90.38	95.76	91.73			
	Rep 3															84.10	74.90		4 start	3 mid	3 start	4 mid	95.76	90.38	85.73	100.8	93.16			
																	73.73	***276.46***									**92.68**			
Test 5	Rep 1	3 alkali	1.4950	53.6216	1.4571	2.1784	**1.1889**	3.3674	64.6921	35.3079	0.4591	1.9541	1.7233	2.4736	70.45	90.35	81.15		6 mid	4 mid	6 start	5 mid	120.7	100.8	115.9	111.1	112.11	11.63	11.39	11.51
	Rep 2	72 water														90.30	81.10		6 start	5 mid	5 mid	6 mid	115.9	111.1	111.1	120.7	114.69			
	Rep 3															91.80	82.60		5 mid	5 mid	5 mid	5 mid	111.1	111.1	111.1	111.1	111.13			
																	81.62	***228.77***									**112.64**			
Test 6	Rep 1	4 alkali	1.5890	51.4035	1.4301	2.2724	**1.1889**	3.4614	65.6510	34.3490	0.4591	2.0481	1.6901	2.4718	68.57	102.40	93.20		7 mid	6 mid	8 mid	7 mid	130.8	120.7	140.4	130.8	130.67	11.69	11.46	11.58
	Rep 2	90 water														101.40	92.20		7 start	7 mid	7 mid	8 start	125.8	130.8	130.8	135.8	130.81			
	Rep 3															102.70	93.50		7 mid	6 mid	7 mid	8 mid	130.8	120.7	130.8	140.4	130.67			
																	92.97	***166.89***									**130.72**			
Test 7	Rep 1	4 alkali	1.7070	48.8660	1.4004	2.3904	**1.1889**	3.5794	66.7833	33.2167	0.4591	2.1661	1.6525	2.4698	66.35	107.40	98.20		9 mid	10 mid	9 mid	10 mid	150.5	160.6	150.5	160.6	155.53	11.73	11.46	11.60
	Rep 2	114 water														111.00	111.0		10 start	9 mid	10 mid	11 start	155	150.5	160.6	164.9	157.75			
	Rep 3															112.20	112.2		11 start	10 mid	11 start	11 start	164.9	160.6	164.9	164.9	163.81			
																	107.13	***97.67***									**159.03**			

Ave. pH *11.57*

APPENDIX M : CO-DISPOSED TAILINGS VANE TESTS – TORQUE-TIME CURVES

Co-disposed tailings – pH 8.6, v : l = 86:14 %

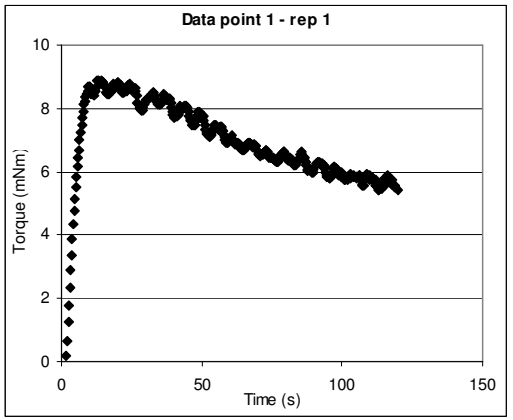

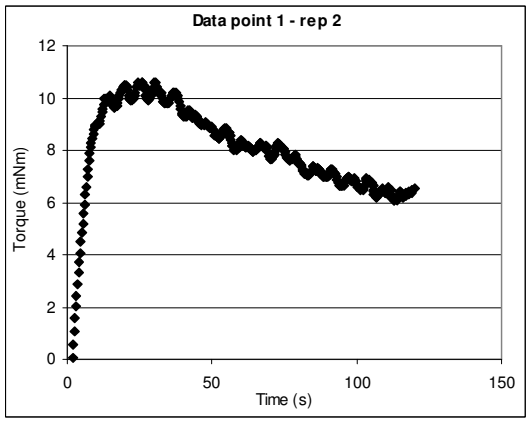

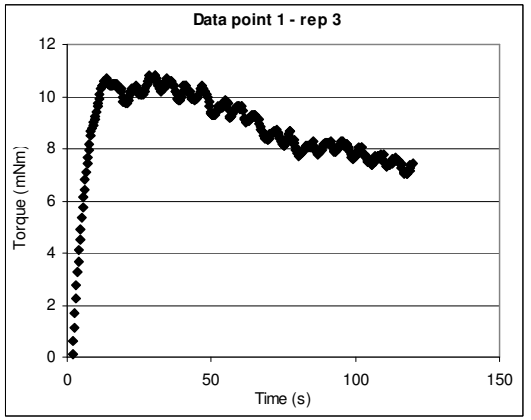

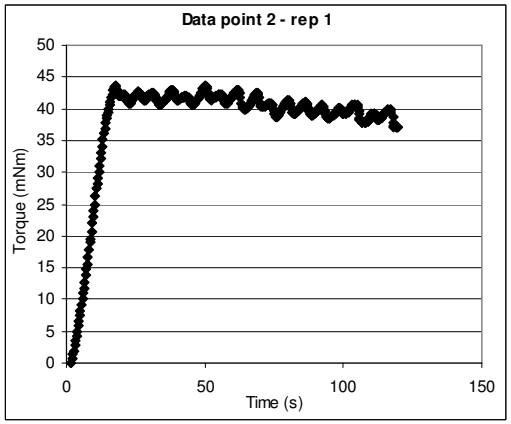

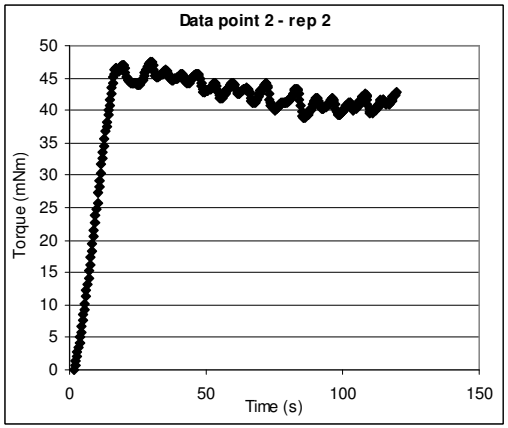

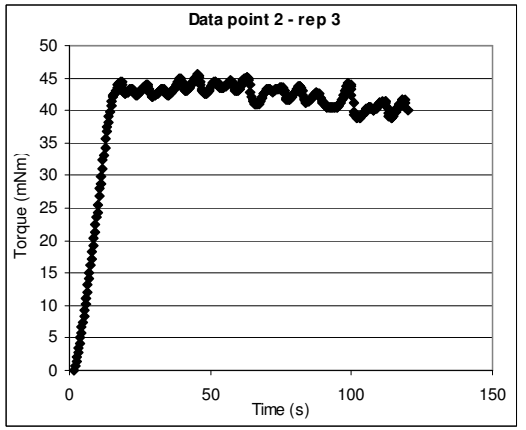

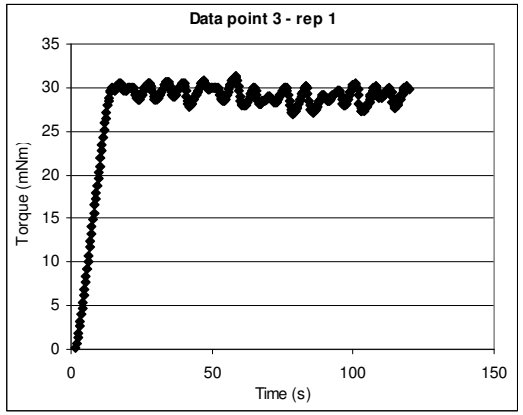
Data point 3 - rep 1
Torque (mNm)
Time (s)
0
5
10
15
20
25
30
35
0
50
100
150

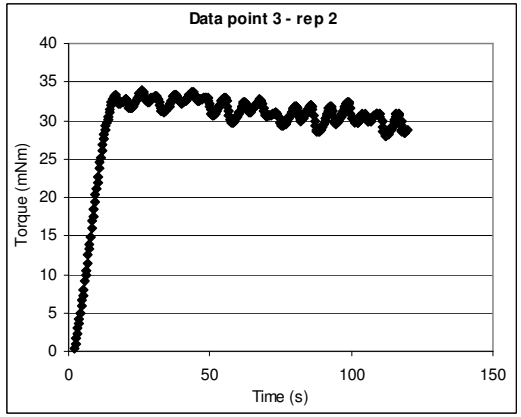
Data point 3 - rep 2
Torque (mNm)
Time (s)
0
5
10
15
20
25
30
35
40
0
50
100
150

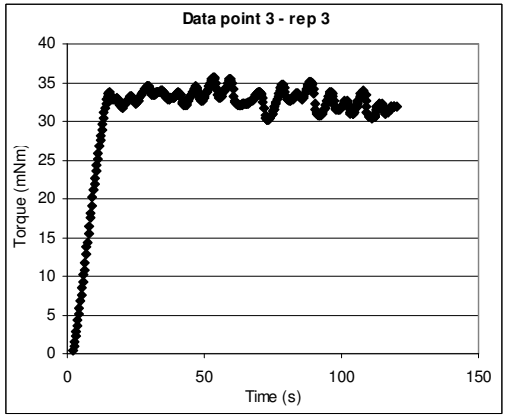
Data point 3 - rep 3
Torque (mNm)
Time (s)
0
5
10
15
20
25
30
35
40
0
50
100
150

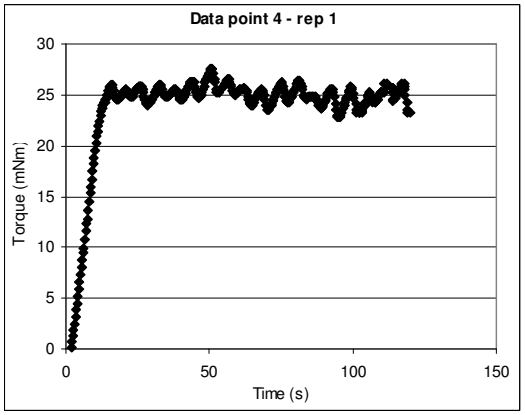
Data point 4 - rep 1
Torque (mNm)
Time (s)
0
5
10
15
20
25
30
0
50
100
150

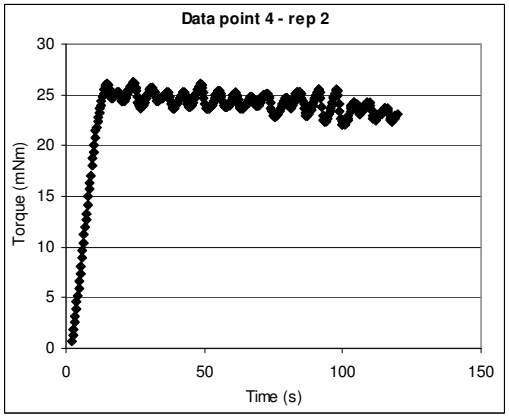
Data point 4 - rep 2
Torque (mNm)
Time (s)
0
5
10
15
20
25
30
0
50
100
150

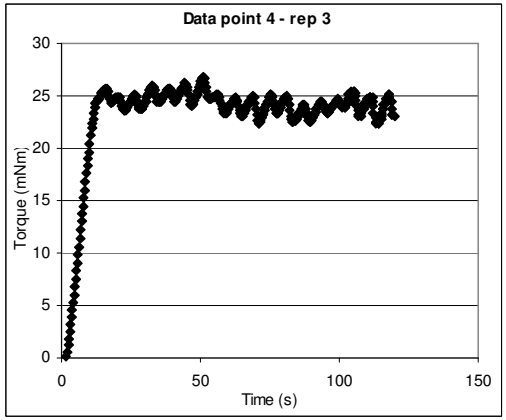
Data point 4 - rep 3
Torque (mNm)
Time (s)
0
5
10
15
20
25
30
0
50
100
150

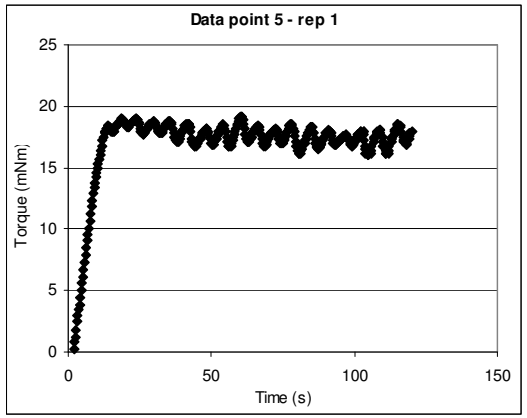
Data point 5 - rep 1
Torque (mNm)
Time (s)
0
5
10
15
20
25
0
50
100
150

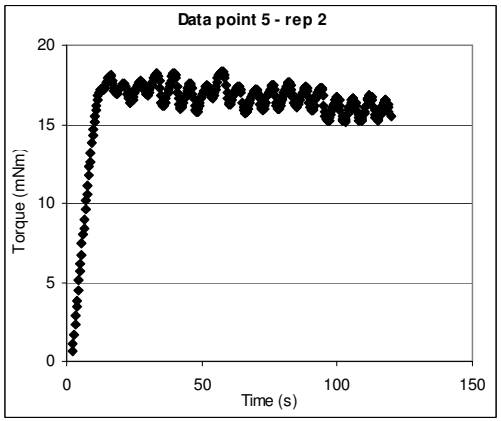
Data point 5 - rep 2
Torque (mNm)
Time (s)
0
5
10
15
20
0
50
100
150

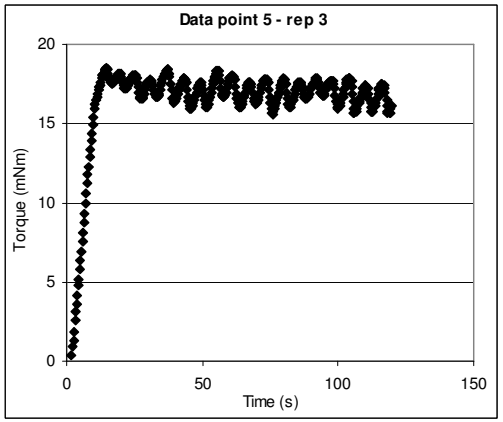
Data point 5 - rep 3
Torque (mNm)
Time (s)
0
5
10
15
20
0
50
100
150

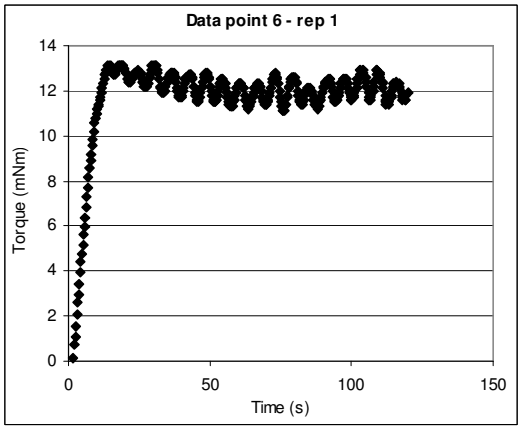
Data point 6 - rep 1
Torque (mNm)
Time (s)
0
2
4
6
8
10
12
14
0
50
100
150

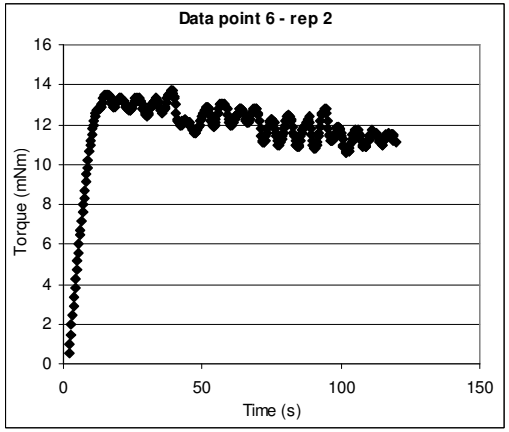
Data point 6 - rep 2
Torque (mNm)
Time (s)
0
2
4
6
8
10
12
14
16
0
50
100
150

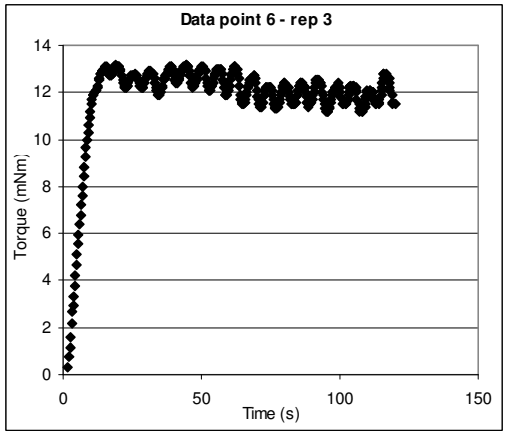
Data point 6 - rep 3
Torque (mNm)
Time (s)
0
2
4
6
8
10
12
14
0
50
100
150

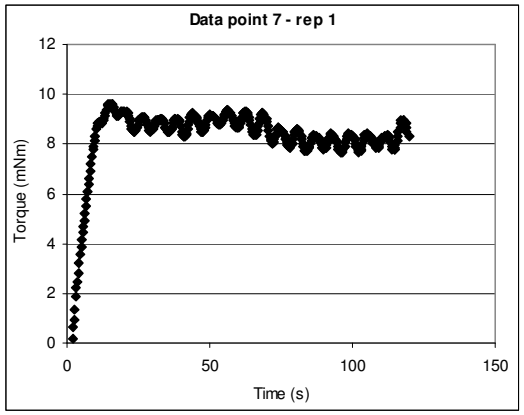
Data point 7 - rep 1
Torque (mNm)
Time (s)
0
2
4
6
8
10
12
0
50
100
150

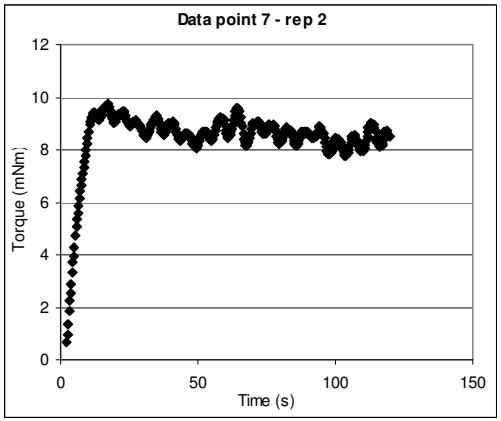
Data point 7 - rep 2
Torque (mNm)
Time (s)
0
2
4
6
8
10
12
0
50
100
150

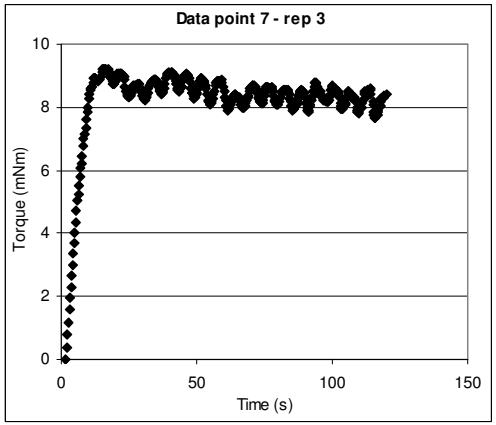
Data point 7 - rep 3
Torque (mNm)
Time (s)
0
2
4
6
8
10
0
50
100
150

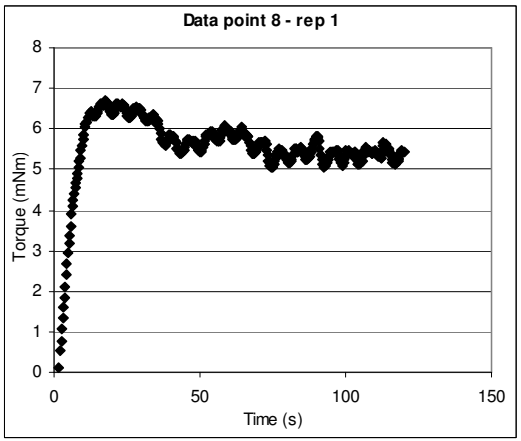
Data point 8 - rep 1
Torque (mNm)
Time (s)
0
1
2
3
4
5
6
7
8
0
50
100
150

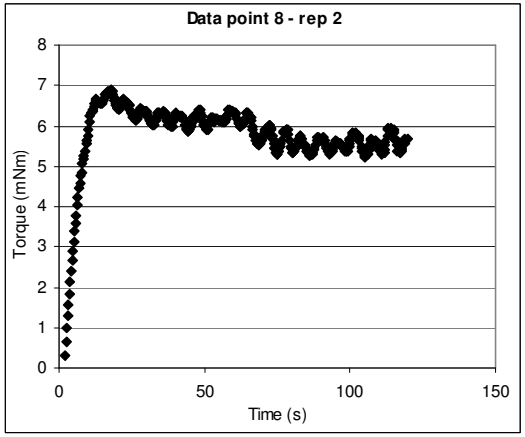
Data point 8 - rep 2
Torque (mNm)
Time (s)
0
1
2
3
4
5
6
7
8
0
50
100
150

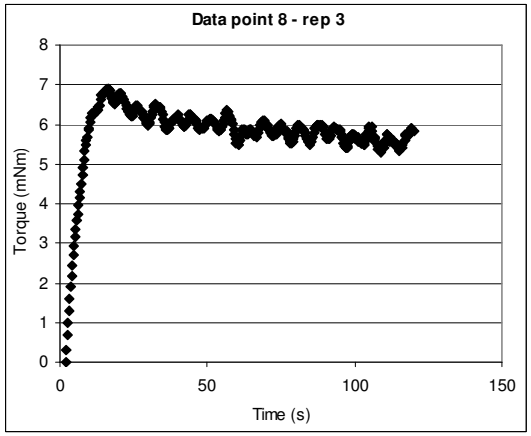
Data point 8 - rep 3
Torque (mNm)
Time (s)
0
1
2
3
4
5
6
7
8
0
50
100
150

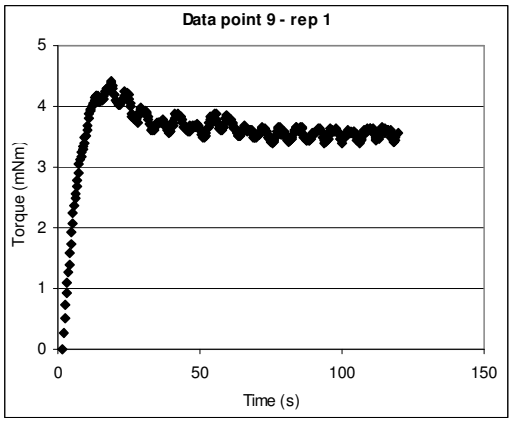
Data point 9 - rep 1
Torque (mNm)
Time (s)
0
1
2
3
4
5
0
50
100
150

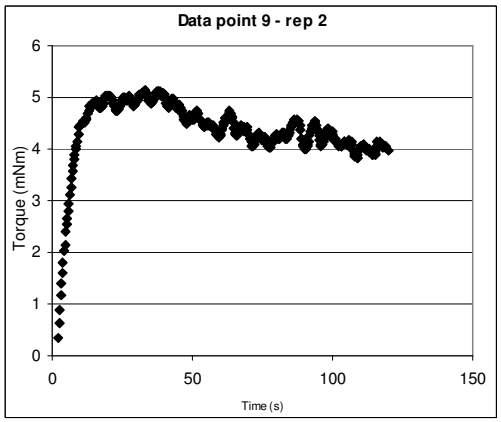
Data point 9 - rep 2
Torque (mNm)
Time (s)
0
1
2
3
4
5
6
0
50
100
150

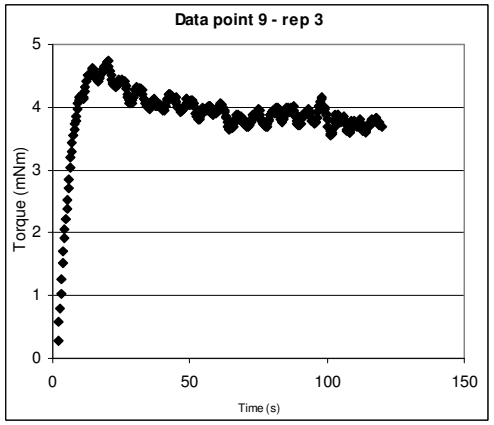
Data point 9 - rep 3
Torque (mNm)
Time (s)
0
1
2
3
4
5
0
50
100
150

Co-disposed tailings – pH 8.6, v : l = 60:40 %

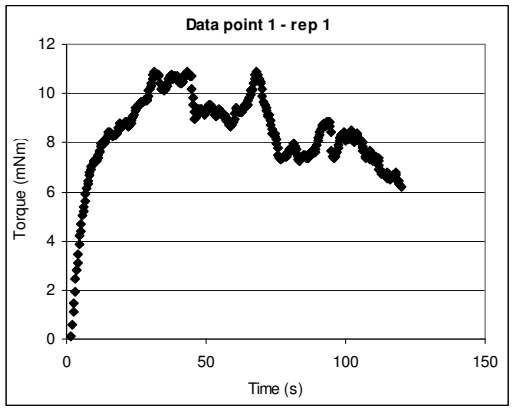

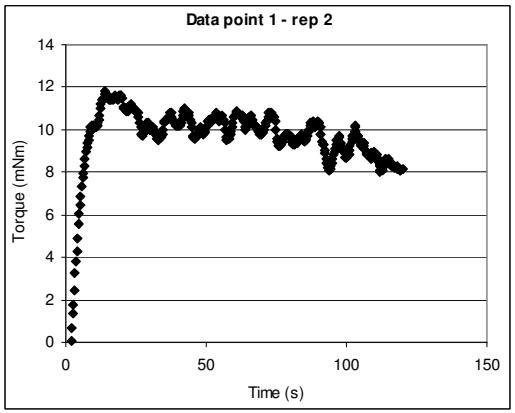

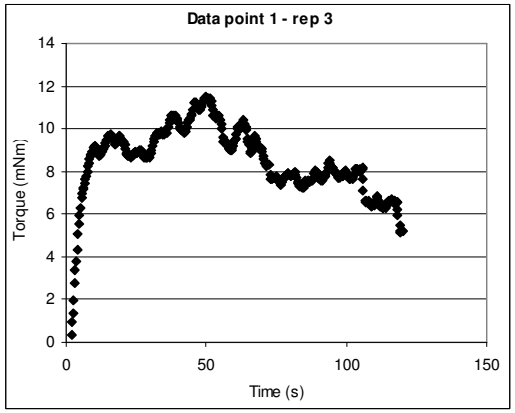

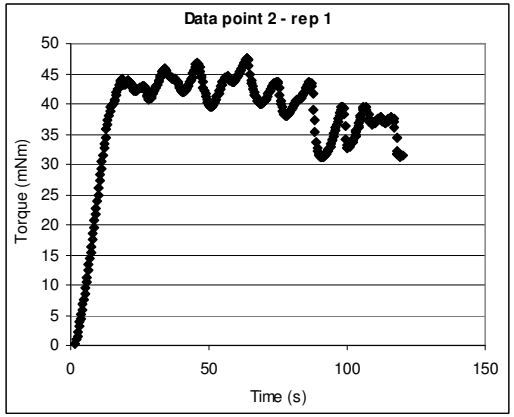

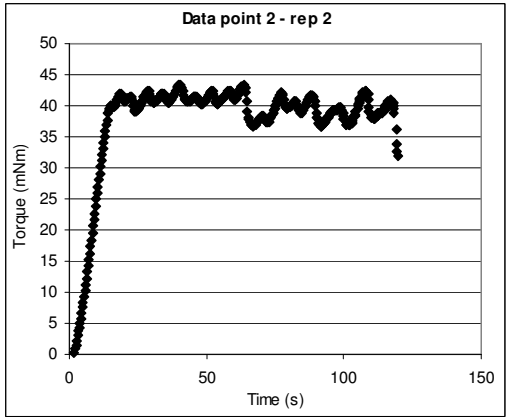

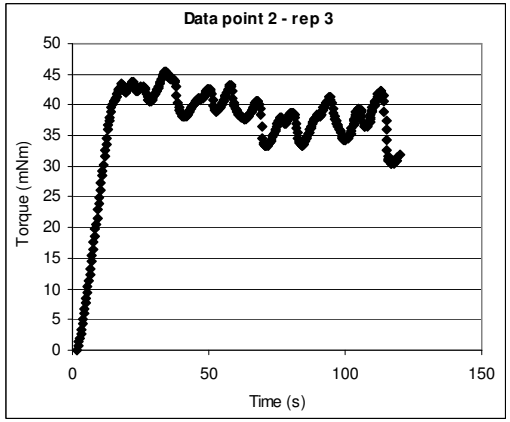

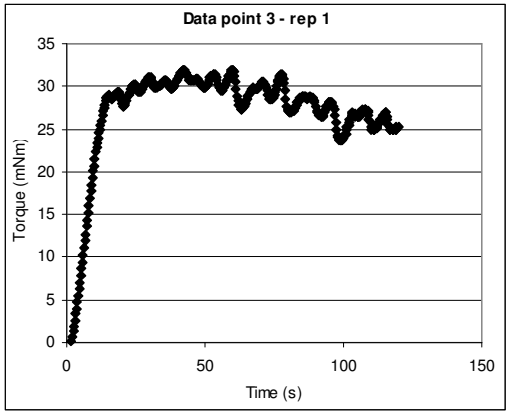
Data point 3 - rep 1
Torque (mNm)
Time (s)
0
5
10
15
20
25
30
35
0
50
100
150

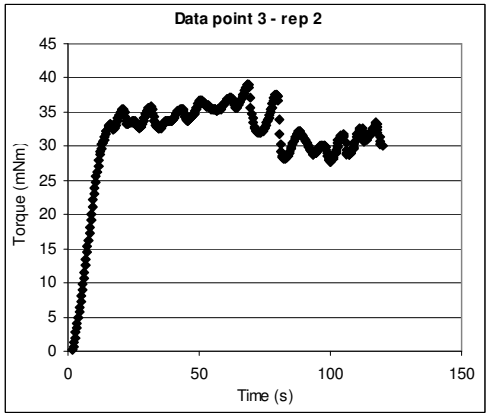
Data point 3 - rep 2
Torque (mNm)
Time (s)
0
5
10
15
20
25
30
35
40
45
0
50
100
150

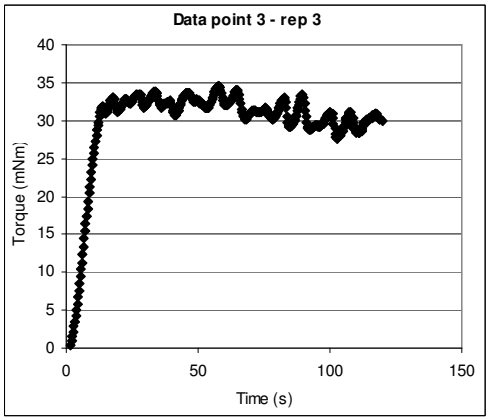
Data point 3 - rep 3
Torque (mNm)
Time (s)
0
5
10
15
20
25
30
35
40
0
50
100
150

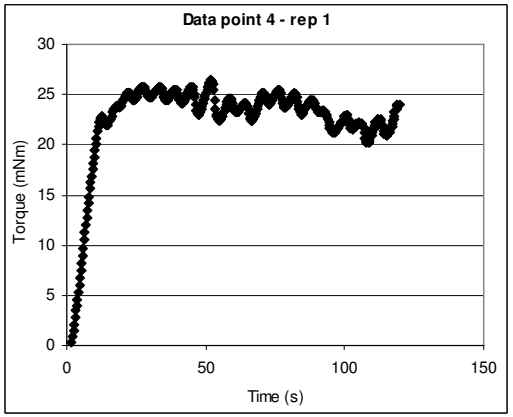
Data point 4 - rep 1
Torque (mNm)
Time (s)
0
5
10
15
20
25
30
0
50
100
150

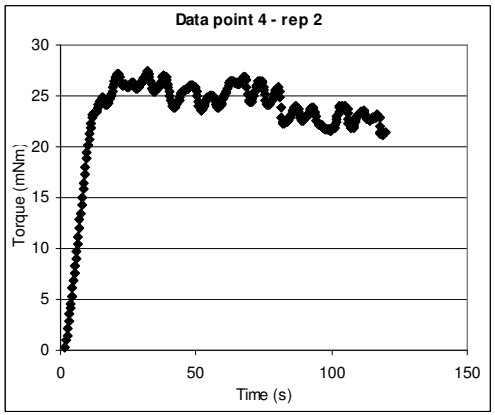
Data point 4 - rep 2
Torque (mNm)
Time (s)
0
5
10
15
20
25
30
0
50
100
150

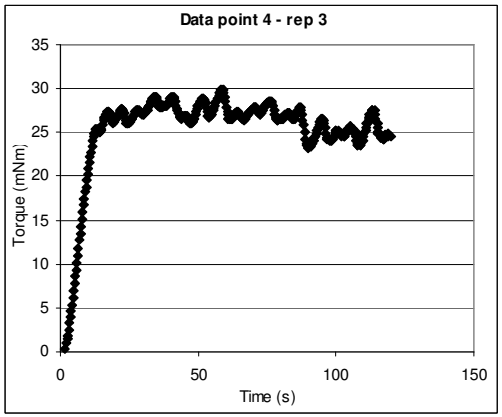
Data point 4 - rep 3
Torque (mNm)
Time (s)
0
5
10
15
20
25
30
35
0
50
100
150

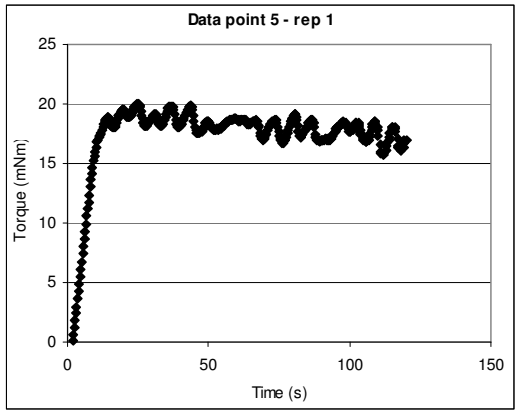
Data point 5 - rep 1
Torque (mNm)
Time (s)
0
5
10
15
20
25
0
50
100
150

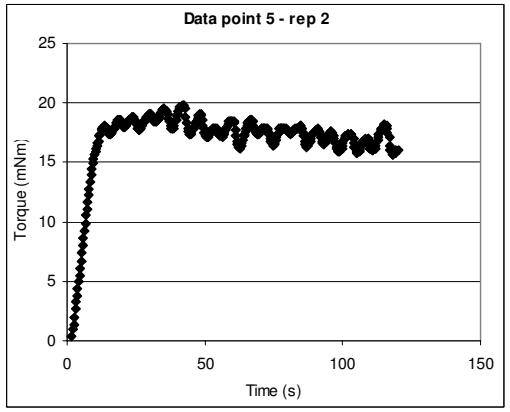
Data point 5 - rep 2
Torque (mNm)
Time (s)
0
5
10
15
20
25
0
50
100
150

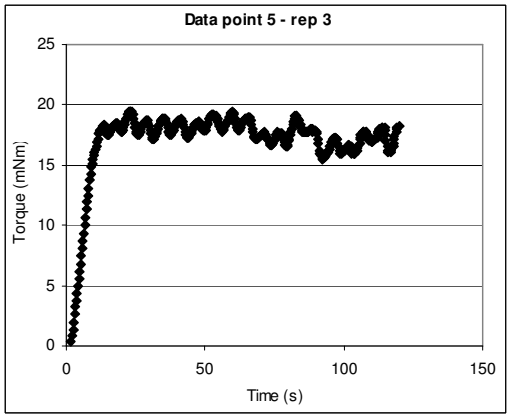
Data point 5 - rep 3
Torque (mNm)
Time (s)
0
5
10
15
20
25
0
50
100
150

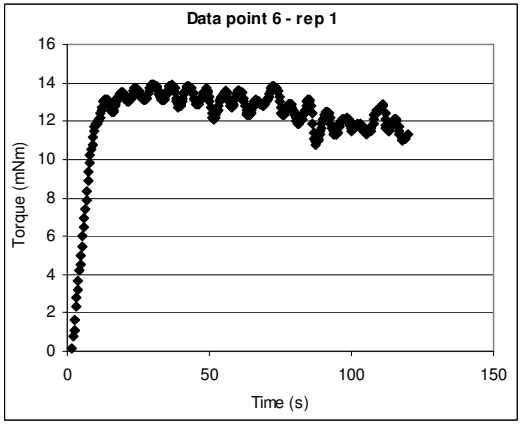
Data point 6 - rep 1
Torque (mNm)
Time (s)
0
2
4
6
8
10
12
14
16
0
50
100
150

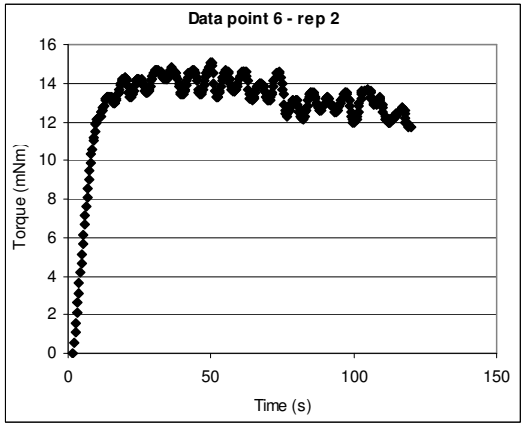
Data point 6 - rep 2
Torque (mNm)
Time (s)
0
2
4
6
8
10
12
14
16
0
50
100
150

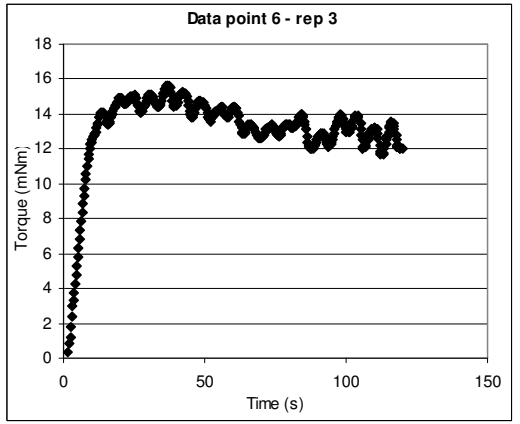
Data point 6 - rep 3
Torque (mNm)
Time (s)
0
2
4
6
8
10
12
14
16
18
0
50
100
150

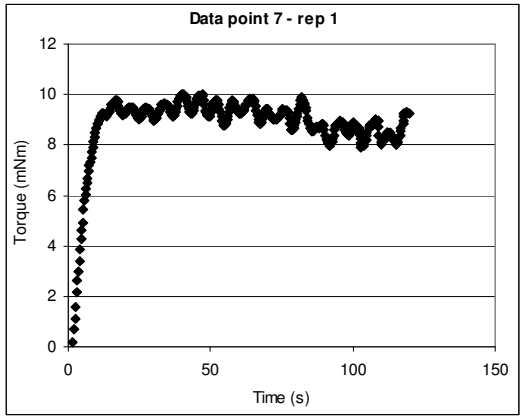
Data point 7 - rep 1
Torque (mNm)
Time (s)
0
2
4
6
8
10
12
0
50
100
150

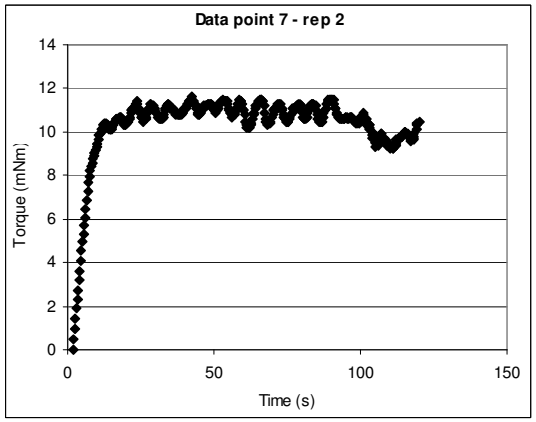
Data point 7 - rep 2
Torque (mNm)
Time (s)
0
2
4
6
8
10
12
14
0
50
100
150

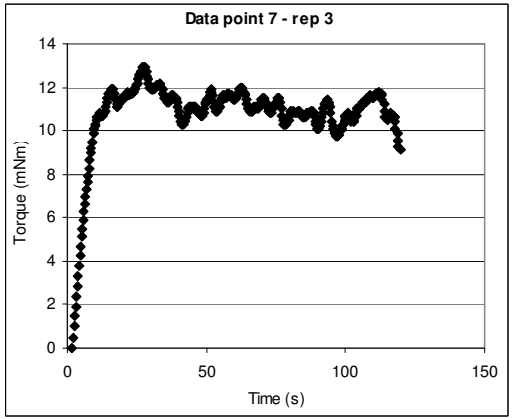
Data point 7 - rep 3
Torque (mNm)
Time (s)
0
2
4
6
8
10
12
14
0
50
100
150

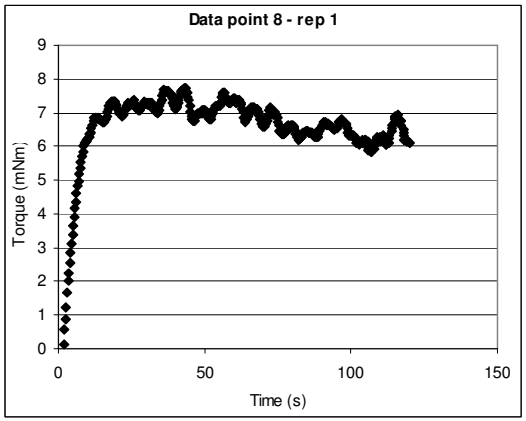
Data point 8 - rep 1
Torque (mNm)
Time (s)
0
1
2
3
4
5
6
7
8
9
0
50
100
150

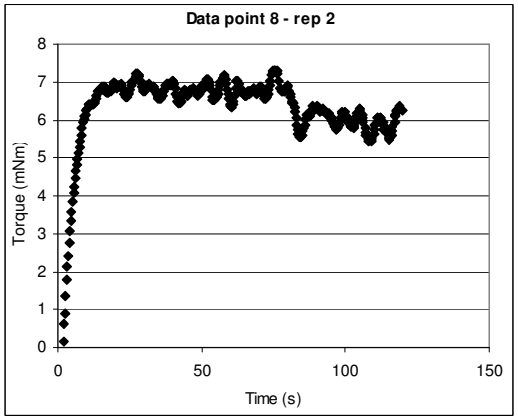
Data point 8 - rep 2
Torque (mNm)
Time (s)
0
1
2
3
4
5
6
7
8
0
50
100
150

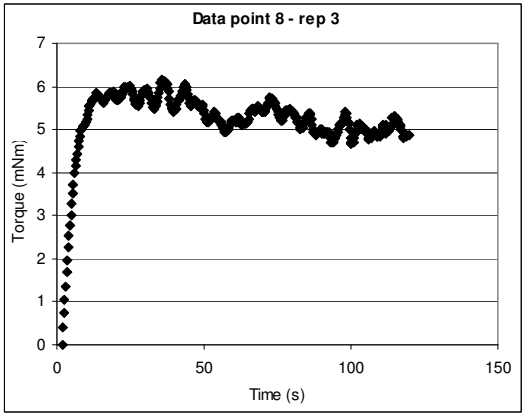
Data point 8 - rep 3
Torque (mNm)
Time (s)
0
1
2
3
4
5
6
7
0
50
100
150

Co-disposed tailings – pH 8.6, v : l = 50:50 %

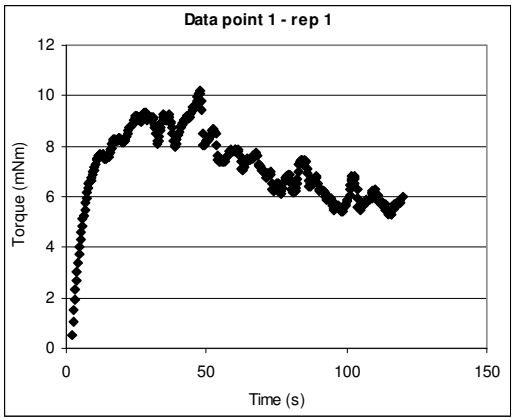

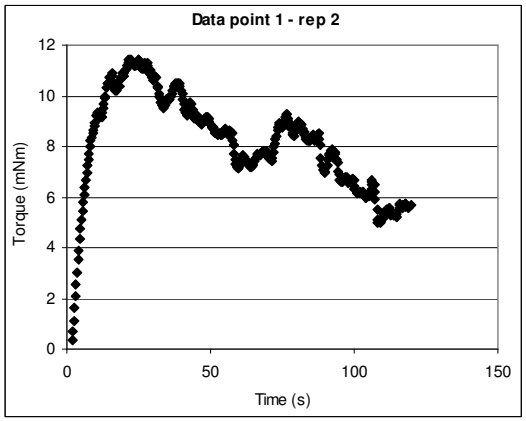

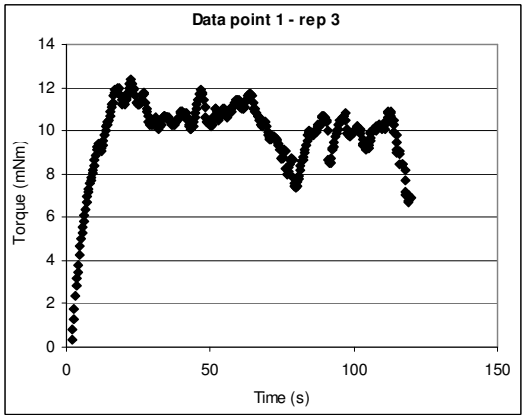

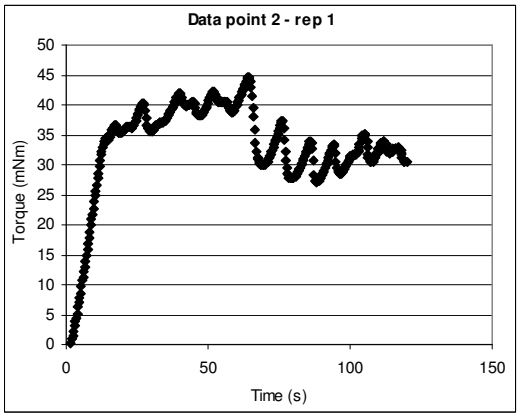

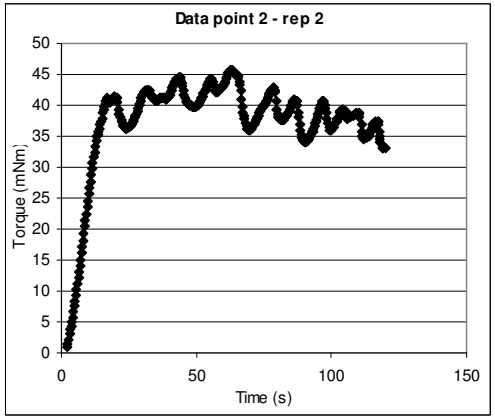

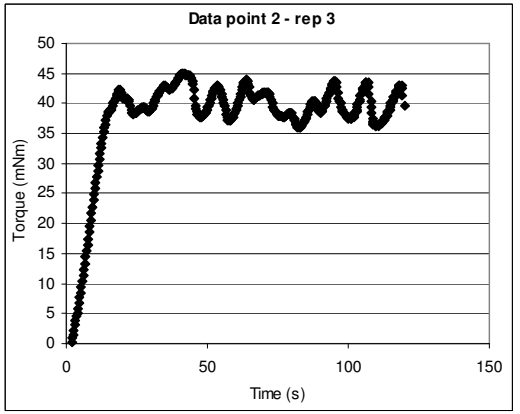

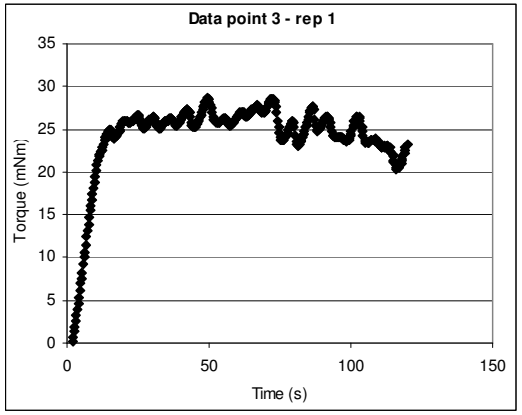
Data point 3 - rep 1
Torque (mNm)
Time (s)
0
5
10
15
20
25
30
35
0
50
100
150

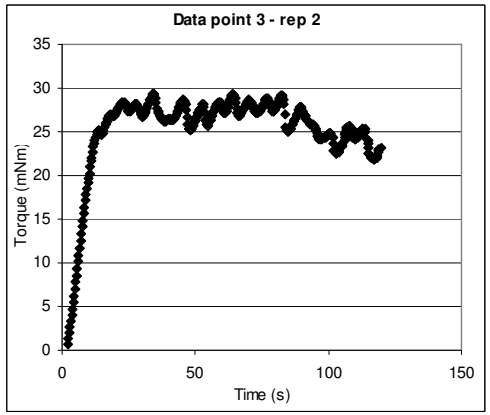
Data point 3 - rep 2
Torque (mNm)
Time (s)
0
5
10
15
20
25
30
35
0
50
100
150

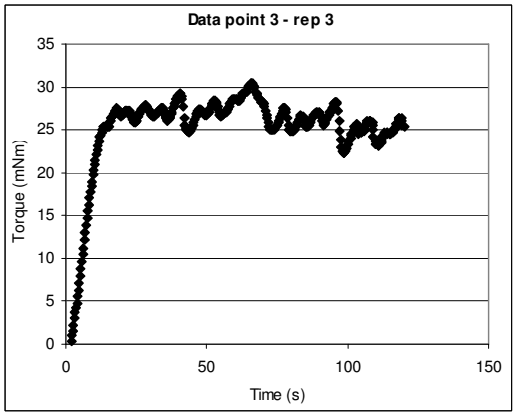
Data point 3 - rep 3
Torque (mNm)
Time (s)
0
5
10
15
20
25
30
35
0
50
100
150

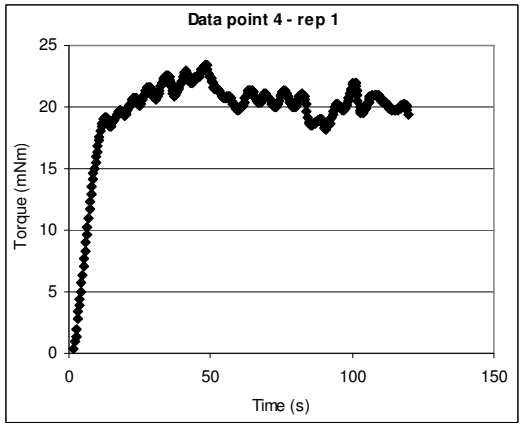
Data point 4 - rep 1
Torque (mNm)
Time (s)
0
5
10
15
20
25
0
50
100
150

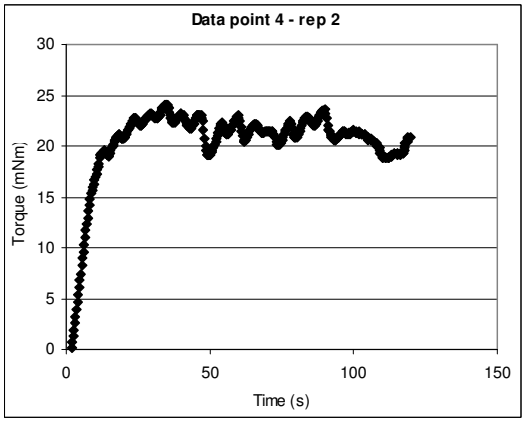
Data point 4 - rep 2
Torque (mNm)
Time (s)
0
5
10
15
20
25
30
0
50
100
150

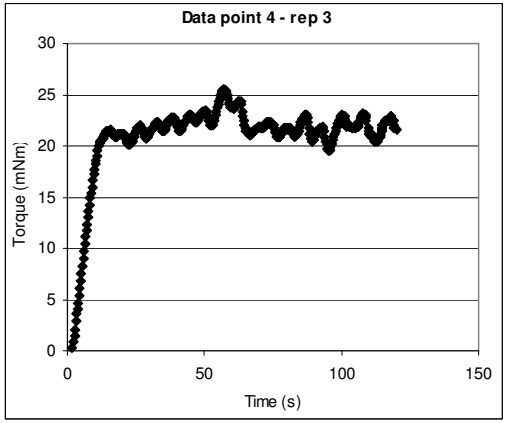
Data point 4 - rep 3
Torque (mNm)
Time (s)
0
5
10
15
20
25
30
0
50
100
150

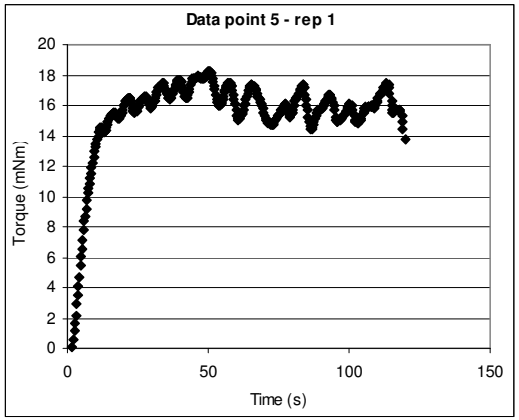
Data point 5 - rep 1
Torque (mNm)
Time (s)
0
2
4
6
8
10
12
14
16
18
20
0
50
100
150

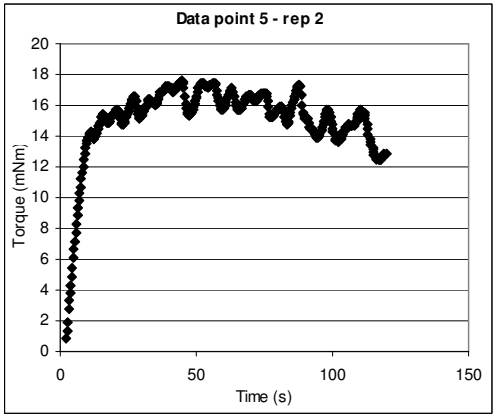
Data point 5 - rep 2
Torque (mNm)
Time (s)
0
2
4
6
8
10
12
14
16
18
20
0
50
100
150

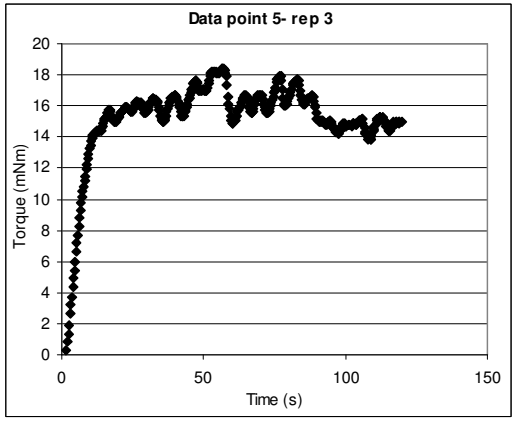
Data point 5- rep 3
Torque (mNm)
Time (s)
0
2
4
6
8
10
12
14
16
18
20
0
50
100
150

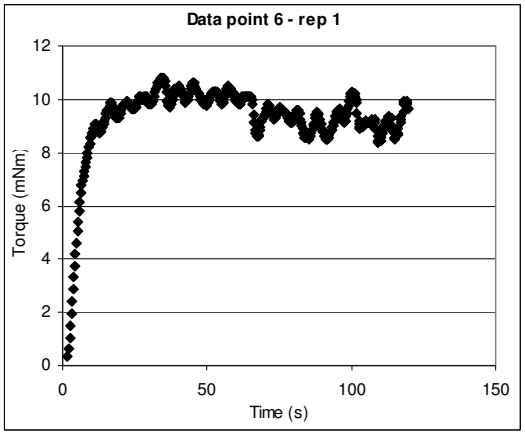
Data point 6 - rep 1
Torque (mNm)
Time (s)
0
2
4
6
8
10
12
0
50
100
150

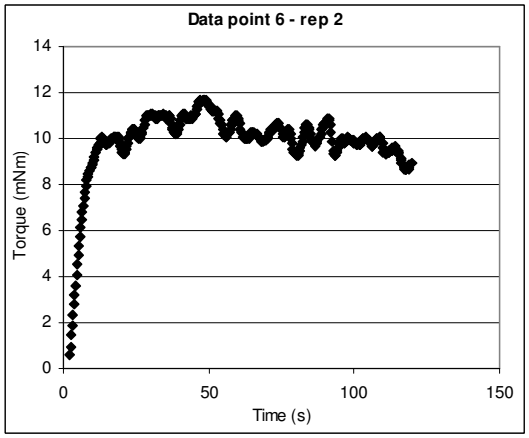
Data point 6 - rep 2
Torque (mNm)
Time (s)
0
2
4
6
8
10
12
14
0
50
100
150

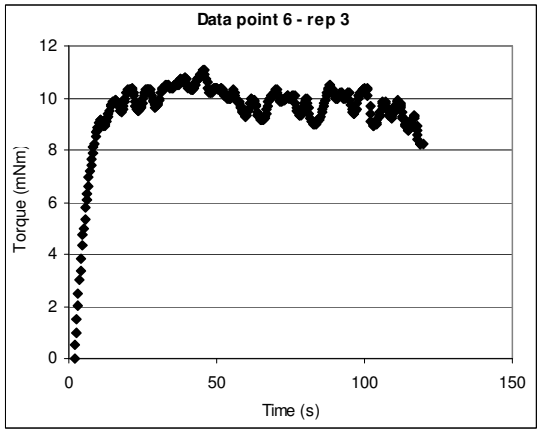
Data point 6 - rep 3
Torque (mNm)
Time (s)
0
2
4
6
8
10
12
0
50
100
150

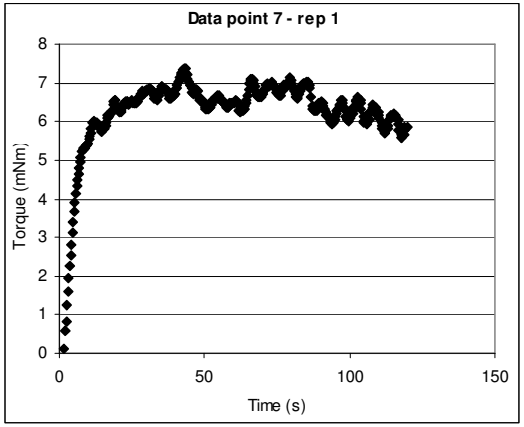
Data point 7 - rep 1
Torque (mNm)
Time (s)
0
1
2
3
4
5
6
7
8
0
50
100
150

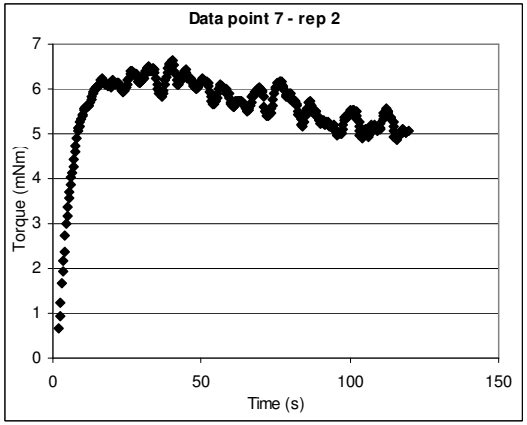
Data point 7 - rep 2
Torque (mNm)
Time (s)
0
1
2
3
4
5
6
7
0
50
100
150

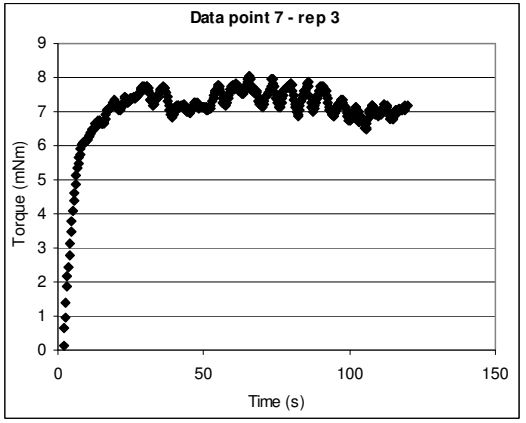
Data point 7 - rep 3
Torque (mNm)
Time (s)
0
1
2
3
4
5
6
7
8
9
0
50
100
150

Co-disposed tailings – pH 6.2, v : l = 86:14 %

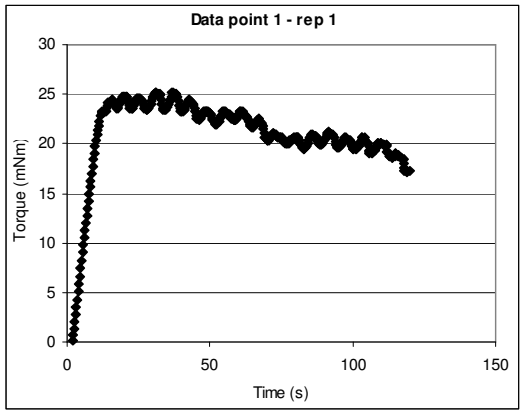

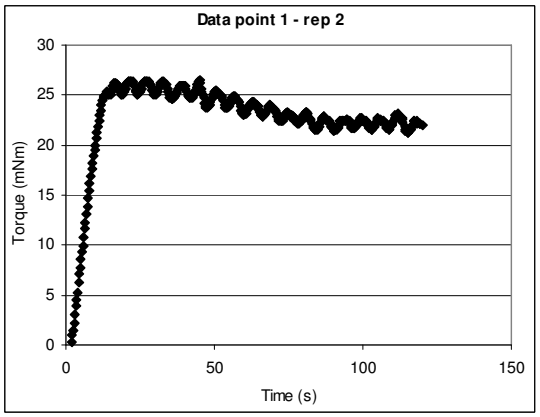

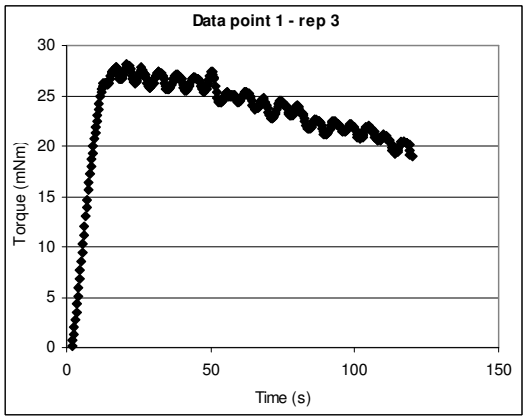

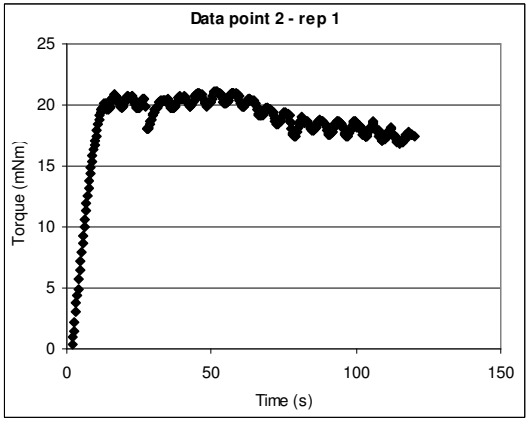

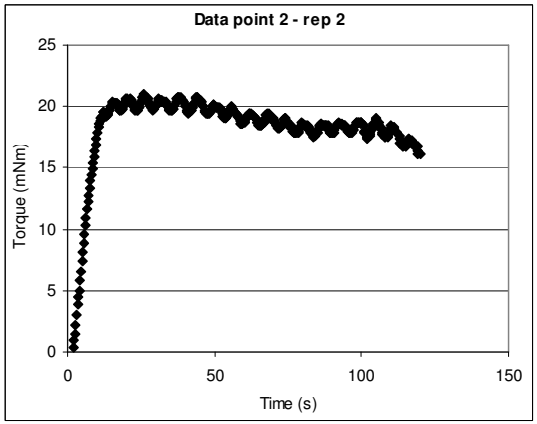

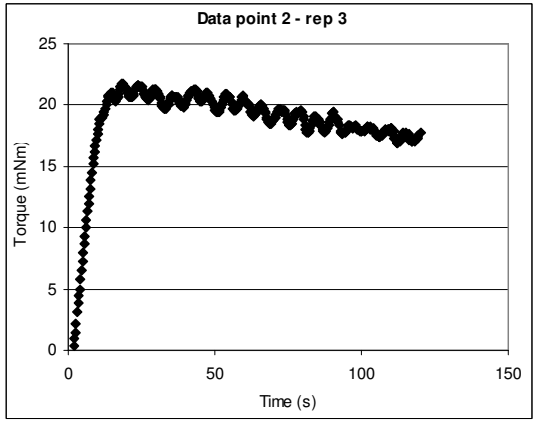

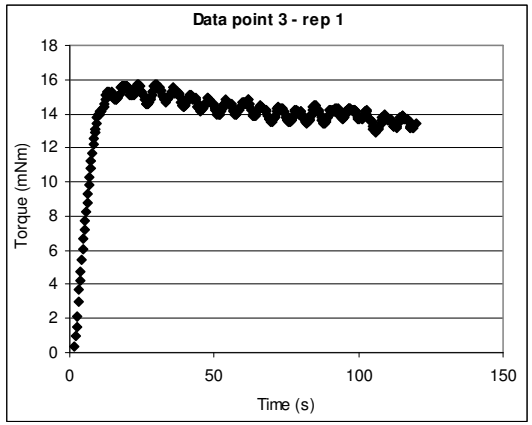
Data point 3 - rep 1
Torque (mNm)
Time (s)
0
2
4
6
8
10
12
14
16
18
0
50
100
150

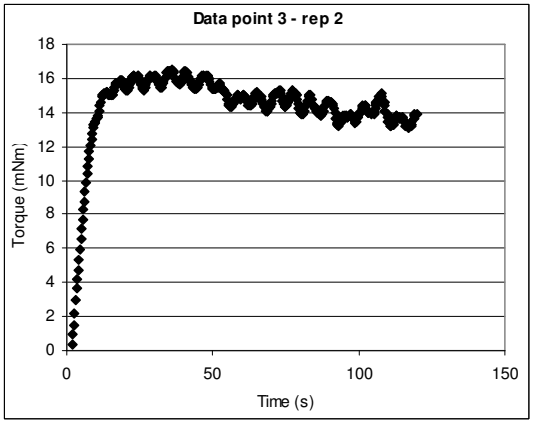
Data point 3 - rep 2
Torque (mNm)
Time (s)
0
2
4
6
8
10
12
14
16
18
0
50
100
150

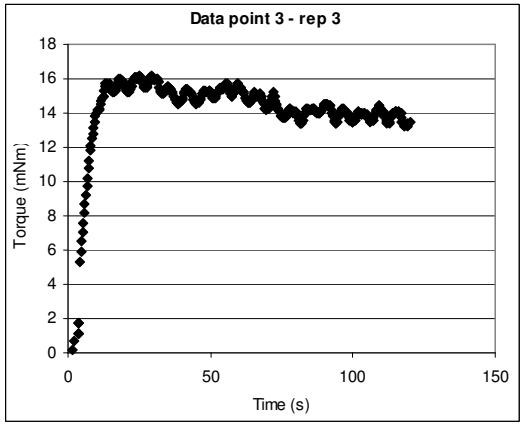
Data point 3 - rep 3
Torque (mNm)
Time (s)
0
2
4
6
8
10
12
14
16
18
0
50
100
150

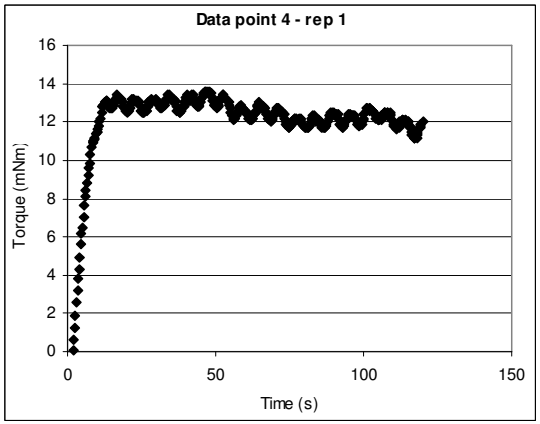
Data point 4 - rep 1
Torque (mNm)
Time (s)
0
2
4
6
8
10
12
14
16
0
50
100
150

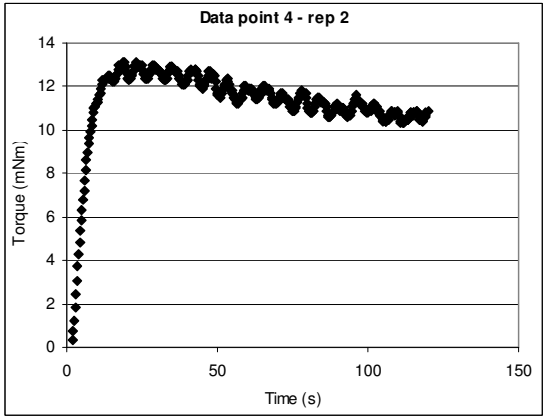
Data point 4 - rep 2
Torque (mNm)
Time (s)
0
2
4
6
8
10
12
14
0
50
100
150

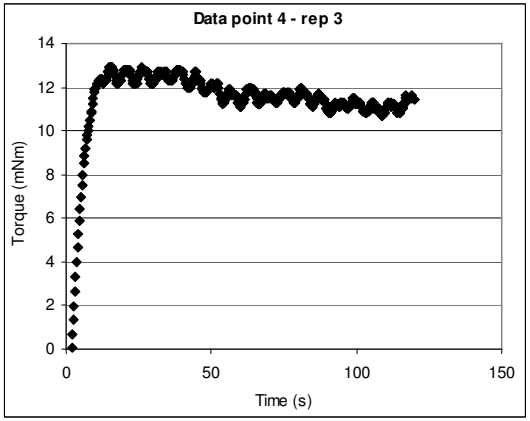
Data point 4 - rep 3
Torque (mNm)
Time (s)
0
2
4
6
8
10
12
14
0
50
100
150

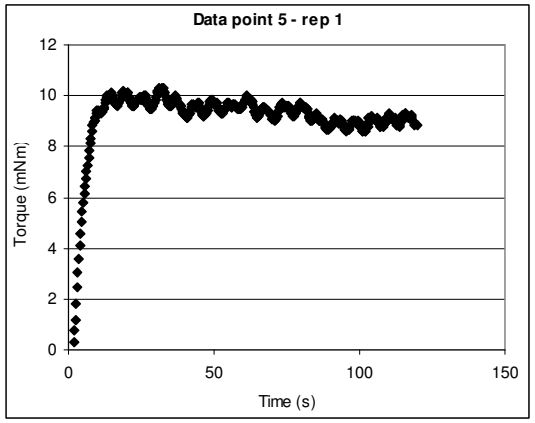
Data point 5 - rep 1
Torque (mNm)
Time (s)
0
2
4
6
8
10
12
0
50
100
150

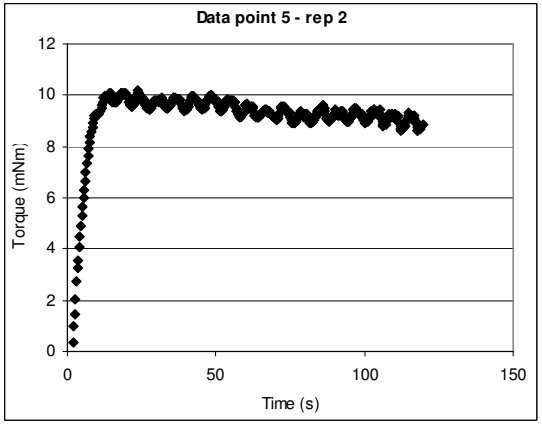
Data point 5 - rep 2
Torque (mNm)
Time (s)
0
2
4
6
8
10
12
0
50
100
150

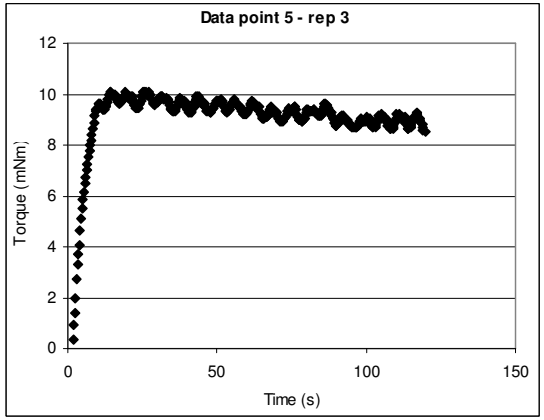
Data point 5 - rep 3
Torque (mNm)
Time (s)
0
2
4
6
8
10
12
0
50
100
150

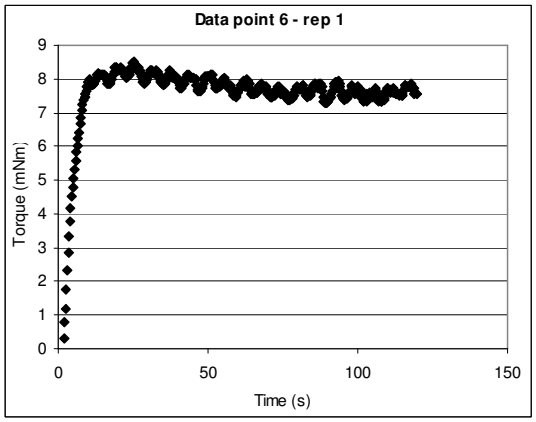
Data point 6 - rep 1
Torque (mNm)
Time (s)
0
1
2
3
4
5
6
7
8
9
0
50
100
150

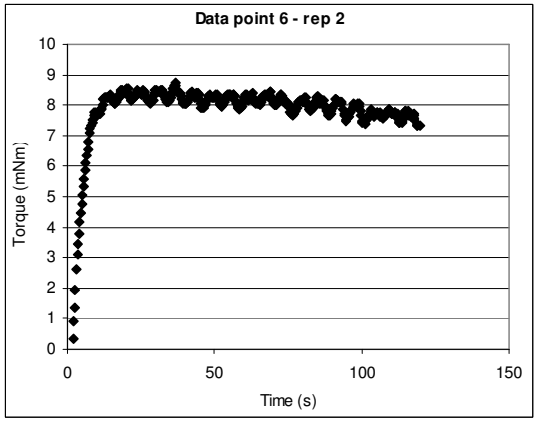
Data point 6 - rep 2
Torque (mNm)
Time (s)
0
1
2
3
4
5
6
7
8
9
10
0
50
100
150

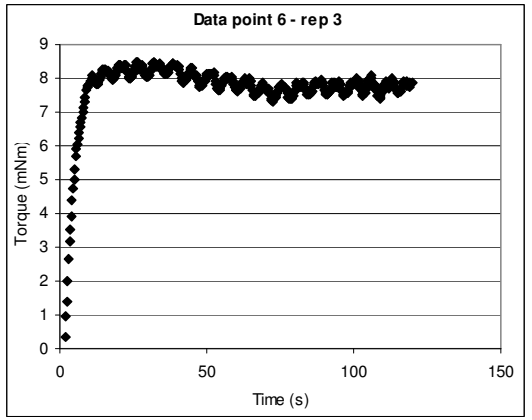
Data point 6 - rep 3
Torque (mNm)
Time (s)
0
1
2
3
4
5
6
7
8
9
0
50
100
150

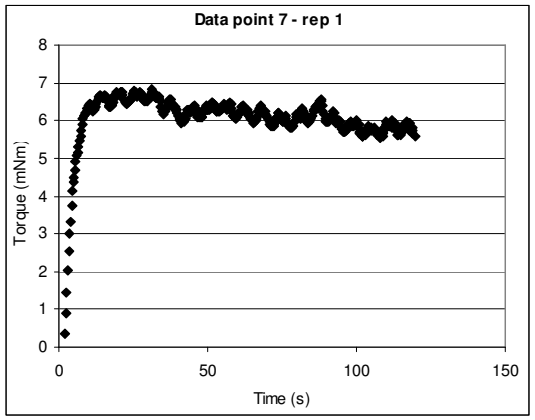
Data point 7 - rep 1
Torque (mNm)
Time (s)
0
1
2
3
4
5
6
7
8
0
50
100
150

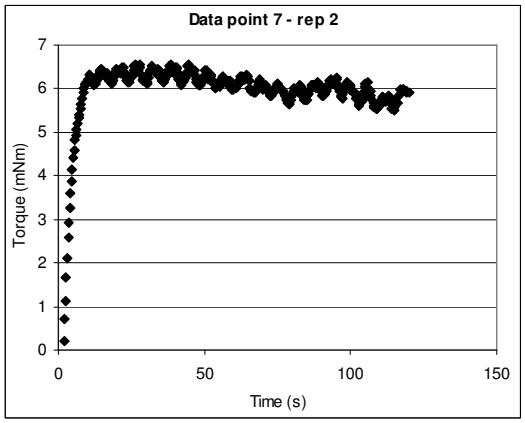
Data point 7 - rep 2
Torque (mNm)
Time (s)
0
1
2
3
4
5
6
7
0
50
100
150

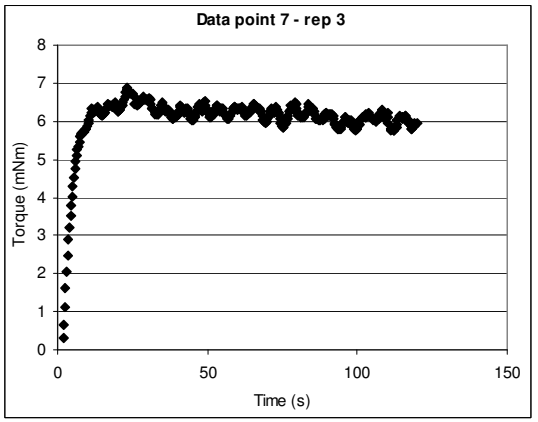
Data point 7 - rep 3
Torque (mNm)
Time (s)
0
1
2
3
4
5
6
7
8
0
50
100
150

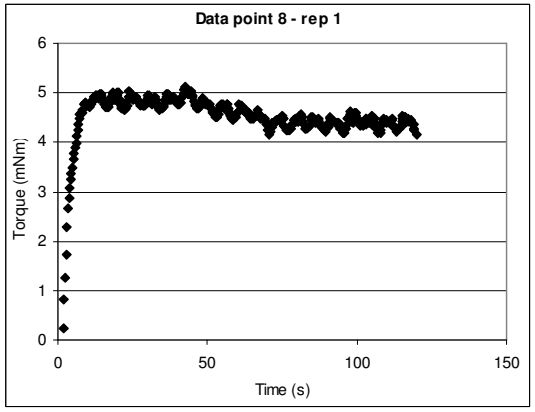
Data point 8 - rep 1
Torque (mNm)
Time (s)
0
1
2
3
4
5
6
0
50
100
150

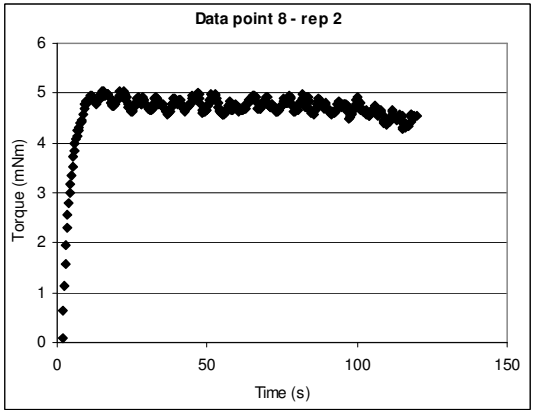
Data point 8 - rep 2
Torque (mNm)
Time (s)
0
1
2
3
4
5
6
0
50
100
150

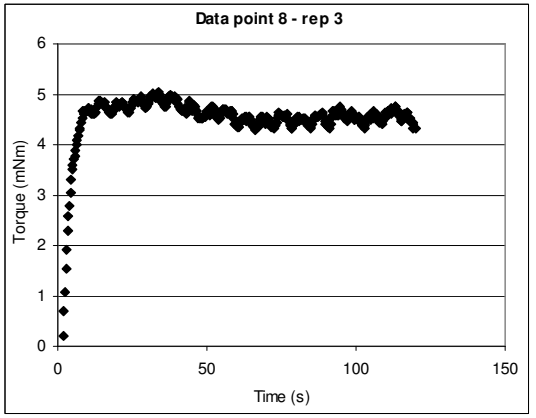
Data point 8 - rep 3
Torque (mNm)
Time (s)
0
1
2
3
4
5
6
0
50
100
150

Co-disposed tailings – pH 6.2, v : l = 60:40 %

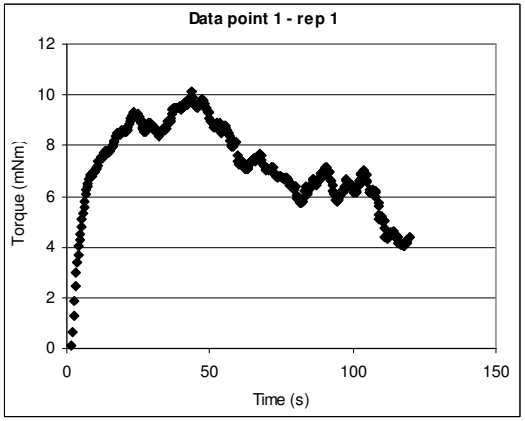

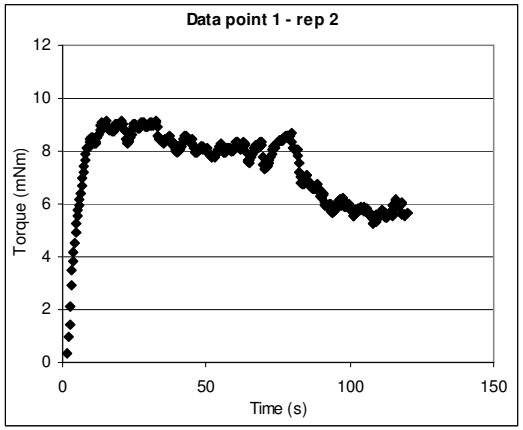

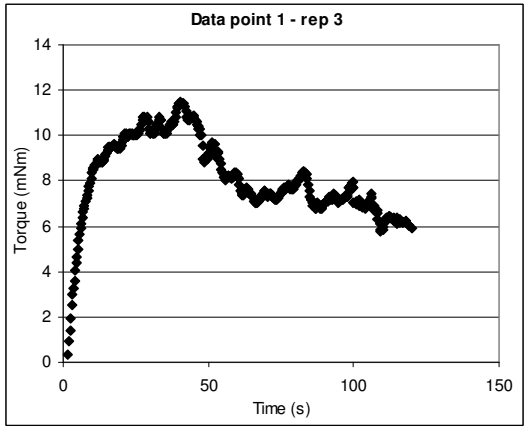

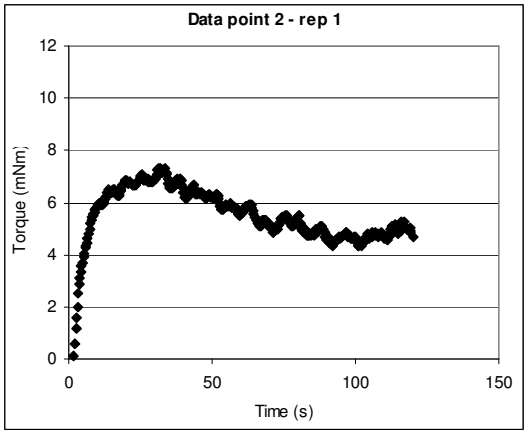

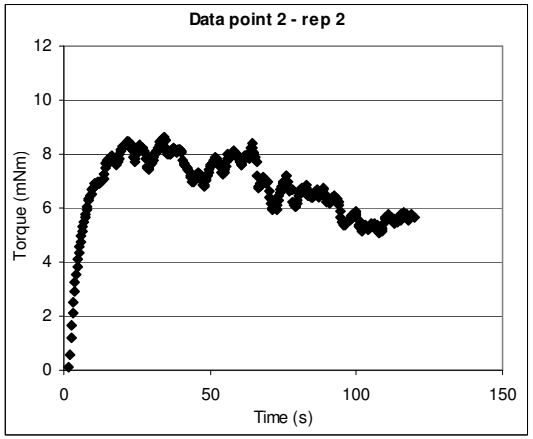

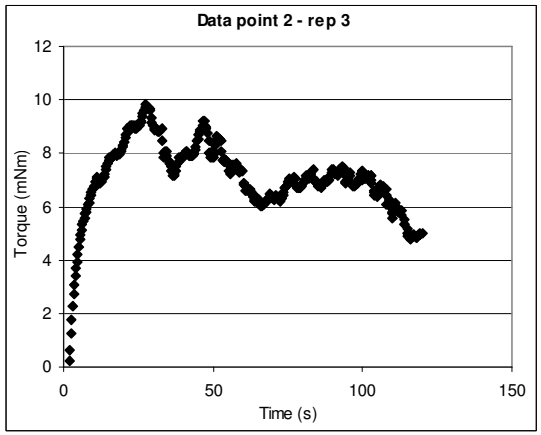

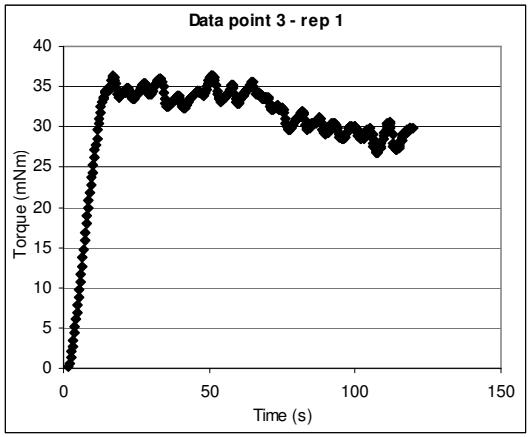
Data point 3 - rep 1
Torque (mNm)
Time (s)
0
5
10
15
20
25
30
35
40
0
50
100
150

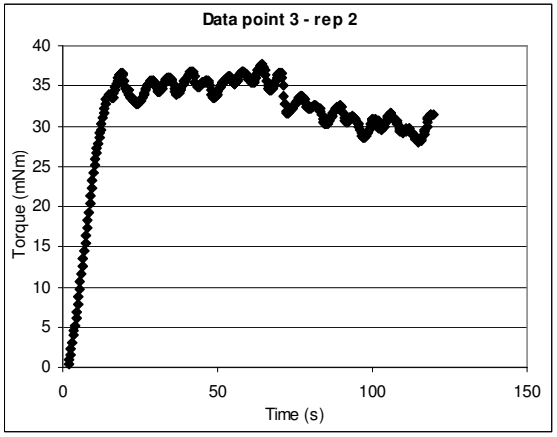
Data point 3 - rep 2
Torque (mNm)
Time (s)
0
5
10
15
20
25
30
35
40
0
50
100
150

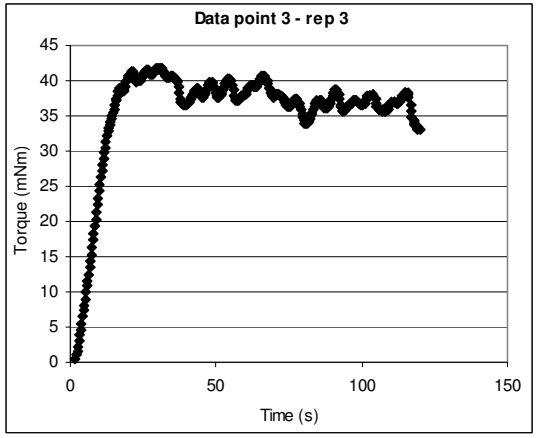
Data point 3 - rep 3
Torque (mNm)
Time (s)
0
5
10
15
20
25
30
35
40
45
0
50
100
150

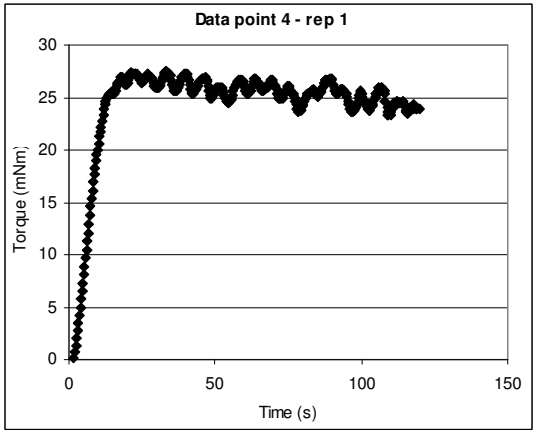
Data point 4 - rep 1
Torque (mNm)
Time (s)
0
5
10
15
20
25
30
0
50
100
150

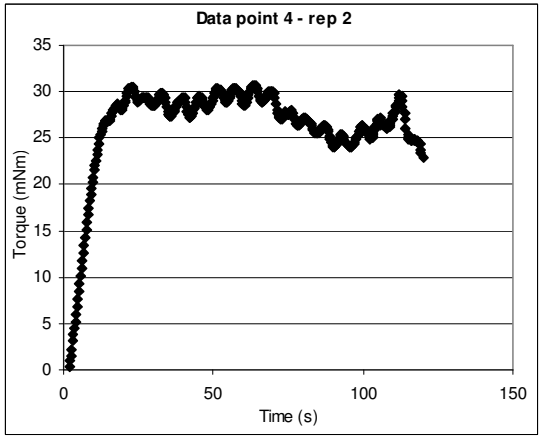
Data point 4 - rep 2
Torque (mNm)
Time (s)
0
5
10
15
20
25
30
35
0
50
100
150

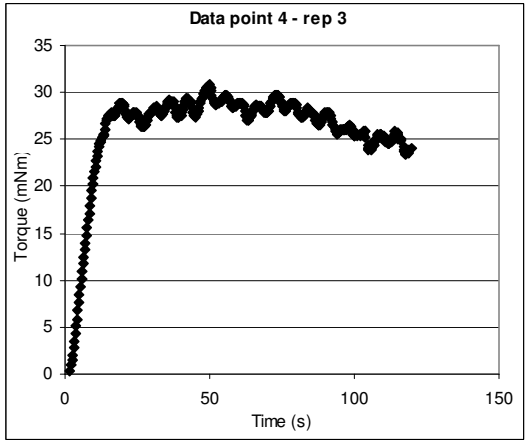
Data point 4 - rep 3
Torque (mNm)
Time (s)
0
5
10
15
20
25
30
35
0
50
100
150

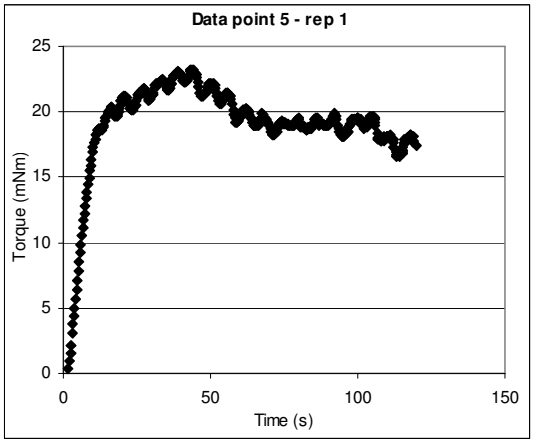
Data point 5 - rep 1
Torque (mNm)
Time (s)
0
5
10
15
20
25
0
50
100
150

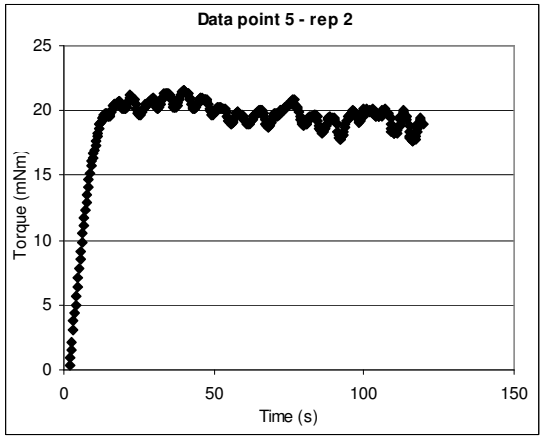
Data point 5 - rep 2
Torque (mNm)
Time (s)
0
5
10
15
20
25
0
50
100
150

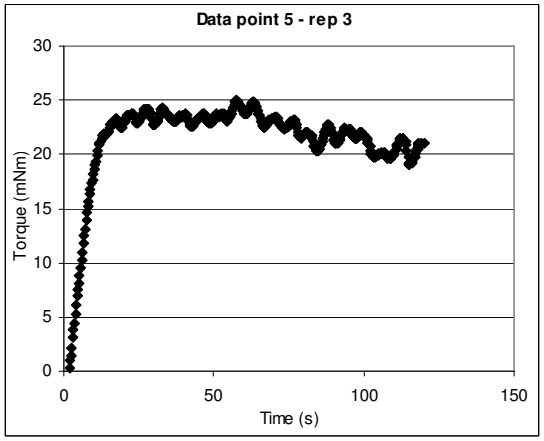
Data point 5 - rep 3
Torque (mNm)
Time (s)
0
5
10
15
20
25
30
0
50
100
150

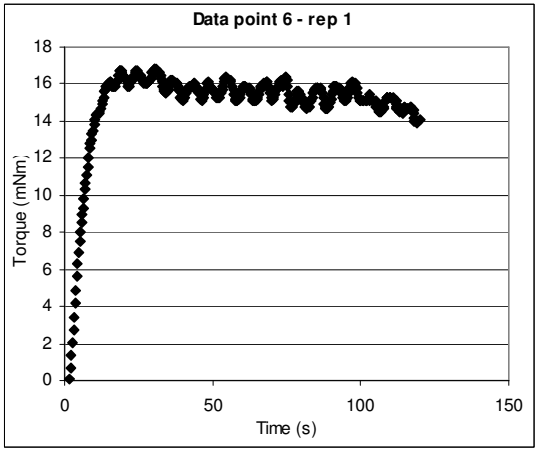
Data point 6 - rep 1
Torque (mNm)
Time (s)
0
2
4
6
8
10
12
14
16
18
0
50
100
150

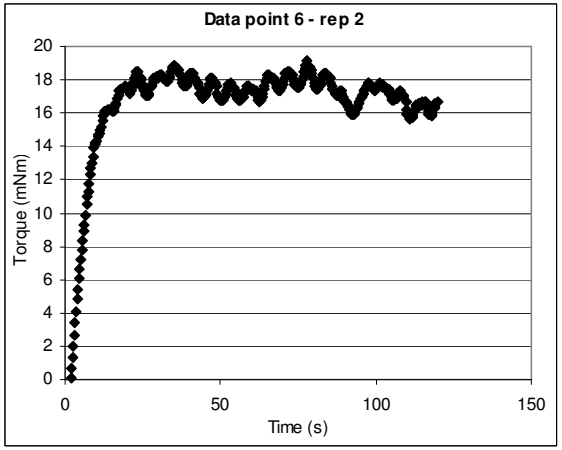
Data point 6 - rep 2
Torque (mNm)
Time (s)
0
2
4
6
8
10
12
14
16
18
20
0
50
100
150

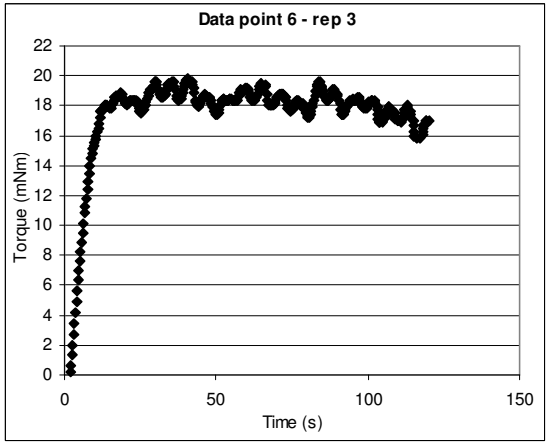
Data point 6 - rep 3
Torque (mNm)
Time (s)
0
2
4
6
8
10
12
14
16
18
20
22
0
50
100
150

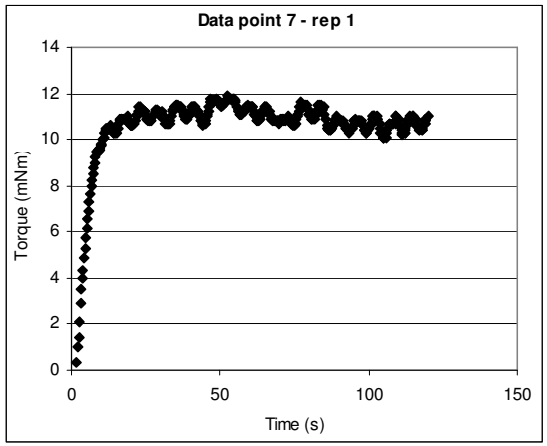
Data point 7 - rep 1
Torque (mNm)
Time (s)
0
2
4
6
8
10
12
14
0
50
100
150

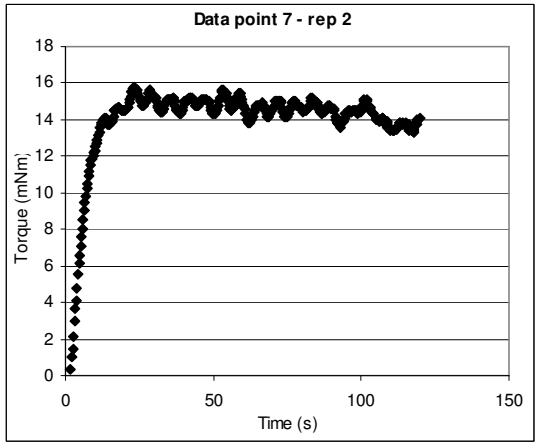
Data point 7 - rep 2
Torque (mNm)
Time (s)
0
2
4
6
8
10
12
14
16
18
0
50
100
150

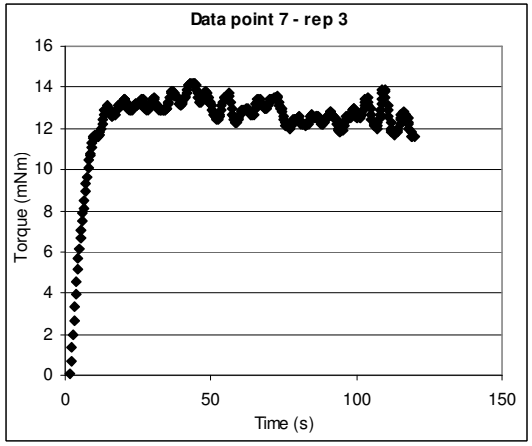
Data point 7 - rep 3
Torque (mNm)
Time (s)
0
2
4
6
8
10
12
14
16
0
50
100
150

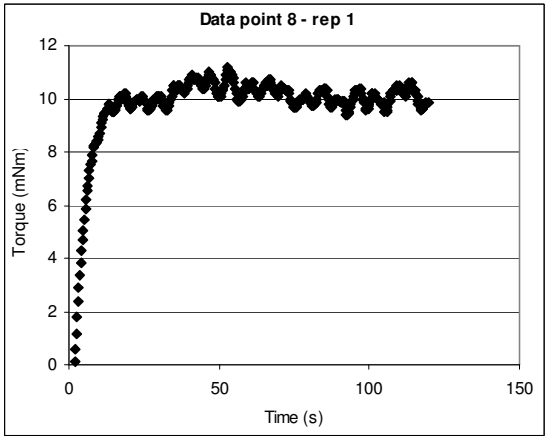
Data point 8 - rep 1
Torque (mNm)
Time (s)
0
2
4
6
8
10
12
0
50
100
150

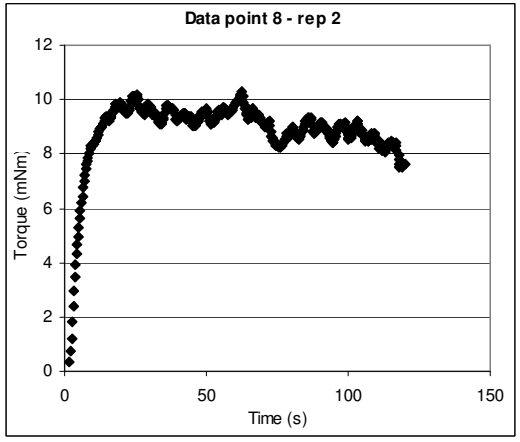
Data point 8 - rep 2
Torque (mNm)
Time (s)
0
2
4
6
8
10
12
0
50
100
150

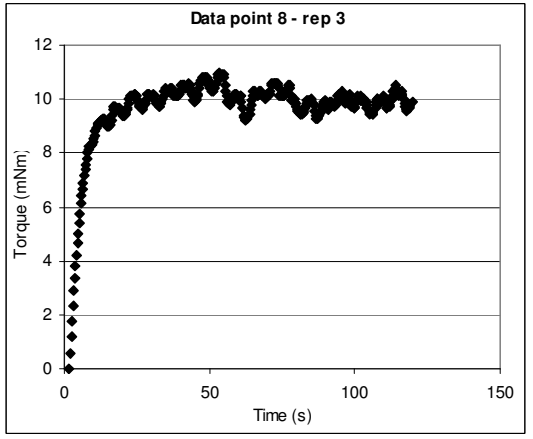
Data point 8 - rep 3
Torque (mNm)
Time (s)
0
2
4
6
8
10
12
0
50
100
150

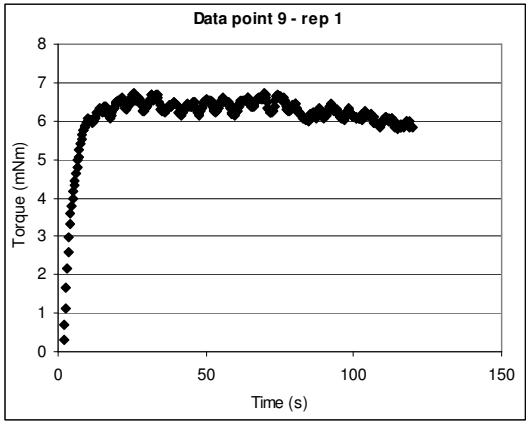
Data point 9 - rep 1
Torque (mNm)
Time (s)
0
1
2
3
4
5
6
7
8
0
50
100
150

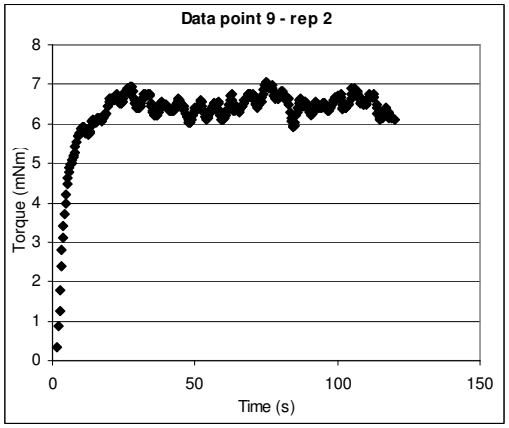
Data point 9 - rep 2
Torque (mNm)
Time (s)
0
1
2
3
4
5
6
7
8
0
50
100
150

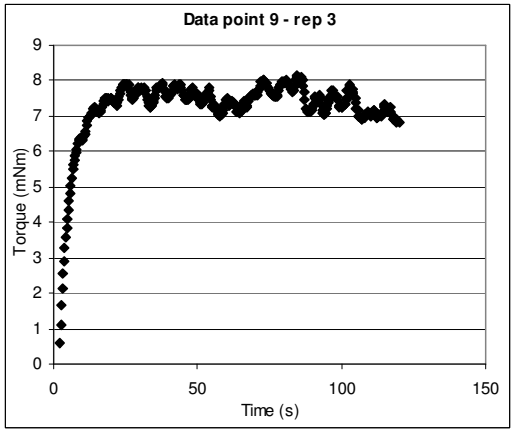
Data point 9 - rep 3
Torque (mNm)
Time (s)
0
1
2
3
4
5
6
7
8
9
0
50
100
150

Co-disposed tailings – pH 6.2, v : l = 50:50 %

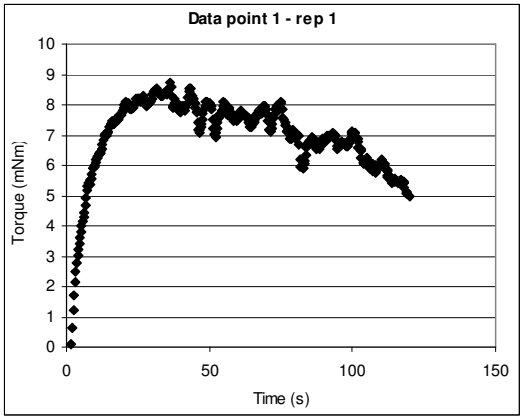

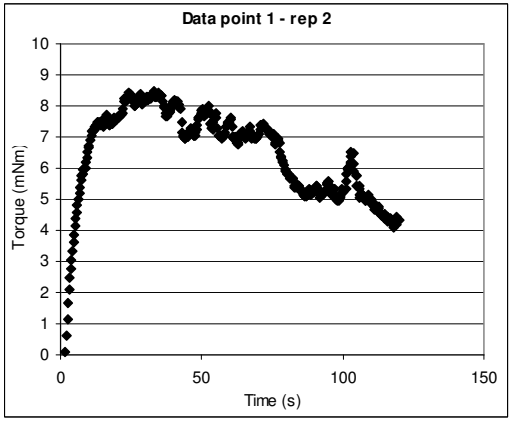

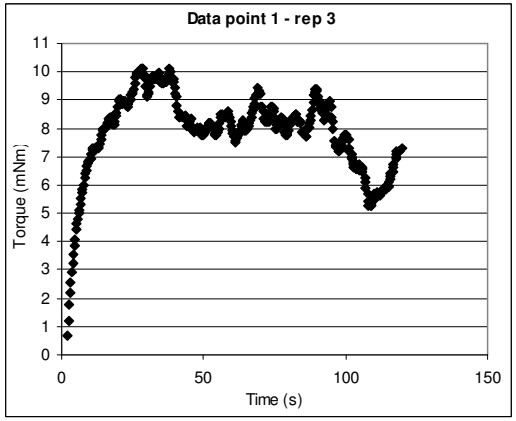

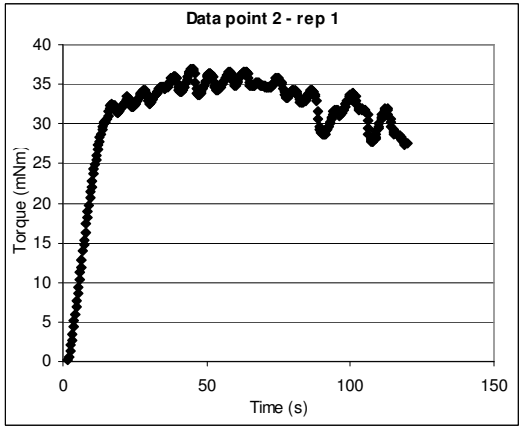

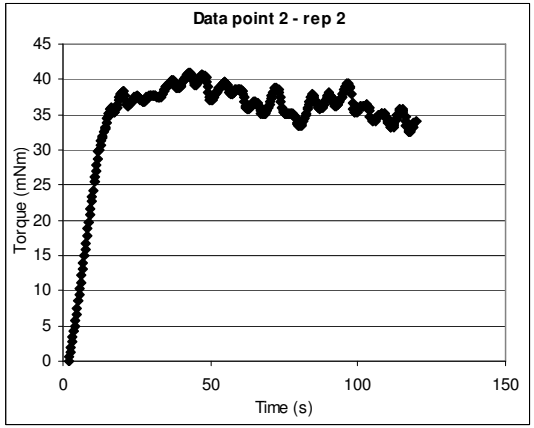

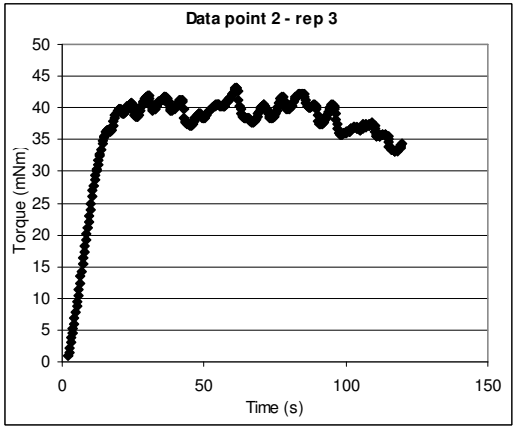

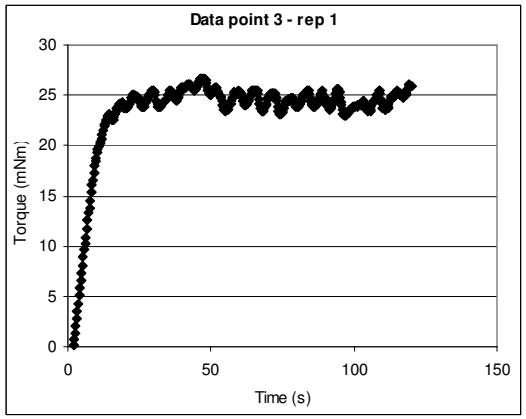
Data point 3 - rep 1
Torque (mNm)
Time (s)
0
5
10
15
20
25
30
0
50
100
150

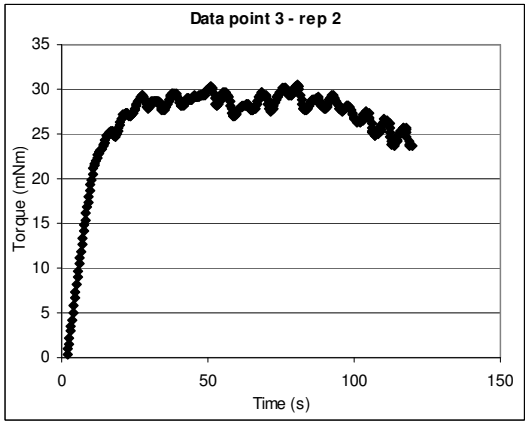
Data point 3 - rep 2
Torque (mNm)
Time (s)
0
5
10
15
20
25
30
35
0
50
100
150

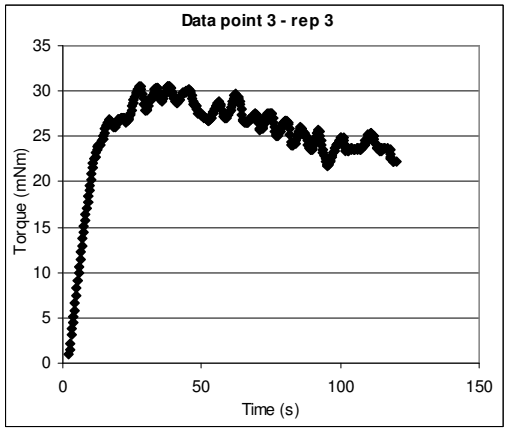
Data point 3 - rep 3
Torque (mNm)
Time (s)
0
5
10
15
20
25
30
35
0
50
100
150

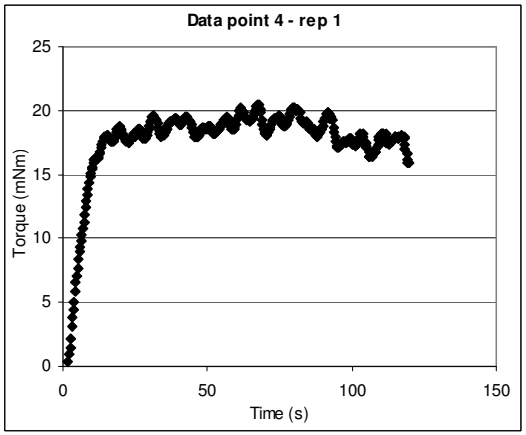
Data point 4 - rep 1
Torque (mNm)
Time (s)
0
5
10
15
20
25
0
50
100
150

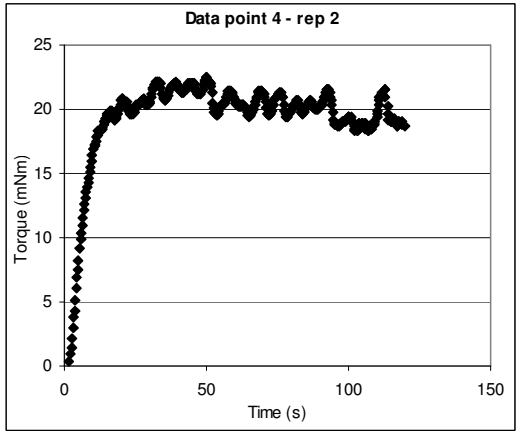
Data point 4 - rep 2
Torque (mNm)
Time (s)
0
5
10
15
20
25
0
50
100
150

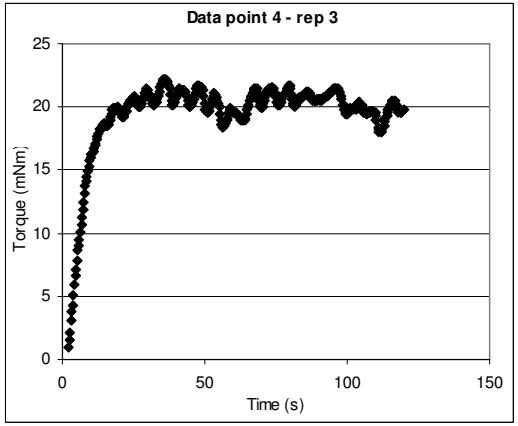
Data point 4 - rep 3
Torque (mNm)
Time (s)
0
5
10
15
20
25
0
50
100
150

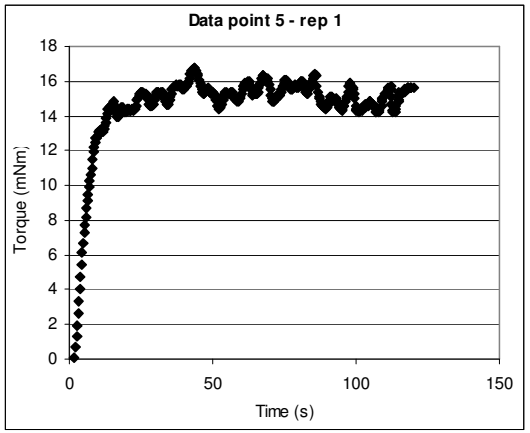
Data point 5 - rep 1
Torque (mNm)
Time (s)
0
2
4
6
8
10
12
14
16
18
0
50
100
150

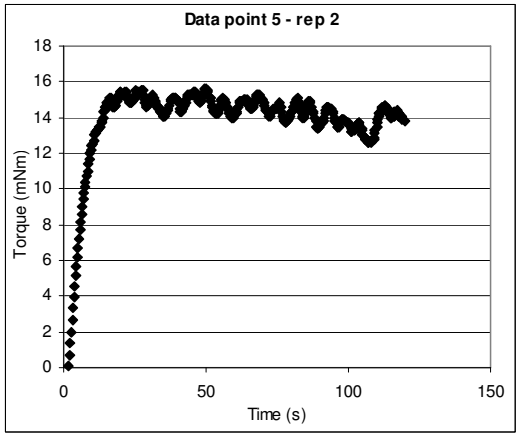
Data point 5 - rep 2
Torque (mNm)
Time (s)
0
2
4
6
8
10
12
14
16
18
0
50
100
150

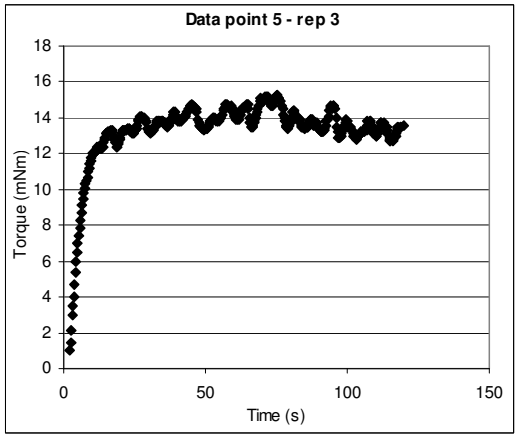
Data point 5 - rep 3
Torque (mNm)
Time (s)
0
2
4
6
8
10
12
14
16
18
0
50
100
150

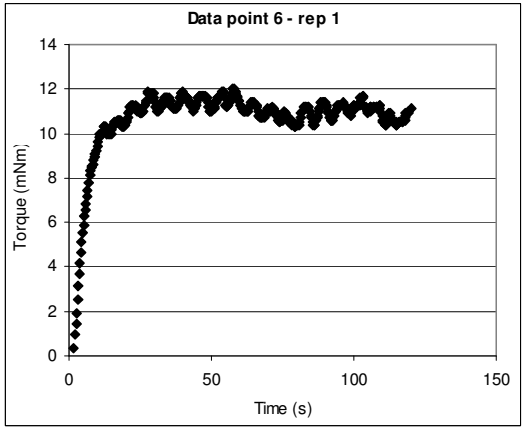
Data point 6 - rep 1
Torque (mNm)
Time (s)
0
2
4
6
8
10
12
14
0
50
100
150

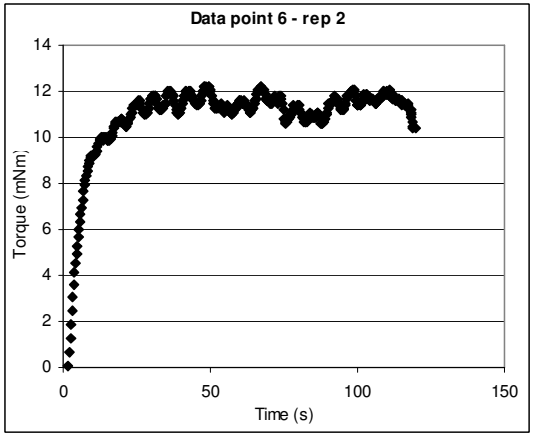
Data point 6 - rep 2
Torque (mNm)
Time (s)
0
2
4
6
8
10
12
14
0
50
100
150

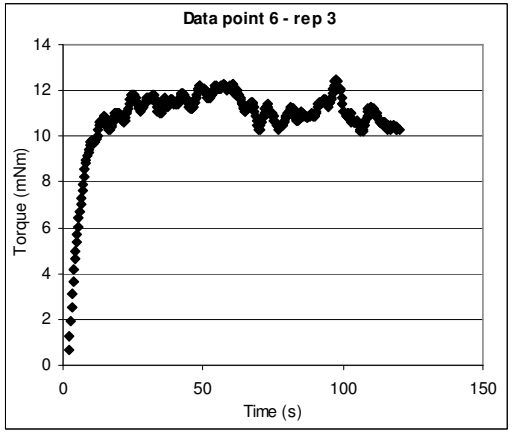
Data point 6 - rep 3
Torque (mNm)
Time (s)
0
2
4
6
8
10
12
14
0
50
100
150

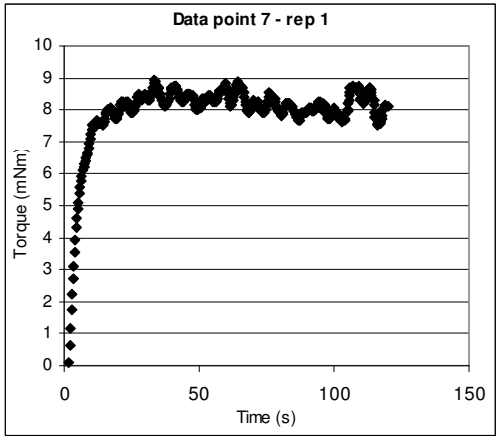
Data point 7 - rep 1
Torque (mNm)
Time (s)
0
1
2
3
4
5
6
7
8
9
10
0
50
100
150

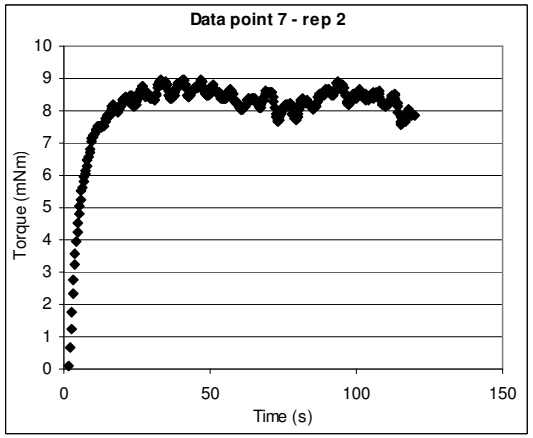
Data point 7 - rep 2
Torque (mNm)
Time (s)
0
1
2
3
4
5
6
7
8
9
10
0
50
100
150

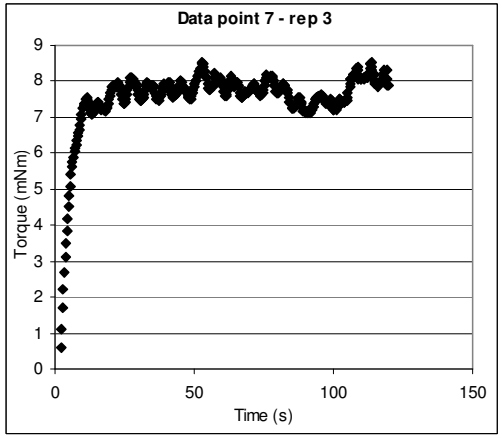
Data point 7 - rep 3
Torque (mNm)
Time (s)
0
1
2
3
4
5
6
7
8
9
0
50
100
150

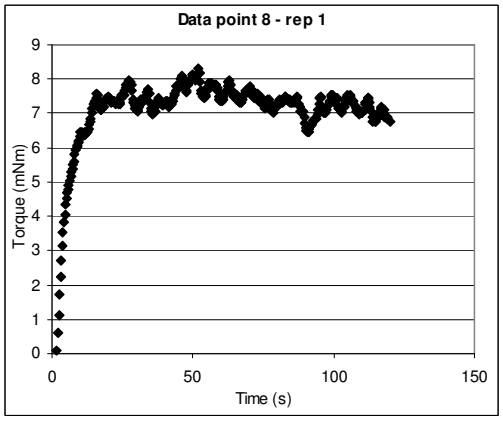
Data point 8 - rep 1
Torque (mNm)
Time (s)
0
1
2
3
4
5
6
7
8
9
0
50
100
150

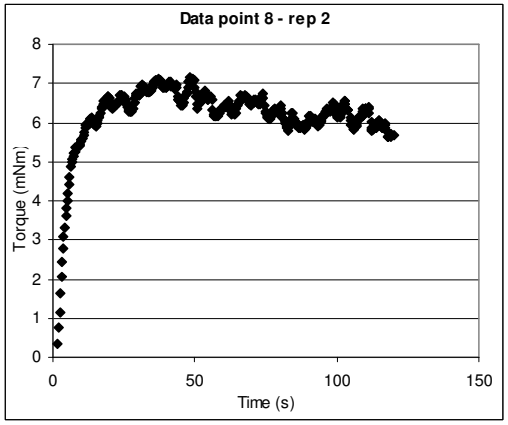
Data point 8 - rep 2
Torque (mNm)
Time (s)
0
1
2
3
4
5
6
7
8
0
50
100
150

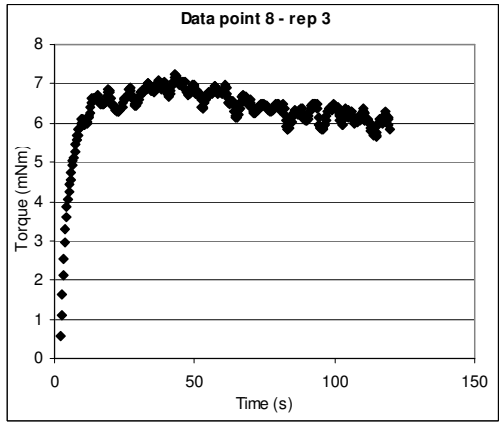
Data point 8 - rep 3
Torque (mNm)
Time (s)
0
1
2
3
4
5
6
7
8
0
50
100
150

Co-disposed tailings – pH 11.5, v : l = 86:14 %

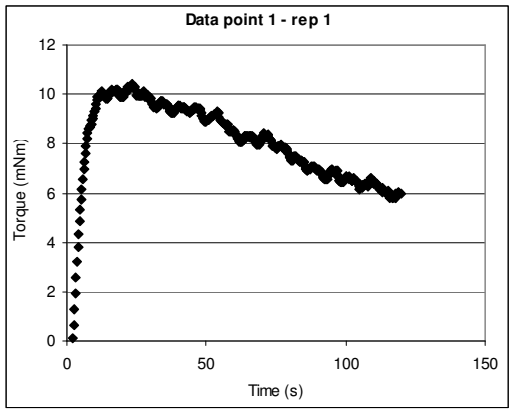

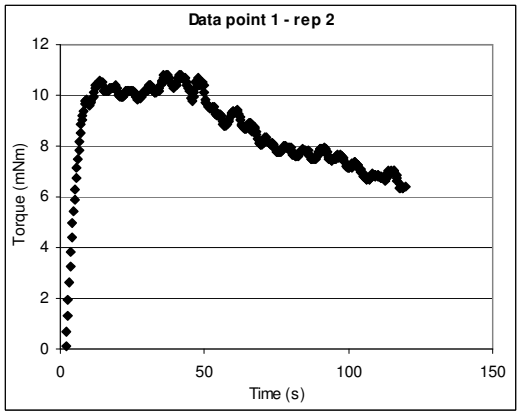

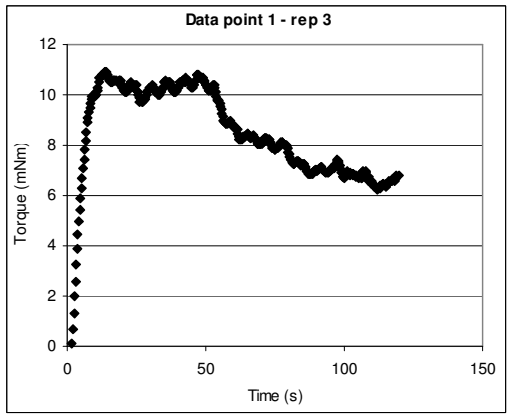

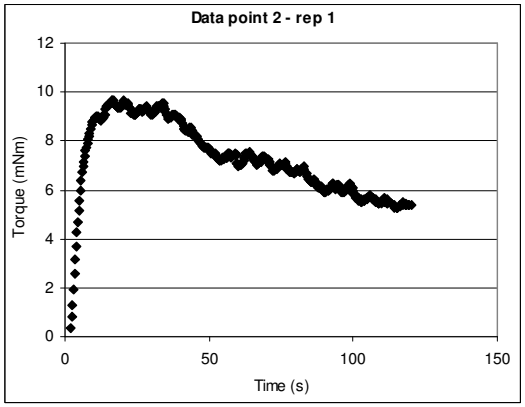

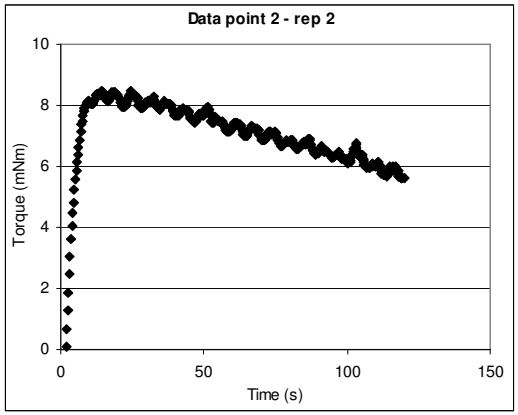

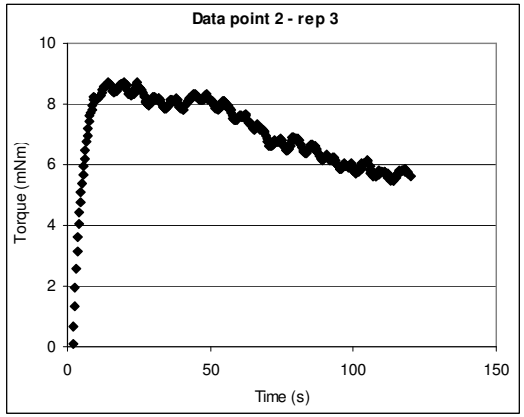

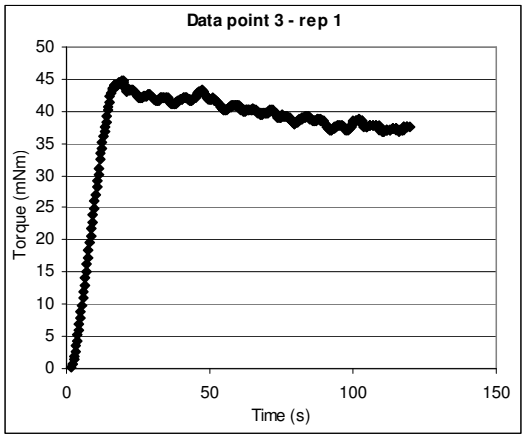
Data point 3 - rep 1
Torque (mNm)
Time (s)
0
5
10
15
20
25
30
35
40
45
50
0
50
100
150

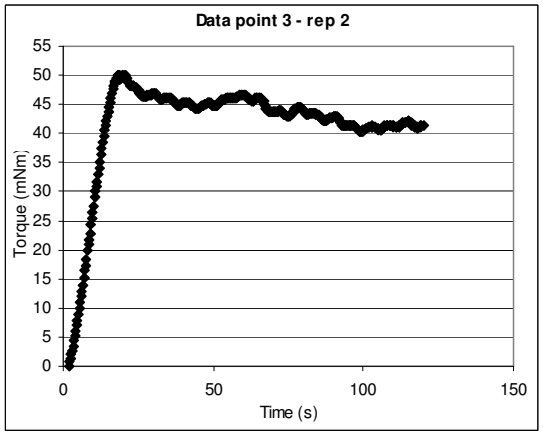
Data point 3 - rep 2
Torque (mNm)
Time (s)
0
5
10
15
20
25
30
35
40
45
50
55
0
50
100
150

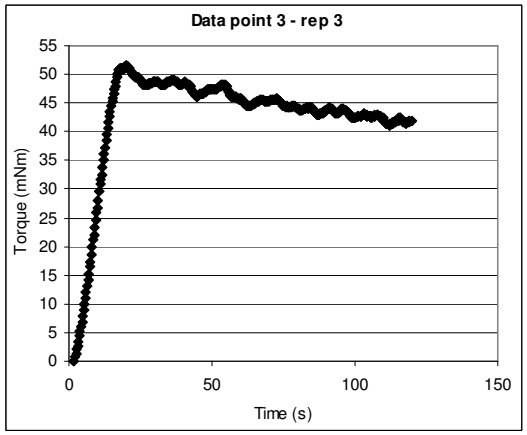
Data point 3 - rep 3
Torque (mNm)
Time (s)
0
5
10
15
20
25
30
35
40
45
50
55
0
50
100
150

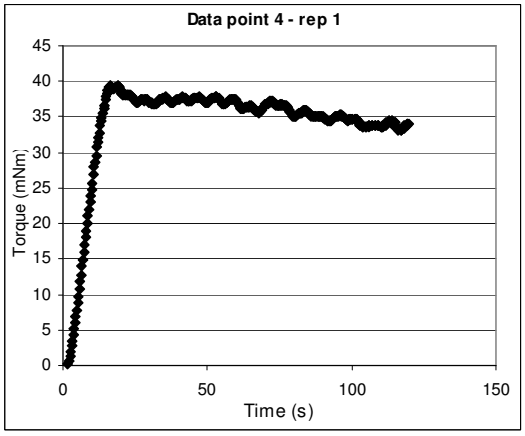
Data point 4 - rep 1
Torque (mNm)
Time (s)
0
5
10
15
20
25
30
35
40
45
0
50
100
150

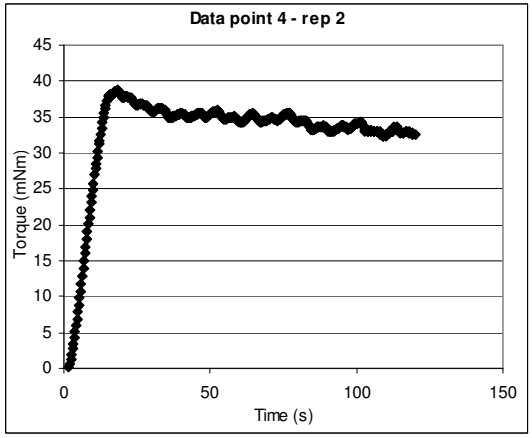
Data point 4 - rep 2
Torque (mNm)
Time (s)
0
5
10
15
20
25
30
35
40
45
0
50
100
150

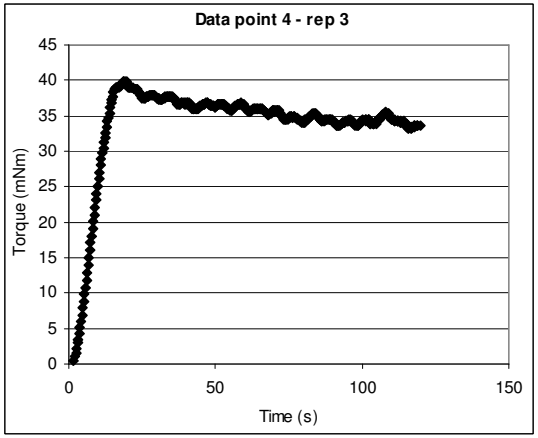
Data point 4 - rep 3
Torque (mNm)
Time (s)
0
5
10
15
20
25
30
35
40
45
0
50
100
150

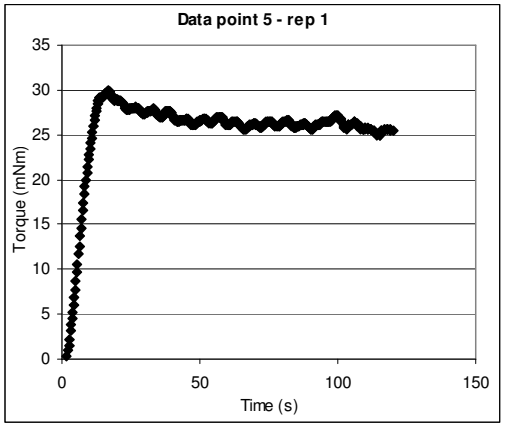
Data point 5 - rep 1
Torque (mNm)
Time (s)
0
5
10
15
20
25
30
35
0
50
100
150

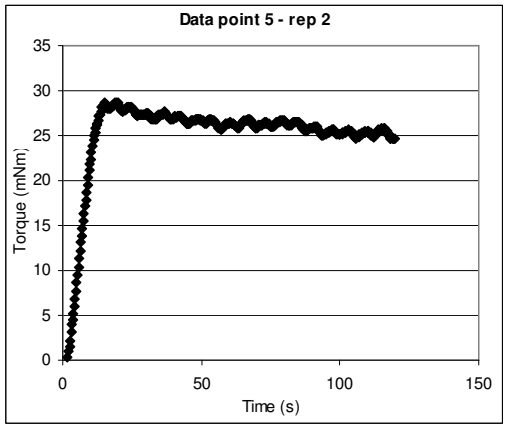
Data point 5 - rep 2
Torque (mNm)
Time (s)
0
5
10
15
20
25
30
35
0
50
100
150

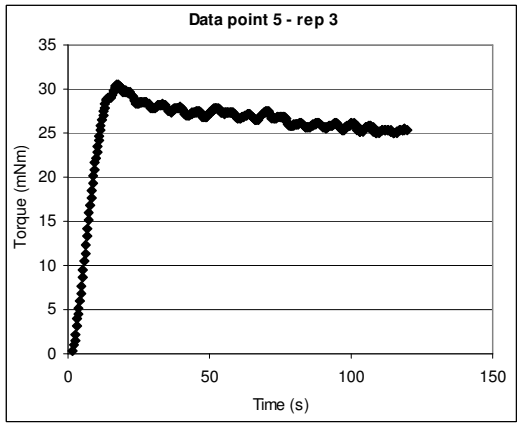
Data point 5 - rep 3
Torque (mNm)
Time (s)
0
5
10
15
20
25
30
35
0
50
100
150

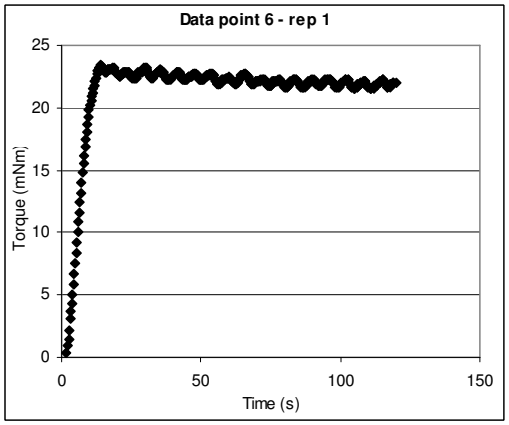
Data point 6 - rep 1
Torque (mNm)
Time (s)
0
5
10
15
20
25
0
50
100
150

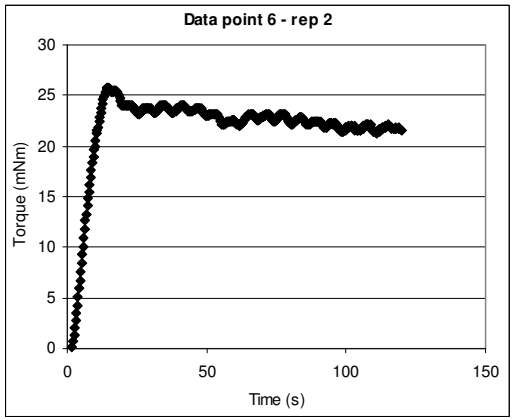
Data point 6 - rep 2
Torque (mNm)
Time (s)
0
5
10
15
20
25
30
0
50
100
150

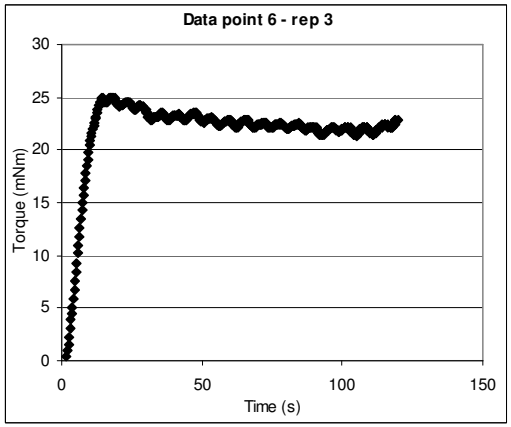
Data point 6 - rep 3
Torque (mNm)
Time (s)
0
5
10
15
20
25
30
0
50
100
150

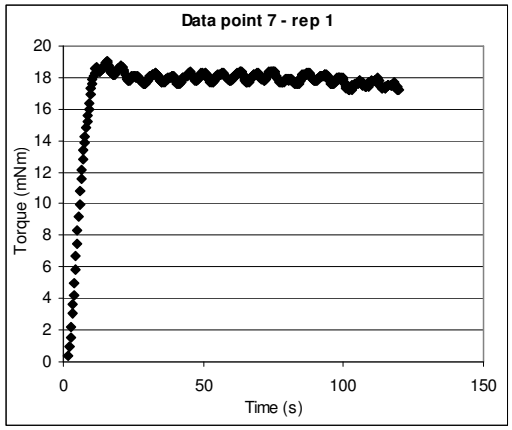
Data point 7 - rep 1
Torque (mNm)
Time (s)
0
2
4
6
8
10
12
14
16
18
20
0
50
100
150

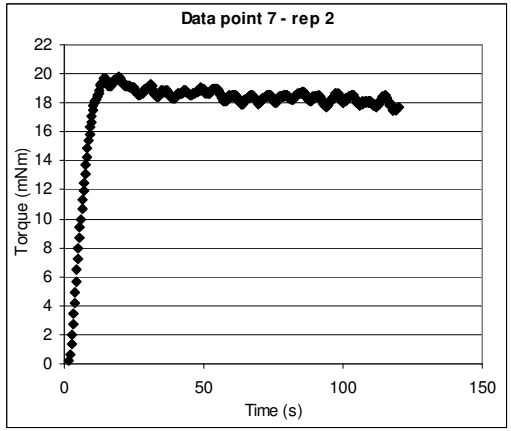
Data point 7 - rep 2
Torque (mNm)
Time (s)
0
2
4
6
8
10
12
14
16
18
20
22
0
50
100
150

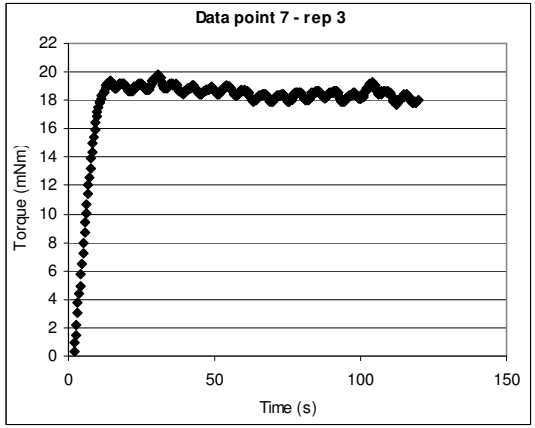
Data point 7 - rep 3
Torque (mNm)
Time (s)
0
2
4
6
8
10
12
14
16
18
20
22
0
50
100
150

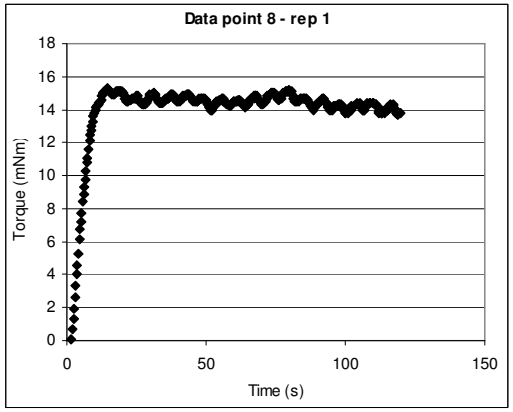
Data point 8 - rep 1
Torque (mNm)
Time (s)
0
2
4
6
8
10
12
14
16
18
0
50
100
150

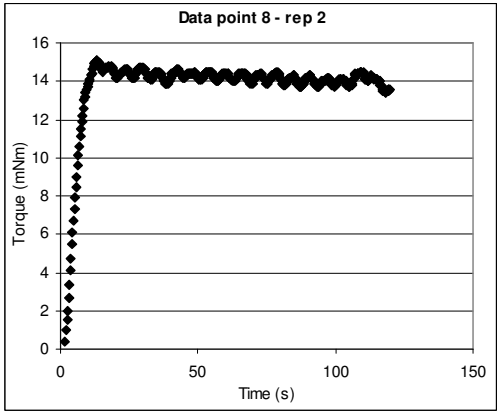
Data point 8 - rep 2
Torque (mNm)
Time (s)
0
2
4
6
8
10
12
14
16
0
50
100
150

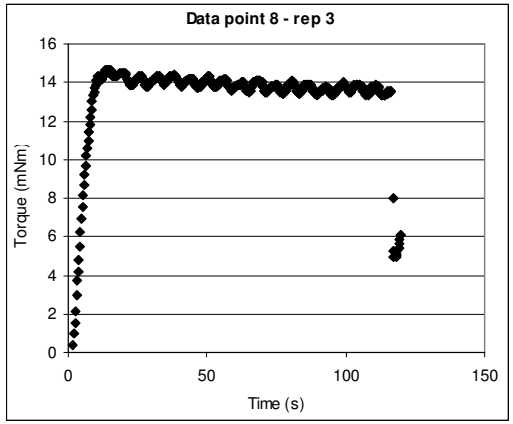
Data point 8 - rep 3
Torque (mNm)
Time (s)
0
2
4
6
8
10
12
14
16
0
50
100
150

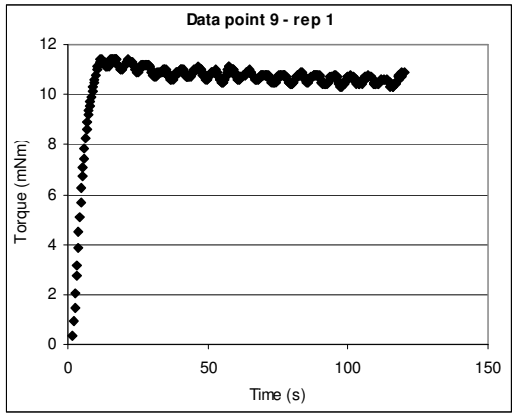
Data point 9 - rep 1
Torque (mNm)
Time (s)
0
2
4
6
8
10
12
0
50
100
150

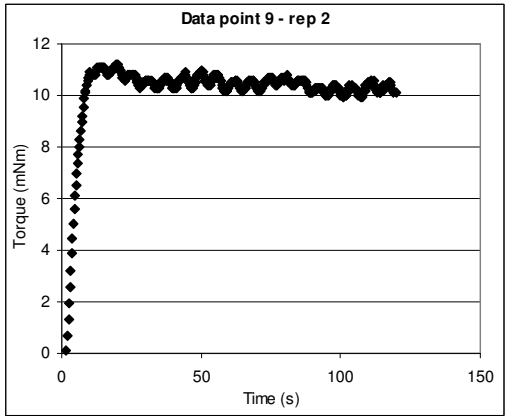
Data point 9 - rep 2
Torque (mNm)
Time (s)
0
2
4
6
8
10
12
0
50
100
150

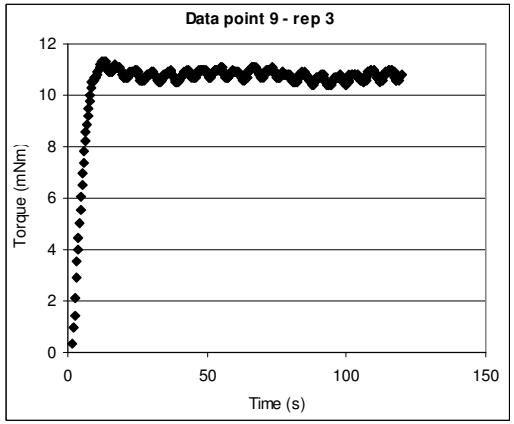
Data point 9 - rep 3
Torque (mNm)
Time (s)
0
2
4
6
8
10
12
0
50
100
150

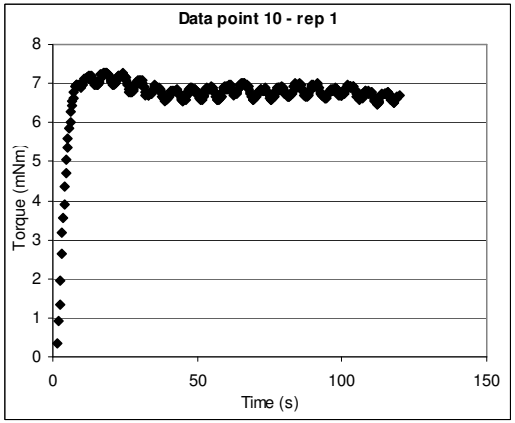
Data point 10 - rep 1
Torque (mNm)
Time (s)
0
1
2
3
4
5
6
7
8
0
50
100
150

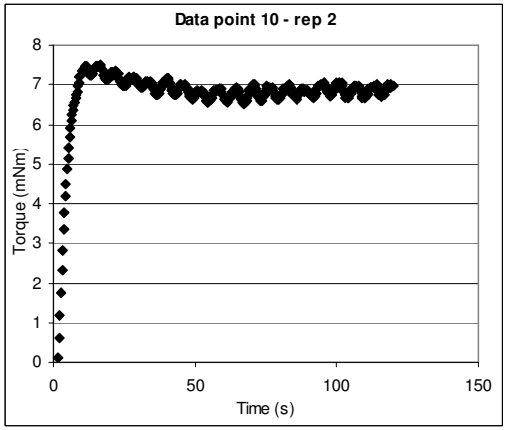
Data point 10 - rep 2
Torque (mNm)
Time (s)
0
1
2
3
4
5
6
7
8
0
50
100
150

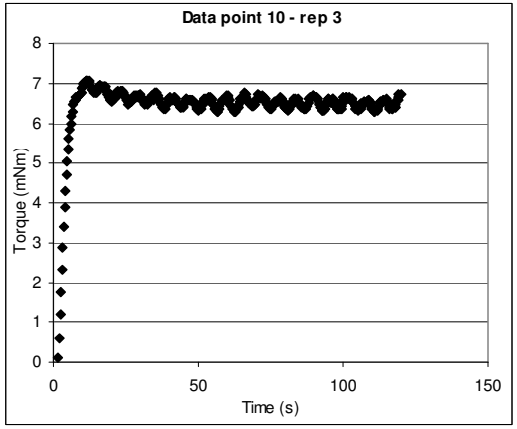
Data point 10 - rep 3
Torque (mNm)
Time (s)
0
1
2
3
4
5
6
7
8
0
50
100
150

Co-disposed tailings – pH 11.5, v : l = 60:40 %

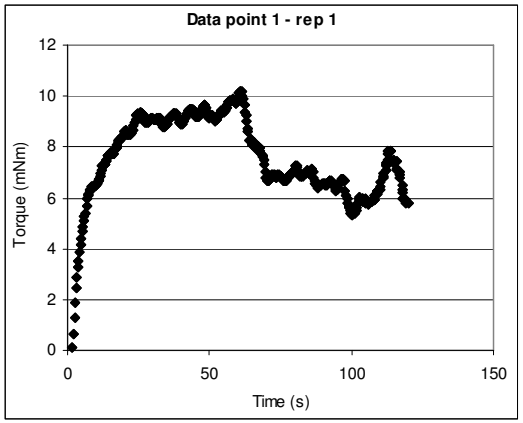

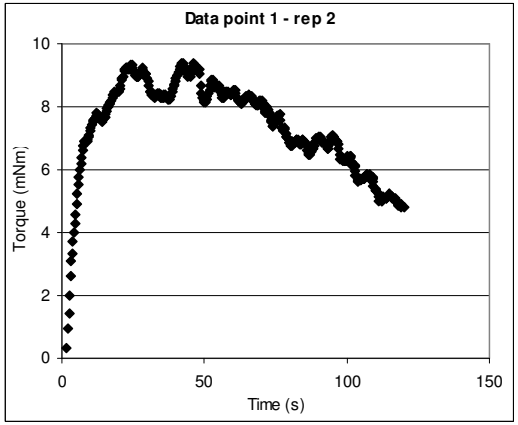

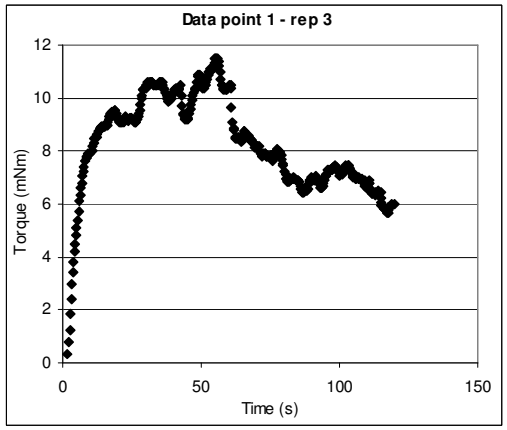

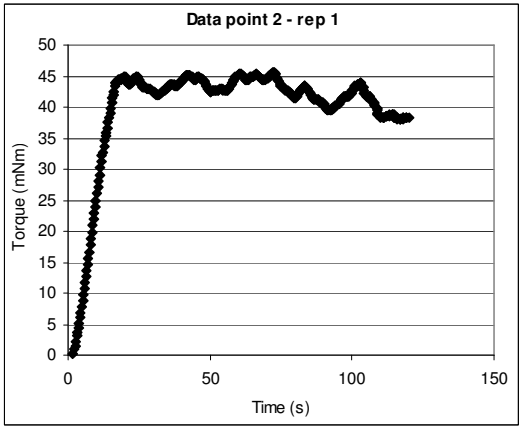

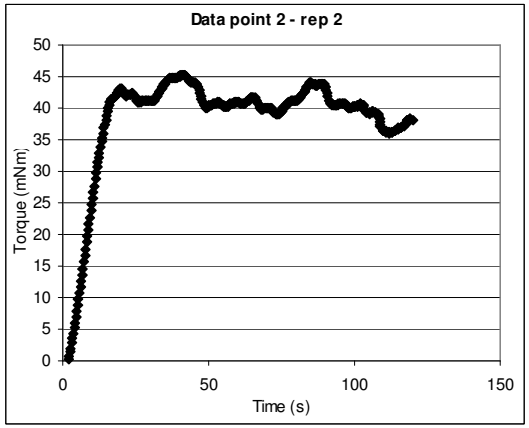

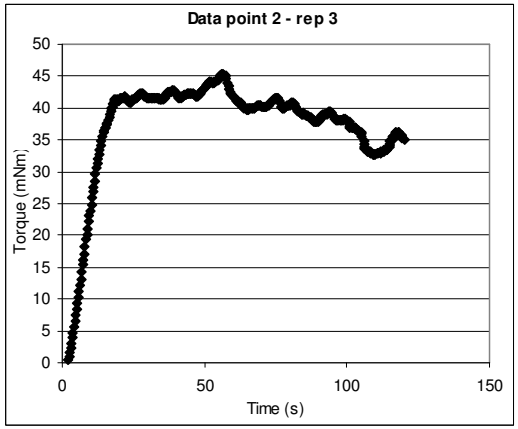

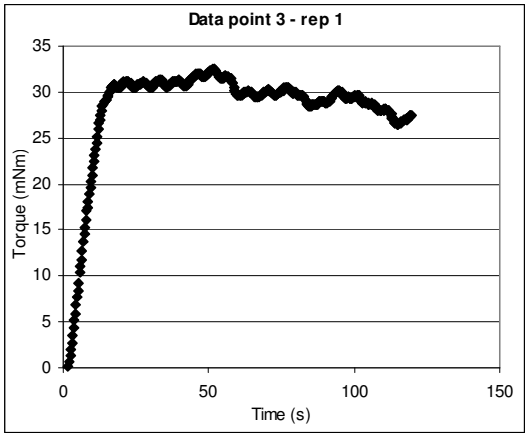
Data point 3 - rep 1
Torque (mNm)
Time (s)
0
5
10
15
20
25
30
35
0
50
100
150

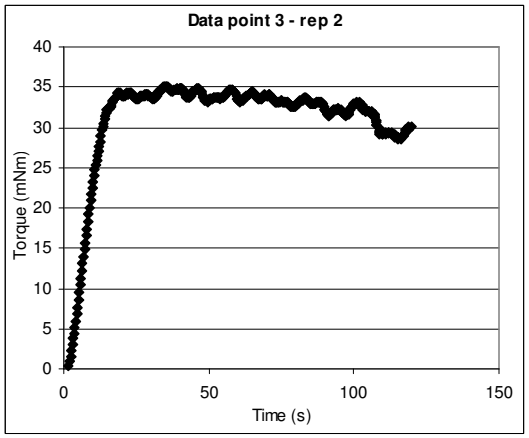
Data point 3 - rep 2
Torque (mNm)
Time (s)
0
5
10
15
20
25
30
35
40
0
50
100
150

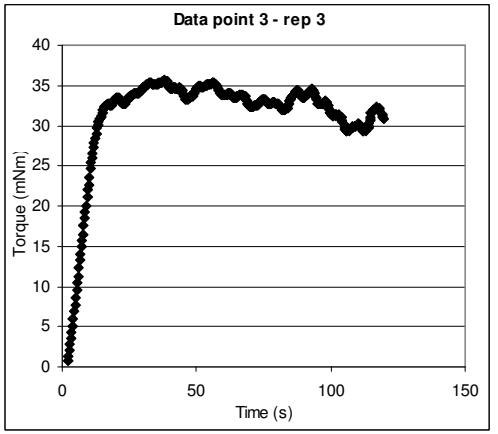
Data point 3 - rep 3
Torque (mNm)
Time (s)
0
5
10
15
20
25
30
35
40
0
50
100
150

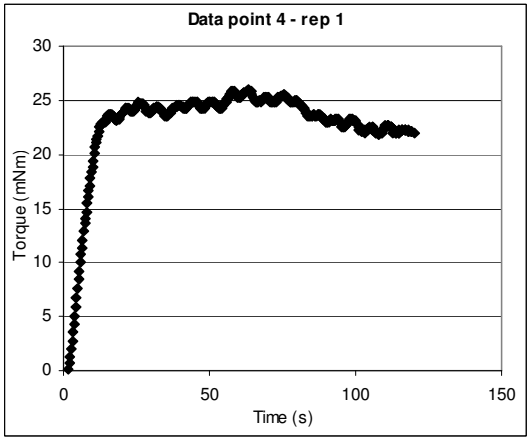
Data point 4 - rep 1
Torque (mNm)
Time (s)
0
5
10
15
20
25
30
0
50
100
150

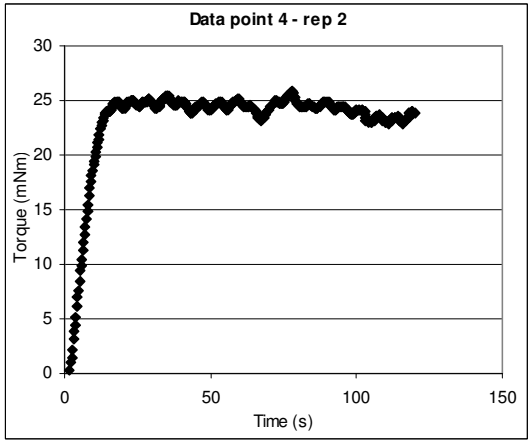
Data point 4 - rep 2
Torque (mNm)
Time (s)
0
5
10
15
20
25
30
0
50
100
150

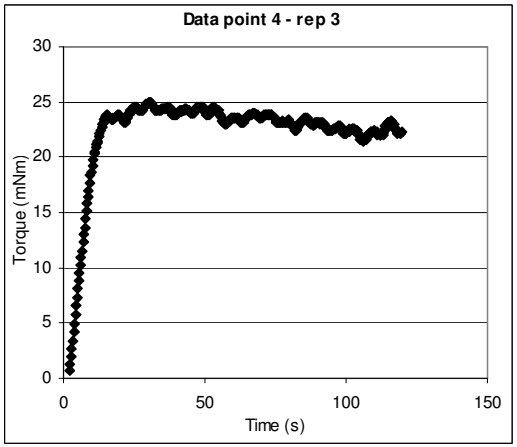
Data point 4 - rep 3
Torque (mNm)
Time (s)
0
5
10
15
20
25
30
0
50
100
150

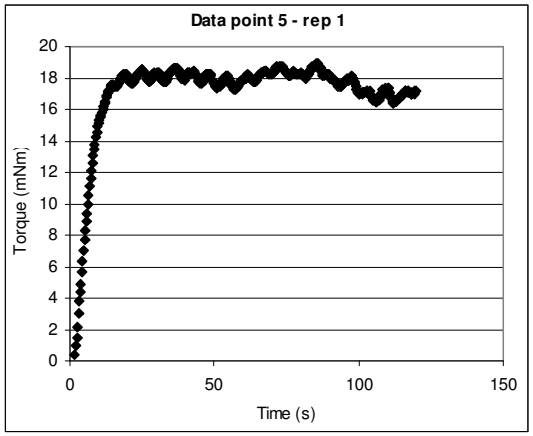
Data point 5 - rep 1
Torque (mNm)
Time (s)
0
2
4
6
8
10
12
14
16
18
20
0
50
100
150

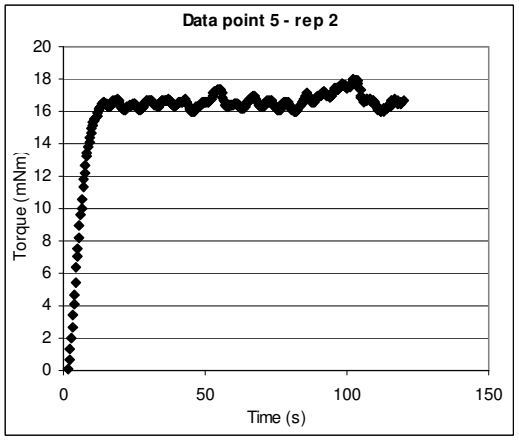
Data point 5 - rep 2
Torque (mNm)
Time (s)
0
2
4
6
8
10
12
14
16
18
20
0
50
100
150

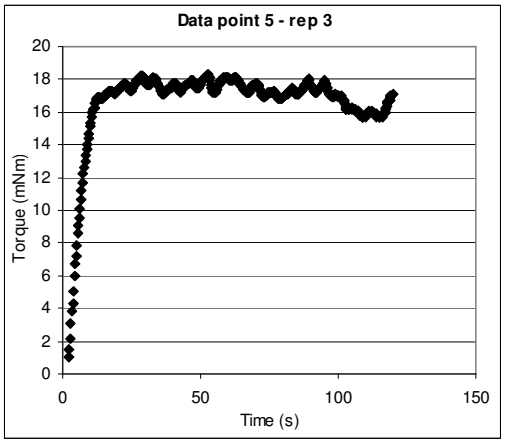
Data point 5 - rep 3
Torque (mNm)
Time (s)
0
2
4
6
8
10
12
14
16
18
20
0
50
100
150

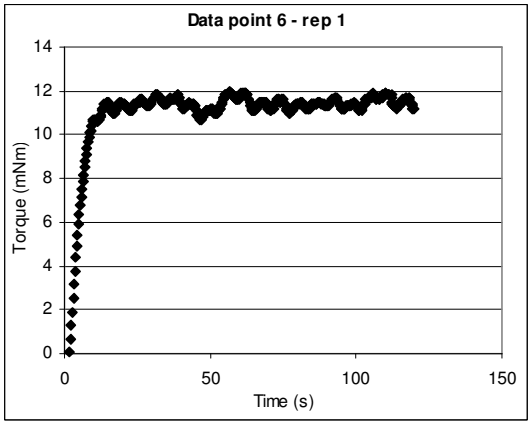
Data point 6 - rep 1
Torque (mNm)
Time (s)
0
2
4
6
8
10
12
14
0
50
100
150

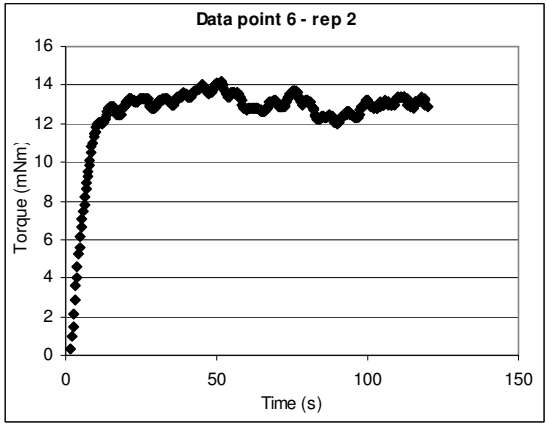
Data point 6 - rep 2
Torque (mNm)
Time (s)
0
2
4
6
8
10
12
14
16
0
50
100
150

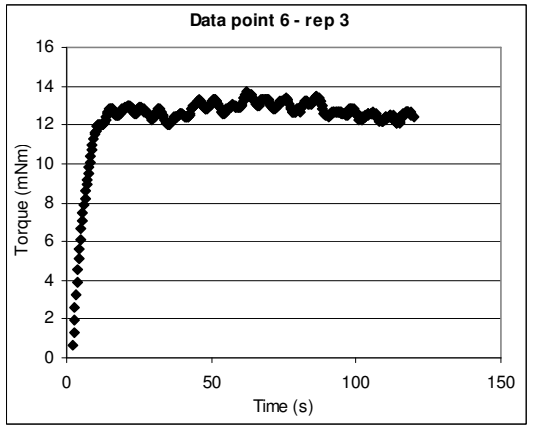
Data point 6 - rep 3
Torque (mNm)
Time (s)
0
2
4
6
8
10
12
14
16
0
50
100
150

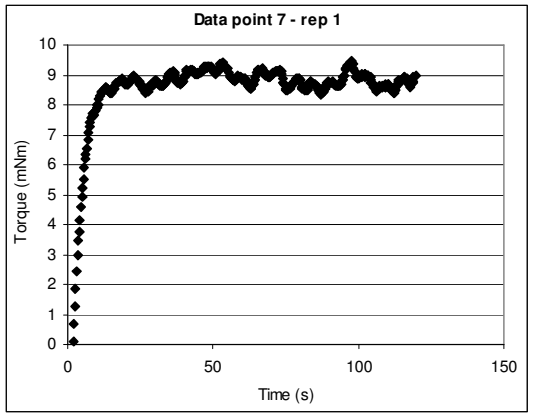
Data point 7 - rep 1
Torque (mNm)
Time (s)
0
1
2
3
4
5
6
7
8
9
10
0
50
100
150

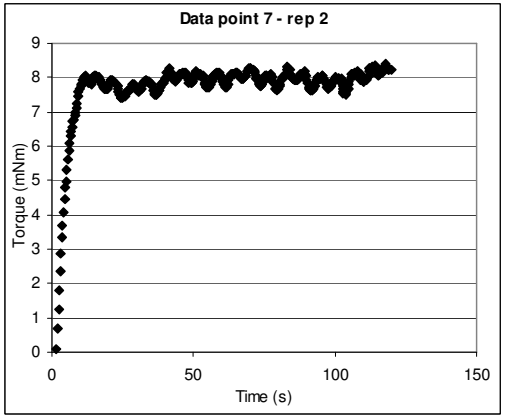
Data point 7 - rep 2
Torque (mNm)
Time (s)
0
1
2
3
4
5
6
7
8
9
0
50
100
150

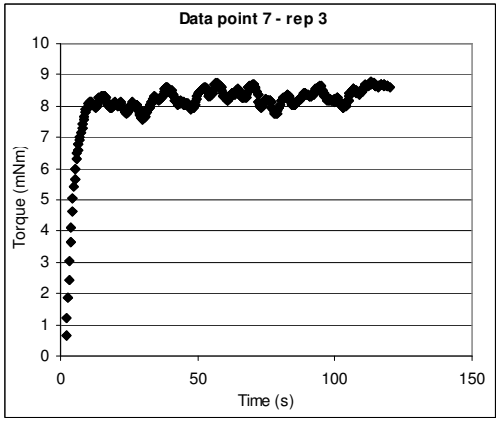
Data point 7 - rep 3
Torque (mNm)
Time (s)
0
1
2
3
4
5
6
7
8
9
10
0
50
100
150

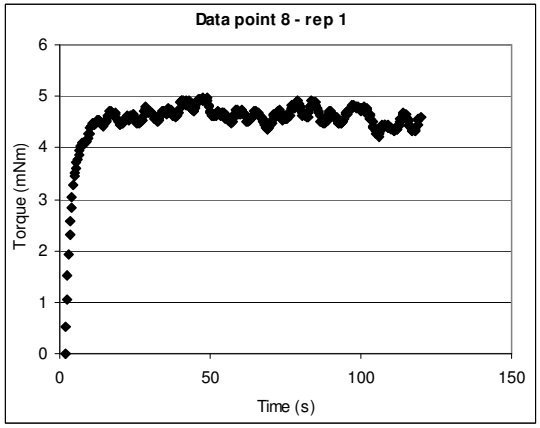
Data point 8 - rep 1
Torque (mNm)
Time (s)
0
1
2
3
4
5
6
0
50
100
150

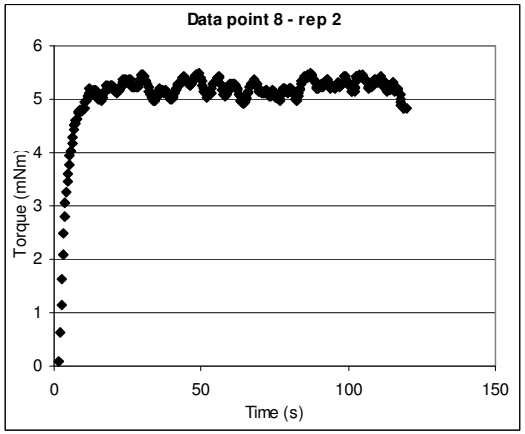
Data point 8 - rep 2
Torque (mNm)
Time (s)
0
1
2
3
4
5
6
0
50
100
150

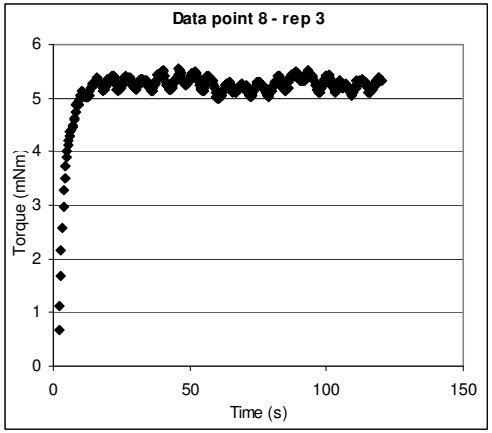
Data point 8 - rep 3
Torque (mNm)
Time (s)
0
1
2
3
4
5
6
0
50
100
150

Co-disposed tailings – pH 11.5, v : l = 50:50 %

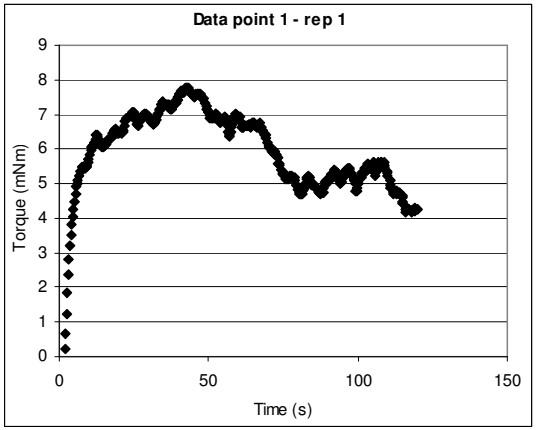

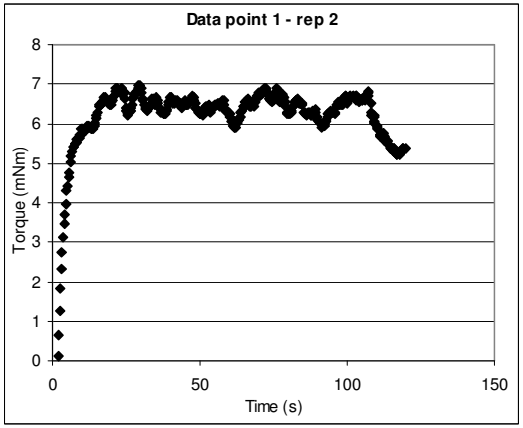

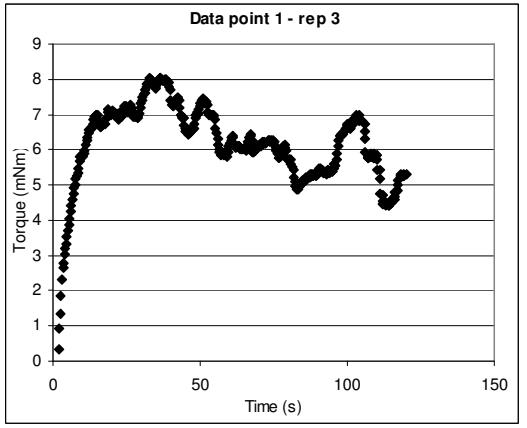

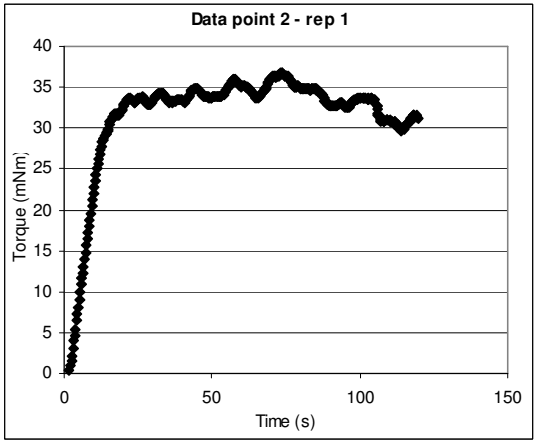

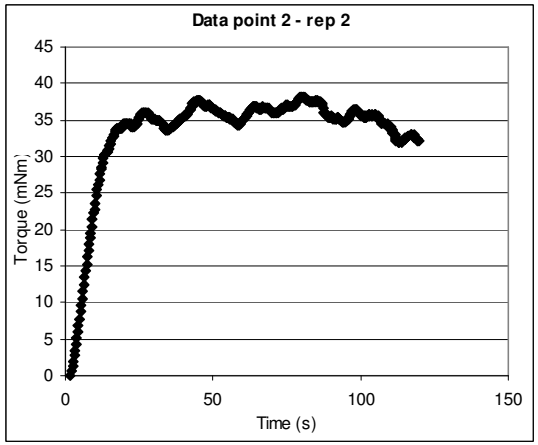

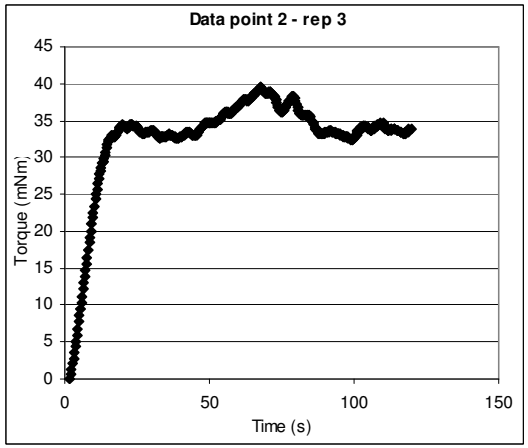

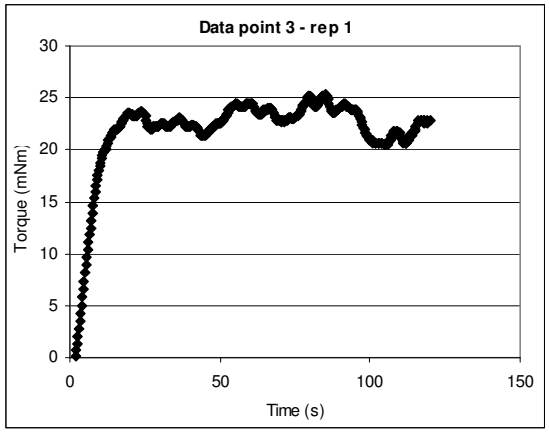
Data point 3 - rep 1
Torque (mNm)
Time (s)
0
5
10
15
20
25
30
0
50
100
150

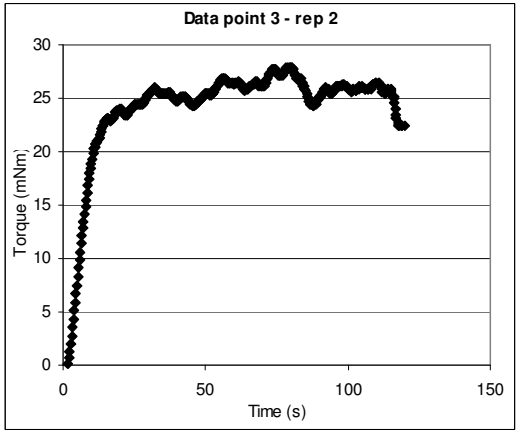
Data point 3 - rep 2
Torque (mNm)
Time (s)
0
5
10
15
20
25
30
0
50
100
150

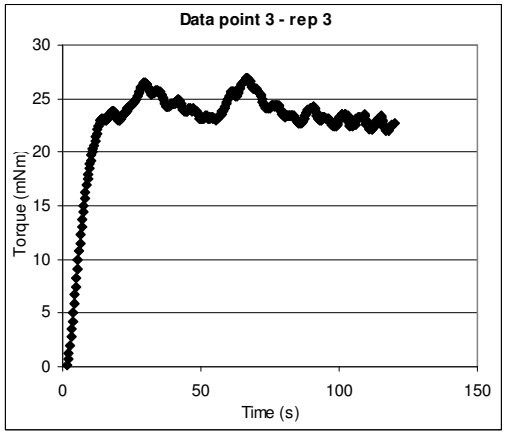
Data point 3 - rep 3
Torque (mNm)
Time (s)
0
5
10
15
20
25
30
0
50
100
150

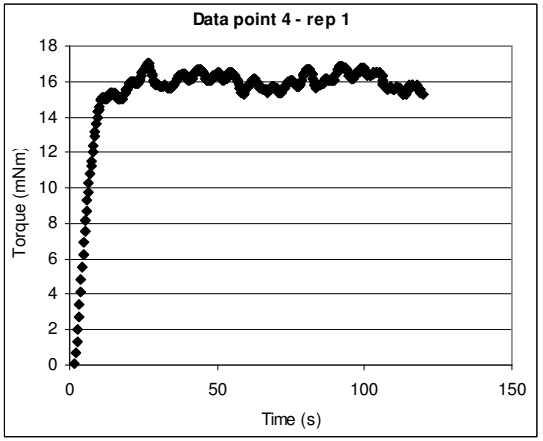
Data point 4 - rep 1
Torque (mNm)
Time (s)
0
2
4
6
8
10
12
14
16
18
0
50
100
150

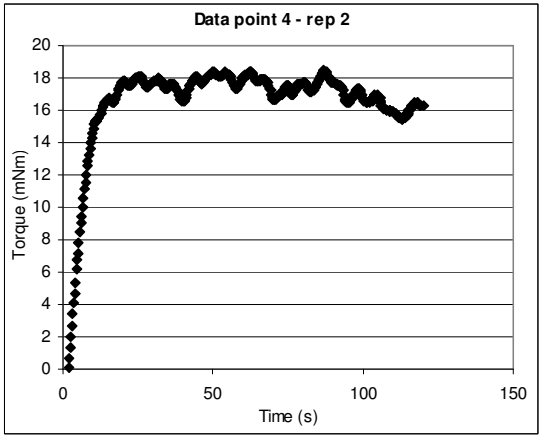
Data point 4 - rep 2
Torque (mNm)
Time (s)
0
2
4
6
8
10
12
14
16
18
20
0
50
100
150

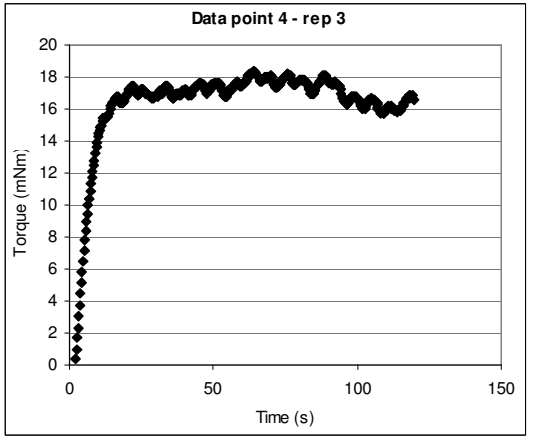
Data point 4 - rep 3
Torque (mNm)
Time (s)
0
2
4
6
8
10
12
14
16
18
20
0
50
100
150

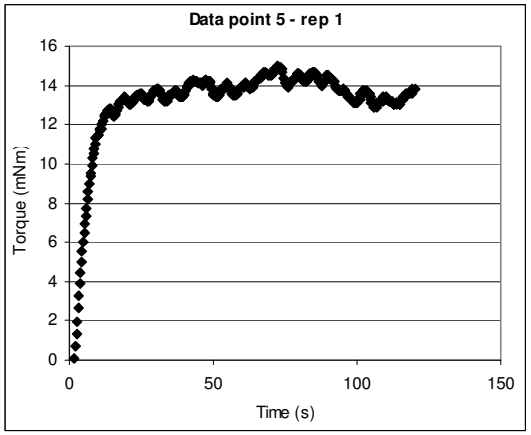
Data point 5 - rep 1
Torque (mNm)
Time (s)
0
2
4
6
8
10
12
14
16
0
50
100
150

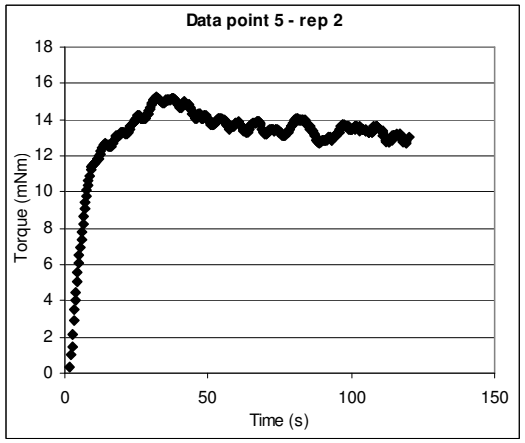
Data point 5 - rep 2
Torque (mNm)
Time (s)
0
2
4
6
8
10
12
14
16
18
0
50
100
150

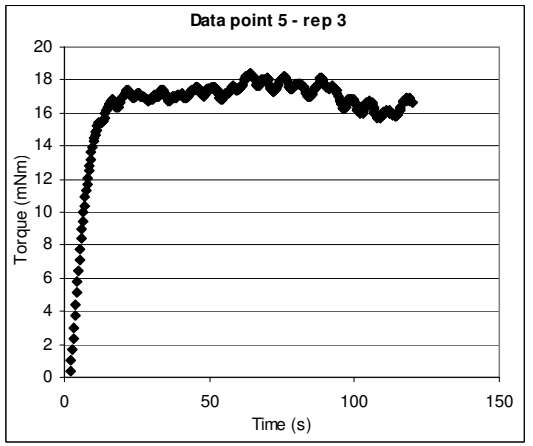
Data point 5 - rep 3
Torque (mNm)
Time (s)
0
2
4
6
8
10
12
14
16
18
20
0
50
100
150

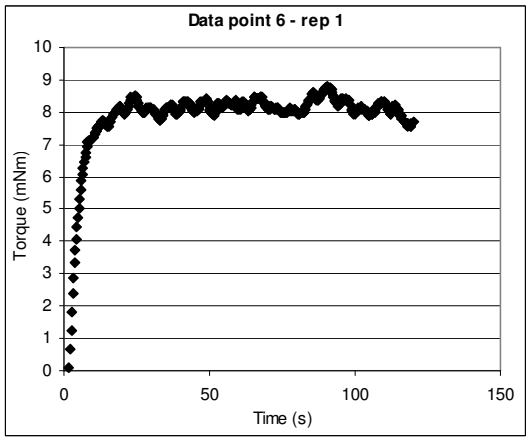
Data point 6 - rep 1
Torque (mNm)
Time (s)
0
1
2
3
4
5
6
7
8
9
10
0
50
100
150

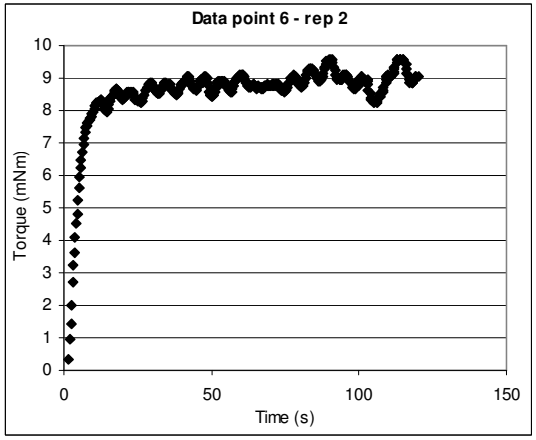
Data point 6 - rep 2
Torque (mNm)
Time (s)
0
1
2
3
4
5
6
7
8
9
10
0
50
100
150

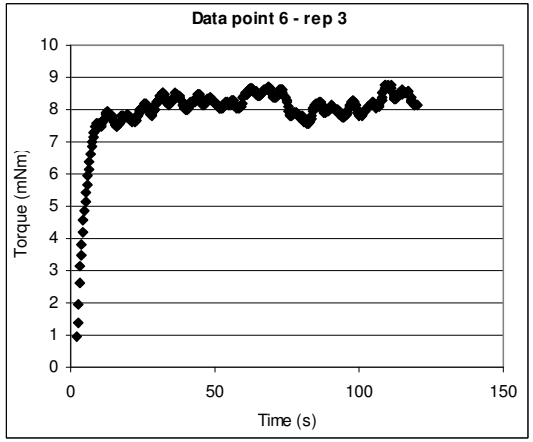
Data point 6 - rep 3
Torque (mNm)
Time (s)
0
1
2
3
4
5
6
7
8
9
10
0
50
100
150

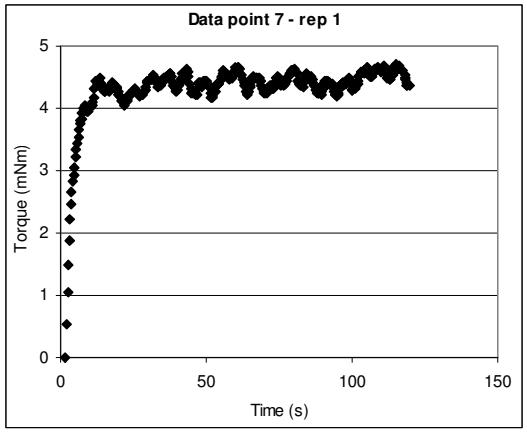
Data point 7 - rep 1
Torque (mNm)
Time (s)
0
1
2
3
4
5
0
50
100
150

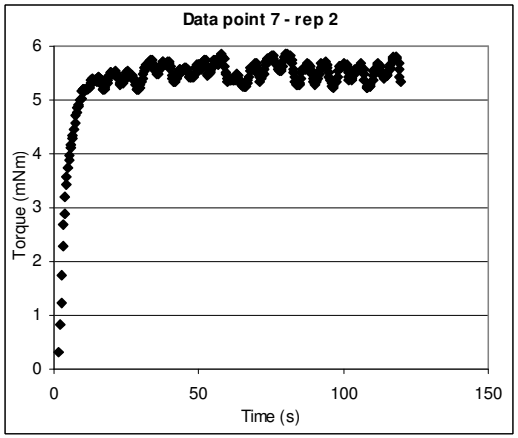
Data point 7 - rep 2
Torque (mNm)
Time (s)
0
1
2
3
4
5
6
0
50
100
150

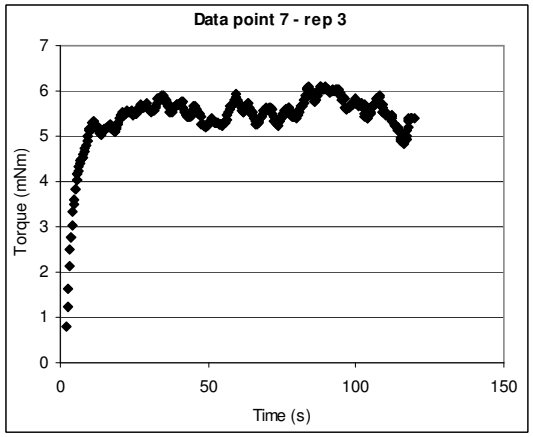
Data point 7 - rep 3
Torque (mNm)
Time (s)
0
1
2
3
4
5
6
7
0
50
100
150